UNIWERSYTET PRZYRODNICZY w LUBLINIE

Wydział Agrobioinżynierii
Dyscyplina naukowa: Rolnictwo i Ogrodnictwo

mgr Magdalena Kusiak

Rozprawa doktorska

Analiza biochemicznej i molekularnej odpowiedzi jęczmienia jarego (*Hordeum vulgare* L.) na dolistną aplikację nanocząstek i jonów miedzi

Analysis of the biochemical and molecular response of spring barley (Hordeum vulgare L.) to foliar application of nanoparticles and copper ions

Rozprawa doktorska wykonana w Instytucie Genetyki, Hodowli i Biotechnologii Roślin

Promotor: dr hab. Izabela Jośko, profesor uczelni

Lublin, rok 2023

Chciałabym serdecznie podziękować
Pani Promotor, dr hab. Izabeli Jośko,
za okazaną pomoc, wsparcie i zaangażowanie
w trakcie wszystkich etapów badań
i pisania tej rozprawy doktorskiej.

Oświadczenie promotora rozprawy doktorskiej

Oświadczam, że niniejsza rozprawa doktorska została przygotowana pod moim kierunkiem i stwierdzam, że spełnia ona warunki do przedstawienia jej w postępowaniu o nadanie stopnia naukowego.

Data ..... Podpis promotora .....

Oświadczenie autora rozprawy doktorskiej

Świadom/a odpowiedzialności prawnej oświadczam, że:

- niniejsza rozprawa doktorska została przygotowana przez mnie samodzielnie pod kierunkiem Promotora/~~Promotorów/Promotora pomocniczego~~* i nie zawiera treści uzyskanych w sposób niezgodny z obowiązującymi przepisami.
- przedstawiona rozprawa doktorska nie była wcześniej przedmiotem procedur związanych
  z uzyskaniem stopnia naukowego.
- niniejsza wersja rozprawy doktorskiej jest tożsama z załączoną na płycie CD/pendrive wersją elektroniczną.

Data ..... Podpis autora .....

* niepotrzebne skreślić

Spis treści

Streszczenie

Miedź jako jeden z mikroelementów jest niezbędna dla prawidłowego wzrostu roślin. Szczególną wrażliwość zarówno na niedobór, jak i nadmiar Cu wykazują zboża, w tym jęczmień jary (*Hordeum vulgare* L.). Deficyt Cu, szczególnie w fazie krzewienia i kłoszenia, może m.in. prowadzić do niezawiązywania się ziaren lub spadku ich wartości odżywczych. Z powodu niezadawalającej efektywności konwencjonalnych nawozów, coraz więcej uwagi koncentruje się na zastosowaniu nano-nawozów. Ze względu na swoje niewielkie rozmiary (1–100 nm) nanocząstki (ang. *engineered nanoparticles*, ENPs) wykazują bardziej efektywne właściwości fizyko-chemiczne od swoich mikro-odpowiedników. W kontekście nawozowym, zdolność ENPs do stopniowego uwalniania m.in. jonów metali może być wykorzystana w celu zapewnienia roślinom długotrwałej dostępności mikroelementów.

Celem pracy była weryfikacja przewagi nanocząstek miedzi nad konwencjonalnymi nawozami miedziowymi. W celu realizacji powyższych założeń, przeprowadzono doświadczenie laboratoryjne i wazonowe, które były poprzedzone przeglądem literatury w zakresie wykorzystania nanotechnologii w uprawie roślin **[PI]**. Celem doświadczenia laboratoryjnego była ocena odpowiedzi roślin jęczmienia (uprawianych w warunkach niedoboru Cu) na dolistną aplikację 100 i 1000 mg Cu L^{-1} nano-Cu względem $CuSO_4$ [**PII**, **PIII**]. Interakcje związków Cu z liśćmi analizowano metodami spektroskopowymi (ICP-OES, FTIR/ATR) i mikroskopowymi (SEM-EDS). Profile zawartości pigmentów, peroksydacji lipidów, aktywności enzymatycznych i zawartości nieenzymatycznych antyoksydantów wraz z analizą ekspresji genów transporterów Cu, akwaporyn oraz antyoksydantów enzymatycznych w roślinach po 1 i 7 dniach ekspozycji posłużyły do oceny skuteczności suplementacji roślin nanocząstkową i jonową formą Cu, w tym komórkowego statusu Cu. W ramach drugiego etapu badań (doświadczenie wazonowe) przeprowadzono ocenę ilościową i jakościową ziarniaków jęczmienia jarego po dolistnej aplikacji nano lub mikrocząstek (nano-Cu, nano-CuO, mikro Cu) i rozpuszczalnych związków Cu ($CuSO_4$, Cu-EDTA) **[PIV]**. Oceniano plon, skład mineralny, zawartość składników pokarmowych, zawartość przeciwutleniaczy oraz bioaktywność ziarniaków.

Przeprowadzone badania wykazały, że aplikacja nano-Cu w dawce 100 mg L^{-1} pozytywnie wpłynęła na kondycję roślin, zwiększając zawartość niskocząsteczkowych antyoksydantów oraz łagodniejszą odpowiedź molekularną niż $CuSO_4$, który potęgował reakcję stresową roślin. Z kolei, analizy ziarniaków wykazały, że nano-Cu mimo,

że skutkował podobnym poziomem akumulacji Cu, jak $CuSO_4$ czy Cu-EDTA, to jego wpływ na pojedyncze parametry biochemiczne (wartość odżywcza, zawartość i aktywność antyoksydantów) był odmienny. Przewaga jednak potencjału nawozowego nano-Cu nad konwencjonalnymi nawozami nie była jednoznaczna.

Słowa kluczowe: *Hordeum vulgare*, nanocząstki Cu, aplikacja dolistna, biofortyfikacja, antyoksydanty

Abstract

Copper as one of the micronutrients is essential for proper plant growth. Cereals, including spring barley (*Hordeum vulgare* L.), are particularly sensitive to both deficiency and excess of Cu. Cu deficiency, especially during tillering and anthesis stages, may result in e.g. pollen abortion or a decrease in their nutritional value. Due to the unsatisfactory efficiency of conventional fertilizers, more attention is being focused on the use of nano-fertilizers. Due to their small size (1- 100 nm), engineered nanoparticles (ENPs) exhibit more effective physico-chemical properties than their bulk counterparts. In the context of fertilization, the ability of ENPs to gradually release metal ions, among other things, can be used to provide plants with long-term source of micronutrients.

The goal of the doctoral dissertation was to verify the advantages of copper nanoparticles over conventional copper fertilizers. Accordingly, 2 experiments (laboratory and pot experiments) were set up, which were preceded by a literature review on the application of nanotechnology in crop production [**PI**]. The laboratory experiment aimed to evaluate the response of barley plants suffering from Cu deficiency to foliar application of nano-Cu versus $CuSO_4$ at two concentrations of 100 and 1000 mg Cu L^{-1} [**PII**, **PIII**]. Cu compounds-plant leaves interactions were analyzed with spectroscopic and microscopic methods (ICP-OES, FTIR/ATR, SEM-EDS). Patterns of pigment content, lipid peroxidation, enzymatic antioxidant activity and non-enzymatic content along with gene expression analysis of Cu transporters, aquaporins, and enzymatic antioxidants in plants after 1 and 7 days of exposure were used to evaluate the efficiency of plant supplementation with nanoparticle and ionic form of Cu, including cellular Cu status. The second stage of the study (pot experiment) involved quantitative and qualitative assessment of spring barley grains after foliar application of nano/microparticles (nano-Cu, nano-CuO, micro Cu) and ionic Cu compounds ($CuSO_4$, Cu-EDTA) [**PIV**]. The yield, mineral composition, nutrient content, antioxidant content, and bioactivity of the grains were evaluated.

The study showed that the application of nano-Cu at a dose of 100 mg L^{-1} had a positive effect on plant health, increasing the content of low-molecular antioxidants and a milder molecular response than $CuSO_4$, which enlarged the plant stress response. On the other hand, the analyses of the grains of the seeds showed that although nano-Cu provided a similar level of Cu accumulation as $CuSO_4$ or Cu-EDTA, their effects on individual biochemical parameters (nutritional value, antioxidant content and activity) were different, but the advantage of nano-Cu over used conventional fertilizers was inconclusive.

Key words: *Hordeum vulgare*, Cu nanoparticles, foliar application, biofortification, antioxidants

Wykaz publikacji wchodzących w skład rozprawy doktorskiej

PI. Kusiak M., Oleszczuk P., Jośko I. (2022). Cross-examination of engineered nanomaterials in crop production: Application and related implications. *Journal of Hazardous Materials*, T. 424 s. 127374, DOI: 10.1016/j.jhazmat.2021.127374

Punkty MEiN: 200 IF: 13.6

PII. Kusiak M., Sierocka M., Świeca M., Pasieczna-Patkowska S., Sheteiwy M., Jośko I. (2023). Unveiling of interactions between foliar-applied Cu nanoparticles and barley suffering from Cu deficiency. *Environmental Pollution*, T. 320 s. 121044, DOI: 10.1016/j.envpol.2023.121044

Punkty MEiN: 100 IF: 8.9

PIII. Kusiak M., Sozoniuk M., Larue C., Grillo R., Kowalczyk K., Oleszczuk P., Jośko I. (2023). Transcriptional response of Cu-deficient barley (*Hordeum vulgare* L.) to foliar-applied nano-Cu: Molecular crosstalk between Cu loading into plants and changes in Cu homeostasis genes. *NanoImpact*, T. 31 s. 100472, DOI: 10.1016/j.impact.2023.100472

Punkty MEiN: 100 IF: 4.9

PIV. Jośko I., **Kusiak M.**, Różyło K., Baranowska-Wójcik E., Sierocka M., Sheteiwy M., Szwajgier D., Świeca M. (2023). The life cycle study revealed distinct impact of foliar-applied nano-Cu on antioxidant traits of barley grain comparing with conventional agents. *Food Research International*, T. 164 s. 112303, DOI: 10.1016/j.foodres.2022.112303

Punkty MEiN: 140 IF: 8.1

Publikacje wchodzące w skład rozprawy doktorskie powstały w ramach realizacji projektu pn. **„Molekularne i biochemiczne mechanizmy regulujące transport nanocząstek miedzi oraz ich wpływ na wzrost, rozwój i plonowanie roślin jęczmienia jarego”**. Narodowe Centrum Nauki. SONATA 13 (2017/26/D/NZ9/00067).

Dane naukometryczne prac wchodzących w skład rozprawy:

Liczba punktów MEiN [według punktacji obowiązującej w roku wydania pracy]: **540**

IF [zgodnie z rokiem opublikowania]: **35.5**

Liczba cytowań wg Web of Science/ Scopus: **8/11**, bez autocytowań **5/7**

1. Wprowadzenie

Uprawy rolne stanowią ważny element gospodarki poprzez dostarczanie produktów roślinnych wykorzystywanych do produkcji żywności, paszy oraz paliwa [1]. Jednakże, obecnie produkcja rolna stoi przed licznymi wyzwaniami wynikającymi m.in. ze zmian klimatycznych, urbanizacji czy zanieczyszczenia środowiska prowadzących do ubytku areału gruntów ornych i spadku produktywności rolnej [2]. Problemy te są dodatkowo potęgowane przez znaczący wzrost zapotrzebowania na żywność i energię, które będą niezbędne do zaspokojenia potrzeb rosnącej liczby ludności. Według raportu Organizacji Narodów Zjednoczonych do spraw Wyżywienia i Rolnictwa (ang. *Food and Agriculture Organization of the United Nations*, FAO) światowa populacja ludzi przekroczy 9 miliardów do 2050 roku, co wymusza intensyfikację produkcji rolniczej o ponad 60% [3]. Jednak dotychczasowo stosowane strategie zwiększania produktywności upraw roślinnych, takie jak nawożenie czy uprawy roślin genetycznie modyfikowanych są kosztowne, mało skuteczne lub ich stosowanie jest ograniczane przez obowiązujące ustawodawstwo ze względu na potencjalne zagrożenia dla zdrowia ludzi (m.in. alergenność, toksyczność) i bezpieczeństwo środowiskowe (np. niekontrolowane rozprzestrzenianie się transgenu w środowisku) [4,5]. Ponadto, na przestrzeni ostatnich trzech dekad zaobserwowano rosnący problem niskiego spożycia i przyswajania mikroelementów oraz witamin [6]. Ten niedobór mikroelementów, nazywany także ukrytym głodem (ang. *hidden hunger*), wynika głównie z ich niskiej zawartości w produktach spożywczych, a nie z niedostatku pożywienia [7]. Według najnowszego raportu FAO szacuje się, że w 2021 roku problem ukrytego głodu dotyczył aż 3 miliardów ludzi na całym świecie (blisko 37,5% światowej populacji ludzkiej) [8]. W zależności od rodzaju witamin/minerałów, stopnia intensywności oraz okresu niedoboru, ukryty głód może prowadzić do pogorszenia się stanu zdrowia, upośledzenia umysłowego, licznych chorób (m.in. anemii, osteoporozy czy chorób układu krążenia), a nawet śmierci [6]. Do obecnie stosowanych metod przeciwdziałania niedoborowi mikroskładników zalicza się m.in. przyjmowanie suplementów diety, wzbogacanie żywności o brakujące składniki oraz biofortyfikację roślin przez nawożenie mineralne [1]. Jednak, stosowanie konwencjonalnych nawozów nieorganicznych wykazuje niską wydajność w dostarczaniu składników odżywczych względem zapotrzebowania roślin [9]. Dlatego też kluczowe jest opracowanie nowego podejścia zapewniającego dostarczenie roślinom optymalnej dawki składników odżywczych adekwatnych do warunków wzrostowych.

Jednym z mikroelementów niezbędnych dla prawidłowego wzrostu i rozwoju roślin jest miedź [10]. Ze względu na udział Cu jako kofaktora w kluczowych procesach metabolicznych (m.in. fotosyntezie, oddychaniu mitochondrialnym czy biosyntezie hormonów), jej niedobór prowadzi do poważnych zaburzeń wzrostu i rozwoju u roślin uprawnych, a także zwiększonej podatności na choroby [10,11]. Wysoką wrażliwość na niedobór Cu wykazują zboża np. jęczmień jary (*Hordeum vulgare* L), szczególnie w fazie krzewienia i kłoszenia [12]. Jest to bezpośrednio związane z rolą miedzi m.in. w procesie lignifikacji czy rozwoju pyłku, przez co długotrwały niedobór Cu w tych kluczowych stadiach rozwojowych prowadzi do długotrwałego krzewienia, wylegania roślin, redukcji płodności kłosków oraz braku zawiązywania ziaren i/lub spadku ich wartości odżywczych [12,13]. W celu zapewnienia roślinom optymalnej zawartości Cu stosowane są nawozy zawierające związki miedzi [14,15]. Jednakże, tradycyjnie stosowane nawozy, np. w formie CuO, $CuSO_4$, i Cu-EDTA, wykazują ograniczoną efektywność, która może wynikać z niskiej biodostępności Cu w glebie (wysokie pH gleby, wiązanie Cu przez materię organiczną, itp.) lub niewielkiej mobilności w przypadku aplikacji doglebowej [16] czy znacznego spłukiwania związków Cu z liści po dolistnym podaniu nawozu [14], co może dodatkowo prowadzić do zanieczyszczenia i degradacji gleby oraz wód gruntowych [17]. Relatywnie niska skuteczność konwencjonalnych nawozów miedziowych wymusza konieczność opracowania bardziej efektywnych związków w suplementacji roślin tym mikroskładnikiem o możliwie najmniejszym wpływie na środowisko [18].

Przeżywająca okres rozkwitu nanotechnologia dostarcza nowych rozwiązań dla szerokiej grupy dziedzin, w tym również dla rolnictwa [**PI**]. Dzięki swoim niewielkim rozmiarom (1–100 nm), nanocząstki (ang. *engineered nanoparticles*, ENPs) nabywają specyficznych, efektywniejszych właściwości (m.in. wyższą reaktywność) w porównaniu do ich mikro-odpowiedników [19]. Z tego względu, prowadzone są badania nad wykorzystaniem ENPs w kierunku zapewnienia zrównoważonej produkcji roślinnej (detekcja patogenów, ochrona upraw przed stresem abiotycznym i biotycznym, nawożenie) (Rys. 1) [20,21] [**PI**]. W kontekście nawożenia roślin, kluczową cechą nieorganicznych ENPs jest zdolność do stopniowego uwalniania jonów metali, co może zapewniać długotrwałe dostarczanie

***Rysunek 1**. Potencjalne zastosowania nanotechnologii w produkcji roślinnej [**PI**].*

mikroelementów [22]. Warto jednak zaznaczyć, że szereg czynników, m.in. morfologia, rozmiar i droga podania ENPs, mogą determinować tempo uwalniania jonów metali, w tym Cu [23]. Przykładowo, Gao i in. [24] zaobserwowali stopniowy wzrost zawartości dostępnego Cu w glebie po podaniu nano-CuO (o około 22% i 60% po 14 i 42 dniach), natomiast Zhao i in. [25] wykazali uwolnienie jedynie 30% Cu z wyjściowej dawki oprysku nano-$Cu(OH)_2$ po upływie 90 dni.

ENPs, dzięki nanometrycznym rozmiarom, mogą w relatywnie łatwy sposób pokonywać barierę komórkową, co sprzyja ich większej absorpcji przez tkanki roślinne w porównaniu do większych cząstek [26,27]. Mechanizmy pobierania i transportu ENPs poprzez liście i korzenie przedstawiono na Rys. 2A. Według dotychczasowych badań,

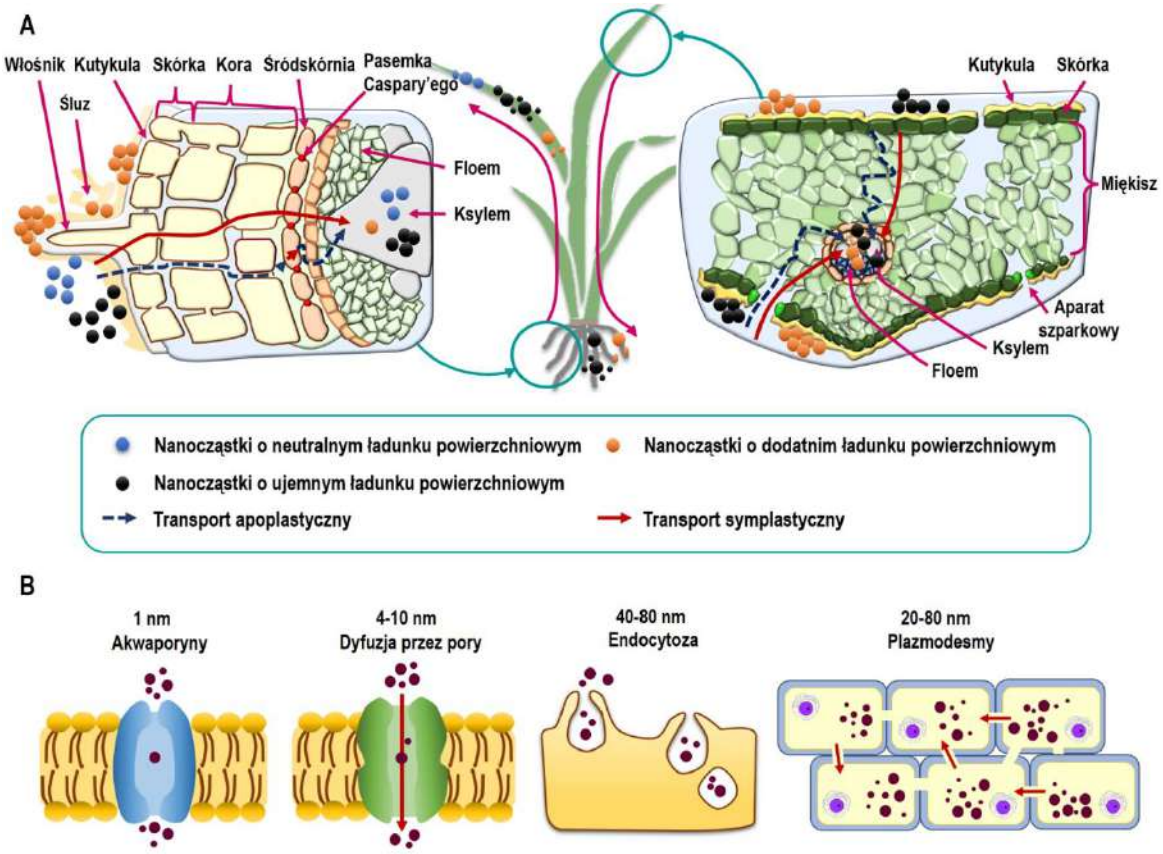

***Rysunek 2**. Schematyczny diagram (A) szlaków pobierania i translokacji nanocząstek w obrębie roślin oraz (B) mechanizmów internalizacji ENPs na poziomie komórkowym (akwaporyny, transport przez pory, endocytoza) i przez plazmodesmy.*

efektywność pobierania i translokacji nanocząstek w obrębie roślin w dużym stopniu zależała od ich właściwości, m.in. rozmiaru i ładunku powierzchniowego (Rys. 2A). Dotychczasowe badania sugerują wzrost efektywności pobierania ENPs przez korzenie [28] i liście [29] wraz ze spadkiem średnicy nanocząstek. Z kolei, Spielman-Sun i in. [30] zauważyli, że nano-CeO_2 o ładunku dodatnim ulegają silnej adhezji do powierzchni korzeni oraz agregacji w eksudacie, co przypuszczalnie ogranicza ich translokację do liści [30].

Odwrotną tendencję obserwowano w przypadku nano-CeO_2 o ładunku neutralnym i ujemnym, gdzie pomimo niskiej zawartości ENPs w korzeniach, zauważono postępującą w czasie kumulację Ce w liściach pszenicy [30]. Przypuszcza się, że takie zachowanie ENPs może wynikać z oddziaływania elektrostatycznego między ujemnie naładowaną powierzchnią korzenia i liści, a badanymi ENPs [31]. Po wniknięciu do tkanki roślinnej, ENPs mogą być transportowane drogą apoplastyczną (siatką ścian komórkowych) lub symplastyczną (poprzez cytozol komórek) [29]. W translokację ENPs drogą symplastyczną do komórek roślinnych zaangażowane są liczne białka transporterowe (do 10 nm), akwaporyny (~1 nm) i proces endocytozy (40-80 nm), podczas gdy transfer nanocząstek pomiędzy sąsiadującymi komórkami odbywa się przy udziale plazmodesmy (20-80 nm) (Rys. 2B) [32]. Z kolei absorpcja nanocząstek poprzez pory komórkowe jest warunkowana głównie ich rozmiarem (5-20 nm), jednak istnieją badania dowodzące uszkadzania błon komórkowych przez ENPs, co toruje drogę pozostałym ENPs [33].

Poza oceną zdolności ENPs do absorpcji przez rośliny, kluczowym aspektem badań nad potencjałem nawozowym ENPs jest ocena wpływu ENPs na rośliny uprawne [18,25,26,34]. Liczne badania wykazały, że reakcja roślin na ENPs jest zależna od wielu czynników, m.in. typu ENPs, stężenia, drogi podania, czasu ekspozycji, gatunku rośliny, itp. [25,26,35]. Dlatego też dotychczasowe analizy nad wykorzystaniem nieorganicznych ENPs zawierających np. Cu do poprawy wzrostu i plonowania roślin uprawnych przynosiły niejednoznaczne rezultaty [22,36,37]. Natomiast Zhao i in. [38] nie wykazali znaczących zmian w biomasie liści czy zawartości chlorofilu u *Spinacia oleracea* po dolistnym podaniu nano-$Cu(OH)_2$ (100 mg L^{-1}), u *Zea mays* zabieg ten skutkował istotnym spadkiem biomasy liści i zawartości barwników fotosyntetycznych [39]. Ponadto, o ile wykazano wzrost wartości odżywczych płodów rolnych w wyniku podawania ENPs opartych na Cu [39–41], to nie można jednoznacznie potwierdzić przewagi ENPs nad odpowiadającymi im solami metali. Dodatkowo, dostępne badania nad ekspresją genów i/lub białek pod wpływem różnych form nano-Cu wskazują na odmienne profile zmian pomiędzy roślinami [22,36,39,42].

Pomimo wielu przeprowadzonych analiz dotyczących wpływu nanocząstek na rośliny na przestrzeni ostatnich dwóch dekad, znacząca większość danych pochodzi z krótkoterminowych badań ekotoksykologicznych stosujących wysokie stężenia ENPs (Rys. 3) [43,44]. Ponadto, w większości badań ocenie podlegały głównie parametry

morfologiczne, fizjologiczne lub biochemiczne, które mimo cennych informacji o kondycji roślin, nie pozwalają na dogłębne zrozumienie interakcji roślina-nanocząstki [45,46].

***Rysunek 3**. Schematyczne przedstawienie uwzględnianych aspektów (niebieski kolor) oraz luk w ówczesnych badaniach nad wpływem ENPs na rośliny (kolor turkusowy).*

Dodatkowo, większość badań skupia się na doglebowym podaniu ENPs, pozostawiając wiele niewiadomych względem potencjalnych interakcji ENPs z liśćmi roślin w dolistnej aplikacji nano-nawozów [36,42,47]. Z kolei analizy transkryptomiczne, mogące pomóc w zrozumieniu mechanizmów działania ENPs we wnętrzu roślin, dotychczas skupiały się na markerach związanych z toksycznością [22,48]. Niewiele jest też wiadomo na temat wpływu aplikacji ENPs na pozyskane plony pod kątem wartości odżywczych i weryfikacji ich przewagi nad tradycyjnymi nawozami [40,49]. Ze względu na mnogość wspomnianych niewiadomych, efekt stosowania ENPs na rośliny powinien zostać poddany wielopoziomowej ocenie, aby uzyskać możliwie całościowy obraz, który mógłby w przyszłości stanowić podstawę do opracowania nowych i efektywnych nawozów.

2. Hipotezy i cele badawcze

Nadrzędnym celem pracy doktorskiej była ocena efektywności nanocząstek miedzi w dolistnym dokarmianiu roślin jęczmienia jarego (*H. vulgare*) względem konwencjonalnych środków nawozowych. Ze względu na złożoność i zakres badań, sformułowano następujące **cele szczegółowe**:

1. Ocena rzeczywistej absorpcji i translokacji miedzi przez rośliny po ekspozycji na nano- miedź i jony miedzi;
2. Analiza biochemicznej odpowiedzi roślin na dolistną aplikację nano-miedzi i ich rozpuszczalnych odpowiedników;
3. Analiza ekspresji genów regulujących transport i detoksykację miedzi w roślinach poddanych działaniu nanocząstek i rozpuszczalnych soli;
4. Ocena potencjału nano-miedzi do biofortyfikacji oraz poprawy cech jakościowych ziarniaków jęczmienia w porównaniu do mikrocząstek i konwencjonalnych nawozów.

Główne **hipotezy badawcze**:

1. Forma miedzi (nanocząstkowa lub jonowa), jej stężenie oraz czas ekspozycji różnicują pobieranie i dystrybucję miedzi w roślinach ze względu na różny stopień uwalniania Cu^{2+} z ENPs i/lub odmienne mechanizmy pobierania nanocząstek i jonów miedzi;
2. Nanocząstki miedzi determinują odmienną reakcję roślin – od poziomu molekularnego do odpowiedzi całego organizmu – w porównaniu do ekspozycji na jony miedzi ze względu na różne tempo i skalę dostarczania Cu do roślin;
3. Nanocząstki miedzi w większym stopniu poprawiają bioaktywność ziarniaków niż po aplikacji mikrocząstek i rozpuszczalnych soli, dzięki stopniowemu i długotrwałemu dostarczaniu Cu z ENPs.

3. Materiały i metody

3.1.Materiały

Związki miedzi

W badaniach wykorzystano różne formy miedzi: nanocząstki miedzi (nano-Cu) i tlenku miedzi (nano-CuO), mikrocząstki Cu (mikro-Cu) (Rys. 4). Ponadto, użyto łatwo rozpuszczalnych związków miedzi, które są powszechnie stosowane w dolistnym nawożeniu roślin [50]: siarczan miedzi ($CuSO_4$) oraz sól disodowa kwasu

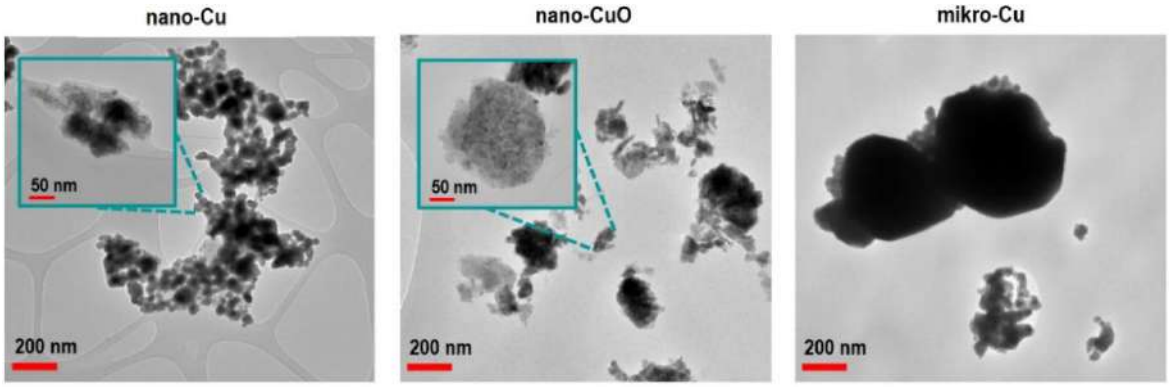

Rysunek 4. *Zdjęcia TEM proszków nano-Cu, nano-CuO i mikro-Cu.*

etylenodiaminotetraoctowego miedzi (II) (Cu-EDTA). Wszystkie związki Cu w postaci proszku o czystości ≥ 95,5% zostały zakupione z Sigma-Aldrich (USA). Podstawowe właściwości fizyko-chemiczne ENPs i mikro-Cu przedstawiono w Tabeli 1. Metody zastosowane do analizy nano- i mikro-proszków pod kątem rozmiaru cząstek, wielkości powierzchni właściwej, składu fazowego opisano w dalszej części pracy.

Tabela 1*. Właściwości fizyko-chemiczne proszków Cu [**PII-PIV**].*

	nano-Cu	nano-CuO	mikro-Cu
$\varnothing_{TEM}$	25 ± 10 nm	50 ± 10 nm	5000 ± 240 nm
S_{BET}	8 m^2 g^{-1}	29 m^2 g^{-1}	b.d.
XRD	62% Cu; 38% Cu_2O	100% CuO	100% Cu

$\varnothing_{TEM}$ –średnica nanocząstek; S_{BET} – powierzchnia właściwa nanocząstek; XRD – skład fazowy; b.d. – brak danych

Roślina testowa

W badaniach jako roślinę testową zastosowano jęczmień jary (*Hordeum vulgare* L.) odmiany Ella. Nasiona pochodziły z kolekcji Zakładu Doświadczalnego Oceny Odmian w Czesławicach. Jęczmień ze względu na znaczenie jako źródło pożywienia i biopaliw jest uważany za czwartą najważniejszą roślinę zbożową na świecie [51,52]. Ziarniaki *H. vulgare* uważane są za źródło wysokoenergetycznego pożywienia, bogatego w fitozwiązki i przeciwutleniacze korzystnie wpływające na zdrowie [7]. Jakość i wielkość plonowania jęczmienia znacząco zależy od poziomu dostępnego dla roślin Cu. Rośliny *H. vulgare* są wrażliwe na niedobór Cu, szczególnie w fazie krzewienia i kłoszenia, co prowadzi do niższych wartości odżywczych nasion, spadku płodności kłosków oraz braku zawiązywania ziaren [11,53].

3.2. Plan badawczy

W celu weryfikacji przyjętych hipotez założono 2 doświadczenia (Rys. 5): laboratoryjne oraz wazonowe. Ze względu na ograniczoną biodostępność Cu w glebie i ograniczoną translokację z korzeni do nadziemnych części roślin w obu doświadczeniach zastosowano aplikację dolistną związków Cu. Zabiegi wykonano w trzech powtórzeniach biologicznych. Wykorzystane w doświadczeniach roztwory Cu scharakteryzowano pod kątem właściwości fizyko-chemicznych, kluczowych dla wyjaśnienia ich wpływu na rośliny.

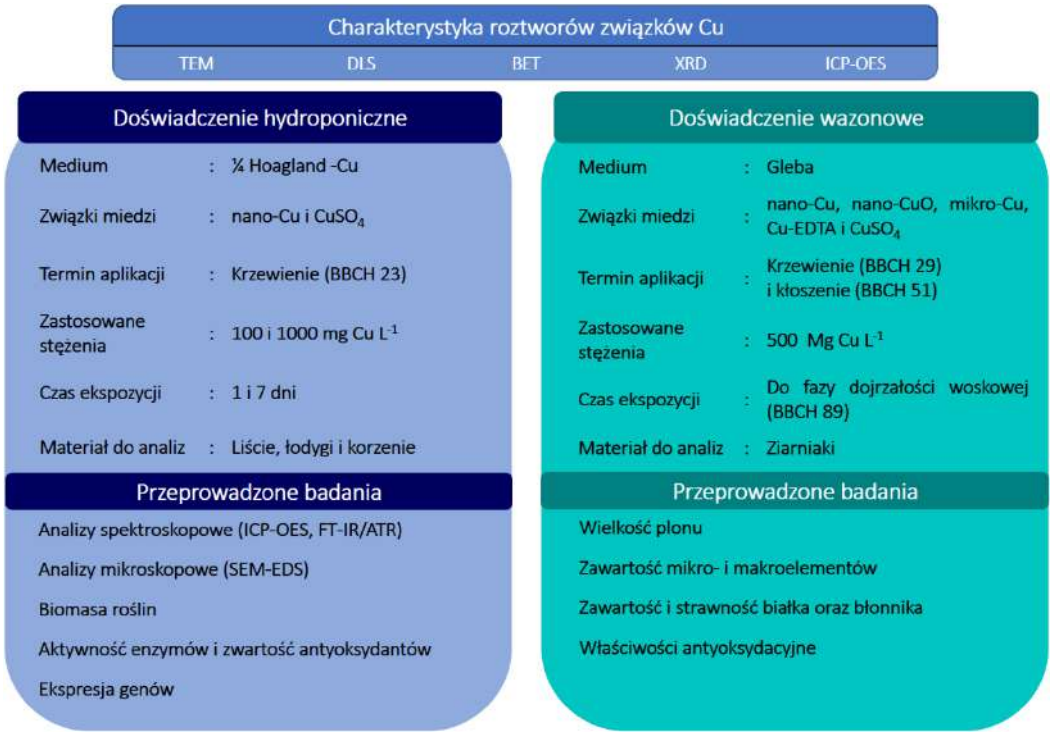

***Rysunek 5**. Plan doświadczenia laboratoryjnego i wazonowego.*

a) **Krótkoterminowe doświadczenie hydroponiczne** w warunkach deficytu Cu miało na celu (i) ocenę interakcji nano-Cu z kutykulą liści i zdolności roślin do pobierania ENPs, (ii) analizę dolistnego dokarmiania roślin jęczmienia jarego pod kątem zmian fizjologicznych i biochemicznych roślin, (iii) ocenę wpływu nano-Cu na redukcję stresu wywołanego niedoborem miedzi oraz zmian w profilach ekspresji genów związanych z transportem, homeostazą i reakcją na stres u roślin.

b) **Doświadczenie wazonowe** uwzględniające cały cykl życiowy roślin umożliwiło ocenę rzeczywistego wpływu ENPs opartych na miedzi w porównaniu do mikro-Cu i Cu^{2+} na (i) plonowanie, (ii) skład chemiczny ziarniaków, (iii) wartość odżywczą i bioaktywność ziarniaków.

3.2.1. Doświadczenie laboratoryjne

Nasiona *H. vulgare* były moczone w wodzie Milli-Q® przez 2 godziny w celu przyspieszenia kiełkowania. Następnie, zostały poddane powierzchniowej sterylizacji poprzez wytrząsanie z 2% podchlorynem wapnia przez 15 min, po czym zostały przemyte

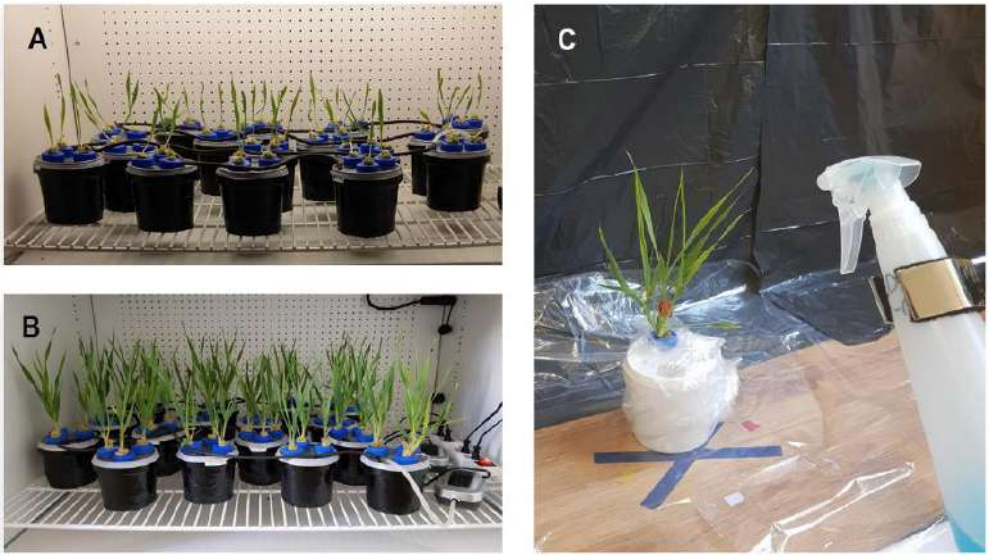

***Rysunek 6**. Zdjęcia uprawy hydroponicznej roślin H. vulgare po (A) 4 dniach i (B) w fazie krzewienia, w której wykonano aplikację oraz (C) zabiegu aplikacji dolistnej.*

70% etanolem (1 min) i trzykrotnie wodą Milli- Q® (3 min). Nasiona umieszczono na bibule laboratoryjnej w szalkach Petriego nasączonej wodą Milli- Q® i inkubowano w temperaturze 24°C w ciemności. Po 4 dniach, młode siewki jęczmienia przeniesiono do pojemników i uprawiano hydroponicznie w stale napowietrzanej pożywce ¼ Hoaglanda zawierającej (mM): 0,457 $MgSO_4 \cdot 7\ H_2O$, 1 KNO_3, 0,1 KH_2PO_4, $Ca(NO_3)_2$, 0,0672 $NaSiO_3\ 5\ H_2O$, 0,001 $Mo_7O_{24}(NH_4)_6$, 0,001 $ZnSO_4$, 0,001 $MnCl_2$, 0,003 H_3BO_3, 0,03 NaFe(III)EDTA, buforowanej przy użyciu 0,02M MES (kwas 4-morfolinoetanosulfonowy, hydrat kwasu

2-(N-morfolino) etanosulfonowego)-KOH i pozbawionej związków Cu. Pojemniki z roślinami zostały umieszczone w fitotronie (Conviron GEN1000) (Rys. 6A,B). W fitotronie przez cały okres trwania eksperymentu utrzymywane były następujące warunki: fotoperiod 16 h (dzień)/ 8 h (noc), temperatura 23 ± 3°C (dzień) i 18 ± 3°C (noc), wilgotność 60 ± 10%.

Po 5 tygodniach uprawy hydroponicznej, w fazie zaawansowanego krzewienia (BBCH: 23), wykonano aplikację dolistną roztworami Cu (Rys. 6C). Nadziemna część roślin jęczmienia jarego została opryskana roztworami nano-Cu lub $CuSO_4$ przygotowanymi w wodzie Milli- Q® w stężeniu 100 i 1000 mg Cu L^{-1} z 0,05% dodatkiem surfaktantu (Tween20, Sigma Aldrich) (Rys. 7). Wyższe stężenie związków Cu zastosowano w celu uzyskania dawki 2 kg Cu na ha, zgodnej z wytycznymi dobrej praktyki rolniczej [54], natomiast niższe stężenie roztworów Cu wybrano na podstawie przeglądu literatury i badań wstępnych [44,55], aby ocenić potencjał nawozowy niższych dawek Cu. Grupę kontrolną stanowiły rośliny spryskane roztworem wody Milli- Q® z dodatkiem 0,05% Tween20. Przed opryskiem, roztwory Cu były sonikowane przez 30 min (25°C, 250 W, 50 Hz) w łaźni ultradźwiękowej. Aplikacja dolistna została wykonana przy użyciu 250 mL ręcznych spryskiwaczy. Przed przystąpieniem do aplikacji, spryskiwacze skalibrowano w celu zapewnienia aplikacji równych objętości roztworów i poziomu zraszania. Ponadto, pojemniki zostały przykryte folią na czas aplikacji, aby zapobiec zanieczyszczeniu miedzią pożywki hydroponicznej oraz ryzyka absorpcji Cu przez korzenie. Masa folii przed i po aplikacji roztworów Cu umożliwiła określenie rzeczywistej ilości roztworów, która pozostała na roślinie (około 28,5 ± 3,0%). W związku z zauważalną silną agregacją ENPs, przeprowadzono analizy stężenia Cu^{2+} w roztworach z nano-Cu przed i po oprysku (po „przejściu" roztworu przez spryskiwacz) w celu sprawdzenia czy agregaty ENPs nie zatkały dyfuzora powodując niższą realną ekspozycję na ENPs od założonej. Brak różnic w stężeniach Cu^{2+} przed i po wykonaniu oprysków świadczy o niezakłóconym przepływie roztworów z ENPs.

***Rysunek 7**. Zdjęcie roztworów nano- Cu i $CuSO_4$ w stężeniu 100 i 1000 mg L^{-1}.*

Po 1 i 7 dniach ekspozycji na Cu, rośliny ścięto i podzielono na części przeznaczone do chemicznych i biologicznych analiz. Bezpośrednio po ścięciu liście flagowe zostały natychmiast roztarte w ciekłym azocie w celu izolacji RNA. Pozostałe liście zostały podzielone na 2 grupy: pierwsza grupa przeznaczona do analiz biochemicznych została

zważona i przechowywana w -80°C. Druga część liści przeznaczona do analiz spektroskopowych i mikroskopowych została opłukana w wodzie Milli-Q® (wyjątek stanowiły analizy FTIR, w których użyto świeże, nieopłukane fragmenty liści). Dodatkowo, w celu usunięcia nano-Cu z powierzchni liści, liście zostały zanurzone w HNO_3 na 30 sek. i 3-krotnie opłukane wodą Milli-Q®. Korzenie roślin były opłukane tylko w wodzie Milli-Q®. Próbki roślinne zostały następnie powietrznie wysuszone, zważone i przechowywane w temperaturze 20°C.

3.2.2. Doświadczenie wazonowe

Doświadczenie wazonowe prowadzono w warunkach polowych w Świdniku (woj. lubelskie) w okresie od 27.03 do 27.07.2020 roku. Glebę wykorzystaną w doświadczeniu scharakteryzowano pod kątem pH oraz dostępnych makro- i mikroskładników. Nasiona jęczmienia jarego zostały wysiane do 50 L donic (50 nasion/donica). Donice zostały wkopane do gleby i otoczone siatką w celu ochrony przed szkodnikami. W późnej fazie kiełkowania (BBCH: 9) rośliny zostały przerzedzone do 20 siewek jęczmienia jarego. Rośliny były podlewane wodą redestylowaną. Aplikację dolistną roztworami nano-Cu, nano-CuO, mikro-Cu, $CuSO_4$ oraz Cu-EDTA (Rys. 8) wykonano dwukrotnie w okresie wzrostu roślin: w fazie zaawansowanego krzewienia (BBCH: 29) oraz na początku kłoszenia (BBCH: 51) (Rys. 9A,B). Zastosowana dawka (6 mL roztworu o stężeniu 500 mg Cu L^{-1}) została przeliczona by sumarycznie uzyskać końcowe stężenie 2 kg Cu na ha. Roztwory badanych związków Cu przygotowano w wodzie Milli-Q® z 0.1% dodatkiem adiuwanta (FASTER, INTERMAG). Przed opryskiem, roztwory Cu były sonikowane przez 30 min (25 °C, 250 W, 50 Hz). Grupę kontrolną

***Rysunek 8**. Zdjęcie zastosowanych roztworów.*

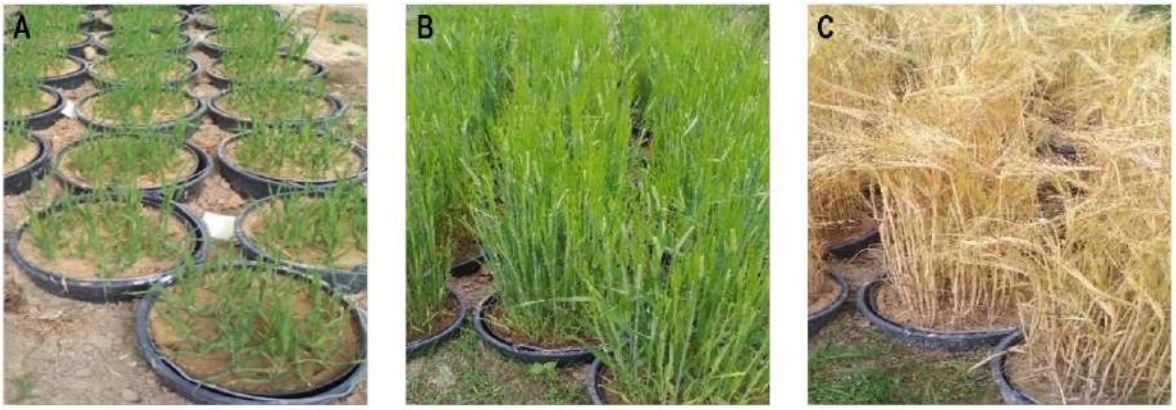

***Rysunek 9**. Zdjęcia uprawy wazonowej roślin H. vulgare w fazie (A) zaawansowanego krzewienia i (B) na początku kłoszenia w których wykonano aplikację oraz (C) w fazie pełnej dojrzałości.*

stanowiły rośliny spryskane roztworem wody Milli-Q® z 0.1% dodatkiem adiuwanta. Aplikację dolistną wykonano przy użyciu ręcznych spryskiwaczy, uprzednio skalibrowanych, podobnie jak w przypadku doświadczenia laboratoryjnego. Na czas aplikacji dolistnej donice z roślinami zostały przeniesione do zadaszonego pomieszczenia by uniknąć zanieczyszczenia sąsiadujących roślin. Po wyschnięciu oprysku, donice przeniesiono na pierwotne miejsce. W próbkach gleby po aplikacji dolistnej oznaczono całkowitą zawartość Cu. Brak znaczących różnic w zawartości Cu w analizowanych próbkach gleby wskazuje na równomierny stopień aplikacji oprysków między grupami. Ziarniaki w fazie pełnej dojrzałości (BBCH: 89) (Rys. 9C) zostały zebrane, powietrznie wysuszone i przechowywane do analiz.

3.3. Opis metod badawczych

3.3.1. Charakterystyka nano- i mikro-cząstek

Nano- i mikro-proszki Cu

Średnia wielkość i **morfologia cząstek** w postaci proszków zostały określone przy użyciu transmisyjnego mikroskopu elektronowego (ang. *transmission electron microscope*, TEM) (JEM–3010 TEM JEOL, Ltd., Japonia). **Powierzchnię właściwą** wyznaczono na podstawie adsorpcji N_2 stosując metodę BET (Brunauer-Emmett-Teller'a). **Strukturę krystaliczną** i **skład fazowy** określono wykorzystując dyfrakcję proszkową (ang. *X-ray powder diffraction,* XRD) (Empyrean, PANalytical, Holandia), używając promieniowania CuKα (λ = 1.54016 Å) przy parametrach 60 keV w zakresie 2θ = 5–95 stopni. Piki odczytane z obrazu dyfrakcyjnego XRD zostały zidentyfikowane przy użyciu bazy danych PDF-2 z Międzynarodowego Centrum Danych Dyfrakcyjnych (ang. *International Centre for Diffraction Data*, ICDD).

Roztwory wodne Cu

Roztwory przeznaczone do aplikacji dolistnej były scharakteryzowane pod kątem **potencjału zeta** i **rozkładu wielkości agregatów** z wykorzystaniem techniki dynamicznego rozpraszania światła (ang. *dynamic light scattering*, DLS) (Zetasizer 3000, Malvern, Wielka Brytania). **Stopień rozpuszczenia** nano-/ mikro-Cu oraz nano-CuO został zmierzony po uprzedniej separacji frakcji rozpuszczonych jonów Cu z roztworu poprzez ultrafiltrację z wykorzystaniem filtrów Omega Membrane 1K (Pall Corporation). Stężenie Cu^{2+} oznaczono przy użyciu optycznej spektrometrii emisyjnej ze wzbudzeniem w plazmie indukowanej (ang. *inductively coupled plasma optical emission spectrometer*, ICP–OES) (Thermo Fisher Scientific, iCAP 7200, USA).

3.3.2. Analiza próbek roślinnych [PII i PIII]

3.3.2.1. Analizy spektroskopowe liści *in situ*

Ocenie poddano **grupy funkcyjne w naskórku liścia**, ich rolę strukturalną, interakcje oraz układ makrocząstkowy ich komponentów wykorzystując spektroskopię osłabionego całkowitego odbicia w podczerwieni (ang. *Fourier transform infrared spectroscopy - attenuated total reflectance*, FT-IR/ATR) (Nicolet 6700 z przystawką Meridian Diamond ATR, Harrick) [33]. Do **zobrazowania powierzchni liści** poddanych ekspozycji na związki miedzi przed i po trawieniu HNO_3 w celu określenia stopnia internalizacji zastosowanych roztworów Cu wykorzystano skaningową mikroskopię elektronową (SEM) z systemem EDS (ang. *energy dispersive spectroscopy*) (Quanta™ 3D FEG, FEI z detektorem EDAX SDD Apollo).

3.3.2.2. Ocena dystrybucji Cu w roślinach

Całkowitą **zawartość Cu** w tkankach roślinnych (korzeniach i częściach nadziemnych) zmierzono po uprzedniej mineralizacji próbek w mieszaninie HNO_3 z 30% H_2O_2 (4:1) w mineralizatorze mikrofalowym (Milestone, ETHOS EASY) w 200°C przez 1h przy użyciu ICP–OES. W celu kontroli jakości mineralizacji, analizy przeprowadzono z wykorzystaniem certyfikowanego materiału referencyjnego (liście pomidora, NIST® SRM® 1573a). Odzysk Cu wynosił 94 ± 2%.

3.3.2.3. Analizy biochemiczne

Zawartość barwników. **Zawartość chlorofilu (a i b)** i **karotenoidów** oznaczono zgodnie z metodyką opisaną przez Nayek i in. [56] z ekstrakcją próbek za pomocą 80% (v/v) acetonu przez 30 minut w temperaturze pokojowej. Uzyskany supernatant wykorzystano do oznaczenia absorbancji chlorofilu a, chlorofilu b i karotenoidów za pomocą spektrofotometru (Lambda 40 UV–Vis, Perkin Elmer), przy długościach fal 663, 645 i 470 nm, odpowiednio.

Analiza peroksydacji lipidów. Analiza opierała się na pomiarze **zawartości aldehydu malonowego** (ang. *malondialdehyde*, MDA) zgodnie z protokołem Wessely-Szpondel [57] z wykorzystaniem 20% kwasu trichlorooctowego. Stężenia MDA odczytano z krzywej standardowej uzyskanej przy użyciu bis-dimetyloacetalu aldehydu malonowego przy długości fali 532 nm.

Zdolność do usuwania wolnych rodników została oznaczona po chemicznej ekstrakcji i trawieniu próbek *in vitro*. Analizy wykonano zgodnie z protokołem Re i in. [58], wykorzystując **ABTS** (2,2'-azobis(3-ety- lobenzotiazolino-6-sulfonian) jako źródło wolnych

rodników. Wyniki wyrażono jako równoważniki troloksu w mg na g świeżej masy.

Aktywność enzymów antyoksydacyjnych. Aktywność **dysmutazy ponadtlenkowej** (ang. *superoxide dismutase*, SOD) (E.C. 1.15.1.1), **katalazy** (ang. *catalase*, CAT) (EC 1.11.1.6) oznaczono z wykorzystaniem zestawów komercyjnych: SOD Assay Kit®, CAT Assay Kit® (Merck, Niemcy), aktywność **peroksydazy** (ang. *peroxidase*, POD) (EC 1.11.1.x) została określona z wykorzystaniem gwajakolu jako substratu reakcji zgodnie z metodyką Ippolito i in. [59], gdzie 1 jednostka utlenia 1 μmol gwajakolu na minutę przy pH 6.4 w 25°C; aktywność **reduktazy glutationowej** (ang. *glutathione reductase*, GR) (EC 1.8.1.7) oznaczono według protokołu Sikory i Świecy [60] z wykorzystaniem 100 mM buforu fosforanu sodu (pH 7.6) zawierającego 3.4 mM EDTA.

Aktywność enzymów związanych z antyoksydantami nieenzymatycznymi. **Aktywność amoniakoliazy fenyloalaniny** (ang. *phenylalanine ammonia-lyase*, PAL) (EC 4.1.3.5) oznaczono z wykorzystaniem 0.02 M L-fenyloalaniny [61]; aktywność **oksydazy polifenolowej** (ang. *polyphenol oxidase*, PPO) (EC.1.10.3.1.) została określona z wykorzystaniem katecholu jako substratu [62];

Zawartość drobnocząsteczkowych antyoksydantów. **Zawartość glutationu utlenionego** (ang. *oxidized glutathione*, GSSG) i **zredukowanego** (ang. *reduced glutathione*, GSH) oznaczono z wykorzystaniem zestawu komercyjnego (Sigma-Aldrich, Niemcy), zgodnie z instrukcją producenta;

Całkowita zawartość polifenoli (ang. *total phenolic content*, TPC). **TPC** została oznaczona po uprzedniej ekstrakcji rozpuszczalnikami (50% metanol, 60 mM HCl w 50% metanolu i 60 mM HCl w 70% acetonie) z użyciem odczynnika Folina-Ciocâlteu [63].

3.3.2.4. Analiza ekspresji genów

RNA wyizolowano ze świeżych liści z zastosowaniem TRIzolu® (Invitrogen, USA) zgodnie z instrukcją producenta. Analizy jakości i ilości materiału dokonano spektrofotometrycznie (NanoDrop 2000). Integralność RNA oceniono za pomocą elektroforezy w 2% żelu agarozowym wybarwionym bromkiem etydyny. Następnie, usunięto genomowe DNA z wykorzystaniem DNAzy I (Thermo Scientific). Reakcję odwrotnej transkrypcji przeprowadzono z wykorzystaniem komercyjnego zestawu NG dART RT kit (EURx). Uzyskane cDNA wykorzystano do oceny poziomu ekspresji wybranych genów **transporterów miedzi** (*RAN1*, *COPT5*, *PAA1*, *PAA2*), **akwaporyn** (*NIP 2;2*, *PIP 1;1*, *TIP 1;1*, *TIP 1;2*) oraz **enzymów antyoksydacyjnych** (*SOD Cu/Zn*, *SOD Fe*, *SOD Mn*, *CAT*) przy zastosowaniu reakcji real-time qPCR używając PowerUpTM SYBRTM Green Master Mix (Applied Biosystems) z wykorzystaniem specyficznych

starterów (Tab. 2). Profile termiczne reakcji oraz stężenie cDNA użyte w reakcji zostały zoptymalizowane dla każdej pary starterów. Reakcje real-time qPCR przeprowadzono na

***Tabela 2**. Sekwencje starterów użytych do reakcji qPCR [**PIII**].*

Gen	Sekwencja startera (5′ → 3′)	Numer wpisu NCBI/ Phytozome	Źródło
ADP	5'-GCGATGAATGCGGCTGAAAT-3' 5'-TCTGAATGTACCAGTGCCGC-3'	AJ508228.2	[64]
ACT	5'-AATCCACGAGACGACCTAC-3' 5'-ACCACTGAGCACGATGTT-3'	AY145451.1	[64]
GAPDH	5'-GACAGCAGGTCCAGCATCTT-3' 5'-GATCAGGTCGACAACACGGT-3'	X60343.1	[65]
COPT5	5'-AAACGAACGTCTGCAATCCC-3' 5'-CCCAAGGTGTGAATGTGTGT-3'	DK830819.1	[64]
RAN1	5'-GCATTAGCGACCTCATTAG-3' 5'-GCCTTATCTTGCTCACTAC-3'	HORVU6Hr1G 031960.1	[64]
PAA1	5'-ATGTGCTCTTGGTCTTGCCA-3' 5'-TCCCTCGCTGTGAGAAGCTA-3'	AK355848.1	[64]
PAA2	5'-TTCGCCATGACACCATCTCTT-3' 5'-CAGATCATCGGGCCCTGGTC-3'	HORVU0Hr1G 009080.5	[64]
NIP2.1	5'-ATCATCGTCACCTTCAACAT-3' 5'-CTAACCCTGCCAACTCAC-3'	AB540229.1	[65]
TIP1.1	5'-TCAGCAGGATCGCCGTGG-3' 5'-GAAGACGAAGATGAGCGTGGAG-3'	AB540221.1	[65]
TIP1.2	5'-GTCTGGGAGAACCACTGG-3' 5'-GCCGATGAAGCAGATGTC-3'	AB540226.1	[65]
PIP1.1	5'-ATCTACAACAGGGAGCAC-3' 5'-TAGGACTTGGTCTTGAATGG	AB286964.1	[65]
SOD Cu-Zn	5'-GGTGACACGACTAATGGAT-3' 5'-TGACGGACTTCATCTTCTG-3'	HORVU7Hr1G 060130.2	[42]
SOD Fe	5'-GTCTCCGAATGCTATCAATC-3' 5'-TTCTCATAATCCAGGTAGTAGG	HORVU7Hr1G 008390.6	[65]
SOD Mn	5'-CTTTGTTGGGAATTGATGTCT-3' 5'-CAGATGTTGGTCAGGTAGT-3'	HORVU2Hr1G 117740.2	[65]
CAT	5'-CACTCAACTACAGGCACAT-3' 5'-ATCATCCAAGAGGCACTTC-3'	HORVU7Hr1G 121700.1	[42]

QuantStudio™ 3 Real-Time PCR System (Applied Biosystems™). Uzyskane dane zostały znormalizowane przy wykorzystaniu genów referencyjnych (*ACT*, *ADP*, *GAPDH*). Relatywny poziom ekspresji został określony wykorzystując metodę $2^{-\Delta\Delta Ct}$. Analiza krzywej topnienia została przeprowadzona w celu potwierdzenia specyficzności powstałych

produktów. Wyniki zostały przeanalizowane z wykorzystaniem dedykowanego programu ThermoFisher Cloud.

3.3.3. Analizy ziarniaków [PIV]

3.3.3.1. Zawartość mikro i makroelementów

Powietrznie wysuszone nasiona jęczmienia jarego zmielono i zmineralizowano w mieszaninie HNO_3 z 30% H_2O_2 (4:1) w mineralizatorze mikrofalowym (Milestone, ETHOS EASY) w 200°C przez 1h. Po ostudzeniu, próbki przefiltrowano (0,45 μm, PTFE), a **zawartość Cu, Zn, Mn, Fe, Ca, Mg, K** oznaczono przy użyciu ICP–OES [42]. Analizy przeprowadzono z wykorzystaniem certyfikowanego materiału (mąka kukurydziana, INCT-CF-3, ICHTJ) jako kontrolę jakości mineralizacji próbek. Odzysk wybranych mikroelementów mieścił się w zakresie 93,0-98,4% (Cu, Zn, Mn, Fe) i 87,4-95,3% (Ca, Mg, K).

3.3.3.2. Wartość odżywcza

Zawartość białka oznaczono metodą Bradforda z wykorzystaniem albumin, globulin, prolamin i gluteiny jako standardy białka [66]. **Strawność białka** *in vitro* została oznaczona z wykorzystaniem metody Minekus i in. [67] z użyciem symulowanego układu pokarmowego. Do oceny **całkowitej zawartości błonnika pokarmowego** zastosowano metodę AOAC 991.43 z wykorzystaniem zestawu komercyjnego (Total Dietary Fiber Assay Kit) [68].

3.3.3.3. Analizy biochemiczne

Analizę **TPC** przeprowadzono po ekstrakcji ziarniaków różnymi rozpuszczalnikami (50% metanol, 60 mM HCl w 50% metanolu i 60 mM HCl w 70% acetonie) z użyciem odczynnika Folina-Ciocâlteu [63]. **Całkowitą zawartość antocyjanin** (ang. *Total anthocyanin content*, TAC) oznaczono z wykorzystaniem metody Lee i in. [69], z pomiarem absorbancji przy długości fal 520 i 700 nm w przeliczeniu na cyjano-3-glukozyd. **Całkowitą zawartość flawonoidów** (ang. *total flavonoid content*, TFC) oznaczono z wykorzystaniem 80% etanolu, 10% Al $(NO_3)_3$ i 1M octanu potasu. Absorbancję próbek zmierzono przy długości fali 415 nm, a wartość TFC została wyrażona w postaci mg odpowiedników kwercetyny na g suchej masy próbki. Do oznaczenia **zawartości tanin** (ang. *content of condensed tannin*, CT) wykorzystano 4% roztwór waniliny w metanolu oraz 35% HCl [70]. **Całkowita zawartość flawanoli** (ang. *total flavanol content*, TFoC) została oznaczona metodą Arancibia-Avila i in. [70] z wykorzystaniem p-aldehydem 4-(dimetyloamino) -cynamonowego (DMACA, 0,1 % w 1 M HCl w MeOH).

Zdolność do usuwania wolnych rodników została określona po chemicznej ekstrakcji i trawieniu *in vitro* próbek z zastosowaniem następujących metod: **ABTS** oznaczono zgodnie z protokołem Re i in. [58], a uzyskane wyniki wyrażono w równoważnikach troloksu; analizy z wykorzystaniem **DPPH•** (rodnik 2,2-difenylo-1-pikrylohydrazylowy) przeprowadzono zgodnie z metodą Brand-Williams'a i in. [71], gdzie wyniki wyrażono w równoważnikach troloksu; **zdolność do redukowania jonów żelaza** (ang. *ferric reducing antioxidant power,* FRAP) oznaczono zgodnie z protokołem wg Hanafy'iego i in. [72], a wyniki wyrażono w równoważnikach troloksu; **zdolność do redukcji jonów miedzi** (ang. *cupric reducing antioxidant capacity,* CUPRAC) przeprowadzono zgodnie z protokołem Oztürk i in. [73], gdzie wynik wyrażono jako ekwiwalent kwercetyny; **zdolność przenoszenia rodników hydroksylowych** (ang. *hydroxyl radical antioxidant capacity,* HORAC) oznaczono według metody opisanej przez Denev i in. [74], a wynik wyrażono w równoważnikach kwasu galusowego; **zdolność do chelatowania** (ang. *chelating power*, ChP) jonów metali przejściowych zmierzono wykorzystując metodę opracowaną przez Guo i in. [75].

3.3.4. Analizy statystyczne

Wszystkie analizy statystyczne wykonano z wykorzystaniem pakietu oprogramowania Statistica 13.1. Różnice pomiędzy badanymi grupami zostały ocenione z wykorzystaniem jedno- i dwukierunkowej analizy wariancji (ANOVA). Następnie przeprowadzono testy wielokrotnego porównania post hoc Dunnett'a, Tukey'a lub test Kruskala-Wallisa ($p < 0,05$), po których wykonano wielokrotne porównanie średnich rang dla par (PMCMR) ($p < 0,05$). Przeprowadzono analizę głównych składowych (ang. *Principal component analysis*, PCA) w celu ustalenia różnic i podobieństw pomiędzy próbami. Zmienne przeanalizowano również przy użyciu korelacji Pearsona.

4. Omówienie wyników i dyskusja

4.1. Charakterystyka roztworów Cu

Analiza literatury w zakresie zastosowania nanotechnologii w produkcji roślinnej, przedstawiona w pracy przeglądowej [**PI**] wykazała, że oddziaływanie ENPs na rośliny jest zależne od wielu czynników, w tym od fizyko-chemicznych właściwości ENPs, takich jak średnica cząstek, wielkość powierzchni właściwej, potencjał zeta (ζ), rozkład wielkości cząstek, rozpuszczalność, itp. [76,77]. Z tego względu roztwory ENPs przeznaczone do aplikacji dolistnej w doświadczeniu laboratoryjnym i wazonowym zostały poddane fizyko-chemicznej charakterystyce.

4.1.1. Roztwory użyte w doświadczeniu laboratoryjnym

Zarówno zdjęcia TEM, jak i analiza rozkładu wielkości cząstek wykazała znaczącą tendencję nano-Cu do tworzenia agregatów w roztworach wodnych (Rys. 10). Średnia wielkość agregatów nano-Cu dla stężenia 100 mg L^{-1} wynosiła 248,8 ± 6 nm, pomiar agregacji dla 10-krotnie wyższego stężenia ENPs nie był możliwy ze względu na zbyt dużą wielkość agregatów i ich szybką sedymentację. Potencjał ζ roztworów nano- Cu przy stężeniach 100 i 1000 mg L^{-1} wynosił odpowiednio -14,6 i -19,6 mV. Przeprowadzone analizy rozpuszczalności w roztworach nano-Cu potwierdziły słabą rozpuszczalność ENPs na bazie miedzi (0,29-0,65 mg L^{-1}, co stanowiło mniej niż 1% zastosowanej puli Cu) [**PII-PIII**]. Niższy stosunek rozpuszczonego Cu w roztworze o stężeniu 1000 mg L^{-1} w porównaniu do 100 mg L^{-1} mógł wynikać m.in. ze zwiększonej agregacji nanocząstek wraz ze wzrostem stężenia [78].

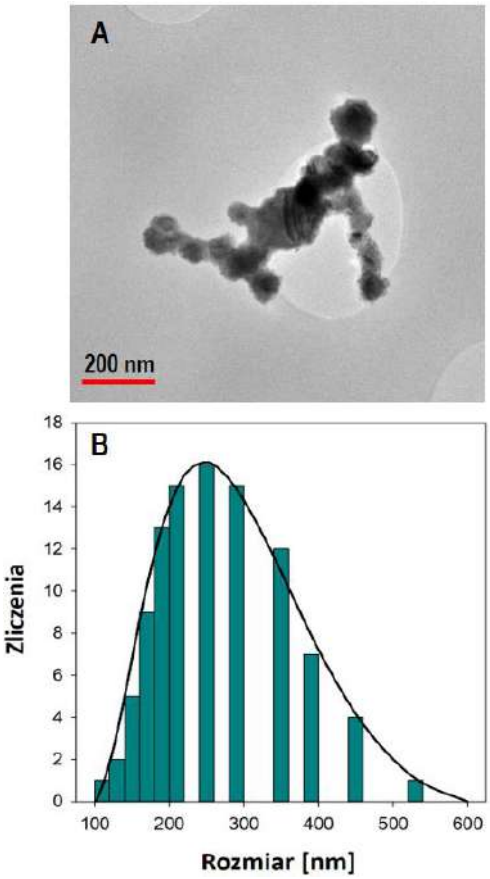

Rysunek 10. *Charakterystyka wodnego roztworu nano-Cu w stężeniu 100 mg L^{-1} (A) obraz TEM oraz (B) rozkład wielkości agregatów* ***[PII, PIII].***

4.1.2. Roztwory użyte w doświadczeniu wazonowym

Wyniki analiz roztworów nano-Cu, nano-CuO oraz mikro-Cu przedstawiono na Rysunku 11. ENPs w roztworach tworzyły agregaty, których średnia wielkość była 14- (nano-Cu) i 9,6-krotnie (nano-CuO) większa od pierwotnej wielkości cząstek. Średni rozmiar agregatów mikro-Cu był ponad 10 razy większy niż ENPs [**PIV**]. Według Landa i in. [22], stopień i wielkość agregacji cząstek mógł następnie warunkować poziom stężenia Cu^{2+} uwolnionych z nano- i mikrocząstek Cu (Rys. 11). Wyższe stężenia Cu^{2+} w roztworach ENPs (0,4-0,5 mg L^{-1}) względem mikro-Cu (0,1 mg L^{-1}) mogą także wynikać z ich większej powierzchni właściwej, a przez to reaktywności. Podobną tendencję obserwowanego w badaniach innych autorów [22,79,80].

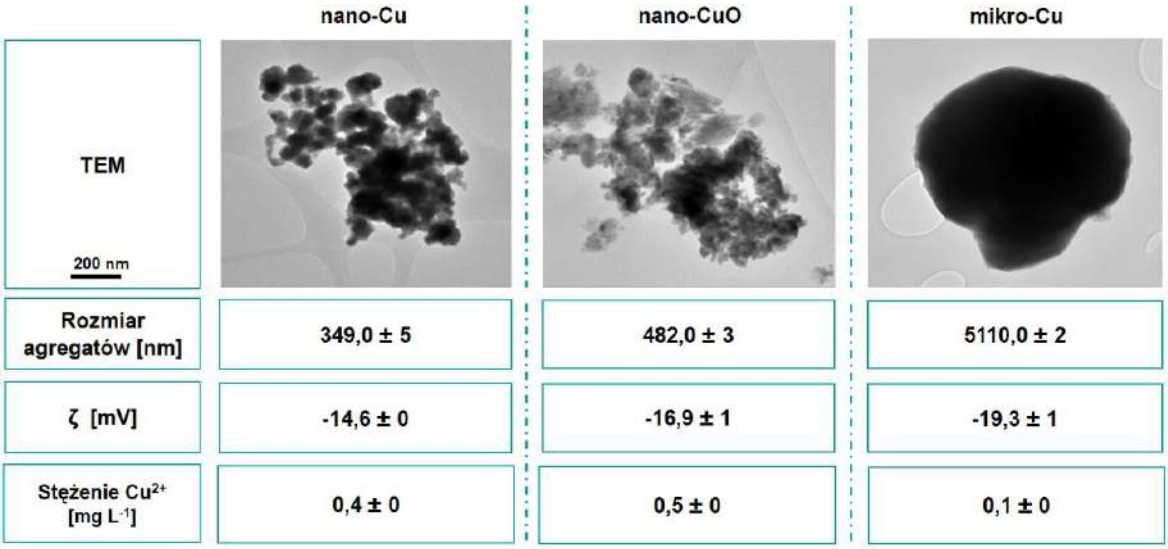

Rysunek 11. *Charakterystyka roztworów nano-Cu, nano-CuO i mikro-Cu o stężeniu 500 mg L^{-1}* ***[PIV]*** *pod względem rozmiaru agregatów, potencjału zeta oraz stężenia rozpuszczonych jonów Cu.*

4.2. Analiza *in situ* interakcji związków Cu z liśćmi *H. vulgare*

Analiza oddziaływania ENPs z rośliną w miejscu ekspozycji była naturalnym krokiem oceny potencjału nawozowego nano-Cu w zakresie ich absorpcji i internalizacji. W ramach tego etapu wykonano mikroskopowe obrazowanie i analizę chemizmu liści, a także analizy całkowitej zwartości Cu w częściach nadziemnych roślin.

Istotny wzrost zawartości Cu w częściach nadziemnych (liście + łodyga) jęczmienia (~4,5-krotny) po 1 dniu zaobserwowano jedynie przy zastosowaniu najwyższej dawki Cu (1000 mg L^{-1}), niezależnie od zastosowanej formy miedzi (Rys. 12A) [**PII**]. Natomiast po 7 dniach wykazano proporcjonalny wzrost zawartości Cu w nadziemnych tkankach roślin wraz ze wzrostem zastosowanej dawki związków miedzi ($p < 0,05$) (Rys. 12B). Podobne obserwacje stwierdzano w dostępnej literaturze naukowej porównującej zawartość Cu

w liściach *Ocimum basilicum* L. [81] czy *Lactuca sativa* L. [34] po dolistnej aplikacji ENPs zawierających Cu. Jednakże, zauważono że całkowita zawartość Cu w tkankach

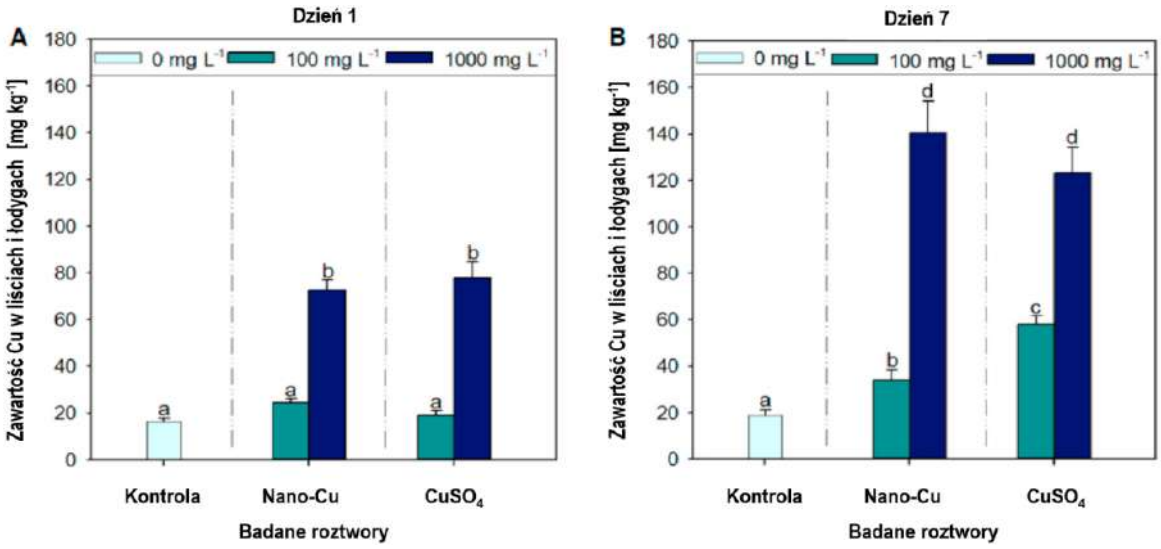

Rysunek 12. *Całkowita zawartość Cu w częściach nadziemnych H. vulgare (liście + łodygi) po aplikacji nano-Cu i $CuSO_4$ (100 i 1000 mg L^{-1}). Słupki błędów przedstawiają błąd standardowy (SE, n = 3 próby). Różne litery oznaczają istotne różnice między zabiegami (test Tukey'a, p < 0,05)* ***[PII].***

nadziemnych roślin eksponowanych na niższą dawkę nano-Cu była aż o 76% niższa niż u roślin traktowanych analogiczną dawką $CuSO_4$ (Rys. 12B) [**PII**]. Mogło to świadczyć o wolniejszym pobieraniu Cu przez rośliny, gdy jego źródłem było nano-Cu w wyniku wcześniej opisanego wolnego uwalniania Cu^{2+} oraz powstawania agregatów ENPs [81]. Jednakże, nie można wykluczyć, że chloroza (zmiany w fenotypie omówione zostały w dalszej części pracy) obserwowana u roślin po oprysku wysokim stężeniem $CuSO_4$ (1000 mg L^{-1}) nie wpłynęła negatywnie na zdolność roślin do pobierania i transportowania Cu.

Należy nadmienić, że po wykonaniu oprysku nano-Cu, na powierzchni liści dostrzegalne były agregaty ENPs (Rys. 13A) [**PII, PIII**]. Jak wykazały analizy SEM-EDS (Rys. 13C, E), pomimo zastosowania wstępnego trawienia próbek w celu usunięcia nano-Cu z powierzchni liści, nie udało się tego całkowicie dokonać. Mogło to spowodować przeszacowanie zawartości Cu w próbkach traktowanych nano-Cu. Obserwowana tendancja nano-Cu do tworzenia agregatów na powierzchni liści może stanowić jednak zaletę jako długotrwałe źródło Cu [39]. W badaniach Zhao i in. [39] wykazano podobną agregację ENPs na powierzchni liści *Zea mays*, co przypuszczalnie wynikało z uwięzienia nano-$Cu(OH)_2$ w kutykuli oraz innych strukturach powierzchniowych liści. Odmienną reakcję obserwowano u roślin eksponowanych na $CuSO_4$ (Rys. 13D, F), co wskazywało na sukcesywne pobieranie całej puli jonów Cu przez roślin jęczmienia jarego. Na podstawie różnic pomiędzy całkowitą zawartością Cu w liściach pomiędzy 1-szym a 7-mym dniem po podaniu 100 mg L^{-1} nano- Cu, nawet po uwzględnieniu błędu pomiarowego spowodowanego obecnością

agregatów nanocząstek, możemy stwierdzić pobieranie miedzi przez rośliny. Z kolei, podobne zawartości Cu w korzeniach grupy kontrolnej i roślin po aplikacji nano-Cu i $CuSO_4$ świadczy o braku translokacji Cu (niezależnie od formy) do części podziemnych. Fakt ten mógł wynikać z krótkiego czasu ekspozycji (7 dni) oraz niskiej mobilności Cu, wynikającej z jej silnego wiązania przez bioligandy.

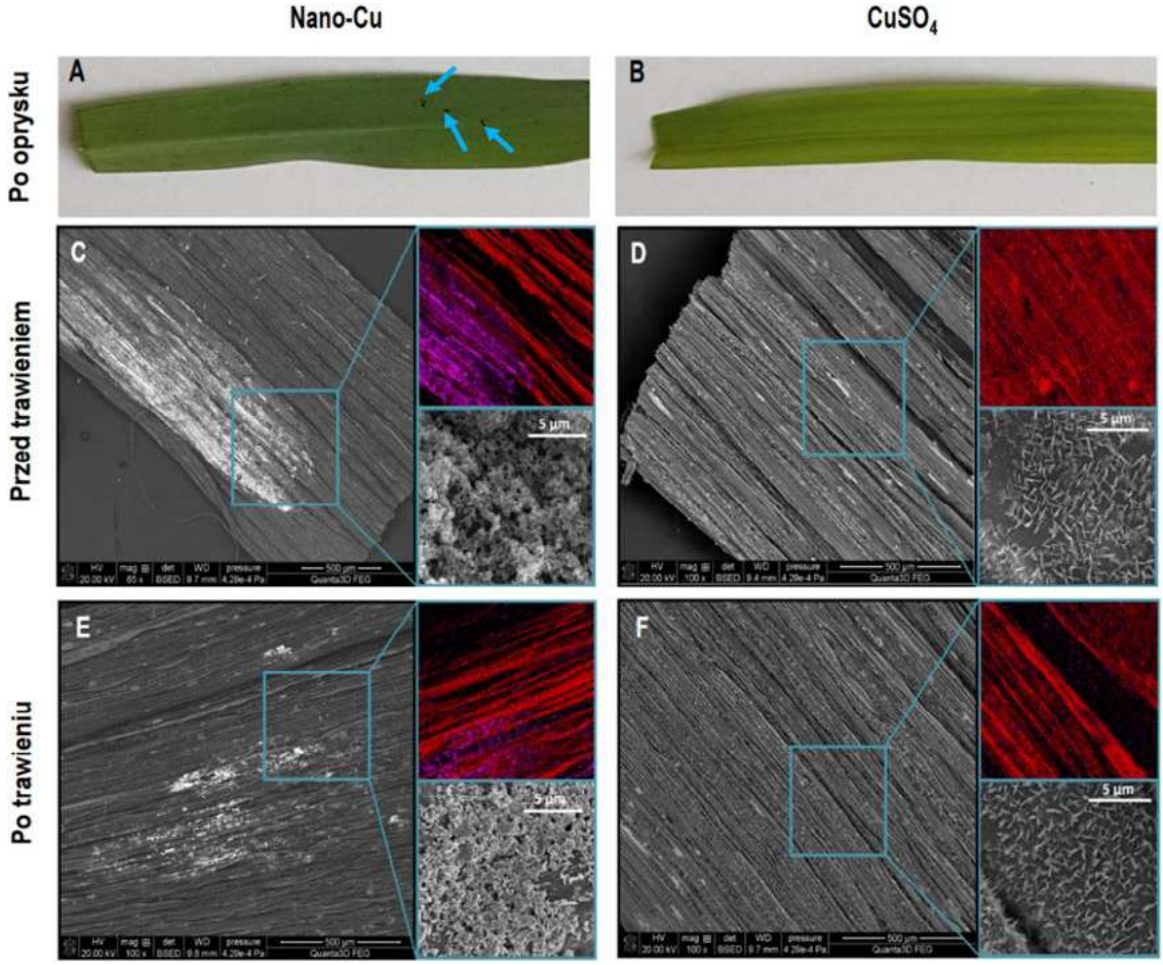

***Rysunek 13**. Zdjęcie liści H. vulgare po oprysku (A) nano-Cu i (B) $CuSO_4$ o stężeniu 100 mg L^{-1} 7 dni po aplikacji dolistnej; Analizę internalizacji Cu przeprowadzono z wykorzystaniem SEM-EDS (C, D, E, F). Zdjęcia wykonano przed (C, D) i po (E, F) wytrawieniu liści H. vulgare poddanych ekspozycji na nano-Cu i $CuSO_4$ (w stężeniu 100 mg L^{-1}) w celu usunięcia cząstek miedzi. Różowy kolor odpowiada obecności Cu [**PII, PIII**].*

Uwzględniając, że dolistna aplikacja zastosowanych roztworów miedzi może wpływać na chemizm powierzchni liści, przeprowadzono analizę FT-IR/ATR próbek roślinnych (Rys. 14) [**PII**]. Badanie to wykazało, że dodatek surfaktantu do badanych roztworów Cu znacząco obniżył pasma $-CH_3$ i $-CH_2-$ (długołańcuchowe woski alifatyczne) oraz C=O (kutyna) względem próbek kontrolnych (woda destylowana). Wskazuje to na istotny wzrost hydrofilności powierzchni liści, co może wynikać z degradacji komórek kutykuli przez surfaktant [82]. Uwzględniając rolę kutykuli w ograniczaniu przenikania

substancji obcych do wnętrza roślin [45], tak znacząca redukcja warstwy kutykuli mogła potencjalnie ułatwiać dyfuzję ENPs do wewnętrznej warstwy liści [45].

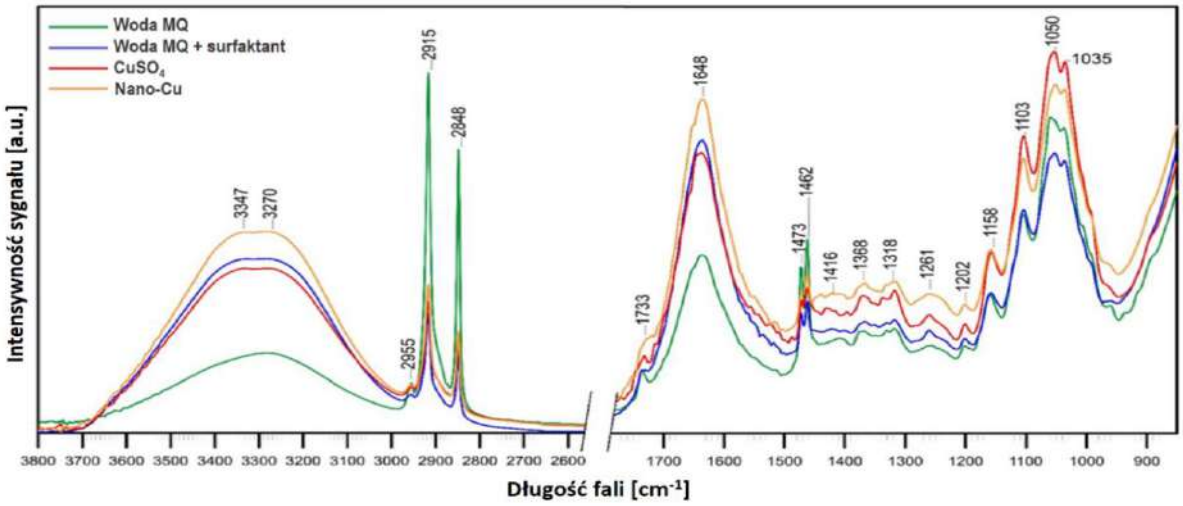

***Rysunek 14**. Widma FT IR/ATR analizowanych próbek. Liście H. vulgare poddano działaniu nano- Cu i $CuSO_4$ (w stężeniu 100 mg L^{-1}) przez 7 dni [**PII**].*

4.3. Ocena odpowiedzi roślin jęczmienia jarego na dolistną aplikację związków miedzi w zależności od formy i stężenia w warunkach deficytu Cu

Zarówno niedobór jak i nadmiar Cu wywołują u roślin kaskadę reakcji w odpowiedzi na stres, np. zmiany aktywności enzymów antyoksydacyjnych [83,84]. Wynika to m.in. z silnych właściwości oksydoredukcyjnych miedzi [83] oraz jej roli jako kofaktora ważnych procesów metabolicznych [13]. Dlatego też podanie związków miedzi w celu przywrócenia homeostazy potencjalnie może ograniczyć negatywny wpływ wywołany wzrostem w warunkach deficytu Cu [83]. Jednakże, o ile dotychczasowe badania wskazują na zależności między drogą podania, dawką i źródłem Cu na reakcje roślin na podane związki Cu (zarówno pozytywne/negatywne) [25,85,86], brak było informacji odnośnie efektów aplikacji ENPs na bazie miedzi roślinom w okresie niedoboru tego mikroelementu.

4.3.1. Wpływ ekspozycji związków miedzi na wzrost roślin

Długotrwały wzrost badanych roślin w warunkach deficytu Cu skutkował wystąpieniem charakterystycznych objawów niedoboru Cu u roślin [10], m.in. chlorozy oraz deformacji i usychania końcówek młodych liści tzw. „choroby nowin" (Rys. 15A) [**PII, PIII**]. Po 1-no dniowej ekspozycji na nano-Cu i $CuSO_4$ nie zaobserwowano widocznych zmian w fenotypie roślin, podczas gdy po 7 dniach odnotowano postępującą chlorozę i zmiany nekrotyczne liści roślin eksponowanych na 1000 mg L^{-1} $CuSO_4$ (Rys. 15B) [**PII,**

PIII]. Efekt ten mógł być spowodowany nadmiarem Cu^{2+}, których cała pula została uwolniona z $CuSO_4$ [85].

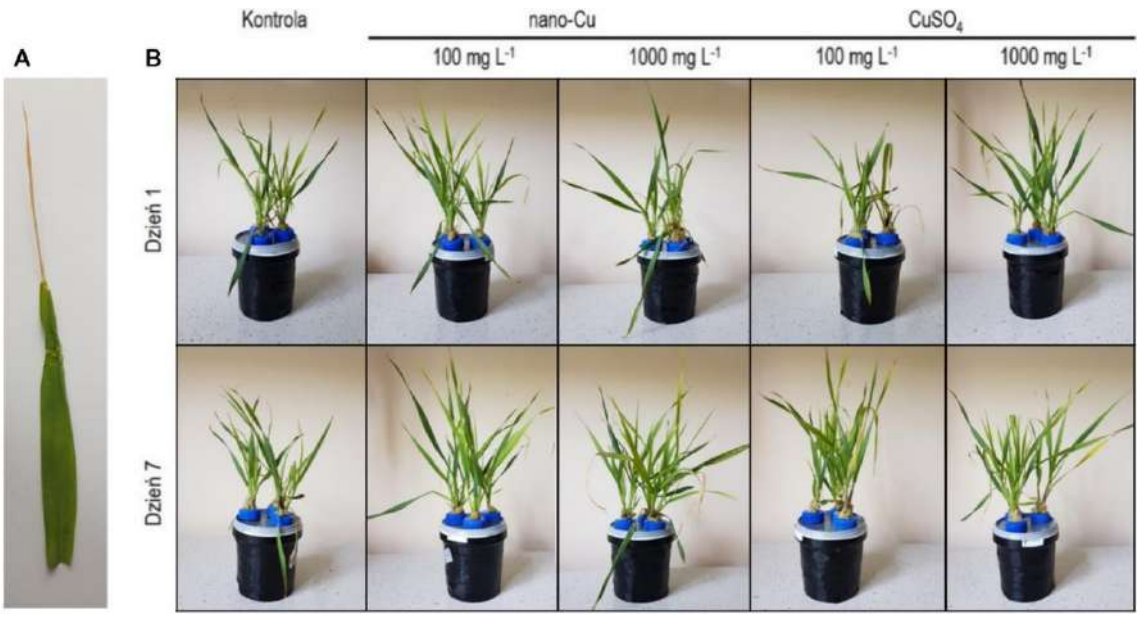

***Rysunek 15**. Zdjęcie liścia H. vulgare (A) z charakterystycznymi objawami niedoboru miedzi wykonane przed aplikacją związków miedzi. Zdjęcia roślin jęczmienia jarego (B) wykonane po 1 i 7 dniach od dolistnej ekspozycji na nano- Cu i $CuSO_4$ (w stężeniu 100 i 1000 mg L^{-1}) [**PII, PIII**].*

Aplikacja zarówno nano-Cu jak i $CuSO_4$ zwiększyła poziom suchej masy nadziemnej części roślin *H. vulgare* po 1-no i 7-mio dniowej ekspozycji (Tab. 3) [**PII**]. Po 1 dniu od aplikacji zauważono, że sucha masa nadziemnych części roślin opryskanych związkami Cu była o 7-22% większa względem roślin z grupy kontrolnej (Tab. 3), podczas gdy nie zauważono znaczących zmian przeprowadzonych zabiegów na suchą masę korzeni (Tab. 3). Z kolei, po 7 dniach, stwierdzono dodatnią zależność między zastosowaną dawką Cu, a suchą masą nadziemnych części roślin. Należy jednak zaznaczyć, że ekspozycja na $CuSO_4$ stymulowała przyrost biomasy w większym stopniu (89-115%) niż nano-Cu (22,7-85%) w porównaniu do roślin kontrolnych. Uzyskane wyniki pozwalają przypuszczać, że zaobserwowany przyrost biomasy roślin wynikał bezpośrednio z dostarczenia Cu roślinom cierpiącym na jego niedobór. Ponadto, tak szybki przyrost masy po aplikacji dolistnej Cu mógł wynikać ze zwiększonego zapotrzebowania na ten pierwiastek podczas fazy krzewienia [12]. Przeprowadzone badania wykazały, że biomasa korzeni wzrosła adekwatnie wraz ze wzrostem zastosowanych dawek nano-Cu (19,5-46,2% w stosunku do kontroli), podczas gdy odwrotny trend zaobserwowano dla zabiegu z $CuSO_4$ (120-82%), pomimo braku translokacji miedzi do tych partii roślin.

***Tabela 3**. Wpływ nano-Cu i $CuSO_4$ (w stężeniu 100 i 1000 mg L-1) na suchą masę korzeni oraz części nadziemnych (pędów i liści) H. vulgare. Średnie, po których następują różne litery, oznaczają istotne różnice między zabiegami (test Tukey'a, $p < 0,05$) [**PII**].*

Roztwór	Stężenie [mg L^{-1}]	Sucha masa [mg]	
		Korzenie	Łodygi + Liście
		Dzień 1	
Kontrola	-	26,10±1,1[a]	98,72±2,2[a]
Nano-Cu	100	28,42±1,3[a]	105,81±1,5[b]
	1000	25,73±1,7 [a]	106,34±3,1[b]
$CuSO_4$	100	29,50±1,3[a]	107,10±1,1[b]
	1000	26,50±1,5[a]	120,61±11,0[c]
		Dzień 7	
Kontrola	-	45,21±0,9[a]	102,73±1,4[a]
Nano-Cu	100	54,00±1,8[b]	126,09±0,9[b]
	1000	66,10±1,0[c]	190,24±0,8[c]
$CuSO_4$	100	99,50±0,8[e]	192,65±1,5[c]
	1000	81,70±1,6[d]	220,24±1,4[d]

4.3.2. Analizy biochemiczne

Zawartości chlorofilu i karotenoidów są ważnymi wskaźnikami intensywności fotosyntezy, stresu i stanu odżywienia roślin [55]. Przeprowadzone analizy wykazały brak istotnych zmian w zawartości barwników fotosyntetycznych po 1 dniu ekspozycji roślin na Cu, niezależnie od podanej formy i dawki [**PII**]. W przypadku zawartości chlorofilu b i karotenoidów podobny trend utrzymał się także po 7 dniach po oprysku. Wykazano natomiast znaczący spadek zawartości chlorofilu a u roślin poddanych działaniu $CuSO_4$ w dawkach 100 i 1000 mg L^{-1} (14,2% i 24,7%, odpowiednio) w porównaniu do roślin kontrolnych oraz obu dawek nano-Cu [**PII**]. Wyniki te są zgodne z obserwowaną chlorozą liści u roślin eksponowanych na sole miedzi (Rys. 15).

Według dostępnej literatury, zarówno deficyt jak i nadmiar Cu mogą indukować stres oksydacyjny w wyniku zaburzenia równowagi w produkcji reaktywnych form tlenu (ang. *reactive oxygen species*, ROS) [35,87]. Nadprodukcja ROS może wywoływać uszkodzenia roślin na poziomie molekularnym poprzez m.in. utlenianie lipidów, białek, pigmentów czy kwasów nukleinowych [22]. W celu określenia odpowiedzi roślin na zastosowane związki miedzi, w pierwszej kolejności analizie poddano zawartość MDA, jako wskaźnika peroksydacji lipidów (Rys. 16A) [**PII**]. Po 1-szym dniu zastosowane roztwory

Cu spowodowały istotne zmiany w zawartości MDA jedynie przy stężeniu 1000 mg L^{-1} nano-Cu (spadek o 29%) i $CuSO_4$ (wzrost o 56%). Po dłuższej ekspozycji, stwierdzono podwyższoną zawartość MDA jedynie u roślin wystawionych na działanie $CuSO_4$, podczas gdy nano-Cu nie miała wpływu na ten parametr. Taka reakcji roślin mogła wynikać z nagłego dostarczenie dużej puli Cu^{2+} z $CuSO_4$, co doprowadziło do peroksydacji lipidów [88]. Ponadto, odnotowany wzrost pojemności antyoksydacyjnej wyrażonej wskaźnikiem ABTS jedynie pod wpływem najwyższej dawki $CuSO_4$ (o 157,4%) w porównaniu do roślin kontrolnych po 1-szym dniu może potwierdzać negatywną reakcję roślin na ekspozycję pełnej puli Cu^{2+} (Rys. 16B).

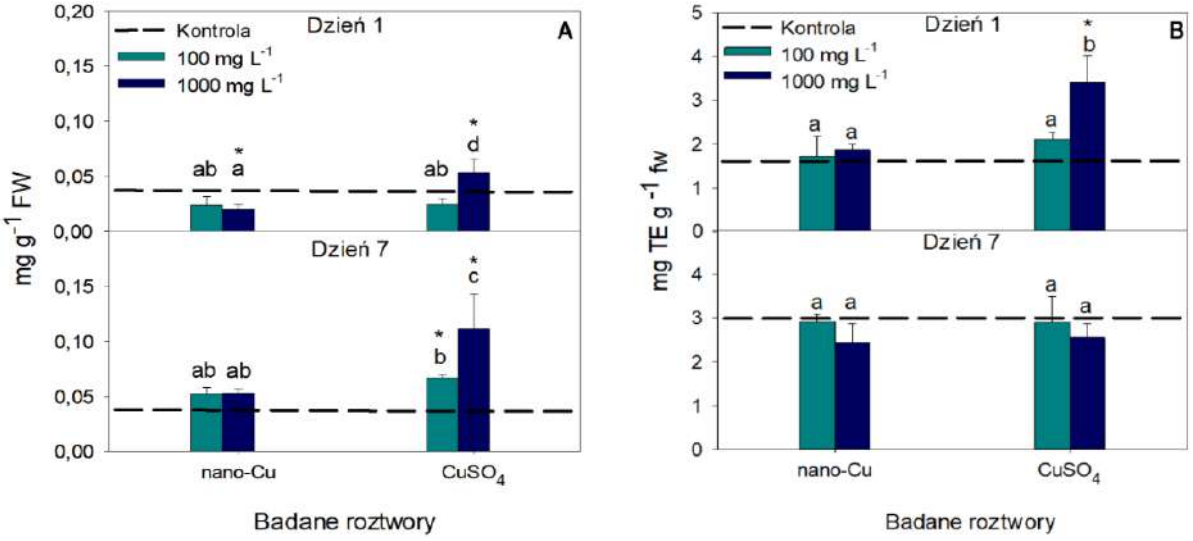

Rysunek 16. *Zawartość malondialdehydu (MDA) (A) oraz zdolność antyoksydacyjna (ABTS) (B) w roślinach H. vulgare eksponowanych na nano-Cu i $CuSO_4$ w stężeniu 100 i 1000 mg L^{-1} przez 1 i 7 dni. Słupki błędów reprezentują błąd standardowy (SE, n=3 próby). Gwiazdki wskazują na istotną różnicę między próbami nietraktowanymi i traktowanymi (test Duncana, $p < 0,05$). Różne litery wskazują na istotne różnice między zabiegami (test Tukey'a, $p < 0,05$) [**PII**].*

W następnym etapie badań, przeanalizowano poziom aktywności/zawartości antyoksydantów enzymatycznych i nieenzymatycznych, które odpowiadają za konwersję ROS do mniej toksycznych form lub ich całkowitą neutralizację [85,89]. Analiza aktywności badanych antyoksydantów pod wpływem zastosowanych związków Cu pozwoliła na (i) zbadanie ich roli w łagodzeniu stresu oksydacyjnego spowodowanego niedoborem Cu, (ii) ocenę potencjalnego wpływu fitotoksycznego wynikającego z nadmiaru Cu^{2+}/obecności nanocząstek [**PII**]. Spośród 4 badanych enzymów, dolistna aplikacja związków Cu istotnie zmieniła aktywność jedynie SOD i GR po 1-dniowej ekspozycji (Rys. 17). W przypadku SOD, wykazano blisko 1,7-krotny spadek aktywności enzymu pod wpływem niskiej dawki obu związków Cu. Jednocześnie, ekspozycja na 1000 mg L^{-1} Cu, niezależnie od formy miedzi, spowodowała aż 9-krotne obniżenie aktywności enzymu SOD u roślin

w porównaniu do roślin kontrolnych. Biorąc pod uwagę, że SOD stanowi pierwszą linię obrony przed stresem oksydacyjnym (kataliza $O_2^{\bullet-}$ do H_2O_2 i O_2), zmiana jego aktywności jest kluczowa dla zachowania równowagi wewnątrzkomórkowej m.in. w odpowiedzi na

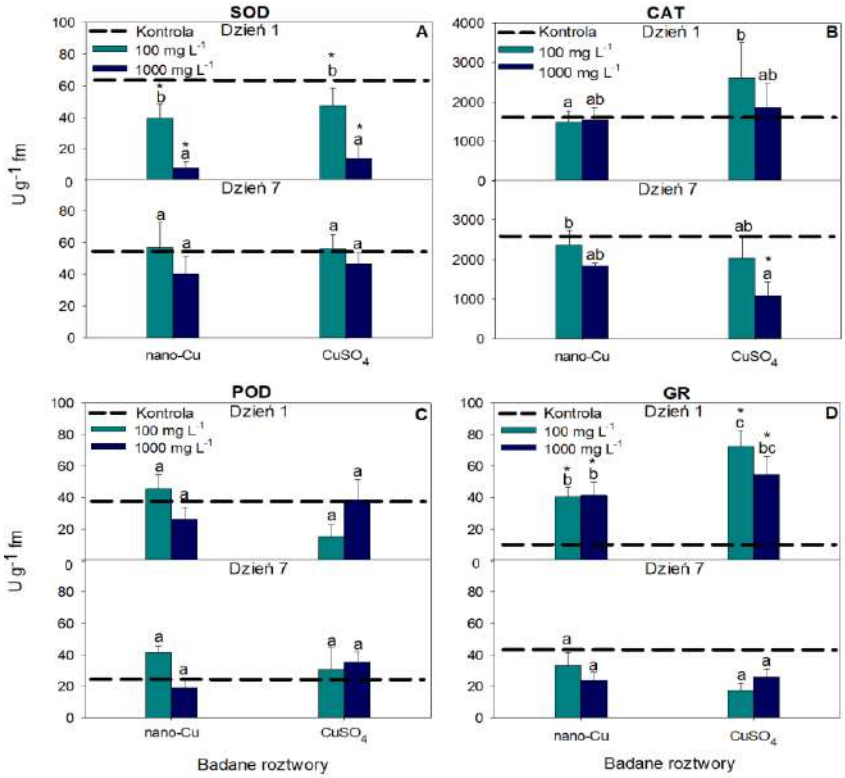

***Rysunek 17**. Aktywność SOD (A), CAT (B), POD (C), GR (D) w H. vulgare pod wpływem działania nano-Cu i $CuSO_4$ (100 i 1000 mg L^{-1}) po 1 i 7 dniach ekspozycji. Słupki błędów reprezentują błąd standardowy (SE, n=3 próby). Gwiazdki wskazują na istotną różnicę między próbami nietraktowanymi i traktowanymi (test Duncana, $p < 0,05$). Różne litery wskazują na istotne różnice między zabiegami (test Tukey'a, $p < 0,05$) [**PII**].*

stres związany z deficytem Cu [83]. Mimo, że jedna z izoform tego metaloenzymu (SOD Cu-Zn) w centrach aktywnych zawiera miedź i dostarczenie tego metalu powinno skutkować szybkim przywróceniem aktywności SOD, to zaobserwowana redukcja enzymu mogła być związana z wybuchem tlenowym w odpowiedzi na silny stres wywołany obecnością obcych cząstek (ENPs) [90] lub toksycznym stężeniem Cu^{2+} ($CuSO_4$) u roślin po długotrwałym okresie niedoboru Cu [85]. Pomimo zaangażowania zarówno enzymu CAT, jak i POD do konwersji H_2O_2 do O_2 oraz H_2O [85], nie wykazano istotnych różnic w poziomie aktywności między roślinami traktowanymi i kontrolnymi ($p > 0,05$) pod kątem aktywności tych enzymów po 1-nym dniu (Rys. 17B,C). Brak zmian aktywności CAT i POD po krótkotrwałej ekspozycji mógł wynikać z opóźnionej lub gatunkowo/odmianowej specyficznej odpowiedzi enzymatycznej roślin [85]. Po 7 dniach od ekspozycji poziom aktywności wszystkich opisywanych enzymów zrównał się z poziomem roślin kontrolnych

z wyjątkiem roślin poddanych ekspozycji na wysokie stężenie $CuSO_4$ (60% redukcja aktywności względem kontroli) (Rys. 17B).

Brak spodziewanego wzrostu aktywności enzymów antyoksydacyjnych mógł być także związany z indukcją innych mechanizmów obronnych rośliny, szczególnie związanych z niskocząsteczkowymi antyoksydantami jak glutation czy polifenole. Znaczący wzrost aktywności GR (Rys. 17D) – enzymu odpowiedzialnego za redukcję GSSG do GSH [91] – już po 1-szym dniu sugeruje, że podanie związków Cu aktywowało szlaki związane z gluationem. Oba stężenia nano-Cu spowodowały około 3,3-krotny wzrost aktywności GR, jednak $CuSO_4$ w jeszcze większym stopniu zwiększył aktywność enzymu tego enzymu w porównaniu do roślin nietraktowanych związkami Cu ($p < 0,05$). Dotychczas,

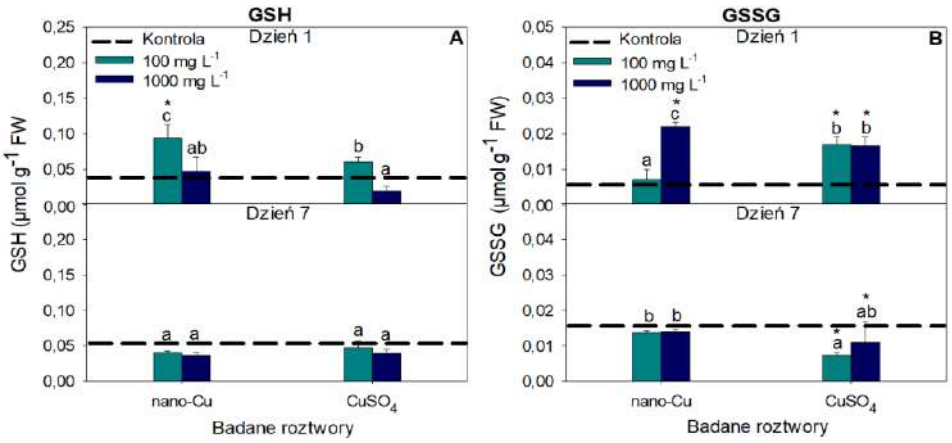

***Rysunek 18**. Wpływ nano-Cu i $CuSO_4$ (w stężeniu 100 i 1000 mg L^{-1}) po 1 i 7 dniach ekspozycji na zawartość glutationu w formie zredukowanej (GSH) (A) i utlenionej (GSSG) (B) w liściach jęczmienia. Słupki błędów reprezentują błąd standardowy (SE, n=3 próby). Gwiazdki wskazują na istotną różnicę między próbami nietraktowanymi i traktowanymi (test Duncana, $p < 0,05$). Różne litery wskazują na istotne różnice między zabiegami (test Tukey'a, $p < 0,05$) [**PII**].*

podwyższony poziom GR obserwowano m.in. u roślin pod wpływem ekspozycji na metale ciężkie, gdzie GR umożliwia utrzymanie puli GSH (Rys. 18) na poziomie umożliwiającym skuteczne zwalczanie ROS, a także chelatację jonów metali [91]. Dlatego znaczny wzrost aktywności enzymu GR pod wpływem $CuSO_4$ mógł świadczyć o nadmiarowych stężeniach Cu^{2+} w komórkach roślinnych i generowaniu ROS [91]. Natomiast uwzględniając niski poziom uwolnionych jonów miedzi z nano-Cu, zaobserwowany efekt mógł być przejawem odpowiedzi obronnej roślin na kombinację obecności obcych cząstek i Cu^{2+}. Warto zaznaczyć, że mimo relatywnie niskiego stężenia jonów Cu w przygotowanych roztworach, nano-Cu po dolistnej aplikacji mogły podlegać transformacjom zarówno na powierzchni liści (np. pod wpływem wilgotności i światła) jak i biotransformacjom wewnątrz roślin, co mogło skutkować zwiększonym uwalnianiem jonów Cu [92]. Analiza zawartości GSH i GSSG wykazała, że jedynie ekspozycja na 100 mg L^{-1} nano-Cu spowodowała wzrost puli

GSH (o 102%) w roślinach po 1 dniu ($p < 0,05$) (Rys. 18). Ze względu na swoją rolę w neutralizowaniu ROS i immobilizowaniu jonów metali, wysoki poziom GSH może prowadzić do zwiększonej tolerancji roślin na czynniki stresowe. Jednocześnie, wyższa dawka nano-Cu oraz obie dawki soli miedzi znacząco zwiększyły zawartość GSSG (odpowiednio 4,5- i 2,8-krotnie). Potwierdza to nadprodukcję ROS pod wpływem tych zabiegów oraz zaangażowanie tego szlaku w reakcji obronnej roślin zarówno na ENPs jak i $CuSO_4$ [**PII**].

Analizie poddano także aktywność kluczowych enzymów szlaku fenylopropanoidowego (PAL, PPO) oraz zawartości jednego z ich produktów – polifenoli (TPC) (Rys. 19) [93]. Nasze badania nie wykazały znaczących zmian w aktywności PAL po

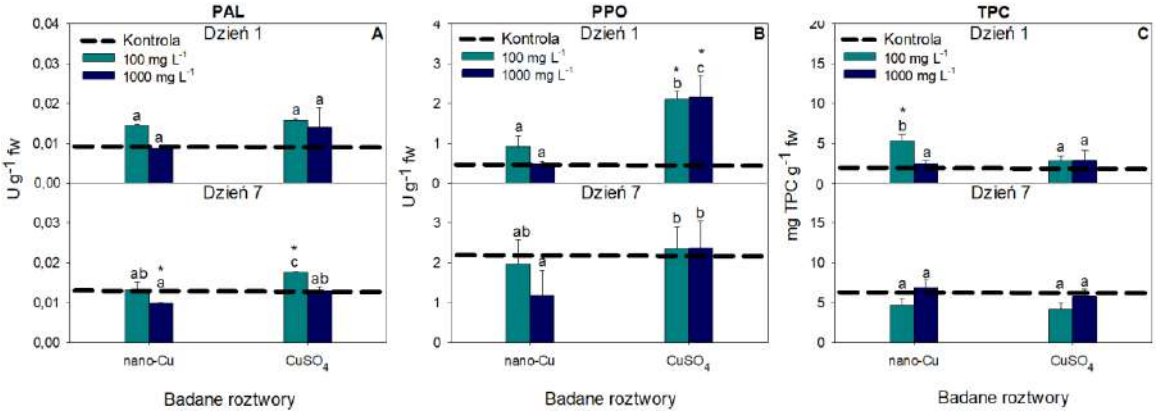

Rysunek 19. *Zmiany aktywności PAL (A), PPO (B) i zawartości TPC (C) w H. vulgare pod wpływem nano-Cu i $CuSO_4$ (w stężeniu 100 i 1000 mg L^{-1}) po 1 i 7 dniach ekspozycji. Słupki błędów reprezentują błąd standardowy (SE, n=3 próby). Gwiazdki wskazują na istotną różnicę między próbami nietraktowanymi i traktowanymi (test Duncana, $p < 0,05$). Różne litery wskazują na istotne różnice między zabiegami (test Tukey'a, $p < 0,05$) [**PII**].*

1-no dniowej ekspozycji roślin względem kontroli (Rys. 19A), podczas gdy badania innych autorów [94] opisywały indukcję PAL w odpowiedzi na stresory takie jak metale ciężkie. W trakcie naszych badań stwierdzono również brak wpływu obu dawek nano-Cu na aktywność PPO, podczas gdy u roślin wystawionych na $CuSO_4$ zaobserwowano ok. 5-krotny wzrost aktywności PPO po 1-szym dniu ekspozycji w porównaniu do roślin kontrolnych ($p < 0,05$). Tak znaczący wzrost aktywności PPO w odpowiedzi na sole miedzi prawdopodobnie wynikał z dostarczenia jonów Cu: PPO jest białkiem wymagającym obecności Cu^{2+}, a w warunkach deficytu jego aktywność spada [85]. Ponadto, aktywność PPO jest związana z utlenianiem polifenoli do chinonów i lignifikacją ścian komórkowych w procesie starzenia w odpowiedzi na stresory [59,85,95]. Jedynie niskie stężenie nano-Cu wykazało efekt stymulujący na TPC (4,3-krotny wzrost) względem roślin kontrolnych po 1 dniu ($p < 0,05$). Biorąc pod uwagę, że związki fenolowe są metabolitami wtórnymi o dużej aktywności antyoksydacyjnej, ich zwiększona akumulacja może świadczyć o prawidłowym

funkcjonowaniu mechanizmu obronnego rośliny i działaniu nano-Cu jako elicytatorów [39]. W przypadku pozostałych zabiegów, stres oksydacyjny mógł zakłócać biosyntezę tych metabolitów i osłabiać zdolności antyrodnikowe roślin [96]. Po dłuższej ekspozycji w większości przypadków, nie obserwowano już znaczącego wpływu zastosowanych roztworów na analizowane parametry, co może sugerować krótkotrwały efekt stymulujący w przypadku niskiej dakwi nano-Cu, lub ich „wykorzystaniu" do neutralizacji ROS.

4.3.3. Analiza ekspresji genów

Ocena zmian na poziomie molekularnym pozwoliła na dogłębną analizę wpływu zastosowanych związków Cu na zmiany w profilach ekspresji genów transporterów miedzi (*RAN1*, *COPT5*, *PAA1*, *PAA2*), akwaporyn (*NIP2.2*, *PIP1.1*, *TIP1.1*, *TIP1.2*) oraz enzymów antyoksydacyjnych (*SOD Cu/Zn*, *SOD Fe*, *SOD Mn*, *CAT*) (Rys. 20) [**PIII**].

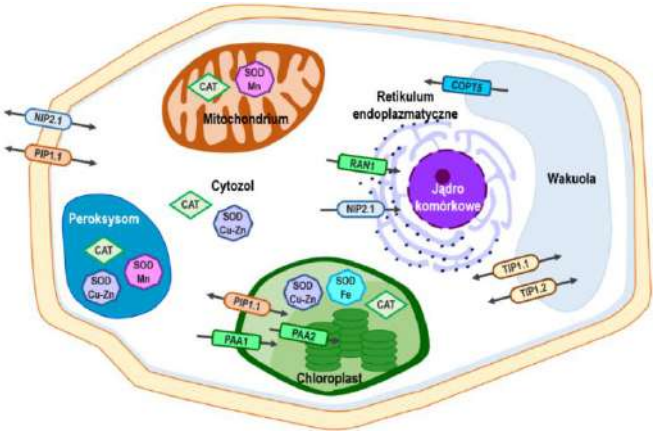

Rysunek 20. *Schemat lokalizacji transporterów Cu, akwaporyn i enzymatycznych antyoksydantów w komórce roślinnej [**PIII**].*

Ekspozycja na 100 mg L^{-1} nano- Cu skutkowała 4-krotnym obniżeniem (*PAA1*) lub brakiem wpływu (*PAA2*, *RAN1*) na ekspresję genów transporterów, natomiast pozostałe roztwory Cu zwiększały poziom ekspresji *PAA2* i *RAN1* (odpowiednio 1,4- i 1,5-3,8-krotnie) (Rys. 21). Badania Ma i in. [97] wskazały na spadek ekspresji transporterów Cu takich jak PAA1 (transport Cu przez błony chloroplastu), PAA2 (transport Cu do centrum chloroplastu) czy RAN1 (transport Cu do jądra komórkowego), w odpowiedzi na nagły wzrost stężenia jonów Cu w komórkach roślinnych, po czym ich poziom ekspresji stopniowo wzrastał w czasie. Pozwala to przypuszczać, że niski poziom ekspresji transporterów Cu jedynie u roślin eksponowanych na 100 mg L^{-1} nano-Cu wynikał z niższej dostępnej roślinom puli jonów Cu ze względu na ich powolne uwalnianie z ENPs [**PII, PIII**]. Jednakże, wraz z wydłużeniem czasu ekspozycji poziomy transkryptów analizowanych genów uległy obniżeniu w odpowiedzi na badane związki Cu niezależnie od dawek (*PAA1* o 64-85%, *PAA2* o 34-53%, *RAN1*o 78-89%) (Rys. 21). Uzyskane wyniki mogą wskazywać na ograniczanie translokacji jonów Cu do organelli komórkowych roślin w celu zapobiegania/łagodzenia efektów gromadzenia się nadmiaru Cu^{2+} wewnątrz komórek *H. vulgare* [97] [**PIII**]. Jednocześnie poziom ekspresji genu *COPT5*, odpowiedzialnego za

transport jonów Cu kumulowanych w wakuoli [98], utrzymywał się na stale obniżonym poziomie zarówno po 1 (o ~50%), jak i po 7 dniach (o 43-84%) (Rys. 21).

W zależności od dostępnej puli jonów Cu potencjał osmotyczny komórek roślinnych podlega zmianom, co może wpłynąć na zmiany profili ekspresji genów akwaporyn (ang. *aquaporines*, AQs) – zaangażowanych w dwustronną dystrybucję jonów metali do/z komórek (NIPs) i organelli komórkowych, takich jak chloroplasty (PIPs) i wakuole (TIPs) (Rys. 20) [99]. Pomimo, iż dotychczasowe badania wiązały spadek ekspresji *AQs* jedynie z regulacją osmotyczną wynikającą z obecności Cu^{2+} [22], w naszych analizach jedynie ekspozycja na nano-Cu w stężeniu 100 mg L^{-1} prowadziła do obniżenia regulacji wszystkich

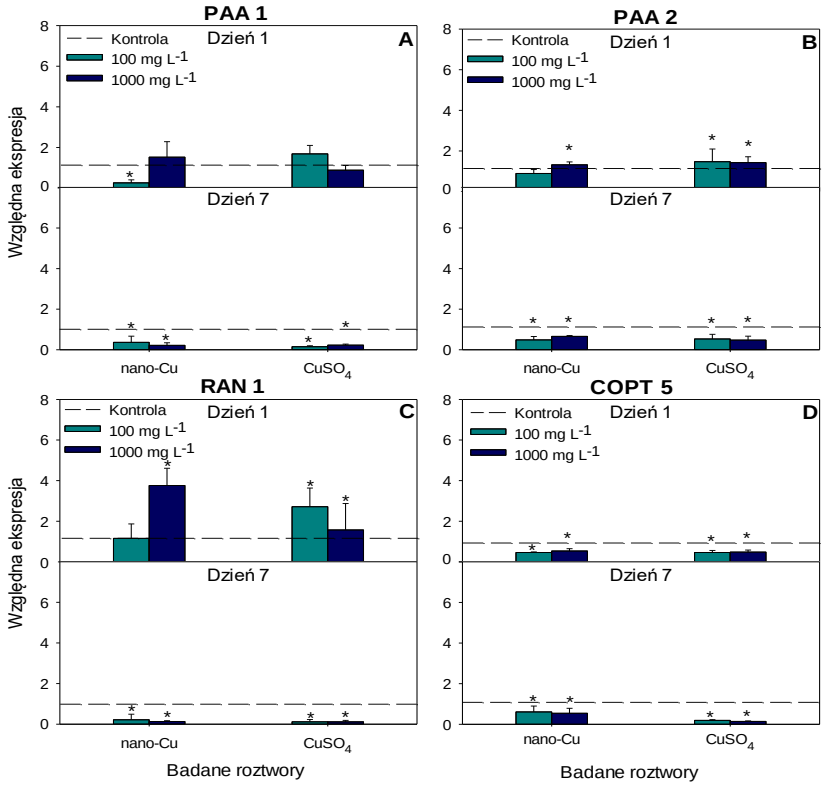

Rysunek 21. *Względna ekspresja genów PAA1 (A), PAA2 (B), RAN1 (C) i COPT5 (D) w liściach H. vulgare pod wpływem ekspozycji na nano-Cu i $CuSO_4$ (100 i 1000 mg L^{-1}) po 1 i 7 dniach ekspozycji. Słupki błędów reprezentują błąd standardowy (SE, n=3 próby). Gwiazdki wskazują na istotną różnicę między próbami nietraktowanymi i traktowanymi (test Duncana, p < 0,05)* ***[PIII]****.*

testowanych genów *AQs* (o 45-64%). Przypuszczalnie, przedłużający się niedobór Cu mógł wpłynąć na reakcje roślin na bodźce [100], co w połączeniu z wcześniej opisaną niższą dostępnością Cu^{2+} z ENPs [**PII, PIII**] prowadziło do odmiennego wzoru ekspresji genów *AQs*. Wraz z wydłużeniem czasu ekspozycji roślin odnotowano istotny wzrost ekspresji wszystkich testowanych *AQs*, jednakże odpowiedź molekularna *NIP2.1*, *PIP1.1* i *TIP1.1* była odwrotnie zależna od dawki: podczas gdy niższe dawki roztworów Cu prowadziły do 1,5-5-krotnej indukcji poziomu transkrypcji genów *AQs*, ekspozycja na roztwory 1000 mg Cu L^{-1} skutkowała wzrostem ekspresji *NIP2.1* (2,7-krotnym). Wyjątek stanowił gen *TIP1.2*,

dla którego wykazano 3,8-5,6-krotny wzrost ekspresji pod wpływem obu dawek nano-Cu i $CuSO_4$. Ze względu na dwukierunkowy transport cząsteczek/cząstek przez akwaporyny oraz nadal niewystarczającą wiedzą na temat ich roli i mechanizmów działania, trudno jednoznacznie zinterpretować oddziaływanie ENPs. Dotychczasowe badania wskazują na podwyższoną ekspresję *AQs* w okresie intensywnego wzrostu roślin w celu zapewnienia efektywniejszej cyrkulacji wody i składników odżywczych [99,101,102], co mogłoby wskazywać na pozytywny wpływ nawożenia Cu w niskich dawkach na gospodarkę wodną i mineralną roślin. Jednak mając na uwadze inne opisane już wcześniej markery, obserwowane zmiany w ekspresji mogły wynikać z reakcji obronnej rośliny polegającej na „wyrzucie" nadmiernych stężeń Cu^+/Cu^{2+} (większa ekspresja *NIP2.2*) i/lub ich sekwestracji w mniej wrażliwych organellach jak wakuole (większa ekspresja *TIP 1.2*) [103].

Uwzględniając negatywny wpływ deficytu Cu na wzrost roślin (stres oksydacyjny, inhibicja białek zawierających Cu) [84], analizie poddaliśmy także ekspresję genów trzech izoform *SOD* oraz *CAT* (Rys. 20). Już po 1 dniu ekspozycji wykazano 4-5-krotny wzrost ekspresji *SOD Cu-Zn* przy równoczesnym gwałtownym spadku ekspresji *SOD Fe* (o około 76%) jedynie u roślin wystawionych na działanie soli miedzi, co prawdopodobnie wynikało z szybkiego uwalniania jonów Cu^{2+} do komórek roślinnych [84,104] w przeciwieństwie do ENPs. Natomiast, niezależnie od formy i dawki Cu oraz czasu ekspozycji, nie odnotowano zmian w ekspresji *SOD Mn* w porównaniu do grupy kontrolnej ($p > 0,05$). Z kolei, stwierdzone zwiększenie ekspresji genu *CAT* zależało głównie od rodzaju związku Cu niż od dawki (1,5- oraz 4,5-krotny wzrost ekspresji dla nano-Cu i $CuSO_4$, odpowiednio). Obserwowana zwiększona ekspresja *SOD Cu-Zn* i *CAT* w odpowiedzi na $CuSO_4$ po 1 dniu może sygnalizować nadprodukcję ROS z powodu szybszego napływu Cu^{2+} i ich nadmiarowej akumulacji [22]. Reakcja ta mogła być również związana z budową SOD Cu-Zn, wymaga jonów Cu, w przypadku ich niedoboru ich rolę mogą „przejmować" inne izoformy tego metaloenzymu. To wytłumaczenie znajduje potwierdzenie w poziomach ekspresji dwóch izofom SOD (SOD Cu-Zn, SOD Fe) zmierzonych po 7 dniach. Mianowicie, w przypadku $CuSO_4$ zauważono dalszy wzrost ekspresji *SOD Cu-Zn* (4- i 13,5-krotny) przy równoczesnym spadku poziomu transkryptu *SOD Fe* (4- i 12,8-krotnym). Jednocześnie wszystkie związki Cu powodowały ok. 60-78% spadek ekspresji genu *CAT* po 7 dniach ekspozycji. Być może wynikało to z zaangażowania innych szlaków związanych z odpowiedzią na stres [87]. W bieżących badaniach nie wykazano istotnej korelacji pomiędzy poziomem ekspresji genów *CAT* i izoform *SOD*, a poziomem aktywności enzymów CAT i SOD, co mogło być spowodowane różnicą w pobranym do badań materiale – do analiz

aktywności enzymów wykorzystano starsze liście, podczas gdy analizy ekspresji genów przeprowadzono na liściach flagowych. Ponadto, taki stan może wynikać z różnic w zawartości nano-Cu/$CuSO_4$ w tych partiach liści oraz odmienny profil ekspresji genów w zależności od tkanki roślinnej [105], co mogło być związane z warunkami wzrostu roślin (niedobór Cu), które wymuszały na roślinie np. priorytetyzację dystrybucji Cu do młodszych liści.

W celu uzyskania całościowego obrazu zmian ekspresji analizowanych genów pod wpływem nano-Cu oraz $CuSO_4$ na rośliny *H. vulgare*, profile ekspresji 12 badanych genów przedstawiono w postaci mapy ciepła (Rys. 22). Po 1 dniu ekspozycji na sole miedzi, w przeciwieństwie do nano-Cu, rośliny wykazywały podobne wzorce ekspresji wszystkich genów niezależnie od dawki. Ta różnica w ekspresji genów najprawdopodobniej wynikała z szybkiego rozpuszczenia i wychwytu Cu^{2+} przy zastosowaniu $CuSO_4$, co bezpośrednio prowadziło do szybkiej indukcji ekspresji genów antyoksydantów. Jednocześnie zauważalny był wyraźny podział w profilu ekspresji genów między niższą dawką nano-Cu,

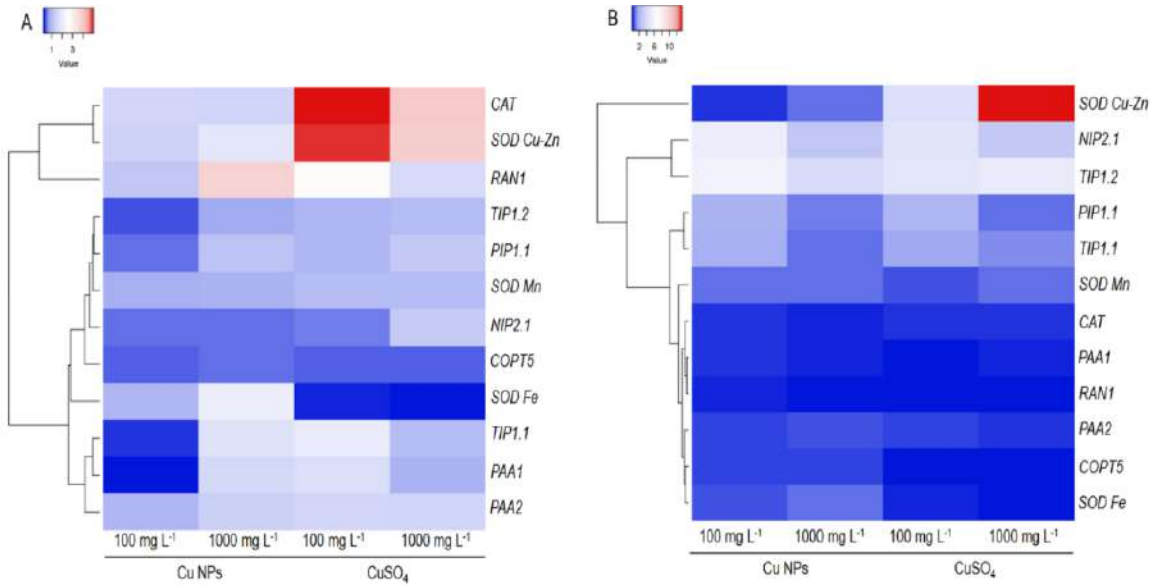

***Rysunek 22**. Mapy ciepła pokazujące zróżnicowaną ekspresję genów homeostazy Cu, akwaporyn i enzymatycznych przeciwutleniaczy w liściach flagowych H. vulgare po 1 (A) i 7 dniach (B) ekspozycji na związki Cu. Każda kolumna reprezentuje ekspresję w liściach flagowych pod wpływem różnych zabiegów Cu (nano-Cu i CuSO4 w stężeniach 100 i 1000 mg L^{-1}), a każdy wiersz reprezentuje jeden gen. Skala kolorów na zdjęciach pokazuje ekspresję genów od niskiej (niebieski) do wysokiej (czerwony). Hierarchiczne grupowanie genów jest pokazane na dendrogramach [**PIII**].*

a pozostałymi grupami (wyższe stężenie nano-Cu, obie dawki $CuSO_4$). Analizy wskazały obecność 2 klastrów genów o podobnym wzorze ekspresji (Rys. 22A). Pierwszy klaster zawierał geny *CAT* i *SOD Cu-Zn*, których poziom ekspresji był ściśle zależny od zastosowanej formy Cu: w przeciwieństwie do obu dawek nano-Cu, podanie $CuSO_4$ skutkowało znaczącym wzrostem ekspresji obu genów. Tymczasem drugi klaster (dolna

część mapy ciepła) zawierał geny wykazujące niski poziom ekspresji, w szczególności geny *AQs* i transporterów Cu. Wyraźnie niższy poziom ekspresji tych genów był obserwowany u roślin pod wpływem ekspozycji na 100 mg L^{-1} nano-Cu, co prawdopodobnie wiąże się z mniejszą ekspozycją na jony Cu uwolnione przy niższej dawce ENPs. Po 7 dniach ekspozycji nie zaobserwowano znaczących różnic w ekspresji badanych genów pomiędzy nano-Cu, a solami miedzi z wyjątkiem genu kodującego *SOD Cu-Zn* (stanowiący osobny klaster) (Rys. 22B). Tak znacząca nadekspresja *SOD Cu-Zn* jedynie u roślin poddanych działaniu $CuSO_4$ mogła wynikać z szybkiego uwalniania Cu^{2+}, które wraz z upływem czasu mogło prowadzić do silnych reakcji stresowych u roślin. Wszystkie pozostałe geny zostały podzielone na kolejne 2 klastry: pierwszy obejmował geny *AQs* o podwyższonym poziomie ekspresji (*NIP2.1* i *TIP1.2*), drugi geny o obniżonej ekspresji (głównie transportery Cu). Spadek ekspresji transporterów Cu do komórki i jej organelli może być przejawem reakcji obronnej roślin przed pobraniem nadmiaru Cu, co sugeruje, że w przeciągu 7 dni rośliny były zdolne do pobrania znaczącej ilości Cu niezależnie od źródła i dawki.

4.4. Analiza wpływu związków miedzi na wartość odżywczą i zawartość antyoksydantów ziarniaków jęczmienia jarego

Ostatni etap badań nad wpływem ENPs na bazie Cu na rośliny, miał na celu ocenę ilości i jakości plonu jęczmienia po dolistnej aplikacji nano-Cu i nano-CuO, mikro-Cu oraz łatwo rozpuszczalnych związków Cu ($CuSO_4$, Cu-EDTA), które są powszechnie stosowane jako nawozy [14,16]. Przeprowadzone analizy wykazały brak znaczącego wpływu testowanych roztworów Cu na wielkość plonowania jęczmienia jarego względem roślin kontrolnych (Tab. 4). Obecnie nie ma dostępnych danych na temat plonowania zbóż po

***Tabela 4**. Masa nasion jęczmienia jarego otrzymanych po ekspozycji na różne roztwory Cu. Średnie, po których następują różne litery, oznaczają istotne różnice między zabiegami (test Tukey'a, $p < 0,05$) [**PIV**].*

	Kontrola	Nano-Cu	Nano-CuO	Mikro-Cu	$CuSO_4$	Cu-EDTA
Waga nasion [g] na 1 donicę	41,5±2,5^a	43,6±3,5^a	35,3±4,2^a	43,7±2,0^a	39,6±3,3^a	40,2±3,5^a
Waga 1000 nasion [g]	38,2±1,7^a	36,0±2,1^a	35,6±2,6^a	39,6±2,3^a	36,6±2,6^a	38,7±2,7^a

dolistnej aplikacji ENPs na bazie Cu. Prawdopodobnie, aplikacja Cu jako mikroelementu może mieć większe znaczenie dla jakości plonów niż jego ilości [**PIV**]. Analizy zawartości Cu w nasionach wykazały ok. 2-krotne większą jej zawartość u roślin traktowanych

nano- Cu oraz rozpuszczalnymi związkami miedzi ($CuSO_4$ i Cu-EDTA) w porównaniu do grupy kontrolnej (2,6 mg kg^{-1}) (Rys. 23). Biorąc pod uwagę uprzednio opisaną niską rozpuszczalność ENPs, wysoka zawartość miedzi w nasionach może być wynikiem pobierania i translokacji nano-Cu w roślinie i do nasion w postaci cząstek. Takie zachowanie było potencjalnie możliwe ze względu na ich niewielkie rozmiary nano-Cu (25 nm) w porównaniu do pozostałych cząstek (nano-CuO = 50 nm, mikro-Cu = 5 µm), dzięki czemu byłyby zdolne do pokonywania naturalnych barier *H. vulgare* poprzez m.in. aparaty szparkowe [17]. Przeanalizowano także zawartość innych mikroelementów (Zn, Fe, Mn) w nasionach jęczmienia (Tab. 5). Mimo, iż dane literaturowe dowodzą, że ENPs mają wpływ na pobieranie i zawartość innych metali [34,41], nasze badania nie wykazały znaczących zmian w zawartości tych mikroelementów po aplikacji nano- i mikro-Cu. Ponadto, nie zaobserwowano także ogólnego trendu zmian w zawartości Ca, K, Mg w nasionach pod wpływem podanych związków Cu (Tab. 5).

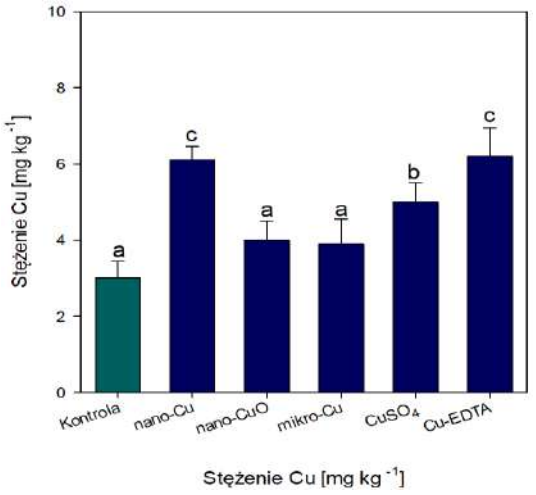

***Rysunek 23**. Zawartość Cu w ziarniakach H. vulgare po ekspozycji na różne związki Cu. Słupki błędów reprezentują błąd standardowy (SE, n=3 próby). Różne litery wskazują na istotne różnice między zabiegami (p < 0,05) [**PIV**].*

***Tabela 5**. Zawartość mikro- i makroskładników w suchej masie nasionach H. vulgare po ekspozycji na różne związki Cu. Różne litery wskazują na istotne różnice między zabiegami (test Kruskala-Wallisa, p < 0,05) [**PIV**].*

	Zn [mg kg^{-1}]	Fe [mg kg^{-1}]	Mn [mg kg^{-1}]	Ca [mg kg^{-1}]	K [mg kg^{-1}]	Mg [mg kg^{-1}]
Kontrola	18,8±0,6^a	28,6±0,9^a	11,6±0,1^a	304,0±22,5^b	5615,7±120,1^a	922,3±37,3^b
Nano-Cu	20,0±1,6^a	28,8±2,6^a	11,1±0,1^a	269,0±36,5^a	5991,3±210,2^b	913,0±29,8^b
Nano-CuO	19,8±1,7^a	24,9±2,4^a	11,1±0,3^a	272,6±19,7^a	5308,5±320,6^a	901,1±21,9^b
Mikro-Cu	22,3±2,6^a	24,7±1,1^a	11,0±0,1^a	269,6±26,0^a	5561,4±114,8^a	922,9±30,8^b
$CuSO_4$	23,2±1,9^b	26,3±1,2^a	10,7±0,1^a	259,2±31,8^a	5399,2±213,7^a	839,7±37,9^a
Cu-EDTA	17,5±0,8^a	31,3±1,1^a	13,1±0,1^b	298,8±30,2^b	5709,0±204,5^a	982,3±40,1^c

Przeprowadzone analizy nie wykazały znaczącego wpływu aplikacji roztworów Cu na zawartość i strawność białka ziarniaków z wyjątkiem $CuSO_4$, który skutkował

zmniejszeniem strawności białka o 6% [**PIV**]. Jednocześnie, istotne zmiany w zawartości błonnika wykazano jedynie po aplikacji nano-Cu (wzrost zawartości błonnika całkowitego i rozpuszczalnego odpowiednio o 19,9% i 43,6%) w porównaniu z kontrolą ($p < 0,05$) [**PIV**], co może wskazywać na potencjał nano-Cu w poprawie właściwości prozdrowotnych ziarniaków.

Analizy wpływu roztworów Cu na zawartość związków fenolowych, uważanych za główne związki przeciwutleniające [39], wykazały istotne zmiany jedynie na poziomie pojedynczych składników polifenoli (Tab. 6). Podczas gdy podanie Cu-EDTA spowodowało wzrost zawartości antocyjanów (o 20%) oraz tanin (o 140%), aplikacja nano- Cu prowadziła do 20% wzrostu zawartości flawanoli (Tab. 6). Taki obraz zmian może

Tabela 6*. Zawartość składników antyoksydacyjnych w nasion H. vulgare po ekspozycji na różne związki Cu. Różne litery wskazują na istotne różnice między zabiegami ($p < 0,05$) [**PIV**].*

	Związki fenolowe [mg GAE/g]	Antocyjany [mg cya-3-glu/ g]	Flawonoidy [mg kwercetyn/ g]	Taniny [mg katechin/ g]	Flawanole [mg katechin/ g]
Kontrola	3,0±0,1^{a}	37,1±0,8^{a}	0,2±0,1^{a}	0,4±0,1^{a}	36,0±2,0^{a}
Nano-Cu	3,5±0,6^{a}	33,9±0,1^{a}	0,1±0,1^{a}	0,5±0,1^{a}	43,0±1,0^{b}
Nano-CuO	2,7±0,0^{a}	40,0±0,1^{a}	0,1±0,1^{a}	0,6±0,1^{a}	36,0±2,0^{a}
Mikro-Cu	2,7±0,5^{a}	38,7±0,1^{a}	0,1±0,1^{a}	0,7±0,1^{a}	37,0±3,0^{a}
$CuSO_4$	3,0±0,3^{a}	32,6±0,1^{a}	0,1±0,1^{a}	0,3±0,1^{a}	38,0±4,0^{a}
Cu-EDTA	2,5±0,4^{a}	44,7±0,1^{b}	0,1±0,1^{a}	0,9±0,1^{b}	34,0±3,0^{a}

wskazywać odmienny sposób oddziaływania cząstkowego i jonowego Cu na produkcję i kumulację związków bioaktywnych w roślinach [35].

Analiza aktywności antyrodnikowej wykazała mniejszą zdolność do neutralizacji rodników $ABTS^{\bullet+}$ i $DPPH^{\bullet}$ w ziarniakach roślin, które były wystawione na działanie związków Cu (Rys. 24). Szczególnie znaczący spadek aktywności antyoksydacyjnej wobec $ABTS^{\bullet+}$odnotowano w wyniku aplikacji $CuSO_4$ (o 66%) względem roślin z grupy kontrolnej ($p < 0,05$), podczas gdy aplikacja mikro-Cu nie miała znaczącego wpływu na ten parametr. Nie wykryto także istotnych zmian w potencjale redukcyjnym FRAP, niezależnie od zastosowanego roztworu Cu ($p \geq 0,05$) (Rys. 24C), podczas gdy test CUPRAC wykazał spadek zdolności redukcyjnych ekstraktu z nasion roślin (o 9,0-39,8%) w wyniku ekspozycji na badane roztwory Cu ($p < 0,05$) (Rys. 24D). Jedyny wyjątek stanowił roztwór nano-Cu,

który nie wpłynął na zdolności redukcyjne ekstraktu (Rys. 24D). Jednocześnie wykazano, że tylko pod wpływem nano-Cu obniżeniu ulegała moc redukująca HORAC (o 21,4 %). Ekspozycja na pozostałe roztwory nie powodowała zmian (mikro-Cu) lub skutkowała

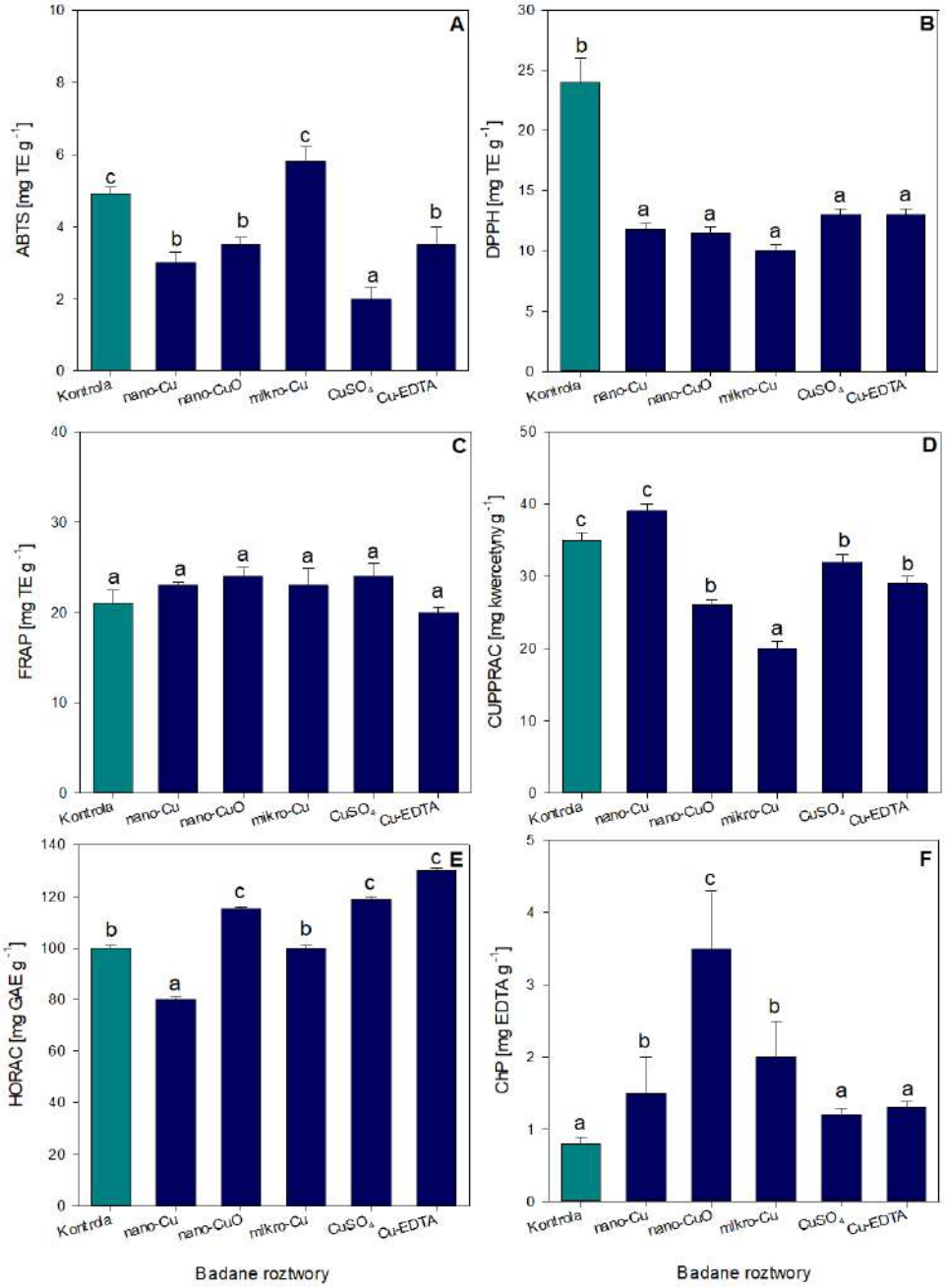

***Rysunek 24**. Aktywność przeciwrodnikowa w ekstraktach ziarniaków H. vulgare wyrażona wskaźnikami: ABTS (A), DPPH (B), FRAP (C), CUPRAC (D), HORAC (E) i zdolnością chelatująca (F). Słupki błędów reprezentują błąd standardowy (SE, n=3 próby). Różne litery wskazują na istotne różnice między zabiegami (p < 0,05) [**PIV**].*

większym potencjałem redukcyjnym ziarniaków (o 12,7-25,7 %) ($p < 0,05$) (Rys. 24E). Warto podkreślić, że aplikacja nano- i mikro-Cu skutkowała 2- i 4-krotnie większą siłą chelatującą ekstraktów nasion względem roślin kontrolnych, podczas gdy oprysk z $CuSO_4$ i Cu-EDTA nie wpłynął na ten parametr (Rys. 24F). Te obserwacje pokrywały się

z analizami Rico i in [106], w których wykazano ograniczenie wychwytywania wolnych rodników w ziarnach ryżu pod wpływem nano-CeO_2, co autorzy przypisali zmniejszonej zawartości TPC. Jednakże, jak wspomniano wcześniej, w naszych badaniach nie stwierdzono zmian w TPC pod wpływem związków Cu (Tab. 6), ale odmienna zdolność przeciwutleniająca może być związana ze zmianami zawartości poszczególnych związków fenolowych [107, 108].

5. Wnioski

Przeprowadzone badania pozwoliły na sformułowanie następujących wniosków:

❖ ENPs w roztworach wodnych wykazały tendencje do tworzenia agregatów 10-14-krotnie (nano-Cu) oraz 9,6-krotnie (nano-CuO) większych od średniej wielkości cząstki oraz stopniowe uwalnianie jonów Cu, co następnie rzutowało na ich oddziaływanie z roślinami.

❖ Ze względu na silną adhezję ENPs do powierzchni liści, jednoznaczne wykazanie pobranej ilości Cu było utrudnione. Jednakże, w oparciu o szereg parametrów biochemicznych i molekularnych istnieją przesłanki potwierdzające pobieranie Cu (nanocząstkowej i/lub jonowej). Analizy te wskazują również na istotny wpływ dawki oraz formy Cu na kinetykę pobierania miedzi.

❖ Nie stwierdzono translokacji aplikowanego Cu z liści do korzeni niezależnie od dawki czy formy Cu, co mogło wynikać z małej mobilności jonów Cu/nanocząstek Cu i/lub z krótkiego okresu ekspozycji roślin.

❖ Krótkotrwała ekspozycja na sole miedzi prowadziła do większego przyrostu biomasy roślin (korzeni i części nadziemnej) niż nano-Cu, co mogło wynikać z dostarczenia pełnej puli deficytowego mikroelementu w fazie intensywnego wzrostu. Jednak po 7 dniach zaobserwowano chlorozę liści po ekspozycji roślin na $CuSO_4$, co prawdopodobnie wynikało z absorpcji toksycznych ilości Cu.

❖ Istotne zmiany aktywności antyoksydantów zaobserwowano głównie po 1 dniu od ekspozycji na związki Cu. Oba badane stężenia $CuSO_4$ jak i wyższa dawka nano-Cu powodowały znacząco większe zmiany w poziomach antyoksydacyjnych markerów wskazujące na wywołanie większego stresu u roślin. Natomiast niższa dawka nano-Cu, zwiększając zawartość niskocząsteczkowych antyoksydantów, mogła wspierać mechanizmy obronne roślin.

❖ Analiza ekspresji genów u roślin po aplikacji związków miedzi wykazała, że zmiany w odpowiedzi molekularnej na różne formy Cu były uzależnione od zastosowanego stężenia Cu, analizowanych genów i czasu ekspozycji. Największe różnice w ekspresji genów związanych z transportem Cu między formą „nano", a jonami Cu obserwowano przy niższej dawce, krótko po aplikacji tych związków. W miarę upływu czasu „efekt nano" ulegał zatarciu, co może oznaczać, że zarówno nano-Cu jak i $CuSO_4$ dostarczyły roślinom Cu w ilościach wymagających uruchomienia mechanizmów jej relokacji w celu ochrony kluczowych organelli. Jednak na podstawie poziomu ekspresji genów antyoksydantów

można stwierdzić, że reakcja na jony Cu ($CuSO_4$) była szybsza i silniejsza niż nano-Cu, co świadczy o łagodniejszym wpływie ENPs na rośliny.

❖ Zwiększoną zawartość Cu w ziarniakach stwierdzono jedynie po aplikacji nano-Cu oraz związków łatwo rozpuszczalnych Cu ($CuSO_4$ i Cu-EDTA). Może to potwierdzać sukcesywną absorpcję i translokację Cu głównie w formie nanocząstek po aplikacji nano-Cu, które wyjściowo charakteryzowały się niewielką rozpuszczalnością.

❖ Mimo, iż aplikacja związków Cu nie zwiększała plonowania jęczmienia jarego, nano-Cu, w przeciwieństwie do pozostałych form Cu, poprawił niektóre cechy jakościowe ziarniaków np. zawartość składników odżywczych (błonnika i flawonoli).

❖ Pomimo, iż ENPs i mikro-Cu wyraźnie zwiększały zdolności chelatujące ekstraktów z ziarniaków, pozostałe testy zdolności antyoksydacyjnej/redukującej wykazały głównie spadek mocy do neutralizacji wolnych rodników pod wpływem aplikacji tych związków Cu, co może wzbudzać obawy przed obniżeniem wartości prozdrowotnej ziarniaków.

6. Bibliografia

[1] K.F. Ofori, S. Antoniello, M.M. English, A.N.A. Aryee, Improving nutrition through biofortification–A systematic review, Frontiers in Nutrition 9 (2022) 1043655. https://doi.org/10.3389/fnut.2022.1043655.

[2] N.D. Mueller, J.S. Gerber, M. Johnston, D.K. Ray, N. Ramankutty, J.A. Foley, Closing yield gaps through nutrient and water management, Nature 490 (2012) 254–257. https://doi.org/10.1038/nature11420.

[3] FAO, The future of Food and Agriculture: Alternative pathways to 2050, Food and Agricultural 8 Organization of the United Nations, Rome, 2018. https://knowledge4policy.ec.europa.eu/publication/future-food-agriculture-alternative-pathways-2050_en (accessed April 28, 2023).

[4] J.L. Azevedo, W.L. Araujo, Genetically modified crops: environmental and human health concerns, Mutation Research/Reviews w Mutation Research 544 (2003) 223–233. https://doi.org/10.1016/j.mrrev.2003.07.002.

[5] A.-R. Sayadi Maazou, J. Tu, J. Qiu, Z. Liu, Breeding for Drought Tolerance in Maize (*Zea mays* L.), American Journal of Plant Sciences 07 (2016) 1858–1870. https://doi.org/10.4236/ajps.2016.714172.

[6] L. Yadav, N. Kumar Maurya, Fight Hidden Hunger through National Programs and Food Based Approaches, w F. Saeed, A. Ahmed, M. Afzaal (Eds.), Combating Malnutrition through Sustainable Approaches, IntechOpen, (2023) https://doi.org/10.5772/intechopen.104459.

[7] S. Narwal, D. Kumar, A.S. Kharub, R.P.S. Verma, Barley biofortification: present status and future prospects, w Wheat and Barley Grain Biofortification, Elsevier, (2020) 275–294. https://doi.org/10.1016/B978-0-12-818444-8.00011-0.

[8] FAO, ed., Transforming food systems for food security, improved nutrition and affordabel healthy diets for all, FAO, Rome, 2021. https://doi.org/10.4060/cb4474en.

[9] A.K. Bhardwaj, S. Chejara, K. Malik, R. Kumar, A. Kumar, R.K. Yadav, Agronomic biofortification of food crops: An emerging opportunity for global food and nutritional security, Frontiers in Plant Science 13 (2022) 1055278. https://doi.org/10.3389/fpls.2022.1055278.

[10] M. van Maarschalkerweerd, R. Bro, M. Egebo, S. Husted, Diagnosing Latent Copper Deficiency in Intact Barley Leaves (*Hordeum vulgare*, L.) Using Near Infrared Spectroscopy, Journal of Agricultural and Food Chemistry 61 (2013) 10901–10910. https://doi.org/10.1021/jf402166g.

[11] N. Rahman, J. Schoenau, Response of wheat, pea, and canola to micronutrient fertilization on five contrasting prairie soils, Scientific Reports 10 (2020) 18818. https://doi.org/10.1038/s41598-020-75911-y.

[12] G. Wojnarowiez, C. Jacquard, P. Devaux, R.S. Sangwan, C. Clément, Influence of copper sulfate on anther culture in barley (*Hordeum vulgare* L.), Plant Science 162 (2002) 843–847. https://doi.org/10.1016/S0168-9452(02)00036-5.

[13] R. Shahzad, S. Jamil, S. Ahmad, A. Nisar, S. Khan, Z. Amina, S. Kanwal, H.M.U. Aslam, R.A. Gill, W. Zhou, Biofortification of Cereals and Pulses Using New Breeding Techniques: Current and Future Perspectives, Frontiers in Nutrition 8 (2021) 721728. https://doi.org/10.3389/fnut.2021.721728.

[14] M. Kah, D. Navarro, R.S. Kookana, J.K. Kirby, S. Santra, A. Ozcan, S. Kabiri, Impact of (nano)formulations on the distribution and wash-off of copper pesticides and fertilisers applied on citrus leaves, Environmental Chemistry 16 (2019) 401. https://doi.org/10.1071/EN18279.

[15] A. Moreira, L.A.C. Moraes, T.R. de Melo, R. Heinrichs, L.G. Moretti, Management of copper for crop production, w Advances in Agronomy, Elsevier, (2022) 257–298. https://doi.org/10.1016/bs.agron.2022.02.005.

[16] R.D. Graham, Micronutrient Deficiencies in Crops and Their Global Significance, w B.J. Alloway (Ed.), Micronutrient Deficiencies in Global Crop Production, Springer Netherlands, Dordrecht, (2008) 41–61. https://doi.org/10.1007/978-1-4020-6860-7_2.

[17] A. Avellan, J. Yun, B.P. Morais, E.T. Clement, S.M. Rodrigues, G.V. Lowry, Critical Review: Role of Inorganic Nanoparticle Properties on Their Foliar Uptake and *in Planta* Translocation,

Environmental Science & Technology 55 (2021) 13417–13431. https://doi.org/10.1021/acs.est.1c00178.
[18] R. Prasad, A. Bhattacharyya, Q.D. Nguyen, Nanotechnology in Sustainable Agriculture: Recent Developments, Challenges, and Perspectives, Frontiers in Microbiology 8 (2017) https://doi.org/10.3389/fmicb.2017.01014.
[19] L. Pagano, A.D. Servin, R. De La Torre-Roche, A. Mukherjee, S. Majumdar, J. Hawthorne, M. Marmiroli, E. Maestri, R.E. Marra, S.M. Isch, O.P. Dhankher, J.C. White, N. Marmiroli, Molecular Response of Crop Plants to Engineered Nanomaterials, Environmental Science & Technology 50 (2016) 7198–7207. https://doi.org/10.1021/acs.est.6b01816.
[20] G.V. Lowry, A. Avellan, L.M. Gilbertson, Opportunities and challenges for nanotechnology in the agri-tech revolution, Nature Nanotechnology 14 (2019) 517–522. https://doi.org/10.1038/s41565-019-0461-7.
[21] Y. Shang, Md.K. Hasan, G.J. Ahammed, M. Li, H. Yin, J. Zhou, Applications of Nanotechnology in Plant Growth and Crop Protection: A Review, Molecules 24 (2019) 2558. https://doi.org/10.3390/molecules24142558.
[22] P. Landa, P. Dytrych, S. Prerostova, S. Petrova, R. Vankova, T. Vanek, Transcriptomic Response of Arabidopsis thaliana Exposed to CuO Nanoparticles, Bulk Material, and Ionic Copper, Environmental Science & Technology 51 (2017) 10814–10824. https://doi.org/10.1021/acs.est.7b02265.
[23] J. Borgatta, C. Ma, N. Hudson-Smith, W. Elmer, C.D. Plaza Pérez, R. De La Torre-Roche, N. Zuverza-Mena, C.L. Haynes, J.C. White, R.J. Hamers, Copper Based Nanomaterials Suppress Root Fungal Disease in Watermelon (*Citrullus lanatus*): Role of Particle Morphology, Composition and Dissolution Behavior, ACS Sustainable Chemistry & Engineering 6 (2018) 14847–14856. https://doi.org/10.1021/acssuschemeng.8b03379.
[24] X. Gao, A. Avellan, S. Laughton, R. Vaidya, S.M. Rodrigues, E.A. Casman, G.V. Lowry, CuO Nanoparticle Dissolution and Toxicity to Wheat (*Triticum aestivum)* in Rhizosphere Soil, Environmental Science & Technology 52 (2018) 2888–2897. https://doi.org/10.1021/acs.est.7b05816.
[25] L. Zhao, Q. Hu, Y. Huang, A.N. Fulton, C. Hannah-Bick, A.S. Adeleye, A.A. Keller, Activation of antioxidant and detoxification gene expression in cucumber plants exposed to a Cu(OH)(2) nanopesticide, Environmental Science: Nano 8 (2017) 1750–1760. https://doi.org/10.1039/c7en00358g.
[26] J. Yang, W. Cao, Y. Rui, Interactions between nanoparticles and plants: phytotoxicity and defense mechanisms, Journal of Plant Interactions. 12 (2017) 158–169. https://doi.org/10.1080/17429145.2017.1310944.
[27] A. Pérez-de-Luque, Interaction of Nanomaterials with Plants: What Do We Need for Real Applications in Agriculture?, Frontiers in Environmental Science 5 (2017) https://doi.org/10.3389/fenvs.2017.00012.
[28] T. Sabo-Attwood, J.M. Unrine, J.W. Stone, C.J. Murphy, S. Ghoshroy, D. Blom, P.M. Bertsch, L.A. Newman, Uptake, distribution and toxicity of gold nanoparticles in tobacco (*Nicotiana xanthi*) seedlings, Nanotoxicology 6 (2012) 353–360. https://doi.org/10.3109/17435390.2011.579631.
[29] A. Avellan, J. Yun, Y. Zhang, E. Spielman-Sun, J.M. Unrine, J. Thieme, J. Li, E. Lombi, G. Bland, G.V. Lowry, Nanoparticle Size and Coating Chemistry Control Foliar Uptake Pathways, Translocation, and Leaf-to-Rhizosphere Transport in Wheat, ACS Nano 13 (2019) 5291–5305. https://doi.org/10.1021/acsnano.8b09781.
[30] E. Spielman-Sun, E. Lombi, E. Donner, D. Howard, J.M. Unrine, G.V. Lowry, Impact of Surface Charge on Cerium Oxide Nanoparticle Uptake and Translocation by Wheat (*Triticum aestivum*), Environmental Science & Technology 51 (2017) 7361–7368. https://doi.org/10.1021/acs.est.7b00813.
[31] N.R. Meychik, I.P. Yermakov, Ion exchange properties of plant root cell walls, Plant and Soil 234 (2001) 181–193. https://doi.org/10.1023/A:1017936318435.
[32] P.K. Shukla, P. Misra, C. Kole, Uptake, Translocation, Accumulation, Transformation, and Generational Transmission of Nanoparticles in Plants, w C. Kole, D.S. Kumar, M.V.

Khodakovskaya (Eds.), Plant Nanotechnology, Springer International Publishing, Cham, (2016) 183–218. https://doi.org/10.1007/978-3-319-42154-4_8.
[33] M.F. Serag, N. Kaji, C. Gaillard, Y. Okamoto, K. Terasaka, M. Jabasini, M. Tokeshi, H. Mizukami, A. Bianco, Y. Baba, Trafficking and Subcellular Localization of Multiwalled Carbon Nanotubes in Plant Cells, ACS Nano 5 (2011) 493–499. https://doi.org/10.1021/nn102344t.
[34] M.Y. Kohatsu, M.T. Pelegrino, L.R. Monteiro, B.M. Freire, R.M. Pereira, P. Fincheira, O. Rubilar, G. Tortella, B.L. Batista, T.A. de Jesus, A.B. Seabra, C.N. Lange, Comparison of foliar spray and soil irrigation of biogenic CuO nanoparticles (NPs) on elemental uptake and accumulation in lettuce, Environmental Science and Pollution Research 28 (2021) 16350–16367. https://doi.org/10.1007/s11356-020-12169-x.
[35] M.Y. Kohatsu, C.N. Lange, M.T. Pelegrino, J.C. Pieretti, G. Tortella, O. Rubilar, B.L. Batista, A.B. Seabra, T.A. de Jesus, Foliar spraying of biogenic CuO nanoparticles protects the defence system and photosynthetic pigments of lettuce (*Lactuca sativa*), Journal of Cleaner Production 324 (2021) 129264. https://doi.org/10.1016/j.jclepro.2021.129264.
[36] F. Yasmeen, N.I. Raja, A. Razzaq, S. Komatsu, Proteomic and physiological analyses of wheat seeds exposed to copper and iron nanoparticles, Biochimica Et Biophysica Acta. Proteins and Proteomics 1865 (2017) 28–42. https://doi.org/10.1016/j.bbapap.2016.10.001.
[37] P.M.G. Nair, I.M. Chung, Physiological and molecular level effects of silver nanoparticles exposure in rice (*Oryza sativa* L.) seedlings, Chemosphere 112 (2014) 105–113. https://doi.org/10.1016/j.chemosphere.2014.03.056.
[38] L. Zhao, Y. Huang, A.S. Adeleye, A.A. Keller, Metabolomics Reveals Cu(OH) $_2$ Nanopesticide-Activated Anti-oxidative Pathways and Decreased Beneficial Antioxidants in Spinach Leaves, Environmental Science & Technology 51 (2017) 10184–10194. https://doi.org/10.1021/acs.est.7b02163.
[39] L. Zhao, Q. Hu, Y. Huang, A.A. Keller, Response at Genetic, Metabolic, and Physiological Levels of Maize (*Zea mays*) Exposed to a Cu(OH)2 Nanopesticide, ACS Sustainable Chemistry & Engineering 5 (2017) 8294–8301. https://doi.org/10.1021/acssuschemeng.7b01968.
[40] S. Rawat, V.L. R. Pullagurala, M. Hernandez-Molina, Y. Sun, G. Niu, J. A. Hernandez-Viezcas, J. R. Peralta-Videa, J. L. Gardea-Torresdey, Impacts of copper oxide nanoparticles on bell pepper (*Capsicum annum* L.) plants: a full life cycle study, Environmental Science: Nano 5 (2018) 83–95. https://doi.org/10.1039/C7EN00697G.
[41] C. Deng, Y. Wang, G. Navarro, Y. Sun, K. Cota-Ruiz, J.A. Hernandez-Viezcas, G. Niu, C. Li, J.C. White, J. Gardea-Torresdey, Copper oxide (CuO) nanoparticles affect yield, nutritional quality, and auxin associated gene expression in weedy and cultivated rice (*Oryza sativa* L.) grains, Science of The Total Environment 810 (2022) 152260. https://doi.org/10.1016/j.scitotenv.2021.152260.
[42] I. Jośko, M. Kusiak, P. Oleszczuk, M. Świeca, M. Kończak, M. Sikora, Transcriptional and biochemical response of barley to co-exposure of metal-based nanoparticles, Science of The Total Environment 782 (2021) 146883. https://doi.org/10.1016/j.scitotenv.2021.146883.
[43] S.J. Bradfield, P. Kumar, J.C. White, S.D. Ebbs, Zinc, copper, or cerium accumulation from metal oxide nanoparticles or ions in sweet potato: Yield effects and projected dietary intake from consumption, Plant Physiology and Biochemistry 110 (2017) 128–137. https://doi.org/10.1016/j.plaphy.2016.04.008.
[44] W.-M. Lee, Y.-J. An, H. Yoon, H.-S. Kweon, Toxicity and bioavailability of copper nanoparticles to the terrestrial plants mung bean (*Phaseolus radiatus*) and wheat (*Triticum aestivum*): plant agar test for water-insoluble nanoparticles, Environmental Toxicology and Chemistry 27 (2008) 1915–1921.
[45] W. Du, J.L. Gardea-Torresdey, R. Ji, Y. Yin, J. Zhu, J.R. Peralta-Videa, H. Guo, Physiological and Biochemical Changes Imposed by CeO2 Nanoparticles on Wheat: A Life Cycle Field Study, Environmental Science & Technology 49 (2015) 11884–11893. https://doi.org/10.1021/acs.est.5b03055.
[46] R. Rafique, Z. Zahra, N. Virk, M. Shahid, E. Pinelli, T.J. Park, J. Kallerhoff, M. Arshad, Dose-dependent physiological responses of *Triticum aestivum* L. to soil applied TiO2 nanoparticles:

Alterations in chlorophyll content, H2O2 production, and genotoxicity, Agriculture, Ecosystems & Environment 255 (2018) 95–101. https://doi.org/10.1016/j.agee.2017.12.010.
[47] J. Trujillo-Reyes, S. Majumdar, C.E. Botez, J.R. Peralta-Videa, J.L. Gardea-Torresdey, Exposure studies of core–shell Fe/Fe3O4 and Cu/CuO NPs to lettuce *(Lactuca sativa*) plants: Are they a potential physiological and nutritional hazard?, Journal of Hazardous Materials 267 (2014) 255–263. https://doi.org/10.1016/j.jhazmat.2013.11.067.
[48] R. Kaveh, Y.-S. Li, S. Ranjbar, R. Tehrani, C.L. Brueck, B. Van Aken, Changes in *Arabidopsis thaliana* Gene Expression in Response to Silver Nanoparticles and Silver Ions, Environmental Science & Technology 47 (2013) 10637–10644. https://doi.org/10.1021/es402209w.
[49] C. Peng, C. Xu, Q. Liu, L. Sun, Y. Luo, J. Shi, Fate and Transformation of CuO Nanoparticles in the Soil–Rice System during the Life Cycle of Rice Plants, Environmental Science & Technology 51 (2017) 4907–4917. https://doi.org/10.1021/acs.est.6b05882.
[50] P.L. Flaten, R.E. Karamanos, F.L. Walley, Mobility of copper from sulphate and chelate fertilizers in soils, Canadian Journal of Soil Science 84 (2004) 283–290. https://doi.org/10.4141/S03-070.
[51] C. Griffey, W. Brooks, M. Kurantz, W. Thomason, F. Taylor, D. Obert, R. Moreau, R. Flores, M. Sohn, K. Hicks, Grain composition of Virginia winter barley and implications for use in feed, food, and biofuels production, Journal of Cereal Science 51 (2010) 41–49. https://doi.org/10.1016/j.jcs.2009.09.004.
[52] C. Tricase, V. Amicarelli, E. Lamonaca, R. Leonardo Rana, Economic Analysis of the Barley Market and Related Uses, w Z. Tadele (Ed.), Grasses as Food and Feed, IntechOpen, (2018) https://doi.org/10.5772/intechopen.78967.
[53] S.M. Wazir, I. Ghobrial, Copper deficiency, a new triad: anemia, leucopenia, and myeloneuropathy, Journal of Community Hospital Internal Medicine Perspectives 7 (2017) 265–268. https://doi.org/10.1080/20009666.2017.1351289.
[54] N.K. Fageria, M.P.B. Filho, A. Moreira, C.M. Guimarães, Foliar Fertilization of Crop Plants, Journal of Plant Nutrition 32 (2009) 1044–1064. https://doi.org/10.1080/01904160902872826.
[55] K.A. Mosa, M. El-Naggar, K. Ramamoorthy, H. Alawadhi, A. Elnaggar, S. Wartanian, E. Ibrahim, H. Hani, Copper Nanoparticles Induced Genotoxicty, Oxidative Stress, and Changes in Superoxide Dismutase (SOD) Gene Expression in Cucumber (*Cucumis sativus*) Plants, Frontiers in Plant Science 9 (2018). https://doi.org/10.3389/fpls.2018.00872.
[56] S. Nayek, I. Choudhury, Haque, J. Nishika, S. Roy, Spectrophotometric Analysis of Chlorophylls and Carotenoids from Commonly Grown Fern Species by Using Various Extracting Solvents, Research Journal of Chemical Sciences 4 (2014) 2231–606. https://doi.org/10.1055/s-0033-1340072.
[57] J. Wessely-Szponder, Z. Bełkot, R. Bobowiec, U. Kosior-Korzecka, M. Wójcik, Transport induced inflammatory responses in horses, Polish Journal of Veterinary Sciences 18 (2015) 407–413. https://doi.org/10.1515/pjvs-2015-0052.
[58] R. Re, N. Pellegrini, A. Proteggente, A. Pannala, M. Yang, C. Rice-Evans, Antioxidant activity applying an improved ABTS radical cation decolorization assay, Free Radical Biology and Medicine 26 (1999) 1231–1237. https://doi.org/10.1016/S0891-5849(98)00315-3.
[59] A. Ippolito, A. El Ghaouth, C.L. Wilson, M. Wisniewski, Control of postharvest decay of apple fruit by *Aureobasidium pullulans* and induction of defense responses, Postharvest Biology and Technology 19 (2000) 265–272. https://doi.org/10.1016/S0925-5214(00)00104-6.
[60] M. Sikora, M. Świeca, Effect of ascorbic acid postharvest treatment on enzymatic browning, phenolics and antioxidant capacity of stored mung bean sprouts, Food Chemistry 239 (2018) 1160–1166. https://doi.org/10.1016/j.foodchem.2017.07.067.
[61] J.S. Assis, R. Maldonado, T. Muñoz, M.I. Escribano, C. Merodio, Effect of high carbon dioxide concentration on PAL activity and phenolic contents in ripening cherimoya fruit, Postharvest Biology and Technology 23 (2001) 33–39. https://doi.org/10.1016/S0925-5214(01)00100-4.
[62] M.A.M. Galeazzi, V.C. Sgarbieri, S.M. Constantinides, Isolation, Purification and Physicochemical Characterization of Polyphenoloxidases (PPO) from a Dwarf Variety of Banana (*Musa cavendishii* L), Journal of Food Science 46 (1981) 150–155. https://doi.org/10.1111/j.1365-2621.1981.tb14551.x.

[63] V.L. Singleton, R. Orthofer, R.M. Lamuela-Raventós, Analysis of total phenols and other oxidation substrates and antioxidants by means of folin-ciocalteu reagent, w Methods in Enzymology, Elsevier, (1999) 152–178. https://doi.org/10.1016/S0076-6879(99)99017-1.
[64] I. Jośko, M. Kusiak, B. Xing, P. Oleszczuk, Combined effect of nano-CuO and nano-ZnO in plant-related system: From bioavailability in soil to transcriptional regulation of metal homeostasis in barley, Journal of Hazardous Materials 416 (2021) 126230. https://doi.org/10.1016/j.jhazmat.2021.126230.
[65] M. Kusiak, M. Sozoniuk, C. Larue, R. Grillo, K. Kowalczyk, P. Oleszczuk, I. Jośko, Transcriptional response of Cu-deficient barley (*Hordeum vulgare* L.) to foliar-applied nano-Cu: Molecular crosstalk between Cu loading into plants and changes in Cu homeostasis genes, NanoImpact 31 (2023) 100472. https://doi.org/10.1016/j.impact.2023.100472.
[66] M.M. Bradford, A rapid and sensitive method for the quantitation of microgram quantities of protein utilizing the principle of protein-dye binding, Analytical Biochemistry 72 (1976) 248–254. https://doi.org/10.1016/0003-2697(76)90527-3.
[67] M. Minekus, M. Alminger, P. Alvito, S. Ballance, T. Bohn, C. Bourlieu, F. Carrière, R. Boutrou, M. Corredig, D. Dupont, C. Dufour, L. Egger, M. Golding, S. Karakaya, B. Kirkhus, S.L. Feunteun, U. Lesmes, A. Macierzanka, A. Mackie, S. Marze, D. Mcclements, O. Ménard, I. Recio, C.N. Santos, R. Singh, G. Vegarud, M. Wickham, W. Weitschies, A. Brodkorb, A standardised static in vitro digestion method suitable for food - an international consensus, Food & Function (2014) https://doi.org/10.1039/c3fo60702j.
[68] B.V. McCleary, N. Sloane, A. Draga, I. Lazewska, Measurement of Total Dietary Fiber Using AOAC Method 2009.01 (AACC International Approved Method 32-45.01): Evaluation and Updates, Cereal Chemistry Journal 90 (2013) 396–414. https://doi.org/10.1094/CCHEM-10-12-0135-FI.
[69] J. Lee, R.W. Durst, R.E. Wrolstad, Collaborators:, T. Eisele, M.M. Giusti, J. Hach, H. Hofsommer, S. Koswig, D.A. Krueger, S. Kupina;, S.K. Martin, B.K. Martinsen, T.C. Miller, F. Paquette, A. Ryabkova, G. Skrede, U. Trenn, J.D. Wightman, Determination of Total Monomeric Anthocyanin Pigment Content of Fruit Juices, Beverages, Natural Colorants, and Wines by the pH Differential Method: Collaborative Study, Journal of AOAC INTERNATIONAL 88 (2005) 1269–1278. https://doi.org/10.1093/jaoac/88.5.1269.
[70] P. Arancibia-Avila, F. Toledo, E. Werner, M. Suhaj, H. Leontowicz, M. Leontowicz, A.L. Martinez-Ayala, P. Paśko, S. Gorinstein, Partial characterization of a new kind of Chilean Murtilla-like berries, Food Research International 44 (2011) 2054–2062. https://doi.org/10.1016/j.foodres.2011.01.016.
[71] W. Brand-Williams, M.E. Cuvelier, C. Berset, Use of a free radical method to evaluate antioxidant activity, LWT - Food Science and Technology 28 (1995) 25–30. https://doi.org/10.1016/S0023-6438(95)80008-5.
[72] D.M. Hanafy, P.D. Prenzler, G.E. Burrows, D. Ryan, S. Nielsen, S.A. El Sawi, T.S. El Alfy, E.H. Abdelrahman, H.K. Obied, Biophenols of mints: Antioxidant, acetylcholinesterase, butyrylcholinesterase and histone deacetylase inhibition activities targeting Alzheimer's disease treatment, Journal of Functional Foods 33 (2017) 345–362. https://doi.org/10.1016/j.jff.2017.03.027.
[73] M. Öztürk, M.E. Duru, Ş. Kivrak, N. Mercan-Doğan, A. Türkoglu, M.A. Özler, In vitro antioxidant, anticholinesterase and antimicrobial activity studies on three Agaricus species with fatty acid compositions and iron contents: A comparative study on the three most edible mushrooms, Food and Chemical Toxicology. 49 (2011) 1353–1360. https://doi.org/10.1016/j.fct.2011.03.019.
[74] P. Denev, M. Kratchanova, M. Ciz, A. Lojek, O. Vasicek, P. Nedelcheva, D. Blazheva, R. Toshkova, E. Gardeva, L. Yossifova, P. Hyrsl, L. Vojtek, Biological activities of selected polyphenol-rich fruits related to immunity and gastrointestinal health, Food Chemistry 157 (2014) 37–44. https://doi.org/10.1016/j.foodchem.2014.02.022.
[75] J.-T. Guo, H.-L. Lee, S.-H. Chiang, F.-I. Lin, C.-Y. Chang, Antioxidant Properties of the Extracts from Different Parts of Broccoli in Taiwan, Journal of Food and Drug Analysis 9 (2020) https://doi.org/10.38212/2224-6614.2795.

[76] A.A. Keller, A.S. Adeleye, J.R. Conway, K.L. Garner, L. Zhao, G.N. Cherr, J. Hong, J.L. Gardea-Torresdey, H.A. Godwin, S. Hanna, Z. Ji, C. Kaweeteerawat, S. Lin, H.S. Lenihan, R.J. Miller, A.E. Nel, J.R. Peralta-Videa, S.L. Walker, A.A. Taylor, C. Torres-Duarte, J.I. Zink, N. Zuverza-Mena, Comparative environmental fate and toxicity of copper nanomaterials, NanoImpact 7 (2017) 28–40. https://doi.org/10.1016/j.impact.2017.05.003.

[77] N. Joudeh, D. Linke, Nanoparticle classification, physicochemical properties, characterization, and applications: a comprehensive review for biologists, Journal of Nanobiotechnology 20 (2022) 262. https://doi.org/10.1186/s12951-022-01477-8.

[78] S.V. Gudkov, I.V. Baimler, O.V. Uvarov, V.V. Smirnova, M.Y. Volkov, A.A. Semenova, A.B. Lisitsyn, Influence of the Concentration of Fe and Cu Nanoparticles on the Dynamics of the Size Distribution of Nanoparticles, Frontiers in Physics 8 (2020) 622551. https://doi.org/10.3389/fphy.2020.622551.

[79] Y. Dai, Z. Wang, J. Zhao, L. Xu, L. Xu, X. Yu, Y. Wei, B. Xing, Interaction of CuO nanoparticles with plant cells: internalization, oxidative stress, electron transport chain disruption, and toxicogenomic responses, Environmental Science: Nano 5 (2018) 2269–2281. https://doi.org/10.1039/C8EN00222C.

[80] C. Kaweeteerawat, C.H. Chang, K.R. Roy, R. Liu, R. Li, D. Toso, H. Fischer, A. Ivask, Z. Ji, J.I. Zink, Z.H. Zhou, G.F. Chanfreau, D. Telesca, Y. Cohen, P.A. Holden, A.E. Nel, H.A. Godwin, Cu Nanoparticles Have Different Impacts in *Escherichia coli* and *Lactobacillus brevis* than Their Microsized and Ionic Analogues, ACS Nano 9 (2015) 7215–7225. https://doi.org/10.1021/acsnano.5b02021.

[81] W. Tan, Q. Gao, C. Deng, Y. Wang, W.-Y. Lee, J.A. Hernandez-Viezcas, J.R. Peralta-Videa, J.L. Gardea-Torresdey, Foliar Exposure of Cu(OH)2 Nanopesticide to Basil (*Ocimum basilicum*): Variety-Dependent Copper Translocation and Biochemical Responses, Journal of Agricultural and Food Chemistry 66 (2018) 3358–3366. https://doi.org/10.1021/acs.jafc.8b00339.

[82] Y. Zhang, J. Yan, A. Avellan, X. Gao, K. Matyjaszewski, R.D. Tilton, G.V. Lowry, Temperature- and pH-Responsive Star Polymers as Nanocarriers with Potential for *in Vivo* Agrochemical Delivery, ACS Nano 14 (2020) 10954–10965. https://doi.org/10.1021/acsnano.0c03140.

[83] K. Ravet, M. Pilon, Copper and Iron Homeostasis in Plants: The Challenges of Oxidative Stress, Antioxidants & Redox Signaling 19 (2013) 919–932. https://doi.org/10.1089/ars.2012.5084.

[84] T. del Pozo, V. Cambiazo, M. González, Gene expression profiling analysis of copper homeostasis in *Arabidopsis thaliana*, Biochemical and Biophysical Research Communications 393 (2010) 248–252. https://doi.org/10.1016/j.bbrc.2010.01.111.

[85] L.L. Martins, M.P. Mourato, Effect of Excess Copper on Tomato Plants: Growth Parameters, Enzyme Activities, Chlorophyll, and Mineral Content, Journal of Plant Nutrition 29 (2006) 2179–2198. https://doi.org/10.1080/01904160600972845.

[86] R.H. Barbosa, L.A. Tabaldi, F.R. Miyazaki, M. Pilecco, S.O. Kassab, D. Bigaton, Foliar copper uptake by maize plants: effects on growth and yield, Ciência Rural 43 (2013) 1561–1568. https://doi.org/10.1590/S0103-84782013000900005.

[87] R.K. Tewari, P. Kumar, P.N. Sharma, Antioxidant responses to enhanced generation of superoxide anion radical and hydrogen peroxide in the copper-stressed mulberry plants, Planta 223 (2006) 1145–1153. https://doi.org/10.1007/s00425-005-0160-5.

[88] Z. Zhang, M. Ke, Q. Qu, W.J.G.M. Peijnenburg, T. Lu, Q. Zhang, Y. Ye, P. Xu, B. Du, L. Sun, H. Qian, Impact of copper nanoparticles and ionic copper exposure on wheat (*Triticum aestivum* L.) root morphology and antioxidant response, Environmental Pollution 239 (2018) 689–697. https://doi.org/10.1016/j.envpol.2018.04.066.

[89] A. Cuypers, J. Vangronsveld, H. Clijsters, Biphasic effect of copper on the ascorbate-glutathione pathway in primary leaves of *Phaseolus vulgaris* seedlings during the early stages of metal assimilation, Physiologia Plantarum 110 (2000) 512–517. https://doi.org/10.1111/j.1399-3054.2000.1100413.x.

[90] M. Rizwan, S. Ali, M.F. Qayyum, Y.S. Ok, M. Adrees, M. Ibrahim, M. Zia-ur-Rehman, M. Farid, F. Abbas, Effect of metal and metal oxide nanoparticles on growth and physiology of

globally important food crops: A critical review, Journal of Hazardous Materials 322 (2017) 2–16. https://doi.org/10.1016/j.jhazmat.2016.05.061.

[91] M.G. Mostofa, M.A. Hossain, M. Fujita, L.-S.P. Tran, Physiological and biochemical mechanisms associated with trehalose-induced copper-stress tolerance in rice, Scientific Reports 5 (2015) 11433. https://doi.org/10.1038/srep11433.

[92] C.O. Ogunkunle, B. Bornmann, R. Wagner, P.O. Fatoba, R. Frahm, D. Lützenkirchen-Hecht, Copper uptake, tissue partitioning and biotransformation evidence by XANES in cowpea (*Vigna unguiculata* L) grown in soil amended with nano-sized copper particles, Environmental Nanotechnology, Monitoring & Management 12 (2019) 100231. https://doi.org/10.1016/j.enmm.2019.100231.

[93] E. Ngadze, D. Icishahayo, T.A. Coutinho, J.E. van der Waals, Role of Polyphenol Oxidase, Peroxidase, Phenylalanine Ammonia Lyase, Chlorogenic Acid, and Total Soluble Phenols in Resistance of Potatoes to Soft Rot, Plant Disease 96 (2012) 186–192. https://doi.org/10.1094/PDIS-02-11-0149.

[94] A.M. Santos-Espinoza, D. González-Mendoza, V.M. Ruiz-Valdiviezo, M.C. Luján-Hidalgo, F. Jonapa-Hernández, B. Valdez-Salas, F.A. Gutiérrez-Miceli, Changes in the physiological and biochemical state of peanut plants (*Arachis hypogaea* L.) induced by exposure to green metallic nanoparticles, International Journal of Phytoremediation 23 (2020) 1–8. https://doi.org/10.1080/15226514.2020.1856037.

[95] B. Printz, S. Lutts, J.-F. Hausman, K. Sergeant, Copper Trafficking in Plants and Its Implication on Cell Wall Dynamics, Frontiers in Plant Science 7 (2016) https://doi.org/10.3389/fpls.2016.00601.

[96] H. Zafar, A. Ali, M. Zia, CuO Nanoparticles Inhibited Root Growth from *Brassica nigra* Seedlings but Induced Root from Stem and Leaf Explants, Applied Biochemistry and Biotechnology 181 (2017) 365–378. https://doi.org/10.1007/s12010-016-2217-2.

[97] Y. Ma, N. Wei, Q. Wang, Z. Liu, W. Liu, Genome-wide identification and characterization of the heavy metal ATPase (HMA) gene family in *Medicago truncatula* under copper stress, International Journal of Biological Macromolecules 193 (2021) 893–902. https://doi.org/10.1016/j.ijbiomac.2021.10.197.

[98] A. Garcia-Molina, N. Andrés-Colás, A. Perea-García, S. del Valle-Tascón, L. Peñarrubia, S. Puig, The intracellular *Arabidopsis* COPT5 transport protein is required for photosynthetic electron transport under severe copper deficiency: Characterization of the *Arabidopsis* COPT5 protein, The Plant Journal 65 (2011) 848–860. https://doi.org/10.1111/j.1365-313X.2010.04472.x.

[99] R. Kapilan, M. Vaziri, J.J. Zwiazek, Regulation of aquaporins in plants under stress, Biological Research 51 (2018) https://doi.org/10.1186/s40659-018-0152-0.

[100] L. Peñarrubia, P. Romero, A. Carrió-Seguí, A. Andrés-Bordería, J. Moreno, A. Sanz, Temporal aspects of copper homeostasis and its crosstalk with hormones, Frontiers in Plant Science 6 (2015) https://doi.org/10.3389/fpls.2015.00255.

[101] I. Johansson, M. Karlsson, U. Johanson, C. Larsson, P. Kjellbom, The role of aquaporins in cellular and whole plant water balance, Biochimica et Biophysica Acta (BBA) - Biomembranes 1465 (2000) 324–342. https://doi.org/10.1016/S0005-2736(00)00147-4.

[102] A. Banerjee, A. Roychoudhury, The role of aquaporins during plant abiotic stress responses, w Plant Life Under Changing Environment, Elsevier, (2020) 643–661. https://doi.org/10.1016/B978-0-12-818204-8.00028-X.

[103] S. Vats, S. Sudhakaran, A. Bhardwaj, R. Mandlik, Y. Sharma, S. Kumar, D.K. Tripathi, H. Sonah, T.R. Sharma, R. Deshmukh, Targeting aquaporins to alleviate hazardous metal(loid)s imposed stress in plants, Journal of Hazardous Materials 408 (2021) 124910. https://doi.org/10.1016/j.jhazmat.2020.124910.

[104] C.M. Cohu, M. Pilon, Cell Biology of Copper, w : R. Hell, R.-R. Mendel (Eds.), Cell Biology of Metals and Nutrients, Springer Berlin Heidelberg, Berlin, Heidelberg, (2010) 55–74. https://doi.org/10.1007/978-3-642-10613-2_3.

[105] W. Jiang, L. Yang, Y. He, H. Zhang, W. Li, H. Chen, D. Ma, J. Yin, Genome-wide identification and transcriptional expression analysis of superoxide dismutase (SOD) family in wheat (*Triticum aestivum*), PeerJ 7 (2019) e8062. https://doi.org/10.7717/peerj.8062.

[106] C.M. Rico, M.I. Morales, A.C. Barrios, R. McCreary, J. Hong, W.-Y. Lee, J. Nunez, J.R. Peralta-Videa, J.L. Gardea-Torresdey, Effect of Cerium Oxide Nanoparticles on the Quality of Rice (*Oryza sativa* L.) Grains, Journal of Agricultural and Food Chemistry 61 (2013) 11278–11285. https://doi.org/10.1021/jf404046v.

[107] L. Lahouar, A. El Arem, F. Ghrairi, H. Chahdoura, H. Ben Salem, M. El Felah, L. Achour, Phytochemical content and antioxidant properties of diverse varieties of whole barley (*Hordeum vulgare* L.) grown in Tunisia, Food Chemistry 145 (2014) 578–583. https://doi.org/10.1016/j.foodchem.2013.08.102.

[108] H. Zhao, W. Fan, J. Dong, J. Lu, J. Chen, L. Shan, Y. Lin, W. Kong, Evaluation of antioxidant activities and total phenolic contents of typical malting barley varieties, Food Chemistry 107 (2008) 296–304. https://doi.org/10.1016/j.foodchem.2007.08.018.

7. Publikacje wchodzące w skład rozprawy doktorskiej oraz oświadczenia współautorów

PI

Kusiak M., Oleszczuk P., Jośko I.

Cross-examination of engineered nanomaterials in crop production: Application and related implications

Journal of Hazardous Materials (2022) T. 424 s. 127374

DOI: 10.1016/j.jhazmat.2021.127374

$IF_{(2022)}$ = 13.6

Punkty MEiN = 200

Journal of Hazardous Materials 424 (2022) 127374

Contents lists available at ScienceDirect

Journal of Hazardous Materials

journal homepage: www.elsevier.com/locate/jhazmat

Review

Cross-examination of engineered nanomaterials in crop production: Application and related implications

Magdalena Kusiak [a], Patryk Oleszczuk [b], Izabela Jośko [a,*]

[a] Institute of Plant Genetics, Breeding and Biotechnology, Faculty of Agrobioengineering, University of Life Sciences, Lublin, Poland
[b] Department of Radiochemistry and Environmental Chemistry, Faculty of Chemistry, Maria Curie–Skłodowska University, Lublin, Poland

ARTICLE INFO

Editor: Guillaume Echevarria

Keywords:
Engineered nanomaterials
Crop production
Plant response
Omics analysis

ABSTRACT

The review presents the current knowledge on the development and implementation of nanotechnology in crop production, giving particular attention to potential opportunities and challenges of the use of nano-sensors, nano-pesticides, and nano-fertilizers. Due to the size-dependent properties, e.g. high reactivity, targeted and controlled delivery of active ingredients, engineered nanomaterials (ENMs) are expected to be more efficient agrochemicals than conventional agents. Growing production and usage of ENMs result in the spread of ENMs in the environment. Because plants constitute an important component of the agri-ecosystem, they are subjected to the ENMs activity. A number of studies have confirmed the uptake and translocation of ENMs by plants as well as their positive/negative effects on plants. Here, these endpoints are briefly summarized to show the diversity of plant responses to ENMs. The review includes a detailed molecular analysis of ENMs-plant interactions. The transcriptomics, proteomics and metabolomics tools have been very recently employed to explore ENMs-induced effects *in planta*. The omics approach allows a comprehensive understanding of the specific machinery of ENMs occurring at the molecular level. The summary of data will be valuable in defining future studies on the ENMs-plant system, which is crucial for developing a suitable strategy for the ENMs usage.

1. Introduction

The global population by 2050 will reach nearly 10 billion people. It has been estimated that agricultural production must increase by 70% to meet the food demand (Mueller et al., 2012). Considering the shrinking amount of arable land, the deficiency of water resources, the climate changes, and the low efficiency of traditional agrochemicals, it is crucial to find an alternative way to increase crop yields (Mueller et al., 2012). Conventional practices of breeding stress-tolerant or high-yielding crop varieties are of low efficiency (Sayadi Maazou et al., 2016), and genetically modified crops raise a public concern about potential risk for human health (e.g. allergenicity, toxicity) and environmental safety (e.g. uncontrolled transgene spread into environment) (Azevedo and Araujo, 2003; Key et al., 2008). Therefore, there is a pressing need to develop new sustainable pathways to protect plants and enhance yield to ensure food security (Prasad et al., 2017). The intense development of nanotechnology over the last two decades has provided numerous innovative applications for electronics, material science, cosmetics, food sector, and also agriculture. Due to nano-metric size (1–100 nm), the larger surface area and the high the surface area to volume ratio, ENMs are characterized by unique physico-chemical properties (e.g. higher reactivity, catalytic activity, magnetic properties) that differ from those of their bulk counterparts (Bowman and Hodge, 2006; Dreaden et al., 2012; Pagano et al., 2016). Because of the superior efficiency of ENMs compared to bulk compounds, ENMs are promising agents in the agri-sector for ensuring sustainable crop production (fertilization, pathogen detection, crop protection from abiotic and biotic stress) (Lowry et al., 2019; Mishra et al., 2017; Shang et al., 2019).

There is a widespread agreement that the growing number of nano-products and their usage (Duhan et al., 2017) lead to increased release and accumulation of ENMs in the environment, including soil (Rajput et al., 2020). It is estimated that around 9–38% of ENMs from nano-products end up in soils, posing a risk of impact on biota (Bundschuh et al., 2018). Therefore, the unravelling effect of ENMs on plants, as one of the most significant components of the agro-ecosystem, is of utmost importance (Mishra et al., 2017). One of the important aspects in studying the ENM-plant interaction is uptake and translocation of ENMs, which is a key of importance due to the risk of ENMs accumulation in the food chain (Avellan et al., 2019; Su et al., 2019). The uptake and further

* Correspondence to: Institute of Plant Genetics, Breeding and Biotechnology, Faculty of Agrobioengineering, Univerisity of Life Sciences in Lublin, 13 Akademicka Street, 20–950 Lublin, Poland.
E-mail address: izabela.josko@up.lublin.pl (I. Jośko).

https://doi.org/10.1016/j.jhazmat.2021.127374
Received 6 April 2021; Received in revised form 21 September 2021; Accepted 26 September 2021
Available online 29 September 2021

Nomenclature

2-DE	Two-dimensional gel electrophoresis
ABA8ox2	ABA 8′-hydroxylase
ABCG22	ATP-binding cassette G22
ABCB4	ATP-Binding Cassette B4
AChE	Acetylcholinesterase
AGL16	Agamous-like MADS-box protein AGL16
AGT	Alanine: glyoxylate aminotransferase
AKR4C8	Aldo-keto reductase family 4 member C8
ALP	Alkaline Phosphatase
AMT	Ammonium transporter
ANS	Anthocyanidin synthase
ANAC042	NAC domain containing protein 42
APTES	3-amminopropyltrimethoxysilane
Aqp2	Water channel protein Aqp2
APX1	L-ascorbate peroxidase 1
ASA1	Anthranilate synthase alpha subunit 1
ATAF1	NAC domain-containing protein 1
ATCTH	Zinc finger protein
ATCHX16	Sodium: hydrogen antiporter
AT4G30170	Peroxidase
ATHSP	Small heat shock protein
ATIREG2	Nickel transmembrane transporter
ATNR	High affinity nitrate transporter
BCB	Copper-ion binding
BCS	Biosilica
BIP3	Heat Shock Protein 70
bHLH	basic Helix–Loop–Helix
BSA	Bovine Serum Albumin
CAT	Catalase
CAX3	Calcium cation antiporter
CCH	Copper chaperone
CIPK6	CBL interacting protein kinase 6
CNT	Carbon nanotubes
COPT	Copper transporter
Cu-CNFs	Cu-carbon nanofibers
CYP	Cytochrome P450
DEGs	Differentially expressed genes
DELTA-OAT	Ornithine-delta-aminotransferase
DELTA-TIP	Delta tonoplast intrinsic protein
DNAJ	DNAJ chaperon protein
DNA-seq	DNA sequencing
ENMs	Engineered nanomaterials
FER	Ferretin
FLS	Flavonol synthase
FRET	Fluorescence resonance energy transfer
FRO	Ferric reduction oxidase
FSD1	Fe superoxide dismutase 1
FSNP	Fluorescent silica nanoparticles
ESP	Endosulfan pesticides
EXO70A1	Exocyst subunit exo70 family protein A1
GC-TOFMS	Gas chromatography/time-of-flight mass spectrometry
GA3ox1	Gibberellin 3-beta-dioxygenase 1
GO	Graphene oxide
GPX	Glutathione peroxidase
GST	Glutathione S-transferase
HeAptDNA	DNA aptamer that binds to hemin
HMA3	Heavy metal ATPase 3
HRGP1	Hydroxyproline-rich glycoproteins 1
IAA	Indole-3-acetic acid
IRT	Iron transporter protein
IRT1	Cadmium, copper, iron, manganese and zinc transporter
IRT2	Iron and zinc transporter
JAC	Jacalin lectin family
JAL5	Jacalin-related lectin 5
LC-MS	Liquid chromatography–mass spectrometry
LM6M	Anti-pectic polysaccharide (α-1,5-arabinan) antibody
LTP2	Lipid transfer proteins 2
MAF2	MADS affecting flowering 2
MALDI	Matrix-assisted laser desorption/ionization
MC8	Metacaspase 8
miRNA	microRNA
MS	Mass spectrometry
MSAP	Methylation sensitive amplification polymorphism
MS/MS	Tandem mass spectrometry
MT	Metallothionein
MTPA2	Zinc ion transmembrane transporter
MTPc3	Cation efflux family protein
MWCNTs	Multi-walled carbon nanotubes
MYB	Myb-related protein
NAC1	NAC domain-containing protein 21
NAS	Nicotianamine synthase
NCED3	9-cis-Epoxycarotenoid Dioxygenase 3
nIR	Near-infrared
NIP	NOD26-like intrinsic proteins
NRAMP1	Manganese transmembrane transporter
NRAMP4	Metal transporter Nramp4
NRT	Nitrate transporter
PAHs	Polycyclic aromatic hydrocarbons
PAL	Phenylalanine ammonia-lyase
PAP1	Phosphatidic acid phosphatase 1
PDC2	Pyruvate decarboxylase 2
PHT	Phosphate transporter
PIPs	Plasma membrane intrinsic proteins
POD	Peroxidase
PR4	Pathogenesis-related 4
PRXCA	Peroxidase 33
QD	Quantum dots
RAPD	Random amplification of polymorphic DNA
RBK1	ROP binding protein kinases 1
RD22	Responsive to desiccation 22
RLK	Receptor-like kinases
RHL41	Zinc finger protein
RHS12	Root hair-specific
RNA-seq	RNA sequencing
ROS	Reactive oxygen species
Rubpy	Tris(bipyridine)ruthenium(II)
SERS	Surface-enhanced Raman scattering
SDS	Sodium dodecyl sulfate
SNRK2	SNF1-related protein kinases
SIPs	Small basic intrinsic proteins
SNRK2–9	SNRK2.9, SNF1-related protein kinase 2.9
SOD	Superoxide dismutase
SULTR1;3	Sulfate transporter
SUS3	Sucrose synthase 3
SWCNTs	Single-walled carbon nanotubes
TCA	Tricarboxylic acid
TIPs	Tonoplast intrinsic proteins
TUA2	Tubulina 2
WRKY	WRKY transcription factor
YSL2	Yellow Stripe-Like2
ZIP	Zinc transporter
XTH14	Xyloglucan endotransglucosylase

translocation of ENMs greatly depend on their properties (size, type, charge, coating) (Yang et al., 2017), method of application (seed dressing/soil/foliar application) (Pradas del Real et al., 2017; Rossi et al., 2019; Vannini et al., 2013), medium type (liquid, soil, agar) (Lee et al., 2012), and characteristics (pH, texture, moisture, content of organic matter, clays) (Dimkpa, 2018; Larue et al., 2018). There is conflicting data regarding possible translocation of ENMs in plants. Although, numerous studies observed roots-to-leaves (Ma et al., 2017; Zhang et al., 2012; Tamez et al., 2019) and leaves-to-roots translocation (Avellan et al., 2019; Lu et al., 2020; Li et al., 2018a) of ENMs and/or released ions in plants. Others confirmed lack (Milewska-Hendel et al., 2017; Birbaum et al., 2010) or trace uptake and loading of ENMs from the application site (Schwab et al., 2016; Avellan et al., 2017), possibly limited by plant system (cell wall, Casparian strip, root exudates) (Schwab et al., 2016; Avellan et al., 2017) and ENMs properties (size, charge, shape, dose) (Liu et al., 2019; Pérez-de-Luque, 2017; Graf et al., 2018). The knowledge about the distribution of ENMs as well as their components *in planta* is crucial for both crop fertilization and protection, as well as for understanding their non-target effects. Such studies would be important for legislation and safety purposes (Amenta et al., 2015; Gupta and Xie, 2018). In the European Union, ENMs are covered by the REACH regulation (*Registration, Evaluation, Authorisation and Restriction of Chemicals*) and CLP (*Classification, Labelling and Packaging*) regulations (European Commission, 2011; OECD, 2013). Other countries have also established a legal framework concerning the use of ENMs in agriculture and food sectors (Bowman and Hodge, 2006).

To date, a number of studies have shown contradictory responses to the ENMs depending on ENMs type (Pagano et al., 2016), size (Syu et al., 2014), coating (Avellan et al., 2017), dose (Rafique et al., 2018), application mode, plant species, growth conditions, and duration of exposure (Avellan et al., 2019; Gogos et al., 2012; Wang et al., 2012). While the positive impact of ENMs on plants and their potential in agriculture have been shown (Gupta et al., 2018; Hong et al., 2005; Yasmeen et al., 2017) (e.g. increased number of grains, higher chlorophyll and protein content) (Gupta et al., 2018; Hong et al., 2005; Yasmeen et al., 2017), many studies have reported adverse effects of ENMs on plants (e.g. decreased biomass, increased ROS accumulation, chromosomal aberrations) (Zhang et al., 2018b; Nair and Chung, 2014; Qian et al., 2013; Pakrashi et al., 2014). The phytotoxicity of ENMs was related with to biochemical reactions, mainly through the generation of ROS triggering oxidative stress (Chung et al., 2019; Landa et al., 2015; Wan et al., 2019). Moreover, the strong tendency of ENMs to form aggregates induced adhesion on surface plant tissues entailing inhibition of water and nutrient transport and a drop of plant growth (Wan et al., 2019; Ma et al., 2018). The majority of current studies have reported morphological, physiological, and biochemical changes in plants upon exposure to ENMs (Rafique et al., 2018; Du et al., 2015; Marchiol et al., 2016). Recently, the molecular effects of ENMs in plants have been increasingly examined (Landa et al., 2017; Taylor et al., 2014; Tiwari et al., 2016). The development of omics techniques (transcriptomics, proteomics, metabolomics) has opened new opportunities for understanding of ENM-specific activity *in planta* (Fig. 1) (Yasmeen et al., 2017; Tiwari et al., 2016; Majumdar and Keller, 2020; Ruotolo et al., 2018). The transcriptomic analysis has been implemented for the identification of predictive biomarkers of ENMs phytotoxicity (Syu et al., 2014; Kohan-Baghkheirati and Geisler-Lee, 2015; Kaveh et al., 2013; Wang et al., 2017). As over 70% of the genes in plants are subjected to alternative splicing (Kim et al., 2007), proteomic and metabolomics analysis are key factors for better understanding correlation between ENMs application and phenotypic responses (Hossain et al., 2020; Li et al., 2018c; Das et al., 2017). The constantly growing database regarding the effects of ENMs on plants needs to be successfully revised to give the full picture of ENM-plant interactions. In this review, we present the state-of-the-art knowledge on plant response to ENMs, from molecular to organism level, which may be valuable to develop strategies for application and the use of ENMs in a plant-friendly and efficient way.

2. ENMs for plant growth and protection

The studies on ENMs application in an agricultural sector primarily focus on 3 areas: pathogen and contaminant detection (Arduini et al., 2016), crop protection against abiotic and biotic stress (Das and Das, 2019; Lamsal et al., 2011) and improvement in yield quantity and quality (Fig. 2) (Kah et al., 2019). Because of the multi-directional

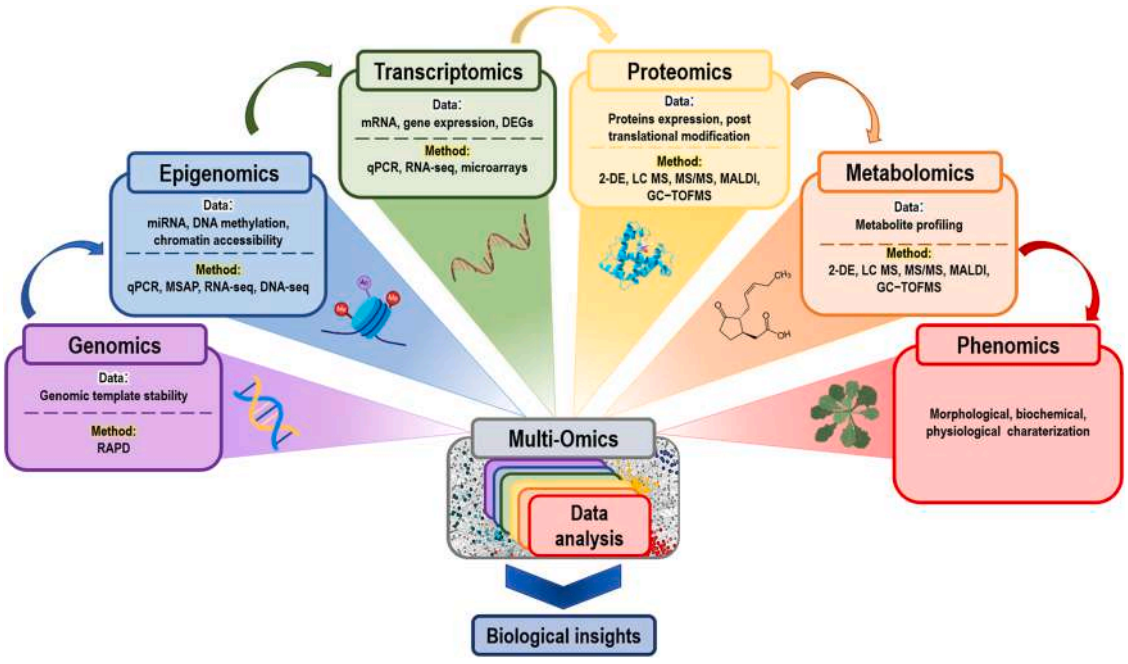

Fig. 1. The overall diagram of relationship between branches of single- and multi-omics data analysis. Although every singular omics have a significant importance for better understanding of plant regulatory mechanisms in response to ENMs, their combined results provide a holistic understanding of regulatory mechanisms of plant responses to ENMs.

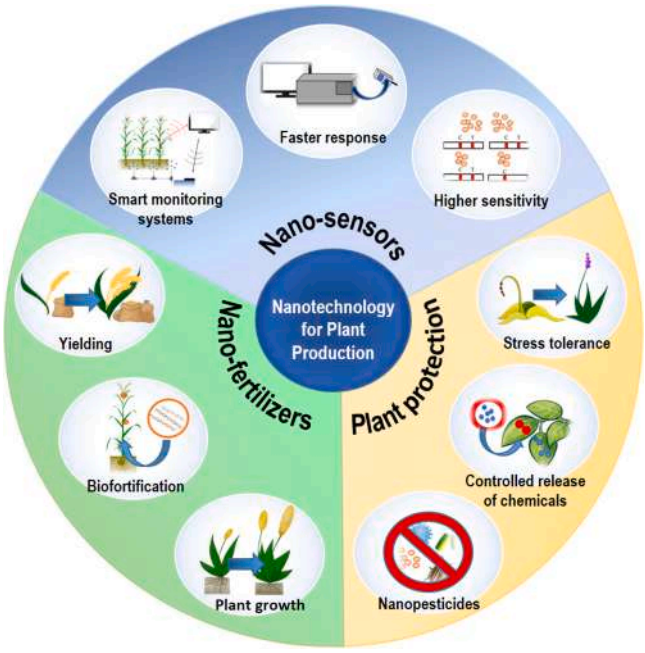

Fig. 2. Potential application of nanotechnology in plant production including 3 of the most extensively studied areas of nanoagrotechnology.

applications of ENMs and their significance for a agri-food sector, agronanotechnology becomes the next revolution in this sector comparable to the Green Revolution (Lowry et al., 2019).

2.1. Nano-sensors

Modern nano-sensors are integrated automated tools capable of detecting and identifying various signals from the environment (Zeinhom et al., 2018). Nano-sensors can be an efficient platform for monitoring the quality of crops, in particular for detecting trace contaminants, e.g. pesticide residues (Mishra et al., 2017; Grewal et al., 2017). Furthermore, studies have shown that functionalized metal- and carbon-based ENMs exhibit increased sensing potential (Arduini et al., 2016; Lupan et al., 2018; Campos et al., 2017) due to the improved ability to bind with biomolecules, which enhances signal amplification and detection (Jianrong et al., 2004). CNTs, especially MWCNTs, have been widely tested for sensing applications due to their rapid electron transfer, high accessible surface area, and mechanical strength (Cai and Du, 2008; Sun et al., 2012; Giraldo et al., 2015; Wu et al., 2020; Pan et al., 2019). For instance, biosensor based on the immobilization of AChE on MWCNTs-cross-linked cellulose acetate composite enabled detection of carbaryl in garlic samples with the accuracy comparable to HPLC method (the relative deviations between these methods were 7.1% to − 8.3%) (Cai and Du, 2008). Chen et al. (2008) also developed an AChE-based sensor enhanced with MWCNTs for the detection of selected organic contaminants in beverages. The coverage of glassy carbon electrodes with MWCNTs increased the surface, facilitated the electrochemical polymerization of prussian blue, and enhanced the enzymatic activity of AChE, which allowed the detection of dichlorvos and carbofuran at the level 0.04 and 0.1 ppb, respectively (Chen et al., 2008). Campos et al. (2017) proved that coating carbon dots with vitamin B_{12} can be used to selectively detect phenolic carbofuran. An increased fluorescence intensity of nano-sensor permitted the determination of the carbofuran phenol 3-Keto pesticide in a concentration range of 12.2×10^{-5}–2.5×10^{-3} M in soy sauce in the presence of other pesticides (Campos et al., 2017). Metal-based ENMs have also demonstrated the feasibility of designing nano-sensors. The benefits of metal-based ENMs include the ability to catalyze various biochemical reactions, facilitated electron transfer and shorter regeneration period in comparison to the conventional homogeneous catalysts (Jianrong et al., 2004). Among ENMs, nano-Au is one of the most often used, especially for the colorimetric and electrochemical-based pesticide detection systems (Goel and Arora, 2018; Tang et al., 2019). Due to high adsorption capacity and stability nano-Au can be easily functionalized for selective testing (Fang et al., 2017). Additionally, size-dependent optical properties of nano-Au (hyper-quenching ability for fluorescence and SERS capability) enhance sensing ability in optical sensors (Halvorson and Vikesland, 2010; Tong et al., 2011; Mortazavi et al., 2011). The use of nano-Au coated films in biosensor led to an increase of the electrochemical response, allowing detection of organochlorine ESP at a concentration of 1 ppm (Goel and Arora, 2018). Additionally, nano-Au catalyzed degradation of ESP into non-toxic products (Goel and Arora, 2018). Embedding of nano-Ag on glass beads surface for SERS resulted in 50- (chlorpyrifos) and 10-times (imidacloprid) lower detection limit of pesticide residues (Tang et al., 2019) in comparison to non-modified SERS method (Huang et al., 2015; Hou et al., 2015).

QDs are associated with FRET technology for a quick detection of biological markers (Zhang et al., 2009; Antonacci et al., 2018). The main advantages of the designed QDs-based FRET sensor were broad excitation spectra with a narrow and defined emission peak as well as a 10–100 times higher molar extinction coefficient compared to non-nano-sensors (Stanisavljevic et al., 2015). A study revealed that multicolor QDs excited from one source by common fluorescent dyes showed no emission signal overlap, which results in brighter probes comparing to conventional fluorophores (Stanisavljevic et al., 2015). That advantage over classical biosensors is further proven by easy modification of surface chemical properties of QDs (Zrazhevskiy et al., 2010). Coating Zn-QDs with APTES (containing SiO_2) prevented QDs from spontaneous aggregation, decomposition in water and enhanced binding capacity with pesticides (Sahoo et al., 2018). Zn-QDs coated with APTES contained free primary amine groups which determined pesticide-specific binding affinity for aldrin, tetradifon, glyphosate, and atrazine. Additionally, the pesticides with strong binding affinity to QDs like aldrin and tetradifon underwent photocatalytic degradation (Sahoo et al., 2018).

Besides the potential application of ENMs as sensors of chemical contaminants, ENMs may be used to detect fungal, bacterial and viral pathogens in crops (Fung and Clark, 2004; Rishi, 2009; Jechalke et al., 2019). A large number of nano-sensors are developed as an alternative for currently widely used methods of biological contaminants detection (ELISA, PCR, RT-PCR, blot immunoassay) (Hariharan and Prasannath, 2021; Khiyami et al., 2014; Fang and Ramasamy, 2015). DNA-functionalized nano-Au probes effectively hybridized with *Phytophthora infestans* ssDNA at a concentration of 0.1 pg mL^{-1} in potato leaves and stems (Zhan et al., 2018). The high specificity of nano-Au biosensor allowed to distinguish between closely related *Phytophthora* species (Zhan et al., 2018) with a 100-times lower detection limit than the previously proposed method based on loop-mediated isothermal amplification assay (Dai et al., 2012). Yao et al. (2009) showed the potential of fluorescent nano-SiO_2 for the detection of *Xanthomonas axonopodis* pv. *vesicatoria* that caused spot disease in the *Solanaceae* plant family. Rubpy-doped nano-SiO_2 exhibited higher and stable fluorescence intensity in comparison to pure Rubpy or nano-SiO_2 (Yao et al., 2009). Thioglycolic acid-modified cadmium-telluride QDs immunosensor presented a comparable or higher sensitivity (5 phytoplasma μL^{-1}) to *Candidatus* Phytoplasma aurantifolia than currently used detection method (Rad et al., 2012). The advantage of the QDs-based FRET biosensor to a DNA-based method is the capacity to distinguish live from dead pathogens (Rad et al., 2012). Nano-sensors have also the potential in the detection of plant stress in real-time (Giraldo et al., 2015; Wu et al., 2020; Chaudhuri et al., 2008; Keinath et al., 2015; Larrieu et al., 2015). Nano-sensors characterized by non/low photobleaching and a high spatiotemporal resolution (single-molecule level per millisecond) detection (Guo et al., 2013; Hong et al., 2015) give new

hopes for field application of sensing tools. Nano-sensors based on SWCNTs functionalized with e.g. polyvinyl-alcohol, Bombolitin II (Wong et al., 2017), HeAptDNA (Wu et al., 2020) have shown high sensitivity and specificity toward various stress signaling molecules like ROS, NO, glucose etc. (Wu et al., 2020; Wong et al., 2017; Kruss et al., 2014). A biosensor designed by Wu et al. (2020) based on SWCNTs coated with HeAptDNA detected H_2O_2 in plant at range of 10–100 μM in response to both environment and pathogen-related stresses with high temporal resolution. In turn, Li et al. (2018b) demonstrated biosensor formed by a pair of functionalized QDs for highly selective detection of glucose in the range from 500 to 1000 μM in photosynthetic tissues.

The detection methods that are currently widely used (e.g. liquid and gas chromatography) require specialized equipment, which makes them cost- and also time-consuming (Fang and Ramasamy, 2015). The decrease of the time needed for analysis and simplification of this process would not only enable common and accurate testing of crops in order to obtain higher yields, but it would also allow detection of the substances potentially hazardous for human (Fung and Clark, 2004; Ohadi Rafsanjani et al., 2012). Various studies on the nano-sensors are aimed to obtain a lab-on-chips that would independently monitor crops with a view to maintaining an optimal environment for crops (amount of soil minerals, soil moisture, temperature) as well as providing protection (detection of fungal, viral and bacterial diseases, detection of chemical stress indicators) and product quality control (amount of fertilizer, pesticide, herbicide and toxin residue) (Guo et al., 2016; Othman and Shazali, 2012). Although the studies on nano-sensors show both no toxicity towards plants and capability for monitoring in real-time (Giraldo et al., 2014), current sensing approaches do not offer the necessary sensitivity for wide application or remote detection from whole plant (Jin et al., 2010; Heller et al., 2009). This brings us to believe that as much as nano-sensors are a promising tool for stress and plant health monitoring, more research is needed to ensure functionality operation under field conditions. As of now, nano-sensors are mostly in phases of laboratory testing. Nanotechnology brings the potential of creating two-way communication channels in real-time between nano-sensors (located within plant/ soil) and electronic devices (smartphones, phenotyping instrumentation etc.) (Giraldo et al., 2019). Mafuta et al. (2013) have designed and deployed the wireless sensor network-based irrigation management system. The self-sustained system collects the information on the soil moisture and temperature and provides an automated response (Mafuta et al., 2013). The concept of lab-on-chip needs further multidisciplinary and collaborative research (Yusof and Isha, 2020), however, these kinds of systems may have a big potential for future agriculture and food production.

2.2. Plant protection and abiotic stress

ENMs find applications in active protection of plants against pathogens and diseases (Zhao et al., 2020) (Fig. 2). The ENMs can be used as active ingredients of pesticides, carriers of active substances, or both (Belava, 2017; Barik et al., 2008). Nano-carriers are characterized by effective delivery, controlled release, and greater capacity of the active substance relative to their conventional counterparts (Johnston, 2010). The ENMs can be also used to promote stress tolerance toward biotic and abiotic stresses by, e.g., mimicking antioxidant enzymes, modifying gene expression, or increasing plant biomass (Zhao et al., 2020).

2.2.1. Biotic stress

Currently, the most frequently studied ENMs in terms of their application in crop protection are nano-Ag and nano-Cu due to their confirmed antifungal and antibacterial activity (Lamsal et al., 2011; Sathiyabama and Manikandan, 2018). Lamsal et al. (2011) demonstrated that nano-Ag applied as spray allowed to control powdery mildew infection in pumpkin and cucumber by inhibiting conidial development and mycelial growth. ENMs act simultaneously as a growth promoter and a fungicide are being designed. For example, nano-Cu-chitosan controlled *Pyricularia grisea infection* in *Eleusine coracanaz* by the significant decrease of spore germination (~80%) and enhanced activity of defense enzymes (Sathiyabama and Manikandan, 2018). Nano-Cu-chitosan also exhibited antifungal activity towards *Fusarium oxysporum* and *Alternaria solani*, responsible for early blight and Fusarium wilt disease of *Solanum lycopersicum* (Sathiyabama and Manikandan, 2018; Saharan et al., 2015). A comparison of the efficacy of ENMs with their bulk counterparts proved significantly greater antifungal efficacy of ENMs (Saharan et al., 2015). Cu-based ENMs applied at low concentrations showed higher antifungal activity on *P. infestans* (a pathogen of *S. lycopersicum* causing substantial yield losses), than commercially used copper based products like Kocide Opti, Cuprofix disperss, and Ridomil Gold Plus (Giannousi et al., 2013).

Because > 90% of traditionally applied pesticides are lost in the environment and/or unable to reach the target area, pesticides are often re-applied or used in quantities exceeding the required amount to achieve desired biological response (Md. Nuruzzaman et al., 2016). A more effective way of substance application is needed. Nano-carriers are a smart delivery system by which chemicals can be delivered in a controlled and targeted manner (Roco, 2003). It can be achieved by encapsulating an active substance in nano-size material (Kah et al., 2013). Besides the delivering role of nano-carriers, they can also protect chemicals from premature degradation and/or too rapid release (Nair et al., 2010). Many types of materials are used for nano-encapsulation, e.g. biodegradable polymer-based materials (Kumari et al., 2010), micelles (Zhang et al., 2013) or porous inorganic nanomaterials (Ao et al., 2013). According to Oliveira et al. (2015) the treatment of *Brassica juncea* with nano-capsules of poly(epsilon-caprolactone) containing atrazine provided a gradual release of herbicide with enhanced activity of the active agents. The encapsulation of atrazine decreased dosage ten-fold compared to conventional formulations, without losses in effectiveness (Oliveira et al., 2015). In turn, Cai et al. (2013) used straw ash-based biochar and BCS to develop a loss-control pesticide. The porous micro/nano structure of BCS and its significantly higher adhesion to the leaf surface showed potential to improve the utilization efficiency of chlorpyrifos. Mesoporous nano-Si demonstrated to be effective against *Botrytis cinerea* in combination with prochloraz , which is marginally absorbed by plants (Zhao et al., 2018). Meanwhile, nano-Si-prochloraz composite displayed relatively quick uptake and translocation in the plant with gradual release of pesticide in plant tissues (Zhao et al., 2018). The analysis of prochloraz residue levels in cucumbers revealed 4–8 times lower concentrations than maximum residue limit values, which indicate a low risk of nano-Si-prochloraz application (Zhao et al., 2018). Controlled biodegradability of nano-enabled chemicals is important for ensuring the effectiveness of nano-pesticides, while simultaneously preventing environmental risk (Khan and Rizvi, 2014). Nano-formulations that degrade faster in the soil than in plants are recently investigated (Khan and Rizvi, 2014). Yan et al. (2005) developed photocatalytic TiO_2/Ag-nanomaterial modified by SDS, which increased both the adsorption of dimethomorph and the photodegradation of residual pesticide in plants and soil. Guan et al. (2010) tested SDS modified Ag/TiO_2 imidacloprid nano-formulation on soybean plants. The results showed that after 20 days, the formulation residues were mostly undetectable in soil and plant (Yan et al., 2005). Next to a decrease of the dosage and reaching target-site, the development of photodegradable agrochemicals is a crucial step for safe and sustainable application of agronanoformulation.

2.2.2. Abiotic stress

Abiotic stress (drought, salinity, heat, heavy metals) causes severe adverse effects on plant growth, development and yielding (Das and Das, 2019). The selected ENMs may improve plant resistance or alleviate stress response to abiotic stress (Das and Das, 2019). Due to different ways of action, those ENMs may be split into two groups: nanozymes mimicking enzyme activities and non-nanozymes (Lee et al., 2013). The effectiveness of a wide group of ENMs nanozymes (nano-Fe_3O_4, CeO_2,

fullerene C60, Au, Pt and Mn_3O_4) was confirmed in the imitation of SOD, CAT, POD and APX enzymes (Boghossian et al., 2013; Wu et al., 2017). Non-nanozymes such as nano-ZnO, SiO_2, TiO_2 do not exhibit enzyme-like properties and mostly they improve plant stress response by triggering up-regulation of genes involved in stress response (Abdel Latef et al., 2018; Siddiqui et al., 2014). The role of ENMs in plant protection from abiotic stress was described in detail in previous reviews (Zhao et al., 2020; Singh, 2019).

2.3. Nano-fertilizers

The development of nanotechnology also provides new solutions to improve the quantity and quality of crops, in particular through fertilization and genetic enhancement of plants (Fig. 2) (Raliya et al., 2016; Dimkpa and Bindraban, 2018). A substantial advantage of nano-fertilizers over conventional agents is their ability to gradually release active substances on a long-term basis (Shang et al., 2019). The potential of ENMs in the crop fertilization has been discussed in detail in previous papers in the area of nanobiotechnology (Prasad et al., 2017; Duhan et al., 2017; Gogos et al., 2012; Dimkpa and Bindraban, 2018; Dimkpa and Bindraban, 2018). Existing studies on the use of nanotechnology for crop fertilization cover a wide group of ENMs, with special attention to metal-based ENMs containing micronutrients (Cu, Fe, Zn) (Shang et al., 2019; Sathiyabama and Manikandan, 2018; He et al., 2019; Dimkpa et al., 2012a; Apodaca et al., 2017; Elanchezhian et al., 2017). Evaluation of the effectiveness of nano-fertilizers has included a wide range of parameters: morphological (plant growth, leaf surface area, root system size and extension, wet and dry matter production) (Shang et al., 2019; Vannini et al., 2013; Elanchezhian et al., 2017; Salehi et al., 2018), physiological (photosynthesis efficiency, chlorophyll and carotenoid content, changes in the amount of produced proteins) (Yasmeen et al., 2017; Mahil and Baburai Nagesh, 2019; de la Rosa et al., 2017; Alkhatib et al., 2019), biochemical (activity of antioxidant enzymes, impact on metabolism) (Elanchezhian et al., 2017; Mahil and Baburai Nagesh, 2019; de la Rosa et al., 2017; Kim et al., 2012) and changes at molecular level (gene and protein expression) (Vannini et al., 2013; Salehi et al., 2018; Khodakovskaya et al., 2011; Mustafa et al., 2015; Marmiroli et al., 2014). Numerous studies confirmed the beneficial effects of ENMs on plants (Duhan et al., 2017; Sathiyabama and Manikandan, 2018; Dimkpa and Bindraban, 2018). However, it is well documented that nano-fertilization efficiency depends on plant species (Song et al., 2013; Lee et al., 2008), type and dose of ENMs (Rafique et al., 2018; Qian et al., 2013; Pramanik et al., 2017), application method, and growing media (He et al., 2019; Hossain et al., 2015). In spite of the fact that the impact and efficiency of nano-fertilizers on crops are extensively studied, the lack of conclusive results causes significant issues with developing commercial products or with establishing regulatory frameworks (Hossain et al., 2015; José Villaverde et al., 2017).

Genetic biofortification can be a substitute or support to fertilization (Cakmak, 2008). Studies in the area of genetic engineering test ENMs as carriers, e.g. of nucleic acids, which will allow DNA fragments to be delivered to desired plant parts (Hussain, 2017). It increases plant productivity or adaptation to climate change or changing conditions (Cunningham et al., 2018). A facilitated system of delivering DNA fragments or active substances into the plant using ENMs is markedly more efficient and causes minimal tissue damage (Ohadi Rafsanjani et al., 2012; Kim et al., 2017). The ability of ENMs to introduce genetic material has been confirmed on the example of mesoporous nano-SiO_2, which was used to deliver plasmid DNA into tobacco and maize cells (Galbraith, 2007). The incorporation of the transporter *AtZIP1* gene to the ubiquitin promoter/terminator cassette of *Hordeum vulgare* led to over-expression of plant membrane transport proteins and doubled the grain Zn concentration (Ramesh et al., 2004). Nano gene delivery system gives the possibility of creating new varieties of agriculturally important crops by genetically integrating desired traits. For example high micronutrient grain content (Datta and Vitolins, 2016) or pest resistance (Perlak et al., 1990) without the need for fertilizer or pesticide application (Kim et al., 2017) may be attained.

3. ENMs *in planta*

3.1. Uptake of ENMs by plants

At the cellular level, uptake of ENMs is dependent on their characteristics such as particle size, which is one of most crucial parameters that determines entrance through the cell wall (Yang et al., 2017). ENMs exhibit the ability to pass by diffusion through cell membrane pores with average size ranges from 4 to 20 nm (Pérez-de-Luque, 2017). A study suggests that ENMs up to about 5 nm are translocated through cell pores, whereas particles up to 20 nm pass through plasmodesma (Ma et al., 2010). Other studies reveal that ENMs ranging from 40 to 50 nm are capable of penetrating into plant cells by endocytosis (Etxeberria et al., 2006), while MWCNTs which range from 30 to 100 nm induce the formation of pores for direct translocation into the cell cytosol (Serag et al., 2011). Aquaporins are supposed to be also involved in the transport of ENMs into plant cells (Kapilan et al., 2018). However, some researchers consider that aquaporins form too small channels to provide free transport of ENMs (Pérez-de-Luque, 2017). It should be remembered that ENMs tend to aggregate, especially at high concentrations, which significantly inhibits their uptake by plants (Ma et al., 2010). Using XANES or fluorescent tagging, it has been confirmed that ENMs are taken up into the plant as particles (Ogunkunle et al., 2019) and to some extent as ions (Zhang et al., 2018b) (Fig. 3). A comparative study of uptake and translocation of nano-Ag and Ag^+ ions in *Oryza sativa* has proved that ENMs undergo assimilation and translocation more efficiently than ions (Yang et al., 2020). Surface ligands on plant parts exposed to ENMs have a large impact on the efficiency of ENMs uptake (Li et al., 2016). In the case of root exposure to ENMs, exudates (low and high molecular weight compounds) significantly affect further fate of ENMs (Liu et al., 2019). If ENMs are applied to the growth medium, they are frequently observed to form aggregates on the root surface (Marchiol et al., 2016) including Casparian strip (Ali et al., 2021). The degree of aggregation of ENMs can be influenced by mucilage released by the root (Avellan et al., 2017; Marchiol et al., 2016). Avellan et al. (2017) have proved that mucilage can trap both positively and negatively charged ENMs. Interestingly, mainly positively charged nano-Au remained immobilized as large agglomerates in the mucilage layer on root tips of *Arabidopsis thaliana*, preventing further uptake (Avellan et al., 2017). In comparison, plants treated with negatively charged nano-Au showed a higher content of Au inside the plant apoplast, proving uptake and translocation (Avellan et al., 2017). Secretion of exudates by plant roots determined the properties of the interface between roots and soil (rhizosphere). Schwabe et al. (2015) revealed that plant roots can prompt the dissolution of nano-CeO_2 in soil, leading to uptake of dissolved Ce (III) that was re-precipitated in plant tissues. Gao et al. (2018) also confirmed the enhanced dissolution of nano-CuO in the rhizosphere of wheat. Moreover, the properties of growth medium are other crucial factor affecting the uptake of ENMs by plants by determining the behavior and transformation of ENMs (Peng et al., 2017; Gao et al., 2019). pH, organic matter and clays content are considered as the most important characteristics that impact the ENMs fate in soil-plant system, which was highlighted in previous works (Zhang et al., 2018b; Gao et al., 2018; Lowry et al., 2012).

During foliar application, ENMs must first overcome the cuticle, which is a protective barrier of leaves against the input of contaminants and pathogens (Pollard et al., 2008). It is estimated that 60–70% of ENMs suspension is delivered onto leaves surface after foliar treatment of ENMs (Su et al., 2019). Two ENMs uptake pathways after foliar application have been described: 1) the lipophilic pathway by diffusion through cuticle wax or 2) hydrophilic pathway through hydathodes, trichomes, or stomata (Eichert et al., 2008). ENMs showed a tendency to

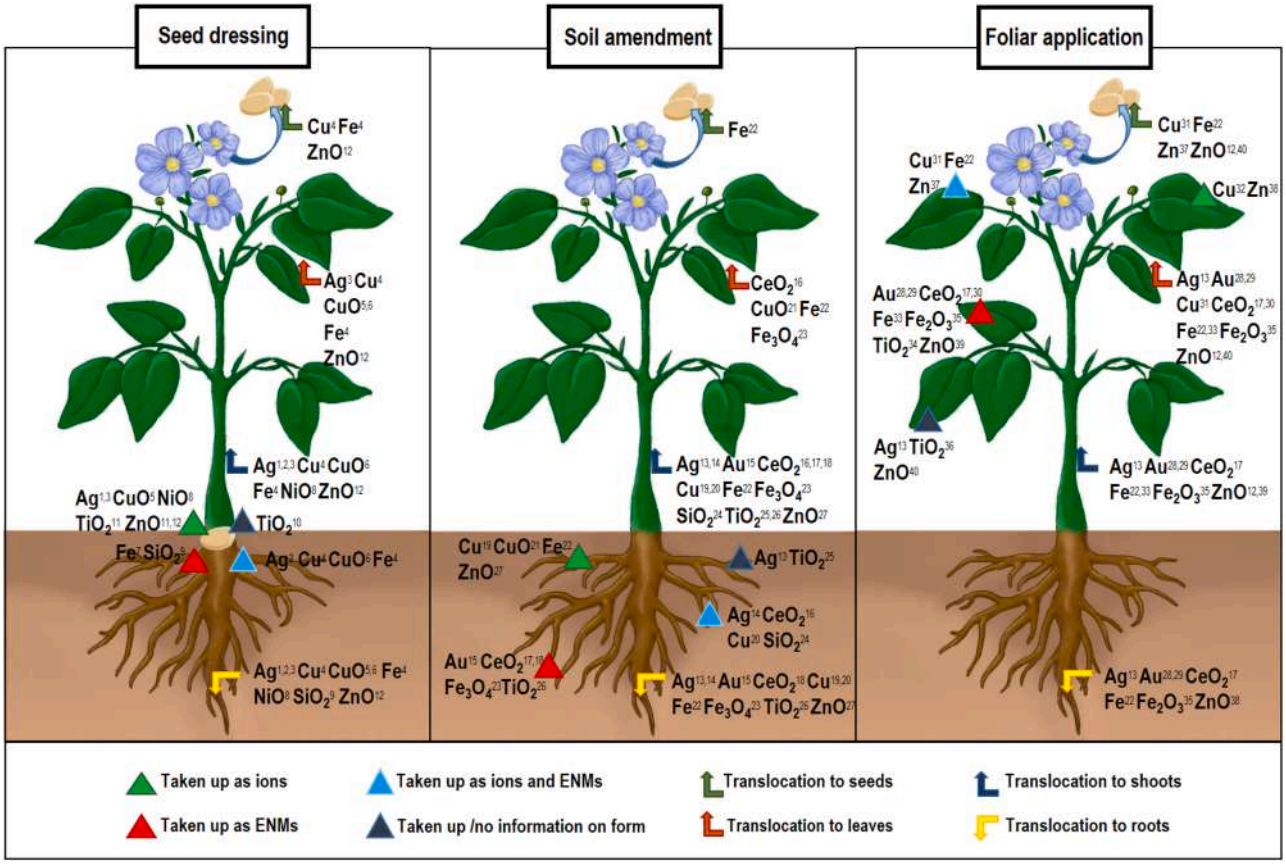

Fig. 3. Selective uptake and translocation of ENMs and/or released metal ions depending on application mode (seed dressing/soil amendment/foliar application) of ENMs. References are provided in Supplementary Material.

accumulate in stomata (Eichert et al., 2008), adjacent parenchyma cells (Corredor et al., 2009) or trichomes (Spielman-Sun et al., 2020). The high number of stomata on leaf surface facilitated rapid and efficient uptake of ENMs (Su et al., 2019). Coating of ENMs is also of great importance in their uptake (Yang et al., 2017). After spraying, uncoated ENMs were distributed by chance on the leaf surface, whereas coated ENMs, like nano-BSA-Au or LM6M-Au, exhibited affinity towards natural leaf openings (trichomes and stomata) (Spielman-Sun et al., 2020).

3.2. Translocation of ENMs

After input into the plant, ENMs can be transported symplastically and apoplastically (Su et al., 2019). Similarly to other compounds, ENMs are transported through vascular bundles, the xylem from the roots to higher plant parts, and via the phloem in the opposite direction (Raliya et al., 2016). However, existing studies revealed that the transport of ENMs or their components in the plant was dependent on their properties (charge, size, chemical composition) and their application mode (Dimkpa et al., 2012b; Zhang et al., 2011) (Fig. 3). A study on the transport of Cu-CNFs showed that the particle diameter determined the pathway of their transport (Ashfaq et al., 2017). Cu-CNFs up to 60 nm were transported through plasmodesma when the diameter of the plasmodesma channel ranged 40–60 nm. Larger Cu-CNFs were transported symplastically and apoplastically (Ashfaq et al., 2017). As in the case of uptake of ENMs, their translocation is determined by the surface charge. For example, negatively charged nano-Zn- chitosan was predominantly translocated to the leaves, whereas almost no transport of positively charged ENMs was observed (Liu et al., 2019). In turn, exposure of wheat and rapeseed to MWCNTs coated with negatively charged gum Arabic or humic acids resulted in a trace uptake and translocation of ENMs (< 0.005‰) from roots to leaves (Larue et al., 2012). Avellan et al. (2019) reported that nano-Au coated with amphiphilic polyvinylpyrrolidone led to higher uptake of ENMs in wheat through the cuticle layer but significantly lower translocation across the mesophyll and the rest of the plant. While only a fraction of nano-Au coated with more hydrophilic citrate entered the leaf, those ENMs were effectively translocated to the plant vasculature (Avellan et al., 2019). Both ENM types showed similar translocation of nano-Au to shoots (10–30%) and roots (10–25%). A small amount of nano-Au (5–15%) was excluded into the rhizosphere (Avellan et al., 2019). Tombuloglu et al. (2019) reported that ENMs were translocated from roots to shoots in *H. vulgare* under treatments in hydroponic conditions. In turn, Ma et al. (2017) proved root-to-shoot-to-root redistribution of nano-CeO_2, which can have significant implications for food safety and human health.

Inside plants, ENMs can undergo various biotransformations (Zhang et al., 2012; Ogunkunle et al., 2019), which may have a major impact on the translocation of released ions/substances (Wang et al., 2012) or potential toxicity (Ogunkunle et al., 2019). Zhang et al. (2012) reported that nano-CeO_2 might be transformed to Ce (III) in cucumber roots with the assistance of reducing substances and organic acids. It was observed that most of the released Ce^{3+} was precipitated as insoluble $CePO_4$ and immobilized in the roots, preventing further translocation of ions. It is supposed that a small part of released Ce^{3+} was transported with nano-CeO_2 to the shoots via xylem (Zhang et al., 2012). It is worth noting that in the stem and leaves Ce (III) occurred as cerium carboxylate, while immobilized insoluble $CePO_4$ remained in the roots (Zhang et al., 2012). A similar reduction of Ce (IV) to Ce (III) was found in *Egeria densa* and the kinetics of the process was negatively correlated with the particle diameter of CeO_2 (Geitner et al., 2018). A study on the transport of nano-CuO from roots to shoots and leaves of *Zea mays* demonstrated that a part of nano-CuO was reduced from Cu (II) to Cu (I) (Wang et al.,

2012). The analysis of the xylem sap showed that only Cu (II) forms occurred. It is suspected that the biotransformation of nano-CuO in *Z. mays* was caused by enzymes such as the reductases and ferredoxins of the plant photosynthetic system or reducing sugars (glucose/fructose) (Wang et al., 2012). The reduction could have occurred partly in the leaves or during the transport through the phloem to the roots due to the interaction with reducing sugars (Wang et al., 2012). Ogunkunle et al. Ogunkunle et al. (2019) showed that all nano-Cu incorporated into the cowpea tissues from the soil underwent biotransformation to Cu^{2+} in the roots. A study on nano-CuO distribution and speciation reported that although ENMs were the dominant form of Cu in roots and mature leaves of *O. sativa*, the concentration of Cu (II) and Cu (I) significantly increased in above-ground tissues and Cu^{2+} was the predominant form in younger leaves (Peng et al., 2015). Shi et al. (2008) indicated that most Cu in *Elsholtzia splendens* roots exists as Cu^{2+}, which has the highest toxicity among Cu species (Keller et al., 2017). Many studies on biotransformation of metal-based ENMs showed that Cu (II) was often bound by phytochelatins, including cysteine, histidine, and nicotianamine, to form chelated complexes (Ogunkunle et al., 2019; Peng et al., 2015).

4. Effects of ENMs on plants

To date, the effects of ENMs on plants have been assessed both in the context of their suitability for plant growth improvement and their potential toxicity (Marchiol et al., 2016; Sathiyabama and Manikandan, 2018; Dimkpa and Bindraban, 2018; Wang et al., 2019). The aspect of risk assessment is gaining an ever greater importance due to the increasing presence of ENMs in the environment, including soils (Rajput et al., 2020). Research on a wide group of ENMs (nano-ZnO, CuO, Au, Ag, TiO_2, C_{60} etc.) has been conducted on many plant species (*Arabidopsis thaliana, Brassica napus, Oryza sativa, Hordeum vulgare*, etc.), on different media (hydroponic, agar, soil) (Chung et al., 2019; Marchiol et al., 2016; Landa et al., 2012; Yue et al., 2017), and under different types of ENM application mode (seed dressing, foliar application, soil application) (Vannini et al., 2013; Zhang et al., 2018b; Sathiyabama and Manikandan, 2018) and duration of exposure (Marchiol et al., 2016; Suriyaprabha et al., 2018). In these studies, the effects of ENMs on plants have been evaluated from the molecular changes through the cell and tissue level to the response of the whole organism (Fig. 4). Both positive and adverse changes in morphological (germination power, biomass) (Nair and Chung, 2014; Kim et al., 2012), physiological (photosynthesis rate, pigments content) (Yasmeen et al., 2017; Trujillo-Reyes et al., 2014), and biochemical parameters (activity of antioxidant enzymes, content of proteins, sugars, starch, and macro- and micronutrients) (Yasmeen et al., 2017; Du et al., 2015) have been reported (Table 1). The analysis of the effects of ENMs on plant growth and development including the role of a number of factors such like ENMs type and dose, mode of application and plant species in plant response was presented in detail in the last reviews (Pradhan and Mailapalli, 2017; Rizwan et al., 2017). Molecular changes in plants under ENMs remain poorly understood. The development of omics techniques offers new possibilities to explore mechanisms of plant-ENM interactions (Fig. 1) (Hossain et al., 2020), which is of utmost importance for the use of ENMs for crop production, and nanotoxicity. Due to the significance and increasing number of omics studies on ENMs *in planta*, the transcriptomic, proteomic and metabolic effects are analyzed below.

4.1. Transcriptomic analysis

Plant response to ENMs at the transcript level has been analyzed based on the whole transcriptome (RNA-sequencing, microarrays) (Wang et al., 2017; Jin et al., 2017) and the expression of selected genes (real-time qPCR) (Syu et al., 2014; García-Sánchez et al., 2015). The impact of ENMs on the plant transcriptome was referred to the activity of their bulk and ion counterparts in order to capture/verify nano-specific effects (Yue et al., 2017; Shi et al., 2014). Metal ions (usually used as metal salts) generally resulted in a higher number of differentially expressed genes (DEGs) at the transcriptome level relative to ENMs or their larger counterparts. Such findings were observed in *A. thaliana* exposed to nano-ZnO (Landa et al., 2015; Wan et al., 2019), nano-CuO (Landa et al., 2017), nano-Al_2O_3 (Jin et al., 2017) as well as in *T. aestivum* upon nano-Cu treatment (Zhang et al., 2018b). Furthermore,

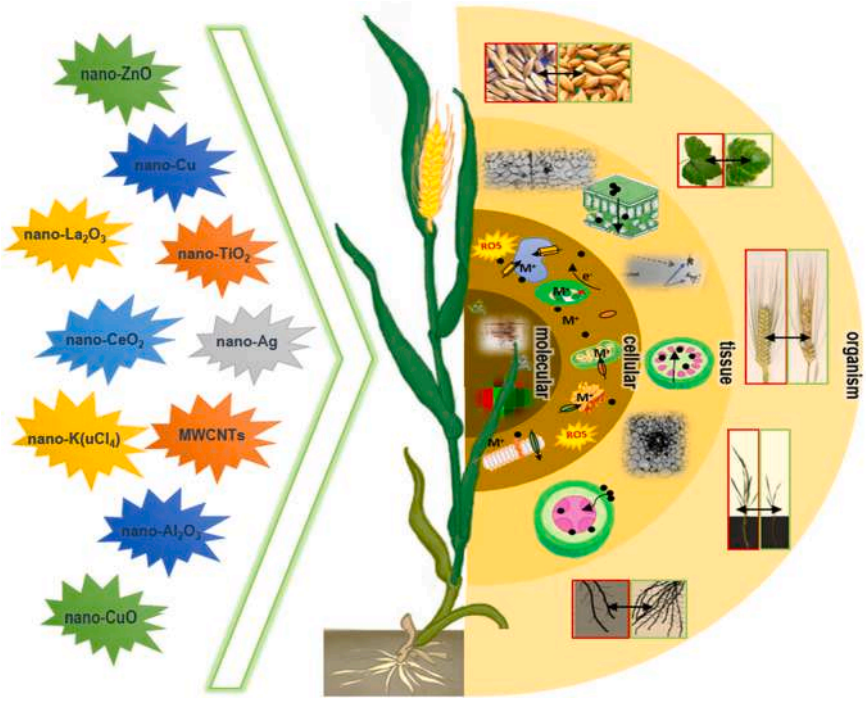

Fig. 4. Schematic presentation of ENMs effects on plants at molecular (genes and proteins expression), cellular (ROS generation, regulation of metal homeostasis), tissue (structural and ultrastructural changes e.g. accumulation of ENMs, blockages and deformations of tissues) and the organism (decreased or increased plant growth and biomass, yield) level. The TEM images were taken from references (Ma et al., 2017; Alkhatib et al., 2019).

Table 1
Morphological, physiological and biochemical changes in plants under ENMs treatments.

ENMs	Plant	Dose	Size [nm]	Analyzed tissues	Exposure route/ Growth media	Age at exposure	Duration of exposure	Remarks			Ref.
								morphological	physiological	biochemical	
Ag	*Arabidopsis thaliana*	100 μM	45	seedling, root	root/ agar	4 days	3 days	↑roots growth	↑anthocyanin accumulation	↑Cu/Zn SOD activity ↑ROS accumulation ↑proteins content ↑chloroplast biogenesis ↑carbohydrate metabolism	(Syu et al., 2014)
	Arabidopsis thaliana	0.5 mg L^{-1}	–	seedling, root	seed/ agar	0 days	14 days	↓roots length ↓seedlings biomass ↑roots number	↓chlorophyll content ↓anthocyanin accumulation		(Qian et al., 2013)
	Oryza sativa	40 ppm	18	leaf, shoot, root	seed/agar	0 days	14 days	↑root, shoot length ↑plant biomass	↑flavonoids accumulation	↑POD, APX, CAT activity	(Gupta et al., 2018)
	Oryza sativa	0.5 mg L^{-1}	20	leaf, shoot, root	root/ aqueous solution	48 h	7 days	↓roots, leaves, stems growth ↓biomass	↓chlorophyll, carotenoids content ↓sugar content	↑lipid peroxidation ↑ROS generation	(Nair and Chung, 2014)
CuO	*Cucumis sativus*	10 mg L^{-1}	50	seedling, root	root/ aqueous solution	5 weeks	5 days	↓plant biomass		↑POD, APX, CAT activity	(Kim et al., 2012)
	Landoltia punctata	1 mg L^{-1}	43	leaf, root	root/ aqueous solution	48 h	9 days	↓plant growth	↓chlorophyll content		(Shi et al., 2011)
	Lactuca sativa	20 mg L^{-1}	20–30	leaf, root	root/ aqueous solution	18 days	15 days	↓plant biomass	↓chlorophyll content	↑CAT activity ↓APX activity	(Trujillo-Reyes et al., 2014)
	Zea mays	100 mg L^{-1}	20–40	leaf, shoot, root	seed and root/ aqueous solution	0 days	8 and 15 days	↓roots length ↓plant biomass		↑ROS accumulation ↑lipid peroxidation	(Wang et al., 2012)
Cu	*Cucumis sativus*	10 mg L^{-1}	50	seedling, root	root/ aqueous solution	5 weeks	5 days	↓plant biomass		↑POD, APX, CAT activity	(Kim et al., 2012)
	Cucumis sativus	100 mg L^{-1}	20	shoot, root	root/ aqueous solution	6 weeks	4 days	↓plant biomass	↑electrolyte leakage ↓chlorophyll content	↑ROS accumulation ↑lipid peroxidation	(Mosa et al., 2018)
	Solanum lycopersicum	250 mg L^{-1}	20–50	leaf, shoot, fruit	foliar/ aqueous solution	93 days	43 days	↑plant biomass ↑fruit weight	↓chlorophyll content	↑glutathione content	(Pérez-Labrada et al., 2019)
	Triticum aestivum	25 ppm	15–30	seed	root/ soil	tillering and anthesis stage	till maturity	↓spike length ↑number of grains	↑sugar content	↑SOD activity ↔ protein content	(Yasmeen et al., 2017)
$Cu(OH)_2$	*Lactuca sativa*	8.75–17.5 mg	50–1000	leaf, root	root/ soil	24 days	4 weeks	↑plant biomass		↑ROS accumulation ↔protein content	(Zhao et al., 2016)
Cu-Chitosan	*Eleusine coracana*	0.15%	88	leaf, shoot, seed	seed and foliar/ soil	0 and 20 days	till maturity	↑shoots, leaves growth ↑plant biomass	↑chlorophyll content	↑protease inhibitors ↑β-1,3 glucanase ↑peroxidase, polyphenol oxidase	(Sathiyabama and Manikandan, 2018)
CeO_2	*Triticum aestivum*	400 mg kg^{-1}	8	seedling, leaf, shoot, root, seed	seed/ soil	0 days	30 days and till maturity		↓chlorophyll content ↑chromatin condensation	↑SOD, CAT activity	(Du et al., 2015)
Fe_3O_4	*Lactuca sativa*	20 mg L^{-1}	50–60	leaf, root	root/ aqueous solution	18 days	15 days	↓leaves biomass	↑chlorophyll content	↑APX activity	(Trujillo-Reyes et al., 2014)
		25 ppm	20–30	seed	root/ soil		till maturity		↑sugar content		

(*continued on next page*)

Table 1 (*continued*)

ENMs	Plant	Dose	Size [nm]	Analyzed tissues	Exposure route/ Growth media	Age at exposure	Duration of exposure	Remarks			Ref.
								morphological	physiological	biochemical	
	Triticum aestivum					seedling emergence				↑SOD activity ↔changes in protein content	(Yasmeen et al., 2017)
SiO_2	*Bt-transgenic cotton*	500 mg L^{-1}	30	shoot, root	root/ aqueous solution	21 days	30 days	↓plant growth ↓roots, shoots biomass		↑SOD. POD activity ↓CAT activity	(Le et al., 2014)
ZnO	*Allium cepa*	0.2 g L^{-1}	75–85	root	root/ aqueous solution	till root reached length of 2–3 cm	24 h		↑cell death ↑impaired cell division ↓ mitotic index	↑ROS accumulation ↑lipid peroxidation ↓CAT activity	(Ghosh et al., 2016)
	Triticum aestivum	40 mg L^{-1}	–	leaf, shoot, seed	foliar/ soil	7 days after anthesis	2, 4, 8, 12 h, 7, 14 and 21 days	↑plant growth ↑number of grains		↑grain protein content	(Deshpande et al., 2018)
TiO_2	*Spinacia oleracea*	2.5‰	–	leaf	seed and foliar/ aqueous solution	0 days	48 h, 7 and 30 days	↑plant biomass ↑ plant growth	↑ chlorophyll content		(Hong et al., 2005)

↑ higher effect, ↓ lower effect, ↔no effect in relation to control sample.

the changes at gene expression as affected by metal ions persist longer than for ENMs. For example, after 3 days of exposure, nearly 70% of DEGs returned to the normal expression level in *A. thaliana* exposed to nano-ZnO compared to 54% in Zn^{2+} treated seedlings. Given that the bioactivity of metal-based ENMs is closely associated with the activity of metal ions released from them, transcriptional changes concerned genes related to, e.g., oxidative stress or metal homeostasis (Landa et al., 2017). Nonetheless, ENMs frequently induced specific changes in plant transcriptome. Nano-ZnO exposure resulted in significant down-regulation of almost 60 genes involved in cell wall organization and structure, while Zn^{2+} caused down-regulation of only 11 such genes. It is suspected that this is caused by the tendency of ENMs to adhere and accumulate in apoplastic spaces (Wan et al., 2019). Landa et al. (2015) also observed transcriptome specific changes in *A. thaliana* treated with nano-ZnO, which might have been caused by aggregation of nano-ZnO on/inside of root tissues, which resulted in blockage of the apoplast and inhibition of water and nutrient transport (Ma et al., 2018). Transcriptomic response of plant upon exposure to ENMs was also tissue-specific, which could have been due to the mode of application of ENMs. Nano-ZnO applied to the growth medium resulted in a higher number of DEGs in *Z. mays* roots than in shoots (Xun et al., 2017). Gene ontology analysis also showed different enriched DEGs patterns between plant tissues: genes involved in nitrogen compound metabolism, the small molecule metabolic process, the nutrient reservoir and cellular components, and the primary and secondary metabolic process were exclusively up- or down-regulated in roots (Xun et al., 2017).

Due to the cost- and time-consumption of analysis of the whole plant transcriptome, studies investigating the expression of selected genes have been used more frequently to evaluate the effects of ENMs on plants (Pagano et al., 2016; Taylor et al., 2014; Xun et al., 2017). Most of these studies have involved analysis of stress response-related genes (Landa et al., 2015; Jin et al., 2017; Valdes et al., 2020) (Fig. 5). Particularly, much attention has been devoted to oxidative stress-related genes (Qian et al., 2013; Kim et al., 2012; Tombuloglu et al., 2019), which are considered to be one of the main reasons for the phytotoxicity of ENMs (Kim et al., 2012; Doğaroğlu and Köleli, 2017; Mosa et al., 2018). Enhanced generation of ROS under the influence of ENMs results in the activation of the plant defense system, including enzymatic and non-enzymatic antioxidants (Chung et al., 2019). Up-regulation of antioxidative enzymes (e.g. *SOD*, *CAT*, *GPX*, *APX*) was induced by nano-Ag (Qian et al., 2013), nano-Al_2O_3 (Jin et al., 2017), nano-ZnO (Wan et al., 2019) and CeO_2 (Ma et al., 2013) in *A. thaliana,* nano-CuO in *Brassica rapa* (Chung et al., 2019), nano-Cu in *C. sativus* (Mosa et al., 2018) and nano-$Cu(OH)_2$ in *Medicago sativa* (Cota-Ruiz et al., 2018). Genes encoding biosynthesis of non-enzymatic antioxidants, e.g. phenolic compounds (*PAP1*, *ANS*, *PAL*, and *FLS*), were up-regulated in *Cicer arietinum* under nano-CuO (Chung et al., 2019). The transcript level of genes involved in the response to biotic and abiotic stress, such as small heat shock proteins (*ATHSP*) under nano-K (AuCl4) (Taylor et al., 2014), or the salicylic and jasmonic acid signaling pathway (*WRKY*) after nano-$Cu(OH)_2$ (Zhao et al., 2017b) and nano--Al_2O_3 (Jin et al., 2017) treatment have also been studied (Fig. 5). Comparative studies of gene expression upon exposure to metal-based ENMs and metal ions have generally revealed effects on the same genes, but differing in the scale and the direction of expression changes. In a study by Tang et al. (2016), nano-CuO induced higher transcripts of oxidative stress-related genes (*RHL41*, *MSRB7*, *BCB, PRXCA*, and *MC8*) in *A. thaliana* than the corresponding Cu^{2+} ions. In turn, up-regulation of *Cu/Zn SOD* was at a similar level after exposure to nano-CuO and Cu^{2+}, but it was higher than after bulk-CuO treatment (Landa et al., 2017). In *Z. mays* exposed to nano-Cu and bulk-Cu (1000 ppm), on the other hand, higher up-regulation of *APX* was observed after adding bulk-Cu (Valdes et al., 2020). In turn, nano-ZnO, bulk-ZnO, and Zn^{2+} up-regulated the genes involved in salt stress and osmotic stress (*SNRK2.8 SNRK2.9, DELTA-OAT, ALP*) to a similar degree (Landa et al., 2015). Specific transcriptome changes under nano-ZnO treatment were related to genes

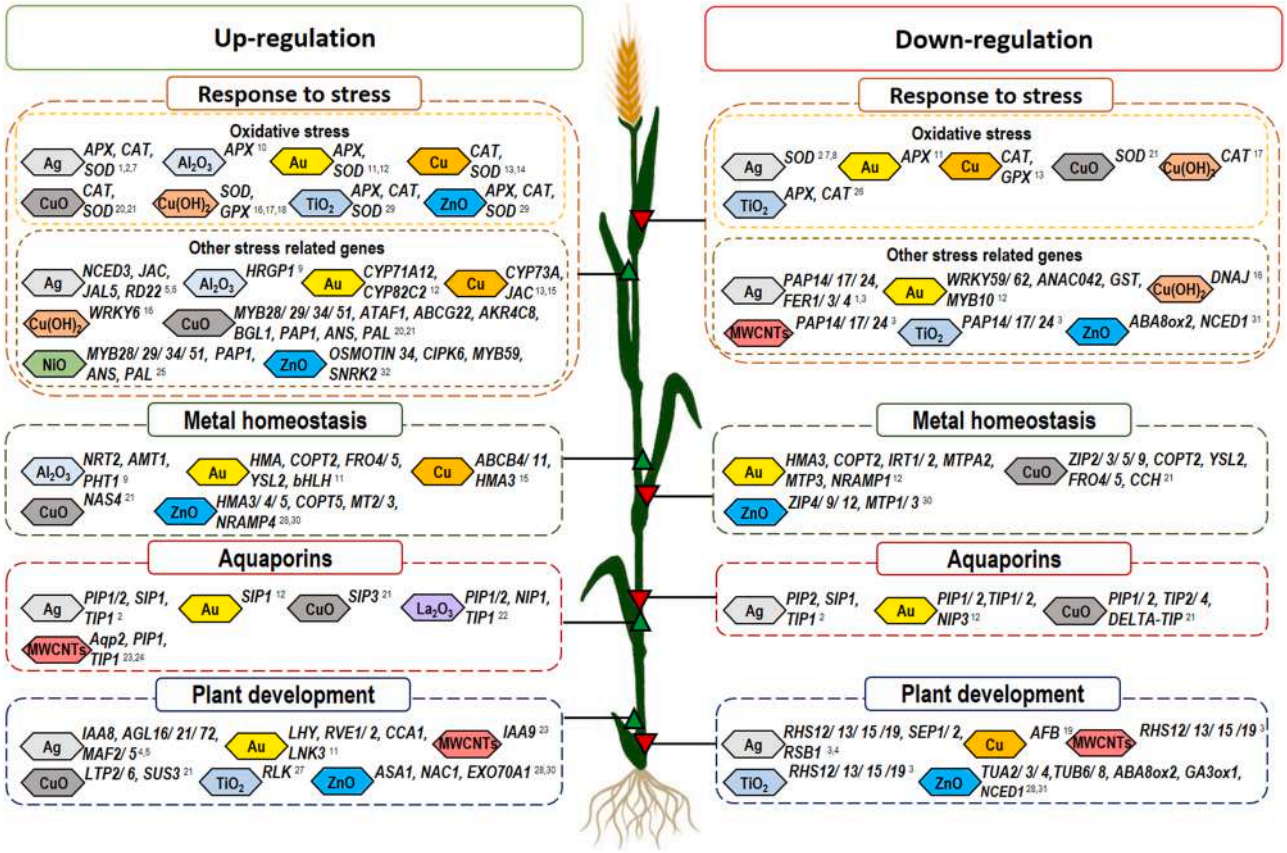

Fig. 5. Transcriptional response of plants to ENMs treatment. Genes have been grouped by their role in plants. References are provided in Supplementary Material.

that played a role in defense response (*RBK1*, *AT4G19925*) to pathogens (*PR4*) or hypoxia (*PDC2*), which could have resulted from strong adhesion of the ENMs to plant roots (Landa et al., 2015). Pagano et al. (2016) also found *BIP3* heat shock protein as a biomarker of ENMs (nano-CuO, La_2O_3, CeO_2) for 3 species: *A. thaliana*, *S. lycopersicum*, and *Cucurbita pepo*. The rate of ENMs has also caused differences in plant response. Foliar application of nano-$Cu(OH)_2$ at 10 mg L^{-1} resulted in up-regulation of *POD1* and *GST1* in *Z. mays*, whereas a 10 times higher concentration reduced the transcript level of other genes involved in response to oxidative stress (*CAT1*) (Zhao et al., 2017c). According to Rizwan et al. (2017), under mild ENMs stress the activity of antioxidant enzymes increases, while at high stress the activity of enzymes decreases due to severe oxidative bursts.

Transcriptional changes in plants under exposure to metal-based ENMs have been evaluated in terms of metal homeostasis (Landa et al., 2017; Taylor et al., 2014; Zhang et al., 2019). Because free metal ions do not occur in plant cells almost at all (on average 1 metal ion per cell), the concentration of metal ions is tightly controlled by the panel of several transporter proteins regulating uptake, cellular compartment, and sequestration of metals (Chen, 2018). Metal-based ENMs are characterized by the different solubility and dissolution rate, which could have driven the differences in the delivery of elements resulting in changes in transcripts of genes regulating metal homeostasis (Landa et al., 2012). A comparative study of the impact of nano-ZnO and Zn^{2+} on *A. thaliana* showed a different expression pattern of genes involved in Fe homeostasis (Wan et al., 2019). Nano-ZnO added to growth medium resulted in up-regulation of 30 and down-regulation of 12 transporter genes, while only 17 genes were up-regulated and 4 down-regulated by Zn^{2+} treatment (Wan et al., 2019). In turn, Landa et al. (2017) showed that nano-CuO, bulk CuO and Cu^{2+} treatment of *A. thaliana* resulted in down-regulation of genes involved in Cu homeostasis (*ZIP2*, *COPT2*, *CCH*, *FSD1*). Nano-CuO caused specific up-regulation of *NAS4* and *SULTR1;3* genes and down-regulation of *ATCTH*, *AT4G30170*, *XTH14* and *AGT* (Landa et al., 2017). Taylor et al. (2014) noted that *A. thaliana* exposure to nano-K(AuCl4) resulted in down-regulation of many transporter genes (e.g. *IRT1*, *IRT2*, *COPT2*, *ATIREG2*, *ATNR 2;1*, *MTPA2*, *MTPc3*, *HMA3*, *ATCHX16*, and *NRAMP1*) in roots, while up-regulating CAX3. An excess of both essential and non-essential metal ions triggers metal homeostasis control mechanisms to avoid metal uptake and subsequent toxicity (Eide et al., 1996). Apart from their impact on transporters characterized by high specificity towards target metals, ENMs have also affected the transcript of genes related to other elements. For example, nano-Al_2O_3 up-regulated N and P transporters (*NRT2:1*, *AMT1:3*, *PHT1:9*) (Jin et al., 2017), which resulted in greater loading of these macronutrients in *A. thaliana*. It is worth noting that Al^{3+} caused down-regulation of *AMT1:3* and impaired N uptake, which is a frequent symptom in abiotic stress conditions (Filiz and Akbudak, 2020).

As regards the contribution of aquaporins to the uptake of water, non-polar solutes (e.g. urea, glycerol) and gases (e.g. CO_2) as well as elements (B) (Maurel et al., 2008) changes in their expression under ENMs treatment have been evaluated. The activity of aquaporins is heavily influenced by a number of stress factors like salinity, pH, low temperature, low humidity, and heavy metals (Qian et al., 2013; Khodakovskaya et al., 2011; Kapilan et al., 2018). Khodakovskaya et al. (2012) demonstrated up-regulation of the *PIP1* gene in tobacco after treatment with MWCNTs. Similar results were obtained by Lahiani et al. (2013): deposition of MWCNTs on the seed surface of barley, corn and soybean enhanced gene expression of several types of aquaporins such as *PIPs*, *TIPs,* and *SIPs* (Lahiani et al., 2013). Increased expression of aquaporins showed a significant impact on the activation and enhancement of seed germination and seedling growth because of stimulation of water uptake. A study on *A. thaliana* treated with nano-K (AuCl4), on the other hand, showed a significant down-regulation of

eleven aquaporin genes (*TIPs*, *NIPs*, *PIPs*). This resulted in strong inhibition of water uptake and increased the toxic effects induced by Au abundance (Taylor et al., 2014). Another non-essential ENMs, nano-La_2O_3, also significantly down-regulated *PIP* genes in *Z. mays,* which led to reduced water uptake and growth inhibition (Yue et al., 2017). In turn, nano-Ag (at 3 mg L^{-1}) induced down-regulation of aquaporins (*PIP2;1*, *PIP2;2*, *SIP1;1*, *TIP1;1*) in *A. thaliana* (Qian et al., 2013), whereas Ag^{2+} did not affect the expression of these genes (except for *PIP2;1*, which was up-regulated). A study on nano-ZnO, bulk, and ionic Zn^{2+} treatments demonstrated down-regulation of *PIP1;4*, *PIP2;3*, and *PIP3* as well as *DELTA-TIP* (Landa et al., 2015).

Recently, ENMs have been found to significantly impact miRNA expression profiles, which may cause crucial changes in plants (Frazier et al., 2014). miRNA is a small single-stranded non-coding RNA molecule involved in RNA silencing and post-transcriptional regulation of gene expression (Bartel, 2018). miRNAs are highly conserved and take part in plant development and tolerance to stress by controlling expression of more than 30% of protein coding genes (Xie et al., 2005; Lewis et al., 2005). Kumar et al. (2013) linked the reduced expression of miR398, miR408 miR167, and miR164 under exposure to nano-Au to enhanced growth and yield in *A. thaliana*. The modulation of miRNA expression by nano-Al_2O_3 (Burklew et al., 2012) and nano-TiO_2 (Xie et al., 2005; Boykov et al., 2019) in *Nicotiana tabacum*, which was associated with resistance to drought and the plant adaptive response to nutrient deficiency, resulted in higher expression miRNA, which was linked to ENMs adverse effect on plants (Xie et al., 2005; Burklew et al., 2012; Boykov et al., 2019).

4.2. Proteomics and metabolics effects

Proteomics and metabolomics analysis (LC MS, MALDI, GC−TOFMS) have increasingly been used to obtain a holistic view of molecular response of plants to ENMs (Zhang et al., 2018a). Proteomics analyzes qualitative and quantitative changes related to proteins, while metabolomics serves as a tool to explore the metabolic status at a particular time point (Li et al., 2018c; Zhao et al., 2019). Unlike transcriptomics, the comparative analysis of metabolic and proteomic effects of ENMs and corresponding bulk particles or dissolved compounds is extremely scarce (Fig. 1.) (Reddy Pullagurala et al., 2018).

A study on the impact of nano-Cu and nano-Fe addition on soil-grown wheat revealed an increase in stress-related proteins (heat shock proteins, luminal binding proteins) and proteins related to protein degradation in seeds (Yasmeen et al., 2017). Nano-Cu showed a significant increase in expression of proteins related to glycolysis and starch degradation, while nano-Fe treatment resulted in increased expression of tricarboxylic acid cycle proteins (Yasmeen et al., 2017). The analysis of protein expression patterns (stress, glycolysis, proteins, amino acid metabolism, etc.) revealed that nano-Cu improved both yield and stress tolerance of wheat in comparison to nano-Fe (Yasmeen et al., 2017). Changes in protein profile expression in soybean also differed among ENMs types (nano-Al_2O_3, ZnO, and Ag) (Hossain et al., 2016). Nano-Al_2O_3 treatment resulted in an abundance of proteins involved in stress signaling, hormonal pathways related to growth and oxidation reduction, which might be crucial for maintaining optimum growth of soybean under ENMs stress. On the other hand, nano-Ag increased the number of proteins related to primary metabolism, while nano-ZnO decreased the amount of proteins involved in stress signaling, secondary metabolism, and hormone metabolism (Hossain et al., 2016). Proteomic analysis of *Eruca sativa* under nano-Ag and Ag^+ indicated similar tendency to accumulation of proteins related to sulfur metabolism (e.g. jacalin lectin family). The study also revealed a nano-specific effect: the proteomic changes caused by nano-Ag were mostly related to ER (strong down-regulation of ER-resident luminal-binding protein 1 and heat shock protein 70), while Ag^+ treatment increased the abundance of several major latex proteins, glutathione-S-transferases, and universal stress protein (Kissen and Bones, 2009).

A study carried out by Zhao et al. (2019) showed that the metabolite profile of *Z. mays* was ENMs-type dependent. The nano-Fe_2O_3 caused the most distinctive metabolic changes (11 altered metabolic pathways), followed by nano-TiO_2 (9 pathways) and nano-SiO_2 (6 pathways). It is worth noting that all the 3 types of ENMs commonly altered 3 metabolic pathways: arginine and proline metabolism, methane metabolism, and pantothenate and CoA biosynthesis, which are crucial for nitrogen and carbohydrate metabolism (Zhao et al., 2019). Untargeted Metabolic Pathway Analysis was used to assess the nanotoxicity of 10 ENMs (nano-Ag, Cu, Fe, ZnO, SiO_2, TiO_2, GO, GOQDs, SWCNTs, and C_{60}) towards rice (Li et al., 2020). Down-regulation of carbohydrate metabolism and up-regulation of amino acid metabolism were the two dominant metabolic changes triggered by all tested ENMs. Nano-specific modulation of *Spinacia oleracea* metabolome was provided in a study testing nano-$Cu(OH)_2$ (Zhao et al., 2017a). Interestingly, both nano- and ionic Cu treatments affected pathways related to plant antioxidative activities but only nano-$Cu(OH)_2$ treatment resulted in nitrogen metabolism perturbation (Zhao et al., 2017a). Metabolome analysis was also employed to record metabolic changes triggered by foliar application of single-walled carbon nanohorns and nano-ZnO to *Sophora alopecuroides* under salt stress (Wan et al., 2020). Both ENMs improved salt tolerance by reprogramming carbon/nitrogen metabolism and stimulating glycolysis and TCA cycle to generate energy and enhancing the levels of unsaturated fatty acids to maintain membrane integrity under salt stress (Wan et al., 2020). In recent time, there have been more and more studies employing an integrated approach and using more than one omics technique for exploration of the ENMs-plant system (Li et al., 2018c; Chen et al., 2018; Sun et al., 2020). Transcriptomics and metabolomics analysis of *A. thaliana* exposed to 1000 mg L^{-1} of carbon nanodot showed oxidative stress, changes in osmotic potential, and interferences with photosynthetic processes (Chen et al., 2018). Foliar application of ZnO to tomato induced changes in gene transcripts and metabolites involved in nutrient element transport, carbon/nitrogen metabolism, and secondary metabolism (Sun et al., 2020). Proteomics and metabolomics tools were also employed to investigate the joint effect of GO and PAHs on rice (Li et al., 2018c). The adverse effect of PAHs on plants was enhanced by co-existing GO, which increased the level of aryl hydrocarbon receptor and cytochrome P450 (related to oxidative stress and transmembrane transport) induced by PAHs (Li et al., 2018c).

5. Conclusions

Over the recent years, nanotechnology has proved its potential for wide applications in crop production. Application of ENMs as crop protection agents, fertilizers or nano-sensors might potentially contribute to increase agricultural production by facilitating adaptation to the negative effects of climate change, increasing crop yields, biofortification, efficient plant protection, and enabling long-time storage without quality loss. These current and potential applications of ENMs result in their release into the environment. The gradually increasing presence of ENMs in the agro-ecosystem may entail their uptake by plants and affect their well-being. The morphological, physiological and biochemical response of plants to ENMs has been intensively studied over the last 20 years, whereas molecular changes *in planta* under ENMs exposure remain under-researched. Due to the last development of omics techniques, the transcriptomic, proteomic and metabolic effects of ENMs are more and more often analyzed. This brings in-depth understanding of interactions of ENMs with plants, which is crucial to efficient plant protection. However, because the above-mentioned molecular analyses are costly and time-consuming, usually one of omics techniques (mostly transcriptome) was used to explore ENM-induced effects. Moreover, molecular studies combined with advanced analytical techniques detecting the speciation and location of ENMs in plants (e.g. μXANES) will provide a greater insight of the specificity of ENMs. Most of the molecular investigations were conducted on a model plant, hydroponically grown *A. thaliana*. There is a pressing need to conduct tests

on agriculturally important plants (soil grown) at environmentally relevant concentrations of ENMs. Further comparative studies of ENMs with corresponding compounds are required to capture nano-specific changes, especially in proteins and metabolite profiles. Even now little is known regarding plant molecular response to long-term exposure to ENMs. Particular attention should be paid to unknown epigenetic changes in plant responses to ENMs exposure. As those modulations may be hereditary, it is of utmost importance to understand and predict the potential impacts of ENMs on crops. As more and more ENMs products are introduced to agri-sector, ensuring long-time safety by extensive testing and introduction of adequate regulations should take priority.

Declaration of Competing Interest

The authors declare that they have no known competing financial interests or personal relationships that could have appeared to influence the work reported in this paper.

Acknowledgments

This study was supported by National Science Centre (Poland) in the frame of SONATA project (2017/26/D/NZ9/00067).

Appendix A. Supporting information

Supplementary data associated with this article can be found in the online version at doi:10.1016/j.jhazmat.2021.127374.

References

Abdel Latef, A.A.H., Srivastava, A.K., El-sadek, M.S.A., Kordrostami, M., Tran, L.-S.P., 2018. Titanium dioxide nanoparticles improve growth and enhance tolerance of broad bean plants under saline soil conditions: $nTiO_2$ application mitigates soil salinity effects on broad bean. Land Degrad. Dev. 29, 1065–1073. https://doi.org/10.1002/ldr.2780.

Ali, S., Mehmood, A., Khan, N., 2021. Uptake, translocation, and consequences of nanomaterials on plant growth and stress adaptation. J. Nanomater. 2021, 1–17. https://doi.org/10.1155/2021/6677616.

Alkhatib, R., Alkhatib, B., Abdo, N., AL-Eitan, L., Creamer, R., 2019. Physio-biochemical and ultrastructural impact of (Fe_3O_4) nanoparticles on tobacco. BMC Plant Biol. 19, 253. https://doi.org/10.1186/s12870-019-1864-1.

Amenta, V., Aschberger, K., Arena, M., Bouwmeester, H., Botelho Moniz, F., Brandhoff, P., Gottardo, S., Marvin, H.J.P., Mech, A., Quiros Pesudo, L., Rauscher, H., Schoonjans, R., Vettori, M.V., Weigel, S., Peters, R.J., 2015. Regulatory aspects of nanotechnology in the agri/feed/food sector in EU and non-EU countries. Regul. Toxicol. Pharmacol. 73, 463–476. https://doi.org/10.1016/j.yrtph.2015.06.016.

Antonacci, A., Arduini, F., Moscone, D., Palleschi, G., Scognamiglio, V., 2018. Nanostructured (Bio)sensors for smart agriculture. TrAC Trends Anal. Chem. 98, 95–103. https://doi.org/10.1016/j.trac.2017.10.022.

Ao, M., Zhu, Y., He, S., Li, D., Li, P., Li, J., Cao, Y., 2013. Preparation and characterization of 1-naphthylacetic acid–silica conjugated nanospheres for enhancement of controlled-release performance. Nanotechnology 24, 035601. https://doi.org/10.1088/0957-4484/24/3/035601.

Apodaca, S.A., Tan, W., Dominguez, O.E., Hernandez-Viezcas, J.A., Peralta-Videa, J.R., Gardea-Torresdey, J.L., 2017. Physiological and biochemical effects of nanoparticulate copper, bulk copper, copper chloride, and kinetin in kidney bean (Phaseolus vulgaris) plants. Sci. Total Environ. 599–600, 2085–2094. https://doi.org/10.1016/j.scitotenv.2017.05.095.

Arduini, F., Cinti, S., Scognamiglio, V., Moscone, D., 2016. Nanomaterials in electrochemical biosensors for pesticide detection: advances and challenges in food analysis. Microchim. Acta 183, 2063–2083. https://doi.org/10.1007/s00604-016-1858-8.

Ashfaq, M., Verma, N., Khan, S., 2017. Carbon nanofibers as a micronutrient carrier in plants: efficient translocation and controlled release of Cu nanoparticles. Environ. Sci. Nano 4, 138–148. https://doi.org/10.1039/C6EN00385K.

Avellan, A., Schwab, F., Masion, A., Chaurand, P., Borschneck, D., Vidal, V., Rose, J., Santaella, C., Levard, C., 2017. Nanoparticle uptake in plants: gold nanomaterial localized in roots of arabidopsis thaliana by X-ray computed nanotomography and hyperspectral imaging. Environ. Sci. Technol. 51, 8682–8691. https://doi.org/10.1021/acs.est.7b01133.

Avellan, A., Yun, J., Zhang, Y., Spielman-Sun, E., Unrine, J.M., Thieme, J., Li, J., Lombi, E., Bland, G., Lowry, G.V., 2019. Nanoparticle size and coating chemistry control foliar uptake pathways, translocation, and leaf-to-rhizosphere transport in wheat. ACS Nano 13, 5291–5305. https://doi.org/10.1021/acsnano.8b09781.

Azevedo, J.L., Araujo, W.L., 2003. Genetically modified crops: environmental and human health concerns. Mutat. Res. Rev. Mutat. Res. 544, 223–233. https://doi.org/10.1016/j.mrrev.2003.07.002.

Barik, T.K., Sahu, B., Swain, V., 2008. Nanosilica—from medicine to pest control. Parasitol. Res. 103, 253–258. https://doi.org/10.1007/s00436-008-0975-7.

Bartel, D.P., 2018. Metazoan microRNAs. Cell 173, 20–51. https://doi.org/10.1016/j.cell.2018.03.006.

Belava, V.N., 2017. The effect of silver and copper nanoparticles on the wheat-pseudocercosporella herpotrichoides pathosystem. Nanoscale Res. Lett. 12, 250.

Birbaum, K., Brogioli, R., Schellenberg, M., Martinoia, E., Stark, W., Günther, D., Limbach, L., 2010. No evidence for cerium dioxide nanoparticle translocation in maize plants. Environ. Sci. Technol. 44, 8718–8723. https://doi.org/10.1021/es101685f.

Boghossian, A.A., Sen, F., Gibbons, B.M., Sen, S., Faltermeier, S.M., Giraldo, J.P., Zhang, C.T., Zhang, J., Heller, D.A., Strano, M.S., 2013. Application of nanoparticle antioxidants to enable hyperstable chloroplasts for solar energy harvesting. Adv. Energy Mater. 3, 881–893. https://doi.org/10.1002/aenm.201201014.

D. Bowman, G. Hodge, 2006. A small matter of regulation: an international review of nanotechnology regulation.

Boykov, I.N., Shuford, E., Zhang, B., 2019. Nanoparticle titanium dioxide affects the growth and microRNA expression of switchgrass (Panicum virgatum). Genomics 111, 450–456. https://doi.org/10.1016/j.ygeno.2018.03.002.

Bundschuh, M., Filser, J., Lüderwald, S., McKee, M.S., Metreveli, G., Schaumann, G.E., Schulz, R., Wagner, S., 2018. Nanoparticles in the environment: where do we come from, where do we go to? Environ. Sci. Eur. 30, 6. https://doi.org/10.1186/s12302-018-0132-6 (6–6).

Burklew, C.E., Ashlock, J., Winfrey, W.B., Zhang, B., 2012. Effects of aluminum oxide nanoparticles on the growth, development, and microrna expression of tobacco (Nicotiana tabacum). PLoS One 7, 34783. https://doi.org/10.1371/journal.pone.0034783.

Cai, D., Wang, L., Zhang, G., Zhang, X., Wu, Z., 2013. Controlling pesticide loss by natural porous micro/nano composites: straw ash-based biochar and biosilica. ACS Appl. Mater. Interfaces 5, 9212–9216. https://doi.org/10.1021/am402864r.

Cai, J., Du, D., 2008. A disposable sensor based on immobilization of acetylcholinesterase to multiwall carbon nanotube modified screen-printed electrode for determination of carbaryl. J. Appl. Electrochem. 38, 1217–1222. https://doi.org/10.1007/s10800-008-9540-4.

Cakmak, I., 2008. Enrichment of cereal grains with zinc: agronomic or genetic biofortification? Plant Soil 302, 1–17. https://doi.org/10.1007/s11104-007-9466-3.

Campos, B.B., Contreras-Cáceres, R., Bandosz, T.J., Jiménez-Jiménez, J., Rodríguez-Castellón, E., da Silva, J.C.G.E., Algarra, M., 2017. Carbon dots coated with vitamin B 12 as selective ratiometric nanosensor for phenolic carbofuran. Sens. Actuators B Chem. 239, 553–561. https://doi.org/10.1016/j.snb.2016.08.055.

Chaudhuri, B., Hörmann, F., Lalonde, S., Brady, S.M., Orlando, D.A., Benfey, P., Frommer, W.B., 2008. Protonophore- and pH-insensitive glucose and sucrose accumulation detected by FRET nanosensors in Arabidopsis root tips. Plant J. 56, 948–962. https://doi.org/10.1111/j.1365-313X.2008.03652.x.

Chen, H., 2018. Metal based nanoparticles in agricultural system: behavior, transport, and interaction with plants. Chem. Speciat. Bioavailab. 30, 123–134. https://doi.org/10.1080/09542299.2018.1520050.

Chen, H., Zuo, X., Su, S., Tang, Z., Wu, A., Song, S., Zhang, D., Fan, C., 2008. An electrochemical sensor for pesticide assays based on carbon nanotube-enhanced acetycholinesterase activity. Analyst 133, 1182–1186. https://doi.org/10.1039/b805334k.

Chen, J., Liu, B., Yang, Z., Qu, J., Xun, H., Dou, R., Gao, X., Wang, L., 2018. Phenotypic, transcriptional, physiological and metabolic responses to carbon nanodot exposure in Arabidopsis thaliana (L.). Environ. Sci. Nano. 5, 2672–2685. https://doi.org/10.1039/C8EN00674A.

Chung, I.-M., Rekha, K., Venkidasamy, B., Thiruvengadam, M., 2019. Effect of copper oxide nanoparticles on the physiology, bioactive molecules, and transcriptional changes in Brassica rapa ssp. rapa seedlings. Water Air Soil Pollut. 230, 48. https://doi.org/10.1007/s11270-019-4084-2.

Corredor, E., Testillano, P.S., Coronado, M.-J., González-Melendi, P., Fernández-Pacheco, R., Marquina, C., Ibarra, M.R., de la Fuente, J.M., Rubiales, D., Pérez-de-Luque, A., Risueño, M.-C., 2009. Nanoparticle penetration and transport in living pumpkin plants: in situ subcellular identification. BMC Plant Biol. 9, 45. https://doi.org/10.1186/1471-2229-9-45.

Cota-Ruiz, K., Hernández-Viezcas, J.A., Varela-Ramírez, A., Valdés, C., Núñez-Gastélum, J.A., Martínez-Martínez, A., Delgado-Rios, M., Peralta-Videa, J.R., Gardea-Torresdey, J.L., 2018. Toxicity of copper hydroxide nanoparticles, bulk copper hydroxide, and ionic copper to alfalfa plants: a spectroscopic and gene expression study. Environ. Pollut. 243, 703–712. https://doi.org/10.1016/j.envpol.2018.09.028.

Cunningham, F.J., Goh, N.S., Demirer, G.S., Matos, J.L., Landry, M.P., 2018. Nanoparticle-mediated delivery towards advancing plant genetic engineering. Trends Biotechnol. 36, 882–897. https://doi.org/10.1016/j.tibtech.2018.03.009.

Dai, T.-T., Lu, C.-C., Lu, J., Dong, S., Ye, W., Wang, Y., Zheng, X., 2012. Development of a loop-mediated isothermal amplification assay for detection of Phytophthora sojae. FEMS Microbiol. Lett. 334, 27–34. https://doi.org/10.1111/j.1574-6968.2012.02619.x.

Das, A., Das, B., 2019. Nanotechnology a potential tool to mitigate abiotic stress in crop plants. In: Bosco de Oliveira, A. (Ed.), Abiotic and Biotic Stress in Plants. IntechOpen. https://doi.org/10.5772/intechopen.83562.

Das, A., Rushton, P.J., Rohila, J.S., 2017. Metabolomic profiling of soybeans (Glycine max L.) reveals the importance of sugar and nitrogen metabolism under drought and heat stress. Plants 6. https://doi.org/10.3390/plants6020021.

Datta, M., Vitolins, M.Z., 2016. Food fortification and supplement use—are there health implications? Crit. Rev. Food Sci. Nutr. 56, 2149–2159. https://doi.org/10.1080/10408398.2013.818527.
Deshpande, P., Dapkekar, A., Oak, M., Paknikar, K., Rajwade, J., 2018. Nanocarrier-mediated foliar zinc fertilization influences expression of metal homeostasis related genes in flag leaves and enhances gluten content in durum wheat. PLoS One 13, 0191035. https://doi.org/10.1371/journal.pone.0191035.
Dimkpa, C.O., 2018. Soil properties influence the response of terrestrial plants to metallic nanoparticles exposure. Curr. Opin. Environ. Sci. Health 6, 1–8. https://doi.org/10.1016/j.coesh.2018.06.007.
Dimkpa, C.O., Bindraban, P.S., 2018. Nanofertilizers: new products for the industry? J. Agric. Food Chem. 66, 6462–6473. https://doi.org/10.1021/acs.jafc.7b02150.
Dimkpa, C.O., McLean, J.E., Britt, D.W., Anderson, A.J., 2012a. Bioactivity and biomodification of Ag, ZnO, and CuO nanoparticles with relevance to plant performance in agriculture. Ind. Biotechnol. 8, 344–357. https://doi.org/10.1089/ind.2012.0028.
Dimkpa, C.O., Mclean, J.E., Britt, D.W., Anderson, A.J., 2012b. CuO and ZnO nanoparticles differently affect the secretion of fluorescent siderophores in the beneficial root colonizer, Pseudomonas chlororaphis O6. Nanotoxicology 6, 635–642. https://doi.org/10.3109/17435390.2011.598246.
Doğaroğlu, Z.G., Köleli, N., 2017. TiO_2 and ZnO nanoparticles toxicity in barley (Hordeum vulgare L.). CLEAN Soil Air Water 45, 1700096. https://doi.org/10.1002/clen.201700096.
Dreaden, E.C., Alkilany, A.M., Huang, X., Murphy, C.J., El-Sayed, M.A., 2012. The golden age: gold nanoparticles for biomedicine. Chem. Soc. Rev. 41, 2740–2779. https://doi.org/10.1039/C1CS15237H.
Du, W., Gardea-Torresdey, J.L., Ji, R., Yin, Y., Zhu, J., Peralta-Videa, J.R., Guo, H., 2015. Physiological and biochemical changes imposed by CeO_2 nanoparticles on wheat: a life cycle field study. Environ. Sci. Technol. 49, 11884–11893. https://doi.org/10.1021/acs.est.5b03055.
Duhan, J.S., Kumar, R., Kumar, N., Kaur, P., Nehra, K., Duhan, S., 2017. Nanotechnology: the new perspective in precision agriculture. Biotechnol. Rep. 15, 11–23. https://doi.org/10.1016/j.btre.2017.03.002.
Eichert, T., Kurtz, A., Steiner, U., Goldbach, H.E., 2008. Size exclusion limits and lateral heterogeneity of the stomatal foliar uptake pathway for aqueous solutes and water-suspended nanoparticles. Physiol. Plant. 134, 151–160. https://doi.org/10.1111/j.1399-3054.2008.01135.x.
Eide, D., Broderius, M., Fett, J., Guerinot, M.L., 1996. A novel iron-regulated metal transporter from plants identified by functional expression in yeast. Proc. Natl. Acad. Sci. 93, 5624–5628. https://doi.org/10.1073/pnas.93.11.5624.
Elanchezhian, R., Kumar, D., Ramesh, K., Biswas, A.K., Guhey, A., Patra, A.K., 2017. Morpho-physiological and biochemical response of maize (Zea mays L.) plants fertilized with nano-iron (Fe_3O_4) micronutrient. J. Plant Nutr. 40, 1969–1977. https://doi.org/10.1080/01904167.2016.1270320.
Etxeberria, E., Gonzalez, P., Baroja-Fernández, E., Romero, J.P., 2006. Fluid phase endocytic uptake of artificial nano-spheres and fluorescent quantum dots by sycamore cultured cells. Plant Signal. Behav. 1, 196–200. https://doi.org/10.4161/psb.1.4.3142.
European Commission, 2011. Commission Recommendation of 18 October 2011 on the definition of nanomaterial Text with EEA relevance. ⟨http://data.europa.eu/eli/reco/2011/696/oj/eng⟩ (Accessed April 11, 2020).
Fang, C., Dharmarajan, R., Megharaj, M., Naidu, R., 2017. Gold nanoparticle-based optical sensors for selected anionic contaminants. TrAC Trends Anal. Chem. 86, 143–154. https://doi.org/10.1016/j.trac.2016.10.008.
Fang, Y., Ramasamy, R.P., 2015. Current and prospective methods for plant disease detection. Biosensors 5, 537–561. https://doi.org/10.3390/bios5030537.
Filiz, E., Akbudak, M.A., 2020. Ammonium transporter 1 (AMT1) gene family in tomato (Solanum lycopersicum L.): bioinformatics, physiological and expression analyses under drought and salt stresses. Genomics 112, 3773–3782. https://doi.org/10.1016/j.ygeno.2020.04.009.
Frazier, T.P., Burklew, C.E., Zhang, B., 2014. Titanium dioxide nanoparticles affect the growth and microRNA expression of tobacco (Nicotiana tabacum). Funct. Integr. Genom. 14, 75–83. https://doi.org/10.1007/s10142-013-0341-4.
Fung, F., Clark, R.F., 2004. Health effects of mycotoxins: a toxicological overview. J. Toxicol. Clin. Toxicol. 42, 217–234. https://doi.org/10.1081/CLT-120030947.
Galbraith, D.W., 2007. Silica breaks through in plants. Nat. Nanotechnol. 2, 272–273. https://doi.org/10.1038/nnano.2007.118.
Gao, X., Avellan, A., Laughton, S., Vaidya, R., Rodrigues, S.M., Casman, E.A., Lowry, G. V., 2018. CuO nanoparticle dissolution and toxicity to wheat (Triticum aestivum) in rhizosphere soil. Environ. Sci. Technol. 52, 2888–2897. https://doi.org/10.1021/acs.est.7b05816.
Gao, X., Rodrigues, S.M., Spielman-Sun, E., Lopes, S., Rodrigues, S., Zhang, Y., Avellan, A., Duarte, R.M.B.O., Duarte, A., Casman, E.A., Lowry, G.V., 2019. Effect of soil organic matter, soil pH, and moisture content on solubility and dissolution rate of CuO NPs in soil. Environ. Sci. Technol. 53, 4959–4967. https://doi.org/10.1021/acs.est.8b07243.
García-Sánchez, S., Bernales, I., Cristobal, S., 2015. Early response to nanoparticles in the Arabidopsis transcriptome compromises plant defence and root-hair development through salicylic acid signalling. BMC Genom. 16, 341. https://doi.org/10.1186/s12864-015-1530-4.
Geitner, N.K., Cooper, J.L., Avellan, A., Castellon, B.T., Perrotta, B.G., Bossa, N., Simonin, M., Anderson, S.M., Inoue, S., Hochella, M.F., Richardson, C.J., Bernhardt, E.S., Lowry, G.V., Ferguson, P.L., Matson, C.W., King, R.S., Unrine, J.M., Wiesner, M.R., Hsu-Kim, H., 2018. Size-based differential transport, uptake, and mass distribution of Ceria (CeO_2) nanoparticles in wetland mesocosms. Environ. Sci. Technol. 52, 9768–9776. https://doi.org/10.1021/acs.est.8b02040.
Ghosh, M., Jana, A., Sinha, S., Jothiramajayam, M., Nag, A., Chakraborty, A., Mukherjee, A., Mukherjee, A., 2016. Effects of ZnO nanoparticles in plants: cytotoxicity, genotoxicity, deregulation of antioxidant defenses, and cell-cycle arrest. Mutat. Res. Genet. Toxicol. Environ. Mutagen 807, 25–32. https://doi.org/10.1016/j.mrgentox.2016.07.006.
Giannousi, K., Avramidis, I., Dendrinou-Samara, C., 2013. Synthesis, characterization and evaluation of copper based nanoparticles as agrochemicals against Phytophthora infestans. RSC Adv. 3, 21743. https://doi.org/10.1039/c3ra42118j.
Giraldo, J., Landry, M., Faltermeier, S., McNicholas, T., Iverson, N., Boghossian, A., Reuel, N., Hilmer, A., Sen, F., Brew, J., Strano, M., 2014. Plant nanobionics approach to augment photosynthesis and biochemical sensing. Nat. Mater. 13, 400–408. https://doi.org/10.1038/nmat3947.
Giraldo, J.P., Landry, M.P., Kwak, S.-Y., Jain, R.M., Wong, M.H., Iverson, N.M., Ben-Naim, M., Strano, M.S., 2015. A ratiometric sensor using single chirality near-infrared fluorescent carbon nanotubes: application to in vivo monitoring. Small 11, 3973–3984. https://doi.org/10.1002/smll.201403276.
Giraldo, J.P., Wu, H., Newkirk, G.M., Kruss, S., 2019. Nanobiotechnology approaches for engineering smart plant sensors. Nat. Nanotechnol. 14, 541–553. https://doi.org/10.1038/s41565-019-0470-6.
Goel, P., Arora, M., 2018. Fabrication of chemical sensor for organochlorine pesticide detection using colloidal gold nanoparticles. MRS Commun. 8, 1000–1007. https://doi.org/10.1557/mrc.2018.125.
Gogos, A., Knauer, K., Bucheli, T.D., 2012. Nanomaterials in plant protection and fertilization: current state, foreseen applications, and research priorities. J. Agric. Food Chem. 60, 9781–9792. https://doi.org/10.1021/jf302154y.
Graf, C., Nordmeyer, D., Sengstock, C., Ahlberg, S., Diendorf, J., Raabe, J., Epple, M., Köller, M., Lademann, J., Vogt, A., Rancan, F., Rühl, E., 2018. Shape-dependent dissolution and cellular uptake of silver nanoparticles. Langmuir 34, 1506–1519. https://doi.org/10.1021/acs.langmuir.7b03126.
Grewal, A., Singla, A., Kamboj, P., Dua, J., 2017. Pesticide residues in food grains, vegetables and fruits: a hazard to human health. J. Med. Chem. Toxicol. 2, 1–7. https://doi.org/10.15436/2575-808X.17.1355.
Guan, H., Chi, D., Yu, J., Li, H., 2010. Dynamics of residues from a novel nano-imidacloprid formulation in soyabean fields. Crop Prot. 29, 942–946. https://doi.org/10.1016/j.cropro.2010.04.022.
Guo, W., Nazim, H., Liang, Z., Yang, D., 2016. Magnesium deficiency in plants: an urgent problem. Crop J. 4, 83–91. https://doi.org/10.1016/j.cj.2015.11.003.
Guo, Z., Park, S., Yoon, J., Shin, I., 2013. Recent progress in the development of near-infrared fluorescent probes for bioimaging applications. Chem. Soc. Rev. 43, 16–29. https://doi.org/10.1039/C3CS60271K.
Gupta, R., Xie, H., 2018. Nanoparticles in daily life: applications, toxicity and regulations. J. Environ. Pathol. Toxicol. Oncol. 37, 209–230. https://doi.org/10.1615/JEnvironPatholToxicolOncol.2018026009.
Gupta, S.D., Agarwal, A., Pradhan, S., 2018. Phytostimulatory effect of silver nanoparticles (AgNPs) on rice seedling growth: an insight from antioxidative enzyme activities and gene expression patterns. Ecotoxicol. Environ. Saf. 161, 624–633. https://doi.org/10.1016/j.ecoenv.2018.06.023.
Halvorson, R.A., Vikesland, P.J., 2010. Surface-Enhanced Raman Spectroscopy (SERS) for environmental analyses. Environ. Sci. Technol. 44, 7749–7755. https://doi.org/10.1021/es101228z.
Hariharan, G., Prasannath, K., 2021. Recent advances in molecular diagnostics of fungal plant pathogens: a mini review. Front. Cell Infect. Microbiol. 10, 600234 https://doi.org/10.3389/fcimb.2020.600234.
He, X., Deng, H., Hwang, H., 2019. The current application of nanotechnology in food and agriculture. J. Food Drug Anal. 27, 1–21. https://doi.org/10.1016/j.jfda.2018.12.002.
Heller, D.A., Jin, H., Martinez, B.M., Patel, D., Miller, B.M., Yeung, T.-K., Jena, P.V., Höbartner, C., Ha, T., Silverman, S.K., Strano, M.S., 2009. Multimodal optical sensing and analyte specificity using single-walled carbon nanotubes. Nat. Nanotechnol. 4, 114–120. https://doi.org/10.1038/nnano.2008.369.
Hong, F., Zhou, J., Liu, C., Yang, F., Wu, C., Zheng, L., Yang, P., 2005. Effect of nano-TiO_2 on photochemical reaction of chloroplasts of spinach. Biol. Trace Elem. Res. 105, 269–280. https://doi.org/10.1385/BTER:105:1-3:269.
Hong, G., Diao, S., Antaris, A.L., Dai, H., 2015. Carbon nanomaterials for biological imaging and nanomedicinal therapy. Chem. Rev. 115, 10816–10906. https://doi.org/10.1021/acs.chemrev.5b00008.
Hossain, Z., Mustafa, G., Komatsu, S., 2015. Plant responses to nanoparticle stress. Int. J. Mol. Sci. 16, 26644–26653. https://doi.org/10.3390/ijms161125980.
Hossain, Z., Mustafa, G., Sakata, K., Komatsu, S., 2016. Insights into the proteomic response of soybean towards Al_2O_3, ZnO, and Ag nanoparticles stress. J. Hazard. Mater. 304, 291–305. https://doi.org/10.1016/j.jhazmat.2015.10.071.
Hossain, Z., Yasmeen, F., Komatsu, S., 2020. Nanoparticles: synthesis, morphophysiological effects, and proteomic responses of crop plants. Int. J. Mol. Sci. 21, 3056. https://doi.org/10.3390/ijms21093056.
Hou, R., Pang, S., He, L., 2015. In situ SERS detection of multi-class insecticides on plant surfaces. Anal. Methods 7, 6325–6330. https://doi.org/10.1039/C5AY01058F.
Huang, S., Hu, J., Guo, P., Liu, M., Wu, R., 2015. Rapid detection of chlorpyriphos residue in rice by surface-enhanced Raman scattering. Anal. Methods 7, 4334–4339. https://doi.org/10.1039/C5AY00381D.
Hussain, T., 2017. Nanotechnology: diagnosis of plant diseases opinion. Agric. Res. Technol. 10 https://doi.org/10.19080/ARTOAJ.2017.10.555777.
Jechalke, S., Schierstaedt, J., Becker, M., Flemer, B., Grosch, R., Smalla, K., Schikora, A., 2019. Salmonella establishment in agricultural soil and colonization of crop plants depend on soil type and plant species. Front. Microbiol. 10, 967. https://doi.org/10.3389/fmicb.2019.00967.

Jianrong, C., Miao, Y., Nongyue, H., Xiaohua, W., Sijiao, L., 2004. Nanotechnology and biosensors. Biotechnol. Adv. 22, 505–518. https://doi.org/10.1016/j.biotechadv.2004.03.004.

Jin, H., Heller, D.A., Kalbacova, M., Kim, J.-H., Zhang, J., Boghossian, A.A., Maheshri, N., Strano, M.S., 2010. Detection of single-molecule H_2O_2 signalling from epidermal growth factor receptor using fluorescent single-walled carbon nanotubes. Nat. Nanotechnol. 5, 302–309. https://doi.org/10.1038/nnano.2010.24.

Jin, Y., Fan, X., Li, X., Zhang, Z., Sun, L., Fu, Z., Lavoie, M., Pan, X., Qian, H., 2017. Distinct physiological and molecular responses in Arabidopsis thaliana exposed to aluminum oxide nanoparticles and ionic aluminum. Environ. Pollut. 228, 517–527. https://doi.org/10.1016/j.envpol.2017.04.073.

Johnston, C.T., 2010. Probing the nanoscale architecture of clay minerals. Clay Miner. 45, 245–279. https://doi.org/10.1180/claymin.2010.045.3.245.

José Villaverde, J., Sevilla-Morán, B., López-Goti, C., Sandín-España, P., Luis Alonso-Prados, J., 2017. An overview of nanopesticides in the framework of European legislation. In: New Pesticides and Soil Sensors. Elsevier, pp. 227–271. https://doi.org/10.1016/B978-0-12-804299-1.00007-2.

Kah, M., Beulke, S., Tiede, K., Hofmann, T., 2013. Nanopesticides: state of knowledge, environmental fate, and exposure modeling. Crit. Rev. Environ. Sci. Technol. 43, 1823–1867. https://doi.org/10.1080/10643389.2012.671750.

Kah, M., Tufenkji, N., White, J.C., 2019. Nano-enabled strategies to enhance crop nutrition and protection. Nat. Nanotechnol. 14, 532–540. https://doi.org/10.1038/s41565-019-0439-5.

Kapilan, R., Vaziri, M., Zwiazek, J.J., 2018. Regulation of aquaporins in plants under stress. Biol. Res. 51, 4. https://doi.org/10.1186/s40659-018-0152-0.

Kaveh, R., Li, Y.-S., Ranjbar, S., Tehrani, R., Brueck, C.L., Van Aken, B., 2013. Changes in Arabidopsis thaliana gene expression in response to silver nanoparticles and silver ions. Environ. Sci. Technol. 47, 10637–10644. https://doi.org/10.1021/es402209w.

Keinath, N.F., Waadt, R., Brugman, R., Schroeder, J.I., Grossmann, G., Schumacher, K., Krebs, M., 2015. Live cell imaging with R-GECO1 sheds light on flg22- and Chitin-induced transient [Ca(2+)]cyt patterns in Arabidopsis. Mol. Plant 8, 1188–1200. https://doi.org/10.1016/j.molp.2015.05.006.

Keller, A.A., Adeleye, A.S., Conway, J.R., Garner, K.L., Zhao, L., Cherr, G.N., Hong, J., Gardea-Torresdey, J.L., Godwin, H.A., Hanna, S., Ji, Z., Kaweeteerawat, C., Lin, S., Lenihan, H.S., Miller, R.J., Nel, A.E., Peralta-Videa, J.R., Walker, S.L., Taylor, A.A., Torres-Duarte, C., Zink, J.I., Zuverza-Mena, N., 2017. Comparative environmental fate and toxicity of copper nanomaterials. NanoImpact 7, 28–40. https://doi.org/10.1016/j.impact.2017.05.003.

Key, S., Ma, J.K.-C., Drake, P.M., 2008. Genetically modified plants and human health. J. R. Soc. Med. 101, 290–298. https://doi.org/10.1258/jrsm.2008.070372.

Khan, M.R., Rizvi, T.F., 2014. Nanotechnology: scope and application in plant disease management. Plant Pathol. J. 13, 214–231. https://doi.org/10.3923/ppj.2014.214.231.

Khiyami, M.A., Almoammar, H., Awad, Y.M., Alghuthaymi, M.A., Abd-Elsalam, K.A., 2014. Plant pathogen nanodiagnostic techniques: forthcoming changes? Biotechnol. Biotechnol. Equip. 28, 775–785. https://doi.org/10.1080/13102818.2014.960739.

Khodakovskaya, M.V., de Silva, K., Nedosekin, D.A., Dervishi, E., Biris, A.S., Shashkov, E. V., Galanzha, E.I., Zharov, V.P., 2011. Complex genetic, photothermal, and photoacoustic analysis of nanoparticle-plant interactions. PNAS 108, 1028–1033. https://doi.org/10.1073/pnas.1008856108.

Khodakovskaya, M.V., de Silva, K., Biris, A.S., Dervishi, E., Villagarcia, H., 2012. Carbon nanotubes induce growth enhancement of tobacco cells. ACS Nano 6, 2128–2135. https://doi.org/10.1021/nn204643g.

Kim, D.H., Gopal, J., Sivanesan, I., 2017. Nanomaterials in plant tissue culture: the disclosed and undisclosed. RSC Adv. 7, 36492–36505. https://doi.org/10.1039/C7RA07025J.

Kim, E., Magen, A., Ast, G., 2007. Different levels of alternative splicing among eukaryotes. Nucleic Acids Res. 35, 125–131. https://doi.org/10.1093/nar/gkl924.

Kim, S., Lee, S., Lee, I., 2012. Alteration of phytotoxicity and oxidant stress potential by metal oxide nanoparticles in Cucumis sativus. Water Air Soil Pollut. 223, 2799–2806. https://doi.org/10.1007/s11270-011-1067-3.

Kissen, R., Bones, A.M., 2009. Nitrile-specifier proteins involved in glucosinolate hydrolysis in Arabidopsis thaliana. J. Biol. Chem. 284, 12057–12070. https://doi.org/10.1074/jbc.M807500200.

Kohan-Baghkheirati, E., Geisler-Lee, J., 2015. Gene expression, protein function and pathways of arabidopsis thaliana responding to silver nanoparticles in comparison to silver ions, cold, salt, drought, and heat. Nanomaterials 5, 436–467. https://doi.org/10.3390/nano5020436.

Kruss, S., Landry, M.P., Vander Ende, E., Lima, B.M.A., Reuel, N.F., Zhang, J., Nelson, J., Mu, B., Hilmer, A., Strano, M., 2014. Neurotransmitter detection using corona phase molecular recognition on fluorescent single-walled carbon nanotube sensors. J. Am. Chem. Soc. 136, 713–724. https://doi.org/10.1021/ja410433b.

Kumar, V., Guleria, P., Kumar, V., Yadav, S.K., 2013. Gold nanoparticle exposure induces growth and yield enhancement in Arabidopsis thaliana. Sci. Total Environ. 461–462, 462–468. https://doi.org/10.1016/j.scitotenv.2013.05.018.

Kumari, A., Yadav, S.K., Yadav, S.C., 2010. Biodegradable polymeric nanoparticles based drug delivery systems. Colloids Surf. B Biointerfaces 75, 1–18. https://doi.org/10.1016/j.colsurfb.2009.09.001.

Lahiani, M.H., Dervishi, E., Chen, J., Nima, Z., Gaume, A., Biris, A.S., Khodakovskaya, M. V., 2013. Impact of carbon nanotube exposure to seeds of valuable crops. ACS Appl. Mater. Interfaces 5, 7965–7973. https://doi.org/10.1021/am402052x.

Lamsal, K., Kim, S.-W., Jung, J.H., Kim, Y.S., Kim, K.S., Lee, Y.S., 2011. Inhibition effects of silver nanoparticles against powdery mildews on cucumber and pumpkin. Mycobiology 39, 26–32. https://doi.org/10.4489/MYCO.2011.39.1.026.

Landa, P., Vankova, R., Andrlova, J., Hodek, J., Marsik, P., Storchova, H., White, J.C., Vanek, T., 2012. Nanoparticle-specific changes in Arabidopsis thaliana gene expression after exposure to ZnO, TiO_2, and fullerene soot. J. Hazard. Mater. 241–242, 55–62. https://doi.org/10.1016/j.jhazmat.2012.08.059.

Landa, P., Prerostova, S., Petrova, S., Knirsch, V., Vankova, R., Vanek, T., 2015. The transcriptomic response of arabidopsis thaliana to zinc oxide: a comparison of the impact of nanoparticle, bulk, and ionic zinc. Environ. Sci. Technol. 49, 14537–14545. https://doi.org/10.1021/acs.est.5b03330.

Landa, P., Dytrych, P., Prerostova, S., Petrova, S., Vankova, R., Vanek, T., 2017. Transcriptomic response of Arabidopsis thaliana exposed to CuO nanoparticles, bulk material, and ionic copper. Environ. Sci. Technol. 51, 10814–10824. https://doi.org/10.1021/acs.est.7b02265.

Larrieu, A., Champion, A., Legrand, J., Lavenus, J., Mast, D., Brunoud, G., Oh, J., Guyomarc'H, S., Pizot, M., Farmer, E.E., Turnbull, C., Vernoux, T., Bennett, M.J., Laplaze, L., 2015. A fluorescent hormone biosensor reveals the dynamics of jasmonate signalling in plants. Nat. Commun. 6, 6043. https://doi.org/10.1038/ncomms7043.

Larue, C., Pinault, M., Czarny, B., Georgin, D., Jaillard, D., Bendiab, N., Mayne-L'Hermite, M., Taran, F., Dive, V., Carrière, M., 2012. Quantitative evaluation of multi-walled carbon nanotube uptake in wheat and rapeseed. J. Hazard. Mater. 227–228, 155–163. https://doi.org/10.1016/j.jhazmat.2012.05.033.

Larue, C., Baratange, C., Vantelon, D., Khodja, H., Surblé, S., Elger, A., Carrière, M., 2018. Influence of soil type on TiO_2 nanoparticle fate in an agro-ecosystem. Sci. Total Environ. 630, 609–617. https://doi.org/10.1016/j.scitotenv.2018.02.264.

Le, V.N., Rui, Y., Gui, X., Li, X., Liu, S., Han, Y., 2014. Uptake, transport, distribution and Bio-effects of SiO_2 nanoparticles in Bt-transgenic cotton. J. Nanobiotechnol. 12, 50. https://doi.org/10.1186/s12951-014-0050-8.

Lee, S.S., Song, W., Cho, M., Puppala, H.L., Nguyen, P., Zhu, H., Segatori, L., Colvin, V.L., 2013. Antioxidant properties of cerium oxide nanocrystals as a function of nanocrystal diameter and surface coating. ACS Nano 7, 9693–9703. https://doi.org/10.1021/nn4026806.

Lee, W.-M., An, Y.-J., Yoon, H., Kweon, H.-S., 2008. Toxicity and bioavailability of copper nanoparticles to the terrestrial plants mung bean (Phaseolus radiatus) and wheat (Triticum aestivum): plant agar test for water-insoluble nanoparticles. Environ. Toxicol. Chem. 27, 1915–1921.

Lee, W.-M., Kwak, J.I., An, Y.-J., 2012. Effect of silver nanoparticles in crop plants Phaseolus radiatus and Sorghum bicolor: media effect on phytotoxicity. Chemosphere 86, 491–499. https://doi.org/10.1016/j.chemosphere.2011.10.013.

Lewis, B.P., Burge, C.B., Bartel, D.P., 2005. Conserved seed pairing, often flanked by adenosines, indicates that thousands of human genes are microRNA targets. Cell 120, 15–20. https://doi.org/10.1016/j.cell.2004.12.035.

Li, C., Wang, P., Lombi, E., Cheng, M., Tang, C., Howard, D.L., Menzies, N.W., Kopittke, P.M., 2018a. Absorption of foliar-applied Zn fertilizers by trichomes in soybean and tomato. J. Exp. Bot. 69, 2717–2729. https://doi.org/10.1093/jxb/ery085.

Li, H., Ye, X., Guo, X., Geng, Z., Wang, G., 2016. Effects of surface ligands on the uptake and transport of gold nanoparticles in rice and tomato. J. Hazard. Mater. 314, 188–196. https://doi.org/10.1016/j.jhazmat.2016.04.043.

Li, J., Wu, H., Santana, I., Fahlgren, M., Giraldo, J.P., 2018b. Standoff optical glucose sensing in photosynthetic organisms by a quantum dot fluorescent probe. ACS Appl. Mater. Interfaces 10, 28279–28289. https://doi.org/10.1021/acsami.8b07179.

Li, X., Mu, L., Hu, X., 2018c. Integrating proteomics, metabolomics and typical analysis to investigate the uptake and oxidative stress of graphene oxide and polycyclic aromatic hydrocarbons. Environ. Sci. Nano 5, 115–129. https://doi.org/10.1039/C7EN00803A.

Li, X., Ban, Z., Yu, F., Hao, W., Hu, X., 2020. Untargeted metabolic pathway analysis as an effective strategy to connect various nanoparticle properties to nanoparticle-induced ecotoxicity. Environ. Sci. Technol. 54, 3395–3406. https://doi.org/10.1021/acs.est.9b06096.

Liu, M., Feng, S., Ma, Y., Xie, C., He, X., Ding, Y., Zhang, J., Luo, W., Zheng, L., Chen, D., Yang, F., Chai, Z., Zhao, Y., Zhang, Z., 2019. Influence of surface charge on the phytotoxicity, transformation, and translocation of CeO_2 nanoparticles in cucumber plants. ACS Appl. Mater. Interfaces 11, 16905–16913. https://doi.org/10.1021/acsami.9b01627.

Lowry, G.V., Gregory, K.B., Apte, S.C., Lead, J.R., 2012. Transformations of nanomaterials in the environment. Environ. Sci. Technol. 46, 6893–6899. https://doi.org/10.1021/es300839e.

Lowry, G.V., Avellan, A., Gilbertson, L.M., 2019. Opportunities and challenges for nanotechnology in the agri-tech revolution. Nat. Nanotechnol. 14, 517–522. https://doi.org/10.1038/s41565-019-0461-7.

Lu, K., Shen, D., Liu, X., Dong, S., Jing, X., Wu, W., Tong, Y., Gao, S., Mao, L., 2020. Uptake of iron oxide nanoparticles inhibits the photosynthesis of the wheat after foliar exposure. Chemosphere 259, 127445. https://doi.org/10.1016/j.chemosphere.2020.127445.

Lupan, O., Wolff, N., Postica, V., Braniste, T., Paulowicz, I., Hrkac, V., Mishra, Y.K., Tiginyanu, I., Kienle, L., Adelung, R., 2018. Properties of a single SnO_2:Zn_2SnO_4 – functionalized nanowire based nanosensor. Ceram. Int. 44, 4859–4867. https://doi.org/10.1016/j.ceramint.2017.12.075.

Ma, C., Chhikara, S., Xing, B., Musante, C., White, J.C., Dhankher, O.P., 2013. Physiological and molecular response of Arabidopsis thaliana (L.) to nanoparticle cerium and indium oxide exposure. ACS Sustain. Chem. Eng. 1, 768–778. https://doi.org/10.1021/sc400098h.

Ma, X., Geisler-Lee, J., Geiser-Lee, J., Deng, Y., Kolmakov, A., 2010. Interactions between engineered nanoparticles (ENPs) and plants: phytotoxicity, uptake and accumulation. Sci. Total Environ. 408, 3053–3061. https://doi.org/10.1016/j.scitotenv.2010.03.031.

Ma, Y., He, X., Zhang, P., Zhang, Z., Ding, Y., Zhang, J., Wang, G., Xie, C., Luo, W., Zhang, J., Zheng, L., Chai, Z., Yang, K., 2017. Xylem and phloem based transport of

CeO_2 nanoparticles in hydroponic cucumber plants. Environ. Sci. Technol. 51, 5215–5221. https://doi.org/10.1021/acs.est.6b05998.
Ma, Y., Yao, Y., Yang, J., He, X., Ding, Y., Zhang, P., Zhang, J., Wang, G., Xie, C., Luo, W., Zhang, J., Zheng, L., Chai, Z., Zhao, Y., Zhang, Z., 2018. Trophic transfer and transformation of CeO_2 nanoparticles along a terrestrial food chain: influence of exposure routes. Environ. Sci. Technol. 52, 7921–7927. https://doi.org/10.1021/acs.est.8b00596.
Mafuta, M., Zennaro, M., Bagula, A., Ault, G., Gombachika, H., Chadza, T., 2013. Successful deployment of a wireless sensor network for precision agriculture in Malawi. Int. J. Distrib. Sens. Netw. 9, 150703 https://doi.org/10.1155/2013/150703.
T. Mahil, A.K. Baburai Nagesh, 2019. Foliar application of nanofertilizers in agricultural crops -a review.
Majumdar, S., Keller, A.A., 2020. Omics to address the opportunities and challenges of nanotechnology in agriculture. Crit. Rev. Environ. Sci. Technol. 0, 1–42. https://doi.org/10.1080/10643389.2020.1785264.
Marchiol, L., Mattiello, A., Pošćić, F., Fellet, G., Zavalloni, C., Carlino, E., Musetti, R., 2016. Changes in physiological and agronomical parameters of barley (Hordeum vulgare) exposed to cerium and titanium dioxide nanoparticles. Int. J. Environ. Res. Public Health 13. https://doi.org/10.3390/ijerph13030332.
Marmiroli, M., Pagano, L., Savo Sardaro, M.L., Villani, M., Marmiroli, N., 2014. Genome-wide approach in Arabidopsis thaliana to assess the toxicity of cadmium sulfide quantum dots. Environ. Sci. Technol. 48, 5902–5909. https://doi.org/10.1021/es404958r.
Maurel, C., Verdoucq, L., Luu, D.-T., Santoni, V., 2008. Plant aquaporins: membrane channels with multiple integrated functions. Annu. Rev. Plant Biol. 59, 595–624. https://doi.org/10.1146/annurev.arplant.59.032607.092734.
Md. Nuruzzaman, M.M.Rahman, Liu, Y., Naidu, R., 2016. Nanoencapsulation, nano-guard for pesticides: a new window for safe application. J. Agric. Food Chem. 64, 1447–1483. https://doi.org/10.1021/acs.jafc.5b05214.
Milewska-Hendel, A., Zubko, M., Karcz, J., Stróż, D., Kurczyńska, E., 2017. Fate of neutral-charged gold nanoparticles in the roots of the Hordeum vulgare L. cultivar Karat. Sci. Rep. 7, 3014. https://doi.org/10.1038/s41598-017-02965-w.
Mishra, S., Keswani, C., Abhilash, P.C., Fraceto, L.F., Singh, H.B., 2017. Integrated approach of agri-nanotechnology: challenges and future trends. Front Plant Sci. 8, 471. https://doi.org/10.3389/fpls.2017.00471.
D. Mortazavi, A.Z. Kouzani, A. Kaynak, W. Duan, 2011. Nano-plasmonic biosensors: a review, in: The 2011 IEEE/ICME International Conference on Complex Medical Engineering. pp. 31–36. https://doi.org/10.1109/ICCME.2011.5876700.
Mosa, K.A., El-Naggar, M., Ramamoorthy, K., Alawadhi, H., Elnaggar, A., Wartanian, S., Ibrahim, E., Hani, H., 2018. Copper nanoparticles induced genotoxicty, oxidative stress, and changes in Superoxide Dismutase (SOD) gene expression in cucumber (Cucumis sativus) plants. Front. Plant Sci. 9, 872. https://doi.org/10.3389/fpls.2018.00872.
Mueller, N.D., Gerber, J.S., Johnston, M., Ray, D.K., Ramankutty, N., Foley, J.A., 2012. Closing yield gaps through nutrient and water management. Nature 490, 254–257. https://doi.org/10.1038/nature11420.
Mustafa, G., Sakata, K., Komatsu, S., 2015. Proteomic analysis of flooded soybean root exposed to aluminum oxide nanoparticles. J. Proteom. 128, 280–297. https://doi.org/10.1016/j.jprot.2015.08.010.
Nair, P.M.G., Chung, I.M., 2014. Physiological and molecular level effects of silver nanoparticles exposure in rice (Oryza sativa L.) seedlings. Chemosphere 112, 105–113. https://doi.org/10.1016/j.chemosphere.2014.03.056.
Nair, R., Varghese, S.H., Nair, B.G., Maekawa, T., Yoshida, Y., Kumar, D.S., 2010. Nanoparticulate material delivery to plants. Plant Sci. 179, 154–163. https://doi.org/10.1016/j.plantsci.2010.04.012.
OECD, 2013. Regulatory frameworks for nanotechnology in foods and medical products: summary results of a survey activity. ⟨https://doi.org/10.1787/5k47w4vsb4s4-en⟩.
Ogunkunle, C.O., Bornmann, B., Wagner, R., Fatoba, P.O., Frahm, R., Lützenkirchen-Hecht, D., 2019. Copper uptake, tissue partitioning and biotransformation evidence by XANES in cowpea (Vigna unguiculata L) grown in soil amended with nano-sized copper particles. Environ. Nanotechnol. Monit. Manag. 12, 100231 https://doi.org/10.1016/j.enmm.2019.100231.
Ohadi Rafsanjani, M., Alvari, A., Samim, M., Hejazi, M., Abdin, M., 2012. Application of novel nanotechnology strategies in plant biotransformation: a contemporary overview. ⟨https://doi.org/10.2174/187220812799789145⟩.
Oliveira, H.C., Stolf-Moreira, R., Martinez, C.B.R., Grillo, R., de Jesus, M.B., Fraceto, L.F., 2015. Nanoencapsulation enhances the post-emergence herbicidal activity of atrazine against mustard plants. PLoS One 10, 0132971. https://doi.org/10.1371/journal.pone.0132971.
Othman, M.F., Shazali, K., 2012. Wireless sensor network applications: a study in environment monitoring system. Procedia Eng. 41, 1204–1210. https://doi.org/10.1016/j.proeng.2012.07.302.
Pagano, L., Servin, A.D., De La Torre-Roche, R., Mukherjee, A., Majumdar, S., Hawthorne, J., Marmiroli, M., Maestri, E., Marra, R.E., Isch, S.M., Dhankher, O.P., White, J.C., Marmiroli, N., 2016. Molecular response of crop plants to engineered nanomaterials. Environ. Sci. Technol. 50, 7198–7207. https://doi.org/10.1021/acs.est.6b01816.
Pakrashi, S., Jain, N., Dalai, S., Jayakumar, J., Chandrasekaran, P.T., Raichur, A.M., Chandrasekaran, N., Mukherjee, A., 2014. In vivo genotoxicity assessment of titanium dioxide nanoparticles by Allium cepa root tip assay at high exposure concentrations. PLoS One 9, 87789. https://doi.org/10.1371/journal.pone.0087789.
Pan, M., Yin, Z., Liu, K., Du, X., Liu, H., Wang, S., 2019. Carbon-based nanomaterials in sensors for food safety. Nanomaterials 9, 1330. https://doi.org/10.3390/nano9091330.
Peng, C., Duan, D., Xu, C., Chen, Y., Sun, L., Zhang, H., Yuan, X., Zheng, L., Yang, Y., Yang, J., Zhen, X., Chen, Y., Shi, J., 2015. Translocation and biotransformation of CuO nanoparticles in rice (Oryza sativa L.) plants. Environ. Pollut. 197, 99–107. https://doi.org/10.1016/j.envpol.2014.12.008.
Peng, C., Xu, C., Liu, Q., Sun, L., Luo, Y., Shi, J., 2017. Fate and transformation of CuO nanoparticles in the soil-rice system during the life cycle of rice plants. Environ. Sci. Technol. 51, 4907–4917. https://doi.org/10.1021/acs.est.6b05882.
Pérez-de-Luque, A., 2017. Interaction of nanomaterials with plants: what do we need for real applications in agriculture? Front. Environ. Sci. 5 https://doi.org/10.3389/fenvs.2017.00012.
Pérez-Labrada, F., López-Vargas, E.R., Ortega-Ortiz, H., Cadenas-Pliego, G., Benavides-Mendoza, A., Juárez-Maldonado, A., 2019. Responses of tomato plants under saline stress to foliar application of copper nanoparticles. Plants 8. https://doi.org/10.3390/plants8060151.
Perlak, F.J., Deaton, R.W., Armstrong, T.A., Fuchs, R.L., Sims, S.R., Greenplate, J.T., Fischhoff, D.A., 1990. Insect resistant cotton plants. Nat. Biotechnol. 8, 939–943. https://doi.org/10.1038/nbt1090-939.
Pollard, M., Beisson, F., Li, Y., Ohlrogge, J.B., 2008. Building lipid barriers: biosynthesis of cutin and suberin. Trends Plant Sci. 13, 236–246. https://doi.org/10.1016/j.tplants.2008.03.003.
Pradas del Real, A.E., Vidal, V., Carrière, M., Castillo-Michel, H., Levard, C., Chaurand, P., Sarret, G., 2017. Silver nanoparticles and wheat roots: a complex interplay. Environ. Sci. Technol. 51, 5774–5782. https://doi.org/10.1021/acs.est.7b00422.
Pradhan, S., Mailapalli, D.R., 2017. Interaction of engineered nanoparticles with the agri-environment. J. Agric. Food Chem. 65, 8279–8294. https://doi.org/10.1021/acs.jafc.7b02528.
Pramanik, A., Datta, A., Gupta, S., 2017. Cadmium sulphide (CDS) and copper oxide (CUO) nanoparticles (NPS) mediated phenotypic mutation in Coriandrum sativum L. (APIACEAE). Int. J. Recent Sci. Res. https://doi.org/10.24327/ijrsr.2017.0810.0918.
Prasad, R., Bhattacharyya, A., Nguyen, Q.D., 2017. Nanotechnology in sustainable agriculture: recent developments, challenges, and perspectives. Front. Microbiol. 8, 1014. https://doi.org/10.3389/fmicb.2017.01014.
Qian, H., Peng, X., Han, X., Ren, J., Sun, L., Fu, Z., 2013. Comparison of the toxicity of silver nanoparticles and silver ions on the growth of terrestrial plant model Arabidopsis thaliana. J. Environ. Sci. 25, 1947–1956. https://doi.org/10.1016/S1001-0742(12)60301-5.
Rad, F., Mohsenifar, A., Tabatabaei, M., Safarnejad, M.R., Shahryari, F., Safarpour, H., Foroutan, A., Mardi, M., Davoudi, D., Fotokian, M., 2012. Detection of candidatus phytoplasma aurantifolia with a quantum dots fret-based biosensor. J. Plant Pathol. 94 https://doi.org/10.4454/JPP.FA.2012.054.
Rafique, R., Zahra, Z., Virk, N., Shahid, M., Pinelli, E., Park, T.J., Kallerhoff, J., Arshad, M., 2018. Dose-dependent physiological responses of Triticum aestivum L. to soil applied TiO2 nanoparticles: Alterations in chlorophyll content, H_2O_2 production, and genotoxicity. Agric. Ecosyst. Environ. 255, 95–101. https://doi.org/10.1016/j.agee.2017.12.010.
Rajput, V., Minkina, T., Mazarji, M., Shende, S., Sushkova, S., Mandzhieva, S., Burachevskaya, M., Chaplygin, V., Singh, A., Jatav, H., 2020. Accumulation of nanoparticles in the soil-plant systems and their effects on human health. Ann. Agric. Sci. 65, 137–143. https://doi.org/10.1016/j.aoas.2020.08.001.
Raliya, R., Franke, C., Chavalmane, S., Nair, R., Reed, N., Biswas, P., 2016. Quantitative understanding of nanoparticle uptake in watermelon plants. Front. Plant Sci. 7, 1288. https://doi.org/10.3389/fpls.2016.01288.
Ramesh, S.A., Choimes, S., Schachtman, D.P., 2004. Over-expression of an arabidopsis zinc transporter in hordeum vulgare increases short-term zinc uptake after zinc deprivation and seed zinc content. Plant Mol. Biol. 54, 373–385. https://doi.org/10.1023/B:PLAN.0000036370.70912.34.
Reddy Pullagurala, V.L., Adisa, I.O., Rawat, S., Kalagara, S., Hernandez-Viezcas, J.A., Peralta-Videa, J.R., Gardea-Torresdey, J.L., 2018. ZnO nanoparticles increase photosynthetic pigments and decrease lipid peroxidation in soil grown cilantro (Coriandrum sativum). Plant Physiol. Biochem. 132, 120–127. https://doi.org/10.1016/j.plaphy.2018.08.037.
Rishi, N., 2009. Significant plant virus diseases in India and a glimpse of modern disease management technology. J. Gen. Plant Pathol. 75, 1–18. https://doi.org/10.1007/s10327-008-0139-8.
Rizwan, M., Ali, S., Qayyum, M.F., Ok, Y.S., Adrees, M., Ibrahim, M., Zia-ur-Rehman, M., Farid, M., Abbas, F., 2017. Effect of metal and metal oxide nanoparticles on growth and physiology of globally important food crops: a critical review. J. Hazard. Mater. 322, 2–16. https://doi.org/10.1016/j.jhazmat.2016.05.061.
Roco, M.C., 2003. Nanotechnology: convergence with modern biology and medicine. Curr. Opin. Biotechnol. 14, 337–346. https://doi.org/10.1016/S0958-1669(03)00068-5.
de la Rosa, G., García-Castañeda, C., Vázquez-Núñez, E., Alonso-Castro, Á.J., Basurto-Islas, G., Mendoza, Á., Cruz-Jiménez, G., Molina, C., 2017. Physiological and biochemical response of plants to engineered NMs: implications on future design. Plant Physiol. Biochem. 110, 226–235. https://doi.org/10.1016/j.plaphy.2016.06.014.
Rossi, L., Fedenia, L.N., Sharifan, H., Ma, X., Lombardini, L., 2019. Effects of foliar application of zinc sulfate and zinc nanoparticles in coffee (Coffea arabica L.) plants. Plant Physiol. Biochem. 135, 160–166. https://doi.org/10.1016/j.plaphy.2018.12.005.
Ruotolo, R., Maestri, E., Pagano, L., Marmiroli, M., White, J.C., Marmiroli, N., 2018. Plant response to metal-containing engineered nanomaterials: an omics-based perspective. Environ. Sci. Technol. 52, 2451–2467. https://doi.org/10.1021/acs.est.7b04121.

Saharan, V., Sharma, G., Yadav, M., Choudhary, M.K., Sharma, S.S., Pal, A., Raliya, R., Biswas, P., 2015. Synthesis and in vitro antifungal efficacy of Cu–chitosan nanoparticles against pathogenic fungi of tomato. Int. J. Biol. Macromol. 75, 346–353. https://doi.org/10.1016/j.ijbiomac.2015.01.027.

Sahoo, D., Mandal, A., Mitra, T., Chakraborty, K., Bardhan, M., Dasgupta, A.K., 2018. Nanosensing of pesticides by zinc oxide quantum dot: an optical and electrochemical approach for the detection of pesticides in water. J. Agric. Food Chem. 66, 414–423. https://doi.org/10.1021/acs.jafc.7b04188.

Salehi, H., Chehregani, A., Lucini, L., Majd, A., Gholami, M., 2018. Morphological, proteomic and metabolomic insight into the effect of cerium dioxide nanoparticles to Phaseolus vulgaris L. under soil or foliar application. Sci. Total Environ. 616–617, 1540–1551. https://doi.org/10.1016/j.scitotenv.2017.10.159.

Sathiyabama, M., Manikandan, A., 2018. Application of copper-chitosan nanoparticles stimulate growth and induce resistance in finger millet (Eleusine coracana Gaertn.) plants against blast disease. J. Agric. Food Chem. 66, 1784–1790. https://doi.org/10.1021/acs.jafc.7b05921.

Sayadi Maazou, A.-R., Tu, J., Qiu, J., Liu, Z., 2016. Breeding for drought tolerance in maize (Zea mays L.). AJPS 07, 1858–1870. https://doi.org/10.4236/ajps.2016.714172.

Schwab, F., Zhai, G., Kern, M., Turner, A., Schnoor, J.L., Wiesner, M.R., 2016. Barriers, pathways and processes for uptake, translocation and accumulation of nanomaterials in plants–critical review. Nanotoxicology 10, 257–278. https://doi.org/10.3109/17435390.2015.1048326.

Schwabe, F., Tanner, S., Schulin, R., Rotzetter, A., Stark, W., von Quadt, A., Nowack, B., 2015. Dissolved cerium contributes to uptake of Ce in the presence of differently sized CeO_2 -nanoparticles by three crop plants. Metallomics 7, 466–477. https://doi.org/10.1039/C4MT00343H.

Serag, M.F., Kaji, N., Gaillard, C., Okamoto, Y., Terasaka, K., Jabasini, M., Tokeshi, M., Mizukami, H., Bianco, A., Baba, Y., 2011. Trafficking and subcellular localization of multiwalled carbon nanotubes in plant cells. ACS Nano 5, 493–499. https://doi.org/10.1021/nn102344t.

Shang, Y., Hasan, Md.K., Ahammed, G.J., Li, M., Yin, H., Zhou, J., 2019. Applications of nanotechnology in plant growth and crop protection: a review. Molecules 24, 2558. https://doi.org/10.3390/molecules24142558.

Shi, J., Wu, B., Yuan, X., Yy, C., Chen, X., Chen, Y., Hu, T., 2008. An X-ray absorption spectroscopy investigation of speciation and biotransformation of copper in Elsholtzia splendens. Plant Soil 302, 163–174. https://doi.org/10.1007/s11104-007-9463-6.

Shi, J., Abid, A.D., Kennedy, I.M., Hristova, K.R., Silk, W.K., 2011. To duckweeds (Landoltia punctata), nanoparticulate copper oxide is more inhibitory than the soluble copper in the bulk solution. Environ. Pollut. 159, 1277–1282. https://doi.org/10.1016/j.envpol.2011.01.028.

Shi, J., Peng, C., Yang, Y., Yang, J., Zhang, H., Yuan, X., Chen, Y., Hu, T., 2014. Phytotoxicity and accumulation of copper oxide nanoparticles to the Cu-tolerant plant Elsholtzia splendens. Nanotoxicology 8, 179–188. https://doi.org/10.3109/17435390.2013.766768.

Siddiqui, M.H., Al-Whaibi, M.H., Faisal, M., Sahli, A.A.Al, 2014. Nano-silicon dioxide mitigates the adverse effects of salt stress on Cucurbita pepo L: nano-SiO_2 mitigates the adverse effects of salt stress. Environ. Toxicol. Chem. 33, 2429–2437. https://doi.org/10.1002/etc.2697.

Singh, S., 2019. Nanomaterials exhibiting enzyme-like properties (nanozymes): current advances and future perspectives. Front. Chem. 7, 46. https://doi.org/10.3389/fchem.2019.00046.

Song, U., Shin, M., Lee, G., Roh, J., Kim, Y., Lee, E.J., 2013. Functional analysis of TiO_2 nanoparticle toxicity in three plant species. Biol. Trace Elem. Res. 155, 93–103. https://doi.org/10.1007/s12011-013-9765-x.

Spielman-Sun, E., Avellan, A., Bland, G.D., Clement, E.T., Tappero, R.V., Acerbo, A.S., Lowry, G.V., 2020. Protein coating composition targets nanoparticles to leaf stomata and trichomes. Nanoscale 12, 3630–3636. https://doi.org/10.1039/C9NR08100C.

Stanisavljevic, M., Krizkova, S., Vaculovicova, M., Kizek, R., Adam, V., 2015. Quantum dots-fluorescence resonance energy transfer-based nanosensors and their application. Biosens. Bioelectron. 74, 562–574. https://doi.org/10.1016/j.bios.2015.06.076.

Su, Y., Ashworth, V., Kim, C., Adeleye, A.S., Rolshausen, P., Roper, C., White, J., Jassby, D., 2019. Delivery, uptake, fate, and transport of engineered nanoparticles in plants: a critical review and data analysis. Environ. Sci. Nano. https://doi.org/10.1039/C9EN00461K.

Sun, L., Wang, Y., Wang, R., Wang, R., Zhang, P., Ju, Q., Xu, J., 2020. Physiological, transcriptomic, and metabolomic analyses reveal zinc oxide nanoparticles modulate plant growth in tomato. Environ. Sci. Nano 7, 3587–3604. https://doi.org/10.1039/D0EN00723D.

Sun, X., Du, S., Wang, X., 2012. Amperometric immunosensor for carbofuran detection based on gold nanoparticles and PB-MWCNTs-CTS composite film. Eur. Food Res. Technol. 235, 469–477. https://doi.org/10.1007/s00217-012-1774-z.

Suriyaprabha, R., Sreeja, K.A., Prabu, M., Prabu, P., Rajendran, V., 2018. Bioaccumulation of transition metal oxide nanoparticles and their influence on early growth stages of Vigna unguiculata seeds. BioNanoScience 8, 752–760. https://doi.org/10.1007/s12668-018-0535-2.

Syu, Y., Hung, J.-H., Chen, J.-C., Chuang, H., 2014. Impacts of size and shape of silver nanoparticles on Arabidopsis plant growth and gene expression. Plant Physiol. Biochem. 83, 57–64. https://doi.org/10.1016/j.plaphy.2014.07.010.

Tamez, C., Hernandez-Molina, M., Hernandez-Viezcas, J.A., Gardea-Torresdey, J.L., 2019. Uptake, transport, and effects of nano-copper exposure in zucchini (Cucurbita pepo). Sci. Total Environ. 665, 100–106. https://doi.org/10.1016/j.scitotenv.2019.02.029.

Tang, J., Chen, W., Ju, H., 2019. Rapid detection of pesticide residues using a silver nanoparticles coated glass bead as nonplanar substrate for SERS sensing. Sens. Actuators B Chem. 287, 576–583. https://doi.org/10.1016/j.snb.2019.02.084.

Tang, Y., He, R., Zhao, J., Nie, G., Xu, L., Xing, B., 2016. Oxidative stress-induced toxicity of CuO nanoparticles and related toxicogenomic responses in Arabidopsis thaliana. Environ. Pollut. 212, 605–614. https://doi.org/10.1016/j.envpol.2016.03.019.

Taylor, A.F., Rylott, E.L., Anderson, C.W.N., Bruce, N.C., 2014. Investigating the toxicity, uptake, nanoparticle formation and genetic response of plants to gold. PLoS One 9, e93793. https://doi.org/10.1371/journal.pone.0093793.

Tiwari, M., Krishnamurthy, S., Shukla, D., Kiiskila, J., Jain, A., Datta, R., Sharma, N., Sahi, S.V., 2016. Comparative transcriptome and proteome analysis to reveal the biosynthesis of gold nanoparticles in Arabidopsis. Sci. Rep. 6, 21733. https://doi.org/10.1038/srep21733.

Tombuloglu, H., Slimani, Y., Tombuloglu, G., Almessiere, M., Baykal, A., 2019. Uptake and translocation of magnetite (Fe_3O_4) nanoparticles and its impact on photosynthetic genes in barley (Hordeum vulgare L.). Chemosphere 226, 110–122. https://doi.org/10.1016/j.chemosphere.2019.03.075.

Tong, L., Zhu, T., Liu, Z., 2011. Approaching the electromagnetic mechanism of surface-enhanced Raman scattering: from self-assembled arrays to individual gold nanoparticles. Chem. Soc. Rev. 40, 1296–1304. https://doi.org/10.1039/C001054P.

Trujillo-Reyes, J., Majumdar, S., Botez, C.E., Peralta-Videa, J.R., Gardea-Torresdey, J.L., 2014. Exposure studies of core–shell Fe/Fe_3O_4 and Cu/CuO NPs to lettuce (Lactuca sativa) plants: are they a potential physiological and nutritional hazard? J. Hazard. Mater. 267, 255–263. https://doi.org/10.1016/j.jhazmat.2013.11.067.

Valdes, C., Cota-Ruiz, K., Flores, K., Ye, Y., Hernandez-Viezcas, J.A., Gardea-Torresdey, J.L., 2020. Antioxidant and defense genetic expressions in corn at early-developmental stage are differentially modulated by copper form exposure (nano, bulk, ionic): nutrient and physiological effects. Ecotoxicol. Environ. Saf. 206, 111197 https://doi.org/10.1016/j.ecoenv.2020.111197.

Vannini, C., Domingo, G., Onelli, E., Prinsi, B., Marsoni, M., Espen, L., Bracale, M., 2013. Morphological and proteomic responses of Eruca sativa exposed to silver nanoparticles or silver nitrate. PLoS One 8, 68752. https://doi.org/10.1371/journal.pone.0068752.

Wan, J., Wang, R., Wang, R., Ju, Q., Wang, Y., Xu, J., 2019. Comparative physiological and transcriptomic analyses reveal the toxic effects of ZnO nanoparticles on plant growth. Environ. Sci. Technol. 53, 4235–4244. https://doi.org/10.1021/acs.est.8b06641.

Wan, J., Wang, R., Bai, H., Wang, Y., Xu, J., 2020. Comparative physiological and metabolomics analysis reveals that single-walled carbon nanohorns and ZnO nanoparticles affect salt tolerance in Sophora alopecuroides. Environ. Sci. Nano 7, 2968–2981. https://doi.org/10.1039/D0EN00582G.

Wang, T., Wu, J., Xu, S., Deng, C., Wu, L., Wu, Y., Bian, P., 2019. A potential involvement of plant systemic response in initiating genotoxicity of Ag-nanoparticles in Arabidopsis thaliana. Ecotoxicol. Environ. Saf. 170, 324–330. https://doi.org/10.1016/j.ecoenv.2018.12.002.

Wang, Y., Chen, R., Hao, Y., Liu, H., Song, S., Sun, G., 2017. Transcriptome analysis reveals differentially expressed genes (DEGs) related to lettuce (Lactuca sativa) treated by TiO_2/ZnO nanoparticles. Plant Growth Regul. 83, 13–25. https://doi.org/10.1007/s10725-017-0280-5.

Wang, Z., Xie, X., Zhao, J., Liu, X., Feng, W., White, J.C., Xing, B., 2012. Xylem- and phloem-based transport of CuO nanoparticles in maize (Zea mays L.). Environ. Sci. Technol. 46, 4434–4441. https://doi.org/10.1021/es204212z.

Wong, M.H., Giraldo, J.P., Kwak, S.-Y., Koman, V.B., Sinclair, R., Lew, T.T.S., Bisker, G., Liu, P., Strano, M.S., 2017. Nitroaromatic detection and infrared communication from wild-type plants using plant nanobionics. Nat. Mater. 16, 264–272. https://doi.org/10.1038/nmat4771.

Wu, H., Tito, N., Giraldo, J.P., 2017. Anionic cerium oxide nanoparticles protect plant photosynthesis from abiotic stress by scavenging reactive oxygen species. ACS Nano 11, 11283–11297. https://doi.org/10.1021/acsnano.7b05723.

Wu, H., Nißler, R., Morris, V., Herrmann, N., Hu, P., Jeon, S.-J., Kruss, S., Giraldo, J.P., 2020. Monitoring plant health with near-infrared fluorescent H_2O_2 nanosensors. Nano Lett. 20, 2432–2442. https://doi.org/10.1021/acs.nanolett.9b05159.

Xie, X., Lu, J., Kulbokas, E.J., Golub, T.R., Mootha, V., Lindblad-Toh, K., Lander, E.S., Kellis, M., 2005. Systematic discovery of regulatory motifs in human promoters and 3′ UTRs by comparison of several mammals. Nature 434, 338–345. https://doi.org/10.1038/nature03441.

Xun, H., Ma, X., Chen, J., Yang, Z., Liu, B., Gao, X., Li, G., Yu, J., Wang, L., Pang, J., 2017. Zinc oxide nanoparticle exposure triggers different gene expression patterns in maize shoots and roots. Environ. Pollut. 229, 479–488. https://doi.org/10.1016/j.envpol.2017.05.066.

Yan, J., Huang, K., Wang, Y., Liu, S., 2005. Study on anti-pollution nano-preparation of dimethomorph and its performance. Chin. Sci. Bull. 50, 108–112. https://doi.org/10.1007/BF02897511.

Yang, J., Cao, W., Rui, Y., 2017. Interactions between nanoparticles and plants: phytotoxicity and defense mechanisms. J. Plant Interact. 12, 158–169. https://doi.org/10.1080/17429145.2017.1310944.

Yang, Q., Xu, W., Liu, G., Song, M., Tan, Z., Mao, Y., Yin, Y., Cai, Y., Liu, J., Jiang, G., 2020. Transformation and uptake of silver nanoparticles and silver ions in rice plant (Oryza sativa L.): the effect of iron plaque and dissolved iron. Environ. Sci. Nano 7, 599–609. https://doi.org/10.1039/C9EN01297D.

Yao, K.S., Li, S.J., Tzeng, K.C., Cheng, T.C., Chang, C.Y., Chiu, C.Y., Liao, C.Y., Hsu, J.J., Lin, Z.P., 2009. Fluorescence silica nanoprobe as a biomarker for rapid detection of plant pathogens. Adv. Mater. Res. 79–82, 513–516. https://doi.org/10.4028/www.scientific.net/AMR.79-82.513.

Yasmeen, F., Raja, N.I., Razzaq, A., Komatsu, S., 2017. Proteomic and physiological analyses of wheat seeds exposed to copper and iron nanoparticles. Biochim. Biophys. Acta Proteins Prote 1865, 28–42. https://doi.org/10.1016/j.bbapap.2016.10.001.

Yue, L., Ma, C., Zhan, X., White, J.C., Xing, B., 2017. Molecular mechanisms of maize seedling response to La_2O_3 NP exposure: water uptake, aquaporin gene expression and signal transduction. Environ. Sci. Nano 4, 843–855. https://doi.org/10.1039/C6EN00487C.

Yusof, N.A., Isha, A., 2020. Nanosensors for early detection of plant diseases. In: Nanomaterials for Agriculture and Forestry Applications. Elsevier, pp. 407–419. https://doi.org/10.1016/B978-0-12-817852-2.00016-0.

Zeinhom, M.M.A., Wang, Y., Sheng, L., Du, D., Li, L., Zhu, M.-J., Lin, Y., 2018. Smart phone based immunosensor coupled with nanoflower signal amplification for rapid detection of Salmonella Enteritidis in milk, cheese and water. Sens. Actuators B Chem. 261, 75–82. https://doi.org/10.1016/j.snb.2017.11.093.

Zhan, F., Wang, T., Iradukunda, L., Zhan, J., 2018. A gold nanoparticle-based lateral flow biosensor for sensitive visual detection of the potato late blight pathogen, Phytophthora infestans. Anal. Chim. Acta 1036, 153–161. https://doi.org/10.1016/j.aca.2018.06.083.

Zhang, C.L., Jiang, H.S., Gu, S.P., Zhou, X.H., Lu, Z.W., Kang, X.H., Yin, L., Huang, J., 2019. Combination analysis of the physiology and transcriptome provides insights into the mechanism of silver nanoparticles phytotoxicity. Environ. Pollut. 252, 1539–1549. https://doi.org/10.1016/j.envpol.2019.06.032.

Zhang, H., Du, W., Peralta-Videa, J.R., Gardea-Torresdey, J.L., White, J.C., Keller, A., Guo, H., Ji, R., Zhao, L., 2018a. Metabolomics reveals how cucumber (Cucumis sativus) reprograms metabolites to cope with silver ions and silver nanoparticle-induced oxidative stress. Environ. Sci. Technol. 52, 8016–8026. https://doi.org/10.1021/acs.est.8b02440.

Zhang, J., Li, M., Fan, T., Xu, Q., Wu, Y., Chen, C., Huang, Q., 2013. Construction of novel amphiphilic chitosan copolymer nanoparticles for chlorpyrifos delivery. J. Polym. Res. 20, 107. https://doi.org/10.1007/s10965-013-0107-7.

Zhang, P., Ma, Y., Zhang, Z., He, X., Zhang, J., Guo, Z., Tai, R., Zhao, Y., Chai, Z., 2012. Biotransformation of ceria nanoparticles in cucumber plants. ACS Nano 6, 9943–9950. https://doi.org/10.1021/nn303543n.

Zhang, X., Guo, Q., Cui, D., 2009. Recent advances in nanotechnology applied to biosensors. Sensors 9, 1033–1053. https://doi.org/10.3390/s90201033.

Zhang, Z., He, X., Zhang, H., Ma, Y., Zhang, P., Ding, Y., Zhao, Y., 2011. Uptake and distribution of ceria nanoparticles in cucumber plants. Metallomics 3, 816–822. https://doi.org/10.1039/c1mt00049g.

Zhang, Z., Ke, M., Qu, Q., Peijnenburg, W.J.G.M., Lu, T., Zhang, Q., Ye, Y., Xu, P., Du, B., Sun, L., Qian, H., 2018b. Impact of copper nanoparticles and ionic copper exposure on wheat (Triticum aestivum L.) root morphology and antioxidant response. Environ. Pollut. 239, 689–697. https://doi.org/10.1016/j.envpol.2018.04.066.

Zhao, L., Ortiz, C., Adeleye, A.S., Hu, Q., Zhou, H., Huang, Y., Keller, A.A., 2016. Metabolomics to detect response of lettuce (Lactuca sativa) to $Cu(OH)_2$ nanopesticides: oxidative stress response and detoxification mechanisms. Environ. Sci. Technol. 50, 9697–9707. https://doi.org/10.1021/acs.est.6b02763.

Zhao, L., Huang, Y., Adeleye, A.S., Keller, A.A., 2017a. Metabolomics reveals $Cu(OH)_2$ nanopesticide-activated anti-oxidative pathways and decreased beneficial antioxidants in spinach leaves. Environ. Sci. Technol. 51, 10184–10194. https://doi.org/10.1021/acs.est.7b02163.

Zhao, L., Hu, Q., Huang, Y., Fulton, A.N., Hannah-Bick, C., Adeleye, A.S., Keller, A.A., 2017b. Activation of antioxidant and detoxification gene expression in cucumber plants exposed to a Cu(OH)(2) nanopesticide, 4, 1750–1760. ⟨https://doi.org/10.1039/c7en00358g⟩.

Zhao, L., Hu, Q., Huang, Y., Keller, A.A., 2017c. Response at genetic, metabolic, and physiological levels of maize (Zea mays) exposed to a $Cu(OH)_2$ nanopesticide. ACS Sustain. Chem. Eng. 5, 8294–8301. https://doi.org/10.1021/acssuschemeng.7b01968.

Zhao, L., Zhang, H., White, J.C., Chen, X., Li, H., Qu, X., Ji, R., 2019. Metabolomics reveals that engineered nanomaterial exposure in soil alters both soil rhizosphere metabolite profiles and maize metabolic pathways. Environ. Sci. Nano 6, 1716–1727. https://doi.org/10.1039/C9EN00137A.

Zhao, L., Lu, L., Wang, A., Zhang, H., Huang, M., Wu, H., Xing, B., Wang, Z., Ji, R., 2020. Nano-biotechnology in agriculture: use of nanomaterials to promote plant growth and stress tolerance. J. Agric. Food Chem. 68, 1935–1947. https://doi.org/10.1021/acs.jafc.9b06615.

Zhao, P., Cao, L., Ma, D., Zhou, Z., Huang, Q., Pan, C., 2018. Translocation, distribution and degradation of prochloraz-loaded mesoporous silica nanoparticles in cucumber plants. Nanoscale 10, 1798–1806. https://doi.org/10.1039/C7NR08107C.

Zrazhevskiy, P., Sena, M., Gao, X., 2010. Designing multifunctional quantum dots for bioimaging, detection, and drug delivery. Chem. Soc. Rev. 39, 4326–4354. https://doi.org/10.1039/B915139G.

Supplementary material

Cross-examination of engineered nanomaterials in crop production: application and related implications

Magdalena Kusiak[1], Patryk Oleszczuk[2], Izabela Jośko[1*]

[1] Institute of Plant Genetics, Breeding and Biotechnology, Faculty of Agrobioengineering, University of Life Sciences, Lublin, Poland

[2] Department of Radiochemistry and Environmental Chemistry, Faculty of Chemistry, Maria Curie–Skłodowska University, Lublin, Poland

* Correspondence to: Izabela Jośko, Institute of Plant Genetics, Breeding and Biotechnology, Faculty of Agrobioengineering, Univerisity of Life Sciences in Lublin, 20–950 Lublin, 13 Akademicka Street, Poland, tel. +48 81 4456675, fax. +48 81 4456031, e–mail: izabela.josko@up.lublin.pl

Journal: *Journal of Hazardous Materials*

Number of pages:7

References for Figure 2:

1. Vannini, C., Domingo, G., Onelli, E., Prinsi, B., Marsoni, M., Espen, L., Bracale, M., 2013. Morphological and proteomic responses of Eruca sativa exposed to silver nanoparticles or silver nitrate. PLoS ONE 8, e68752. https://doi.org/10.1371/journal.pone.0068752
2. Yin, L., Cheng, Y., Espinasse, B., Colman, B.P., Auffan, M., Wiesner, M., Rose, J., Liu, J., Bernhardt, E.S., 2011. More than the Ions: The Effects of Silver Nanoparticles on *Lolium multiflorum*. Environmental Science & Technology 45, 2360–2367. https://doi.org/10.1021/es103995x
3. okhrel, L.R., Dubey, B., 2013. Evaluation of developmental responses of two crop plants exposed to silver and zinc oxide nanoparticles. Sci. Total Environ. 452–453, 321–332. https://doi.org/10.1016/j.scitotenv.2013.02.059
4. Yasmeen, F., Raja, N.I., Razzaq, A., Komatsu, S., 2017. Proteomic and physiological analyses of wheat seeds exposed to copper and iron nanoparticles. Biochim Biophys Acta Proteins Proteom 1865, 28–42. https://doi.org/10.1016/j.bbapap.2016.10.001
5. Rajput, V., Minkina, T., Fedorenko, A., Sushkova, S., Mandzhieva, S., Lysenko, V., Duplii, N., Fedorenko, G., Dvadnenko, K., Ghazaryan, K., 2018. Toxicity of copper oxide nanoparticles on spring barley (Hordeum sativum distichum). Science of The Total Environment 645, 1103–1113. https://doi.org/10.1016/j.scitotenv.2018.07.211
6. Shi, J., Peng, C., Yang, Y., Yang, J., Zhang, H., Yuan, X., Chen, Y., Hu, T., 2014. Phytotoxicity and accumulation of copper oxide nanoparticles to the Cu-tolerant plant Elsholtzia splendens. Nanotoxicology 8, 179–188. https://doi.org/10.3109/17435390.2013.766768
7. Kasote, D.M., Lee, J.H.J., Jayaprakasha, G.K., Patil, B.S., 2019. Seed Priming with Iron Oxide Nanoparticles Modulate Antioxidant Potential and Defense-Linked Hormones in Watermelon Seedlings. ACS Sustainable Chemistry & Engineering 7, 5142–5151. https://doi.org/10.1021/acssuschemeng.8b06013
8. Chung, I.-M., Venkidasamy, B., Thiruvengadam, M., 2019. Nickel oxide nanoparticles cause substantial physiological, phytochemical, and molecular-level changes in Chinese cabbage seedlings. Plant Physiology and Biochemistry 139, 92–101. https://doi.org/10.1016/j.plaphy.2019.03.010
9. Suriyaprabha, R., Karunakaran, G., Yuvakkumar, R., Rajendran, V., Kannan, N., 2012. Silica Nanoparticles for Increased Silica Availability in Maize (Zea mays. L) Seeds Under Hydroponic Conditions. CNANO 8, 902–908. https://doi.org/10.2174/157341312803989033
10. Khan, Z., Shahwar, D., Yunus Ansari, Mohd.K., Chandel, R., 2019. Toxicity assessment of anatase (TiO2) nanoparticles: A pilot study on stress response alterations and DNA damage studies in Lens culinaris Medik. Heliyon 5, e02069. https://doi.org/10.1016/j.heliyon.2019.e02069
11. Doğaroğlu, Z.G., Köleli, N., 2017. TiO2 and ZnO Nanoparticles Toxicity in Barley (Hordeum vulgare L.). CLEAN – Soil, Air, Water 45, 1700096. https://doi.org/10.1002/clen.201700096
12. Hussain, A., Ali, S., Rizwan, M., Zia ur Rehman, M., Javed, M.R., Imran, M., Chatha, S.A.S., Nazir, R., 2018. Zinc oxide nanoparticles alter the wheat physiological response and reduce the cadmium uptake by plants. Environmental Pollution 242, 1518–1526. https://doi.org/10.1016/j.envpol.2018.08.036
13. Cocozza, C., Perone, A., Giordano, C., Salvatici, M.C., Pignattelli, S., Raio, A., Schaub, M., Sever, K., Innes, J.L., Tognetti, R., Cherubini, P., 2019. Silver nanoparticles enter the tree stem faster through leaves than through roots. Tree Physiology 39, 1251–1261. https://doi.org/10.1093/treephys/tpz046

14. Pradas del Real, A.E., Vidal, V., Carrière, M., Castillo-Michel, H., Levard, C., Chaurand, P., Sarret, G., 2017. Silver Nanoparticles and Wheat Roots: A Complex Interplay. Environ. Sci. Technol. 51, 5774–5782. https://doi.org/10.1021/acs.est.7b00422
15. Li, H., Ye, X., Guo, X., Geng, Z., Wang, G., 2016. Effects of surface ligands on the uptake and transport of gold nanoparticles in rice and tomato. Journal of Hazardous Materials 314, 188–196. https://doi.org/10.1016/j.jhazmat.2016.04.043
16. Liu, M., Feng, S., Ma, Y., Xie, C., He, X., Ding, Y., Zhang, J., Luo, W., Zheng, L., Chen, D., Yang, F., Chai, Z., Zhao, Y., Zhang, Z., 2019. Influence of Surface Charge on the Phytotoxicity, Transformation, and Translocation of CeO2 Nanoparticles in Cucumber Plants. ACS Appl. Mater. Interfaces 11, 16905–16913. https://doi.org/10.1021/acsami.9b01627
17. Ma, Y., Yao, Y., Yang, J., He, X., Ding, Y., Zhang, P., Zhang, Junzhe, Wang, G., Xie, C., Luo, W., Zhang, Jing, Zheng, L., Chai, Z., Zhao, Y., Zhang, Z., 2018. Trophic Transfer and Transformation of CeO2 Nanoparticles along a Terrestrial Food Chain: Influence of Exposure Routes. Environ. Sci. Technol. 52, 7921–7927. https://doi.org/10.1021/acs.est.8b00596
18. Ma, Y., He, X., Zhang, P., Zhang, Z., Ding, Y., Zhang, Junzhe, Wang, G., Xie, C., Luo, W., Zhang, Jing, Zheng, L., Chai, Z., Yang, K., 2017. Xylem and Phloem Based Transport of CeO2 Nanoparticles in Hydroponic Cucumber Plants. Environ. Sci. Technol. 51, 5215–5221. https://doi.org/10.1021/acs.est.6b05998
19. Zhang, Z., Ke, M., Qu, Q., Peijnenburg, W.J.G.M., Lu, T., Zhang, Q., Ye, Y., Xu, P., Du, B., Sun, L., Qian, H., 2018. Impact of copper nanoparticles and ionic copper exposure on wheat (Triticum aestivum L.) root morphology and antioxidant response. Environmental Pollution 239, 689–697. https://doi.org/10.1016/j.envpol.2018.04.066
20. AlQuraidi, A.O., Mosa, K.A., Ramamoorthy, K., 2019. Phytotoxic and Genotoxic Effects of Copper Nanoparticles in Coriander (Coriandrum sativum—Apiaceae). Plants 8, 19. https://doi.org/10.3390/plants8010019
21. Shi, J., Abid, A.D., Kennedy, I.M., Hristova, K.R., Silk, W.K., 2011. To duckweeds (Landoltia punctata), nanoparticulate copper oxide is more inhibitory than the soluble copper in the bulk solution. Environ. Pollut. 159, 1277–1282. https://doi.org/10.1016/j.envpol.2011.01.028
22. Hussain, A., Ali, S., Rizwan, M., Rehman, M.Z. ur, Qayyum, M.F., Wang, H., Rinklebe, J., 2019. Responses of wheat (Triticum aestivum) plants grown in a Cd contaminated soil to the application of iron oxide nanoparticles. Ecotoxicology and Environmental Safety 173, 156–164. https://doi.org/10.1016/j.ecoenv.2019.01.118
23. Tombuloglu, H., Slimani, Y., Tombuloglu, G., Almessiere, M., Baykal, A., 2019. Uptake and translocation of magnetite (Fe3O4) nanoparticles and its impact on photosynthetic genes in barley (Hordeum vulgare L.). Chemosphere 226, 110–122. https://doi.org/10.1016/j.chemosphere.2019.03.075
24. Le, V.N., Rui, Y., Gui, X., Li, X., Liu, S., Han, Y., 2014. Uptake, transport, distribution and Bio-effects of SiO2 nanoparticles in Bt-transgenic cotton. J Nanobiotechnology 12, 50. https://doi.org/10.1186/s12951-014-0050-8
25. Rafique, R., Zahra, Z., Virk, N., Shahid, M., Pinelli, E., Park, T.J., Kallerhoff, J., Arshad, M., 2018. Dose-dependent physiological responses of Triticum aestivum L. to soil applied TiO2 nanoparticles: Alterations in chlorophyll content, H2O2 production, and genotoxicity. Agriculture, Ecosystems & Environment 255, 95–101. https://doi.org/10.1016/j.agee.2017.12.010
26. Tiwari, M., Sharma, N.C., Fleischmann, P., Burbage, J., Venkatachalam, P., Sahi, S.V., 2017. Nanotitania Exposure Causes Alterations in Physiological, Nutritional and Stress

Responses in Tomato (Solanum lycopersicum). Front Plant Sci 8, 633. https://doi.org/10.3389/fpls.2017.00633
27. Tripathi, D.K., Mishra, R.K., Singh, Swati, Singh, Samiksha, Singh, V.P., Singh, P.K., Chauhan, D.K., Prasad, S.M., Dubey, N.K., Pandey, A.C., 2017. Nitric oxide ameliorates zinc oxide nanoparticles phytotoxicity in wheat seedlings: Implication of the ascorbate-glutathione cycle. Front. Plant Sci. 8. https://doi.org/10.3389/fpls.2017.00001
28. Raliya, R., Franke, C., Chavalmane, S., Nair, R., Reed, N., Biswas, P., 2016. Quantitative Understanding of Nanoparticle Uptake in Watermelon Plants. Front Plant Sci 7, 1288. https://doi.org/10.3389/fpls.2016.01288
29. Avellan, A., Yun, J., Zhang, Y., Spielman-Sun, E., Unrine, J.M., Thieme, J., Li, J., Lombi, E., Bland, G., Lowry, G.V., 2019. Nanoparticle Size and Coating Chemistry Control Foliar Uptake Pathways, Translocation, and Leaf-to-Rhizosphere Transport in Wheat. ACS Nano 13, 5291–5305. https://doi.org/10.1021/acsnano.8b09781
30. Salehi, H., Chehregani, A., Lucini, L., Majd, A., Gholami, M., 2018. Morphological, proteomic and metabolomic insight into the effect of cerium dioxide nanoparticles to Phaseolus vulgaris L. under soil or foliar application. Science of The Total Environment 616–617, 1540–1551. https://doi.org/10.1016/j.scitotenv.2017.10.159
31. Pérez-Labrada, F., López-Vargas, E.R., Ortega-Ortiz, H., Cadenas-Pliego, G., Benavides-Mendoza, A., Juárez-Maldonado, A., 2019. Responses of Tomato Plants under Saline Stress to Foliar Application of Copper Nanoparticles. Plants (Basel) 8. https://doi.org/10.3390/plants8060151
32. Sathiyabama, M., Manikandan, A., 2018. Application of Copper-Chitosan Nanoparticles Stimulate Growth and Induce Resistance in Finger Millet (Eleusine coracana Gaertn.) Plants against Blast Disease. J. Agric. Food Chem. 66, 1784–1790. https://doi.org/10.1021/acs.jafc.7b05921
33. Corredor, E., Testillano, P.S., Coronado, M.-J., González-Melendi, P., Fernández-Pacheco, R., Marquina, C., Ibarra, M.R., de la Fuente, J.M., Rubiales, D., Pérez-de-Luque, A., Risueño, M.-C., 2009. Nanoparticle penetration and transport in living pumpkin plants: in situ subcellular identification. BMC Plant Biol. 9, 45. https://doi.org/10.1186/1471-2229-9-45
34. Mohammadi, R., Maali-Amiri, R., Abbasi, A., 2013. Effect of TiO2 Nanoparticles on Chickpea Response to Cold Stress. Biological Trace Element Research 152, 403–410. https://doi.org/10.1007/s12011-013-9631-x
35. Lu, K., Shen, D., Liu, X., Dong, S., Jing, X., Wu, W., Tong, Y., Gao, S., Mao, L., 2020. Uptake of iron oxide nanoparticles inhibits the photosynthesis of the wheat after foliar exposure. Chemosphere 259, 127445. https://doi.org/10.1016/j.chemosphere.2020.127445
36. Abdel Latef, A.A.H., Srivastava, A.K., El-sadek, M.S.A., Kordrostami, M., Tran, L.-S.P., 2018. Titanium Dioxide Nanoparticles Improve Growth and Enhance Tolerance of Broad Bean Plants under Saline Soil Conditions: nTiO $_2$ Application Mitigates Soil Salinity Effects on Broad Bean. Land Degradation & Development 29, 1065–1073. https://doi.org/10.1002/ldr.2780
37. Deshpande, P., Dapkekar, A., Oak, M., Paknikar, K., Rajwade, J., 2018. Nanocarrier-mediated foliar zinc fertilization influences expression of metal homeostasis related genes in flag leaves and enhances gluten content in durum wheat. PLOS ONE 13, e0191035. https://doi.org/10.1371/journal.pone.0191035
38. Li, C., Wang, P., Lombi, E., Cheng, M., Tang, C., Howard, D.L., Menzies, N.W., Kopittke, P.M., 2018. Absorption of foliar-applied Zn fertilizers by trichomes in soybean and

tomato. Journal of Experimental Botany 69, 2717–2729. https://doi.org/10.1093/jxb/ery085
39. Rossi, L., Fedenia, L.N., Sharifan, H., Ma, X., Lombardini, L., 2019. Effects of foliar application of zinc sulfate and zinc nanoparticles in coffee (Coffea arabica L.) plants. Plant Physiology and Biochemistry 135, 160–166. https://doi.org/10.1016/j.plaphy.2018.12.005
40. Salama, D.M., Osman, S.A., Abd El-Aziz, M.E., Abd Elwahed, M.S.A., Shaaban, E.A., 2019. Effect of zinc oxide nanoparticles on the growth, genomic DNA, production and the quality of common dry bean (Phaseolus vulgaris). Biocatalysis and Agricultural Biotechnology 18, 101083. https://doi.org/10.1016/j.bcab.2019.101083

References for Figure 4:

1. Zhang, C.L., Jiang, H.S., Gu, S.P., Zhou, X.H., Lu, Z.W., Kang, X.H., Yin, L., Huang, J., 2019. Combination analysis of the physiology and transcriptome provides insights into the mechanism of silver nanoparticles phytotoxicity. Environmental Pollution 252, 1539–1549. https://doi.org/10.1016/j.envpol.2019.06.032
2. Qian, H., Peng, X., Han, X., Ren, J., Sun, L., Fu, Z., 2013. Comparison of the toxicity of silver nanoparticles and silver ions on the growth of terrestrial plant model Arabidopsis thaliana. Journal of Environmental Sciences 25, 1947–1956. https://doi.org/10.1016/S1001-0742(12)60301-5
3. Pokhrel, L.R., Dubey, B., 2013. Evaluation of developmental responses of two crop plants exposed to silver and zinc oxide nanoparticles. Sci. Total Environ. 452–453, 321–332. https://doi.org/10.1016/j.scitotenv.2013.02.059
4. Almutairi, Z.M., 2017. Expression profiling of certain MADS-box genes in Arabidopsis thaliana plant treated with silver nanoparticles. Czech J. Genet. Plant Breed. 53, 30–36. https://doi.org/10.17221/130/2015-CJGPB
5. Syu, Y., Hung, J.-H., Chen, J.-C., Chuang, H., 2014. Impacts of size and shape of silver nanoparticles on Arabidopsis plant growth and gene expression. Plant Physiol. Biochem. 83, 57–64. https://doi.org/10.1016/j.plaphy.2014.07.010
6. Vannini, C., Domingo, G., Onelli, E., Prinsi, B., Marsoni, M., Espen, L., Bracale, M., 2013. Morphological and proteomic responses of Eruca sativa exposed to silver nanoparticles or silver nitrate. PLoS ONE 8, e68752. https://doi.org/10.1371/journal.pone.0068752
7. Nair, P.M.G., Chung, I.M., 2014. Physiological and molecular level effects of silver nanoparticles exposure in rice (Oryza sativa L.) seedlings. Chemosphere 112, 105–113. https://doi.org/10.1016/j.chemosphere.2014.03.056
8. Gupta, S.D., Agarwal, A., Pradhan, S., 2018. Phytostimulatory effect of silver nanoparticles (AgNPs) on rice seedling growth: An insight from antioxidative enzyme activities and gene expression patterns. Ecotoxicology and Environmental Safety 161, 624–633. https://doi.org/10.1016/j.ecoenv.2018.06.023
9. Jin, Y., Fan, X., Li, X., Zhang, Z., Sun, L., Fu, Z., Lavoie, M., Pan, X., Qian, H., 2017. Distinct physiological and molecular responses in Arabidopsis thaliana exposed to aluminum oxide nanoparticles and ionic aluminum. Environmental Pollution 228, 517–527. https://doi.org/10.1016/j.envpol.2017.04.073
10. Burklew, C.E., Ashlock, J., Winfrey, W.B., Zhang, B., 2012. Effects of Aluminum Oxide Nanoparticles on the Growth, Development, and microRNA Expression of Tobacco (Nicotiana tabacum). PLOS ONE 7, e34783. https://doi.org/10.1371/journal.pone.0034783
11. Tiwari, M., Krishnamurthy, S., Shukla, D., Kiiskila, J., Jain, A., Datta, R., Sharma, N., Sahi, S.V., 2016. Comparative transcriptome and proteome analysis to reveal the biosynthesis

of gold nanoparticles in Arabidopsis. Sci Rep 6, 21733. https://doi.org/10.1038/srep21733
12. Taylor, A.F., Rylott, E.L., Anderson, C.W.N., Bruce, N.C., 2014. Investigating the Toxicity, Uptake, Nanoparticle Formation and Genetic Response of Plants to Gold. PLoS One 9. https://doi.org/10.1371/journal.pone.0093793
13. Hernández-Hernández, H., Juárez-Maldonado, A., Benavides-Mendoza, A., Ortega-Ortiz, H., Cadenas-Pliego, G., Sánchez-Aspeytia, D., González-Morales, S., 2018. Chitosan-PVA and Copper Nanoparticles Improve Growth and Overexpress the SOD and JA Genes in Tomato Plants under Salt Stress. Agronomy 8, 175. https://doi.org/10.3390/agronomy8090175
14. Mosa, K.A., El-Naggar, M., Ramamoorthy, K., Alawadhi, H., Elnaggar, A., Wartanian, S., Ibrahim, E., Hani, H., 2018. Copper Nanoparticles Induced Genotoxicty, Oxidative Stress, and Changes in Superoxide Dismutase (SOD) Gene Expression in Cucumber (Cucumis sativus) Plants. Front. Plant Sci. 9. https://doi.org/10.3389/fpls.2018.00872
15. Zhang, Z., Ke, M., Qu, Q., Peijnenburg, W.J.G.M., Lu, T., Zhang, Q., Ye, Y., Xu, P., Du, B., Sun, L., Qian, H., 2018. Impact of copper nanoparticles and ionic copper exposure on wheat (Triticum aestivum L.) root morphology and antioxidant response. Environmental Pollution 239, 689–697. https://doi.org/10.1016/j.envpol.2018.04.066
16. Zhao, L., Hu, Q., Huang, Y., Fulton, A.N., Hannah-Bick, C., Adeleye, A.S., Keller, A.A., 2017. Activation of antioxidant and detoxification gene expression in cucumber plants exposed to a Cu(OH)(2) nanopesticide 4, 1750–1760. https://doi.org/10.1039/c7en00358g
17. Zhao, Lijuan, Hu, Q., Huang, Y., Keller, A.A., 2017. Response at Genetic, Metabolic, and Physiological Levels of Maize (Zea mays) Exposed to a Cu(OH)2 Nanopesticide. ACS Sustainable Chem. Eng. 5, 8294–8301. https://doi.org/10.1021/acssuschemeng.7b01968
18. Cota-Ruiz, K., Hernández-Viezcas, J.A., Varela-Ramírez, A., Valdés, C., Núñez-Gastélum, J.A., Martínez-Martínez, A., Delgado-Rios, M., Peralta-Videa, J.R., Gardea-Torresdey, J.L., 2018. Toxicity of copper hydroxide nanoparticles, bulk copper hydroxide, and ionic copper to alfalfa plants: A spectroscopic and gene expression study. Environmental Pollution 243, 703–712. https://doi.org/10.1016/j.envpol.2018.09.028
19. Wang, Z., Xu, L., Zhao, J., Wang, X., White, J.C., Xing, B., 2016. CuO Nanoparticle Interaction with Arabidopsis thaliana: Toxicity, Parent-Progeny Transfer, and Gene Expression. Environ. Sci. Technol. 50, 6008–6016. https://doi.org/10.1021/acs.est.6b01017
20. Chung, I.-M., Rekha, K., Venkidasamy, B., Thiruvengadam, M., 2019a. Effect of Copper Oxide Nanoparticles on the Physiology, Bioactive Molecules, and Transcriptional Changes in Brassica rapa ssp. rapa Seedlings. Water, Air, & Soil Pollution 230. https://doi.org/10.1007/s11270-019-4084-2
21. Landa, P., Dytrych, P., Prerostova, S., Petrova, S., Vankova, R., Vanek, T., 2017. Transcriptomic Response of Arabidopsis thaliana Exposed to CuO Nanoparticles, Bulk Material, and Ionic Copper. Environ. Sci. Technol. 51, 10814–10824. https://doi.org/10.1021/acs.est.7b02265
22. Yue, L., Ma, C., Zhan, X., White, J.C., Xing, B., 2017. Molecular mechanisms of maize seedling response to La2O3 NP exposure: water uptake, aquaporin gene expression and signal transduction. Environ. Sci.: Nano 4, 843–855. https://doi.org/10.1039/C6EN00487C
23. Khodakovskaya, M.V., Silva, K. de, Nedosekin, D.A., Dervishi, E., Biris, A.S., Shashkov, E.V., Galanzha, E.I., Zharov, V.P., 2011. Complex genetic, photothermal, and

photoacoustic analysis of nanoparticle-plant interactions. PNAS 108, 1028–1033. https://doi.org/10.1073/pnas.1008856108
24. Lahiani, M.H., Dervishi, E., Chen, J., Nima, Z., Gaume, A., Biris, A.S., Khodakovskaya, M.V., 2013. Impact of Carbon Nanotube Exposure to Seeds of Valuable Crops. ACS Applied Materials & Interfaces 5, 7965–7973. https://doi.org/10.1021/am402052x
25. Chung, I.-M., Venkidasamy, B., Thiruvengadam, M., 2019b. Nickel oxide nanoparticles cause substantial physiological, phytochemical, and molecular-level changes in Chinese cabbage seedlings. Plant Physiology and Biochemistry 139, 92–101. https://doi.org/10.1016/j.plaphy.2019.03.010
26. Silva, S., Ferreira de Oliveira, J.M.P., Dias, M.C., Silva, A.M.S., Santos, C., 2019. Antioxidant mechanisms to counteract TiO2-nanoparticles toxicity in wheat leaves and roots are organ dependent. Journal of Hazardous Materials 380, 120889. https://doi.org/10.1016/j.jhazmat.2019.120889
27. Amini, S., Maali-Amiri, R., Mohammadi, R., Kazemi- Shahandashti, S.-S., 2017. cDNA-AFLP analysis of transcripts induced in chickpea plants by TiO2 nanoparticles during cold stress. Plant Physiology and Biochemistry 111, 39–49. https://doi.org/10.1016/j.plaphy.2016.11.011
28. Landa, P., Vankova, R., Andrlova, J., Hodek, J., Marsik, P., Storchova, H., White, J.C., Vanek, T., 2012. Nanoparticle-specific changes in Arabidopsis thaliana gene expression after exposure to ZnO, TiO2, and fullerene soot. Journal of Hazardous Materials 241–242, 55–62. https://doi.org/10.1016/j.jhazmat.2012.08.059
29. Wang, Y., Chen, R., Hao, Y., Liu, H., Song, S., Sun, G., 2017. Transcriptome analysis reveals differentially expressed genes (DEGs) related to lettuce (Lactuca sativa) treated by TiO2/ZnO nanoparticles. Plant Growth Regulation 83, 13–25. https://doi.org/10.1007/s10725-017-0280-5
30. Nair, P.M.G., Chung, I.M., 2017. Regulation of morphological, molecular and nutrient status in Arabidopsis thaliana seedlings in response to ZnO nanoparticles and Zn ion exposure. Science of The Total Environment 575, 187–198. https://doi.org/10.1016/j.scitotenv.2016.10.017
31. Sheteiwy, M.S., Dong, Q., An, J., Song, W., Guan, Y., He, F., Huang, Y., Hu, J., 2017. Regulation of ZnO nanoparticles-induced physiological and molecular changes by seed priming with humic acid in Oryza sativa seedlings. Plant Growth Regulation 83, 27–41. https://doi.org/10.1007/s10725-017-0281-4
32. Landa, P., Prerostova, S., Petrova, S., Knirsch, V., Vankova, R., Vanek, T., 2015. The Transcriptomic Response of Arabidopsis thaliana to Zinc Oxide: A Comparison of the Impact of Nanoparticle, Bulk, and Ionic Zinc. Environmental Science & Technology 49, 14537–14545. https://doi.org/10.1021/acs.est.5b03330

Lublin, 28.08.2023r.

Magdalena Kusiak
Instytut Genetyki, Hodowli i
Biotechnologii Roślin
Uniwersytet Przyrodniczy w Lublinie
Ul. Akademicka 15,
20-950 Lublin
Tel: 508 789 096
magdalena.kusiak@up.lublin.pl

Rada Dyscypliny Rolnictwo i Ogrodnictwo
Uniwersytetu Przyrodniczego
w Lublinie

Oświadczenie o współautorstwie

Oświadczam, że mój udział w pracy "*Cross-examination of engineered nanomaterials in crop production: Application and related implication*" [Journal of Hazardous Materials, 2022] wynosi 70%.

Mój wkład polegał na opracowaniu koncepcji publikacji, zebraniu literatury wraz z jej analizą oraz na przygotowaniu manuskryptu i odpowiedzi na recenzje pracy.

Magdalena Kusiak

Podpis

Lublin, 28.07.2023

Prof. dr hab. Patryk Oleszczuk
Katedra Radiochemii i
Chemii Środowiskowej
Uniwersytet Marii Curie-Skłodowskiej
pl. Marii Curie-Skłodowskiej 3/425
20-031 Lublin
Tel. 81 537 55 15
patryk.oleszczuk@mail.umcs.pl

Rada Dyscypliny Rolnictwo i Ogrodnictwo
Uniwersytetu Przyrodniczego
w Lublinie

Oświadczenie o współautorstwie

Oświadczam, że mój udział w pracy "*Cross-examination of engineered nanomaterials in crop production: Application and related implication*" [Journal of Hazardous Materials, 2022] wynosi 10%.

Mój wkład polegał na opracowaniu koncepcji publikacji i redagowaniu manuskryptu.

.....
Podpis

Lublin, 03.07.2023

Dr hab. Izabela Jośko, prof. uczelni
Instytut Genetyki, Hodowli
i Biotechnologii Roślin
Uniwersytet Przyrodniczy w Lublinie
Ul. Akademicka 15,
20-950 Lublin
Tel. 814456675
izabela.josko@up.lublin.pl

Rada Dyscypliny Rolnictwo i Ogrodnictwo
Uniwersytetu Przyrodniczego
w Lublinie

Oświadczenie o współautorstwie

Oświadczam, że mój udział w pracy "*Cross-examination of engineered nanomaterials in crop production: Application and related implication*" [Journal of Hazardous Materials, 2022] wynosi 20%.

Mój wkład polegał na opracowaniu koncepcji publikacji oraz na redagowaniu manuskryptu do publikacji i odpowiedzi na otrzymane recenzje pracy.

Izabela Jośko

Podpis

PII

Kusiak M., Sierocka M., Świeca M., Pasieczna-Patkowska S., Sheteiwy M., Jośko I.

Unveiling of interactions between foliar-applied Cu nanoparticles and barley suffering from Cu deficiency

Environmental Pollution (2023) T. 320 s. 121044

DOI: 10.1016/j.envpol.2023.121044

$IF_{(2023)} = 8.9$

Punkty MEiN = 100

Environmental Pollution 320 (2023) 121044

Contents lists available at ScienceDirect

Environmental Pollution

journal homepage: www.elsevier.com/locate/envpol

Unveiling of interactions between foliar-applied Cu nanoparticles and barley suffering from Cu deficiency☆

Magdalena Kusiak [a], Małgorzata Sierocka [b], Michał Świeca [b], Sylwia Pasieczna-Patkowska [c], Mohamed Sheteiwy [d], Izabela Jośko [a,*]

[a] Institute of Plant Genetics, Breeding and Biotechnology, Faculty of Agrobioengineering, University of Life Sciences, Lublin, Poland
[b] Department of Biochemistry and Food Chemistry, Faculty of Food Science and Biotechnology, University of Life Sciences, Lublin, Poland
[c] Department of Chemical Technology, Faculty of Chemistry, Maria Curie–Skłodowska University, Lublin, Poland
[d] Department of Agronomy, Faculty of Agriculture, Mansoura University, Mansoura, Egypt

ARTICLE INFO

Keywords:
Hordeum vulgare
Cu nanoparticles
Antioxidants
Foliar exposure

ABSTRACT

The objective of this study was to evaluate nano-Cu-plant interactions under Cu deficiency. Nano-Cu at rates of 100 and 1000 mg L^{-1} was applied as foliar spray to *Hordeum vulgare* L. during increased demand for nutrients at tillering stage. Corresponding treatment with $CuSO_4$ was used to exam the nano-specific effects. Cu compounds-plant leaves interactions were analyzed with spectroscopic and microscopic methods (ICP-OES, FTIR/ATR, SEM-EDS). Moreover, the effect of Cu compounds on plants in terms of biomass, pigments content, lipid peroxidation, antiradical properties, the activity of enzymes involved in plant defense against stress (SOD, CAT, POD, GR, PAL, PPO) and the content of non-enzymatic antioxidants (GSH, GSSG, TPC) was determined after 1 and 7 days of exposure. Cu loading to plant leaves increased over time, but the content of Cu under treatment with nano-Cu at 100 mg L^{-1} was lower by 76% than $CuSO_4$ at 7th day of exposure. The changes induced by applied Cu compounds in biochemical traits were mostly observed after 1 day. Our data showed that $CuSO_4$ exposure induce oxidative stress (increased MDA level and GSSG content) when compared to control and nano-Cu treated plants. Noteworthy, nano Cu at 100 mg L^{-1} demonstrated enhanced stress tolerance as indicated by boosted GSH content. After 7 days, the antioxidant response was almost same compared to control sample. However, based on other indicators (pigment content, chlorosis sign, biomass), it should be noted that $CuSO_4$ caused serve oxidative burst of plant which may resulted in damage of defense system. Nano-Cu, especially at 100 mg L^{-1}, showed promising effect on plant health, and obtained results may be useful for optimizing of nano-Cu application as fertilizer agent.

1. Introduction

It is estimated that the global population will reach over 10 billion people by 2050, thus the agricultural production must be increased by 70% to meet the food demand (Kohatsu et al., 2021). To ensure the food security, agrochemicals are profusely used in agriculture to improve the quality and quantity of the crop yields (Hasegawa et al., 2018). However, the application of conventional chemicals is of low efficiency resulting in unachieved fertilizing objectives as well as environmental degradation (Hasegawa et al., 2018). The need to develop alternative strategies for sustainable agriculture leads to increased interest in nanotechnology as a feasible tool to increase agricultural production rates (Kohatsu et al., 2021). Engineered nanoparticles (ENPs) are inorganic, organic, or hybrid materials characterized by unique properties due to their size (1–100 nm), larger surface area and a high the surface area to volume ratio, that make them different from their bulk counterparts (Doğaroğlu and Köleli, 2017; Pagano et al., 2016). ENPs have a potential to increase crop production as nano-fertilizers through gradual release of active substances on a long-term basis (Wang et al., 2016), reduction of the mobile nutrients losses (Kah et al., 2019), and through enhanced accessibility of poorly-available nutrients (Doğaroğlu and Köleli, 2017).

☆ This paper has been recommended for acceptance by Handling editor Manzer H. Siddiqui.

* Corresponding author. Izabela Jośko, Institute of Plant Genetics, Breeding and Biotechnology, Faculty of Agrobioengineering, Univerisity of Life Sciences in Lublin, 20–950 Lublin, 13 Akademicka Street, Poland.
E-mail address: izabela.josko@up.lublin.pl (I. Jośko).

https://doi.org/10.1016/j.envpol.2023.121044
Received 1 September 2022; Received in revised form 9 November 2022; Accepted 6 January 2023
Available online 10 January 2023

Cu is an essential microelement required for plant growth and development, specifically, for photosynthesis, mitochondrial respiration, cell wall metabolism, protein synthesis etc. (Rahman and Schoenau, 2020; Ravet and Pilon, 2013). Moreover, Cu plays an important role in boosting of plant tolerance to abiotic stresses such as drought, heat or salinity under changed plant growth conditions *via* e.g. improved osmotic adjustment and the stimulation of oxidative defense system through increased activity of antioxidant enzymes and enhanced synthesis of non-enzyme antioxidants (Iqbal et al., 2018; Waraich et al., 2011). Because of the limited uptake and translocation of Cu in plants as a result of low bioavailability in soil and mobility of this element, deficiency symptoms such as stunted growth, chlorosis, curling of leaf margins, defects in photosynthetic activity, altered plant morphology and increased susceptibility to diseases (e.g. ergot) may occur (Rahman and Schoenau, 2020; van Maarschalkerweerd et al., 2013). Cereals such as barley (*Hordeum vulgare* L.) are sensitive to Cu deficiency, especially during the tillering and anthesis stages (Rahman and Schoenau, 2020). Prolonged Cu deficiency results in pollen abortion and male sterility (Rahman and Schoenau, 2020) or diminished Cu and protein content in grains, reducing its nutritional value and increasing the micronutrient deficiencies in humans (Wazir and Ghobrial, 2017). Up to 40% of soils in Poland are at risk of Cu-deficiency (Alloway, 2005). Therefore, efficient Cu fertilization is crucial to ensure plant health and crop quality (Rahman and Schoenau, 2020; Wazir and Ghobrial, 2017). Cu-based fertilizers are most often applied by foliar spray rather than soil irrigation due to direct uptake of the microelement by the target organs of crop plants (Kohatsu et al., 2021). However, currently used agrochemicals are significantly inefficient, as up to 50% of the applied nutrients do not reach their target (Avellan et al., 2021) and 93% of Cu provided as conventional ionic $CuSO_4$ is lost by wash-off from leaves (Kah et al., 2019) and then contaminates the soil and groundwater, which consequently leads to the accumulation of potentially toxic Cu concentrations in the environment (Avellan et al., 2021).

Despite the fact that the potential of ENPs, including Cu-based ENPs, as agrochemicals has been widely discussed, the studies on the efficiency of foliar applied ENPs remain in the minority (Kohatsu et al., 2021; Lafmejani et al., 2018). Especially, data on the integrated analysis of interactions of Cu-based ENPs–plant leaves and plant response (e.g. at physiological and biochemical level) are scarce. The scant studies on the absorption mechanisms of ENPs by plant leaves indicate the important role of the chemistry of leaf surface, depending on plant species and their growth stage, for the penetration of plant tissue by e.g. Zn-based ENPs (Du et al., 2015). Thus, the *in situ* analysis and visualization of nano-Cu with plant leaves is crucial for the examination of actual absorption and of the potential of ENPs for long-term delivery of metal ions. Further, to obtain a complete picture of nano-Cu utility for plant fertilization, the physiological and biochemical traits need to be included. Moreover, the evaluation of fertilizing efficiency of these ENPs should be performed in the conditions, when the plants are suffering from Cu deficiency. In the conditions of deficiency (and excess as well) of Cu, which is a redox-active metal, overproduction of reactive oxygen species (ROS) occurs resulting in oxidative stress, DNA damage, lipid peroxidation etc. (Angelé-Martínez et al., 2017). To tackle the cellular imbalance of ROS, plants activate a defense system consisting of enzyme and non-enzyme antioxidants (Puig and Peñarrubia, 2009). However, so far the antioxidant response of plant under the treatment with Cu-based ENPs has been mostly examined in the ecotoxicological studies, in which ENPs were tested in excessive conditions triggering the oxidative stress and antioxidant stress response (Dimkpa et al., 2012; Shaw et al., 2014; Tang et al., 2016). For example, nano-Cu induced an increase of H_2O_2 and copper-zinc superoxide dismutase gene expression in cucumber after the application of ENPs to hydroponic solution (Mosa et al., 2018). The study by Shaw et al. (2014) showed enhanced ascorbate peroxidase and glutathione reductase activity in rice seedlings exposed to nano-CuO at 1.0 and 1.5 mM. However, there is no data on the antioxidant response of foliar application of ENPs containing Cu under Cu-deficiency. Considering plants needs of a relatively low amount of Cu (Tang et al., 2016), the application of conventional compounds releasing the whole pool of Cu ions may easily exceed plant requirement for this transition metal, thus exacerbating oxidative stress. Cu-based ENPs, characterized by gradual dissolution, may deliver Cu ions at the desired rate to plants suffering from Cu deficiency, thus reducing oxidative stress (Wang et al., 2016).

This study was aimed to give an insight into the impact of foliar sprayed nano-Cu on *H. vulgare* grown under Cu deficiency conditions. *H. vulgare*, the fourth most important cereal in the world, is widely used for food, feed and brewing (Doğaroğlu and Köleli, 2017). Due to its economic importance and sensitivity to Cu deficiency, the impact of nano-Cu on barley needs to be examined. Further, the comparison of the effects of ENPs and their dissolved compounds on the plant antioxidant activity needs to be conducted to evaluate the nano-specific activity. Our study included the *in situ* spectroscopic analysis of the nano-Cu-leaf interaction and the physiological and biochemical response of plant to Cu compounds (nano-Cu/$CuSO_4$). The analysis of changes in the activity of a wide range of antioxidative enzymes and the content of non-enzyme biomolecules in *H. vulgare* under treatment with nano-Cu was aimed to explore their role and path in the mitigation of oxidative burst caused by Cu deficiency. We hypothesized that nano-Cu, by gradually deliver of Cu ions, will give better effects for the plant health grown in Cu scarcity than under treatment with $CuSO_4$. The holistic approach to the interactions of nano-Cu-barley plant will shed light on the potential utility of nano-Cu as foliar fertilizer.

2. Materials and methods

2.1. Characterization of chemicals

Cu nanoparticles (nano-Cu) (purity ≥95.5%) were purchased from Sigma-Aldrich (USA). $CuSO_4$ as a dissolved Cu compound (purity ≥95.5%) was applied to compare the effects of ENPs and ionic forms of the metal. Nano-Cu was characterized by the primary particle size of 25 ± 10 nm, as determined with a transmission electron microscope (TEM) (JEM–3010 TEM JEOL, Ltd., Japan). The TEM image of nano-Cu is presented in Fig. 1A. The surface area of nano-Cu estimated by BET analysis was 8 $m^2\ g^{-1}$. Oxidation state, phase formation and crystallography of nano-Cu were determined with powder XRD (Empyrean, PANalytical, the Netherlands) using CuK_α radiation ($\lambda = 1.54016$ Å) at 60 keV over the range of $2\theta = 5$–$95°$. The peaks in the XRD pattern were identified by comparison with the PDF-2 database of the International Centre for Diffraction Data (ICDD). The XRD pattern analysis was conducted with the Rietveld refinement method. Obtained XRD pattern (Fig. 1B) confirmed the presence of copper (Cu 62%) and cuprite (Cu_2O 38%) in nano-Cu powder. The existence of narrow peaks in the XRD spectrum revealed the crystalline phase of nano-powder. The size of nano-Cu crystallite was estimated based on the diffraction peak broadening using the Scherrer equation. The average crystallite size of nano-Cu was found to be 32.6 ± 3.7 nm. The absence of additional peaks attributed to typical possible impurities confirmed the purity of the tested nano-powder.

2.2. Experimental design

The nano-Cu solutions for foliar spray were prepared by suspending nano-powder of nano-Cu in redistilled water ($\Omega < 0.05$ μS cm^{-1}) at concentration of 100 and 1000 mg of L^{-1}. In our study, all Cu solutions were prepared with the addition of 0.05% Tween 20 as an anti-foaming adjuvant to improve the spreading and adhesion of the metal compound on the leaf surface (Hu et al., 2020). Next, the solutions were sonicated in an ultrasonic bath (25 °C, 250 W, 50 Hz) for 30 min. The solutions of ENPs were characterized in terms of zeta potential (ζ-potential), the distribution of aggregate sizes and dissolution rate. ζ-potential and the distribution of particle sizes in nano-Cu solutions were examined with

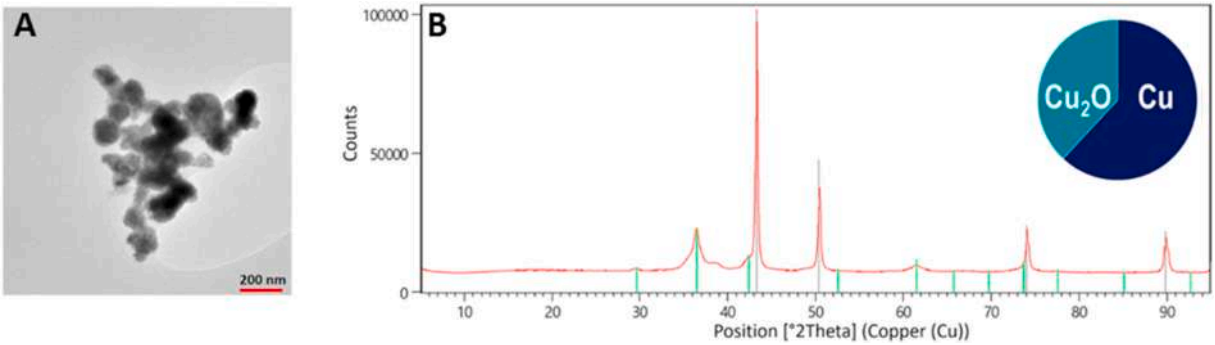

Fig. 1. TEM image (A) and XRD pattern (B) of nano-Cu.

the dynamic light scattering technique (DLS) (Zetasizer 3000, Malvern, UK). The nano-Cu in solution was imaged with TEM by the application of a drop of solution on the polymeric film. The separation of the dissolved metal fraction from the solution of nano-Cu was performed using ultrafiltration with a Microsep Advance Centrifugal Devices with Omega Membrane 1K (Pall Corporation). The concentration of Cu ions in nano-Cu solutions from before and after spraying was determined with an Inductively Coupled Plasma Optical Emission Spectrometer, ICP–OES (Thermo Fisher Scientific, iCAP 7200, USA). Axial configuration was used for Cu determinations. The spectral line (324.754 nm) was chosen to obtain the highest sensitivity and minimum interference.

2.3. Plant growth and foliar application of Cu solutions

Seeds of *H. vulgare* cultivar Ella were soaked for 2 h in redistilled water. The seeds were surface sterilized with 2% calcium hypochlorite (15 min) and then with 70% ethanol (1 min). The seeds were then rinsed 3 times with redistilled water. Next, the sterilized seeds were transferred to Petri dishes containing filter paper soaked in redistilled water for germination. Further, the Petri dishes were placed in a growth chamber at 24 °C in the dark. After 4 days, seedlings were transferred to a modified Hoagland's solution containing (mM) 0.457 $MgSO_4{\cdot}7\ H_2O$, 1 KNO_3, 0.1 KH_2PO_4, $Ca(NO_3)_2$, 0.0672 $NaSiO_3$ 5 H_2O, 0.001 $Mo_7O_{24}(NH_4)_6$, 0.001 $ZnSO_4$, 0.001 $MnCl_2$, 0.003 H_3BO_3, 0.03 NaFe(III) EDTA buffered with 0.02 MES (4-Morpholineethanesulfonic acid, 2-(N-Morpholino) ethanesulfonic acid hydrate)-KOH. The barley plants were grown in Cu deprived Hoagland's solution to induce Cu deficiency. No control with addition of Cu in the growth medium was conducted due to (i) limited translocation of Cu from roots to shoots and (ii) foliar application mode of Cu compounds determining different mechanism of adsorption and plant response than under root exposure (Jośko et al., 2021). The hydroponic solutions were replaced once a week with fresh medium and constantly aerated. Plants were cultivated under hydroponic conditions in a growth chamber (Conviron GEN1000) with a relative humidity of 60 ± 10% and at 16 h light/8 h dark cycle at 23 ± 3 °C (day time) and 18 ± 3 °C (night time) and with a light intensity at 450 μmol m^{-2} s^{-1}. 5 week-aged plants (at advanced tillering stage, BBCH: 23) were sprayed with 10 mL of nano-Cu or $CuSO_4$ solutions with 0.05% Tween 20 at concentration of 100 and 1000 mg L^{-1} using hand-held diffusive sprayer in three biological replicates. The concentrations of nano-Cu were selected on the basis of preliminary tests and available literature (Lee et al., 2008; Mosa et al., 2018). The higher dose of Cu-compounds was calculated to obtain a rate of 2 kg of Cu per ha using in agricultural practice (Fageria et al., 2009). A rate of 100 mg L^{-1} was used to evaluate the opportunity for reducing the amount of Cu used in nano-fertilizers. A solution of redistilled water with the surfactant was used as the control treatment. Each pot lid was covered with foil to prevent the entrance of solutions into roots. Additionally, the foil was weighed before and after spraying to evaluate the volume of solutions left on above-ground parts of plants. These volume values are provided in Supplementary Materials (Table S1).

1 and 7 days after treatment, plants were harvested and prepared for analysis. The plant tissues (roots and leaves) destined for metal content and microscopic analysis were rinsed with Milli-Q® water. Additionally, to remove nano-Cu attached to the leaf surface, leaves were next rinsed with 2.2 M HNO_3 for 30 s and then rinsed 3 times with redistilled water. Then plant samples were air-dried, weighted and stored (in darkness at 20 °C) for Cu content analysis. Fresh leaves for biochemical analysis were weighted and stored in −80 °C.

2.4. Plant tissues analysis

2.4.1. In situ microscopic and spectroscopic analysis

Scanning electron microscopy (SEM) with Energy Dispersive Spectrometry (EDS) (Quanta™ 3D FEG, FEI with EDAX SDD Apollo detector) was employed to image the treated leaves with Cu-compounds before and after etching with HNO_3 in order to determine the internalization of applied Cu solutions into *H. vulgare*. Due to the initial interactions of foliar applied solutions was with the cuticle (Avellan et al., 2019), the characterization of plant cuticles was provided by using Fourier transform infrared spectroscopy – attenuated total reflectance (FT-IR/ATR). It allowed to obtain significant information on the nature of functional groups present in the cuticle matrix and on the structural role, interaction and macromolecular arrangement of their components (Heredia-Guerrero et al., 2014). The spectra were recorded in the 4000-400 cm^{-1} range, resolution 4 cm^{-1}, at room temperature using Nicolet 6700 spectrometer and Meridian Diamond ATR accessory (Harrick). Fresh leaf samples were directly applied onto the diamond crystal and close contact was made with the crystal surface by a pressure tower in such a way as not to destroy the structure of the leaf. Interferograms of 512 scans were averaged for each spectrum. Dry potassium bromide (48h, 105 °C) was used as a reference material to collect ATR spectra. All ATR spectra were corrected for water vapor and carbon dioxide and ATR correction was applied. No smoothing functions were used. All spectral measurements were performed in triplicate.

2.4.2. The total Cu content determination in plant tissues

Dry roots and leaves were digested with a mixture of HNO_3:H_2O_2 (4:1) in Teflon vessels in a microwave oven (Milestone ETHOS EASY, Italy) for 1 h at 200 °C. Cooled samples were filtered (0.45 μm, PTFE), diluted with redistilled–water to 25 mL, and analyzed with ICP–OES (iCAP 7200). All analyses included blanks. Certified material (tomato leaves, NIST® SRM® 1573a) was used for the quality control of the sample digestion. Cu recovery was at the level of 94 ± 2%.

2.4.3. Biochemical analysis

The content of photosynthetic pigments. Chlorophyll and carotenoids content was determined according to the method described by Nayek et al. (2014). Homogenized leaves samples (0.25 g) were extracted with 5 mL of 80% (v/v) acetone for 30 min at room temperature using a

multi-rotator (RS-60, Biosan) (300 rpm). The samples were centrifuged (15 min, 13 000×*g*) and the supernatant were separated and 0.5 mL of it is mixed with 4.5 mL of 80% acetone. The supernatant was used to determine the absorbance of chlorophyll *a*, chlorophyll *b* and carotenoids with a spectrophotometer (Lambda 40 UV–Vis spectrophotometer, PerkinElmer), at the respective wavelengths of 663, 645 and 470 nm.

Lipid peroxidation assay. Lipid peroxidation was determined by measuring malondialdehyde (MDA) content following the protocol described by Wessely-Szponder et al. (2015). The leaves were homogenized with 1.5 mL of 20% trichloroacetic acid (TCA) and centrifuged at 10 000×*g* (15 min, 4 °C). The aliquots of plasma were mixed with TCA and thiobarbituric acid and thereafter heated for 20 min in a boiling water bath. After cooling to room temperature, 2 mL of n-butanol was added and the mixture was shaken for 3 min and centrifuged for 10 min at 1500×*g*. After the transfer of the upper n-butanol layer to a glass cuvette, its absorbance was measured at 532 nm. Concentrations of MDA were estimated on the basis of the standard curve obtained by using malondialdehyde bis-dimethylacetal.

Antioxidant activity assay. Antiradical properties was assayed according to Re et al. (1999). The free radical scavenging abilities (ABTS) were determined in samples obtained after chemical extraction and digestion *in vitro* and expressed as Trolox equivalents in mg per g of fresh weight.

Enzyme activity assays. All enzyme extract procedures were conducted at 4 °C. Superoxide dismutase (SOD), catalase (CAT) and glutathione were determined using commercial kits: SOD Assay Kit® (Cat. No. 19160-1 KT-F, Merck Germany), CAT Assay Kit® (Cat. No. 219265-1KIT, Merck, Germany) and Quantification kit for oxidized (GSSG) and reduced glutathione (GSH) (Sigma-Aldrich, Cat. No. 38185, Sigma-Aldrich, Germany) with accordance to manufacture procedure. Guaiacol peroxidase (POD) activity was determined using guaiacol as a substrate (Ippolito et al., 2000). The activity was expressed in units per g of fresh weight (fw), where one unit oxidizes 1.0 μmol of guaiacol per minute at pH 6.4 at 25 °C. For glutathione reductase (GR), 1 g of the sample was ground with 5 mL of 100 mM sodium phosphate buffer (pH 7.6) containing 3.4 mM EDTA. The extracts were then homogenized and centrifuged at 12 000×*g* at 4 °C for 30 min, and the supernatant was collected (Sikora and Świeca, 2018).

The activity of enzyme associated with low molecular antioxidants. For phenylalanine ammonia-lyase (PAL), 1 g of fresh sample was ground with 5 mL extracting buffer (0.2 M boric acid buffer containing, 1 mM EDTA, and 50 mM β-mercaptoethanol, pH 8.8). PAL assay was determined using 0.02 M L-phenylalanine. One unit was defined as the amount of enzyme that produced 1.0 μmol trans-cinnamic acid per min under the assay conditions. The results were presented as U per g fw (Assis et al., 2001). For polyphenol oxidase (PPO) 1 g of the sample was ground with 5 mL of 100 mM sodium phosphate buffer (pH 6.4) containing 0.2 g of polyvinylpolypyrrolidone. PPO was determined using catechol as a substrate (Galeazzi et al., 1981). The activity was expressed in units per g fw, where U = 0.001 ΔOD_{420} min^{-1} in the assay.

The total content of phenolics. For the extraction of phenolics, samples were subsequently extracted for 1 h at room temperature (300 rpm) in a capped centrifuge tube with 5 mL of different solvents: 50% methanol, 60 mM HCl in 50% methanol, and finally with 60 mM HCl in 70% acetone. The mixture was centrifuged (15 min, 3000×*g*, 22 °C) and the supernatants from all steps were combined (Sikora et al., 2020). The total phenolic content (TPC) was determined using the Folin–Ciocalteau reagent (Singleton et al., 1999). The amount of phenolics was expressed as mg gallic acid equivalents (GAE) per g of fw.

2.4.4. Statistical analysis

All statistical analyses were performed using the Statistica 13.1 software package. The differences between treatments were determined using a one-way and two-way analysis of variance (ANOVA) followed by Tukey's or Dunnett's post hoc test at a significance level of 0.05. Two-tailed Pearson correlation analysis was performed to test the variables. The principal components analysis (PCA) was performed to summarize the similarities and differences among all sample groups.

3. Results and discussion

3.1. Characteristics of nano-Cu solution

Nano-Cu in solution was characterized with ζ-potential of −19.6 mV. The average particle size of nano-Cu (248.8 ± 6 nm) (Fig. 2) in solution confirmed the strong tendency of ENPs to aggregation (Jośko et al., 2017). The concentration of dissolved Cu^{2+} in 100 and 1000 mg L^{-1} of nano-Cu solutions amounted to 0.29% and 0.065% of stock suspensions, respectively (Table S2). The low concentration of dissolved Cu^{2+} in stock suspensions might result from low solubility and dissolution rate of Cu-based ENPs (Lee et al., 2008). Moreover, the low concentration of dissolved Cu^{2+} may be caused by oxidation of nano-Cu powder (Fig. 1B), the strong aggregation of nano-Cu in solutions (Fig. 2A), and the presence of non-ionic surfactant. The formation of a passive layer on nano-Cu might lead to protection from the release of Cu^{2+} from particle core (Conway et al., 2015). The aggregation of ENPs reduces the surface area of ENPs resulting in a decrease of their dissolution rate (Conway et al., 2015). It was also previously observed that a non-ionic surfactant might prevent particle dissolution by stabilizing the ENPs dispersion in the solution (Lee et al., 2008). The decrease in the ratio of dissolved Cu^{2+} in 1000 mg L^{-1} solution compared to 100 mg L^{-1} might stem from increased aggregation of particles at higher concentrations (Lee et al., 2008). The particle size distribution could not be analyzed at 1000 mg L^{-1} of nano-Cu because of too high suspension. It is worth to note that despite the formation of nano-Cu aggregates, which may clog the nozzle of diffusive sprayers, only minimal changes were observed in the concertation of Cu^{2+} in solutions before and after application (Table S2). It proved no clogging of the sprayer, thus allowing an undisturbed spray of the solutions to plants.

3.2. ENPs – plant interactions

The analysis of Cu content in plant parts exposed to ENPs is crucial for the evaluation of their potential for plant fertilization, especially long-term nutrient loading (Kusiak et al., 2022). As Fig. 3A shows, after 1-day of exposure to nano-Cu and $CuSO_4$ treatments, the Cu content in above-ground parts was affected only at 1000 mg L^{-1}, where ~4.5-fold higher Cu content (72.4–77.9 mg kg^{-1} d. w.) was found than in untreated plants. Longer exposure to Cu compounds (7 days) caused a definitely higher Cu content in above-ground plant tissues (Fig. 3B) compared to 1-day exposure. Xiong et al. (2017) also observed a similar tendency of increased Cu content in lettuce and cabbage leaves with increased duration of exposure to foliar applied nano-CuO. Moreover after 7 days, Cu content in above-ground plant parts increased at both used rates of Cu compounds ($p < 0.05$) with a positive dose-effect relation. Only at the rate of 100 mg L^{-1}, the Cu content was differed between plants exposed to nano-Cu and $CuSO_4$: Cu content was higher after $CuSO_4$ by 76% compared to the application of nano-Cu (33.8 mg kg^{-1} d. w.). A difference in Cu leaf content under nanoparticulate and ionic Cu was also noted in a study by Tan et al. (2018), in which $CuSO_4$ due to ionization provided a higher accumulation of Cu in basil leaves, by ~1.7–2.6-fold, than nano-$Cu(OH)_2$. However, at the rate of 1000 mg L^{-1} both Cu-compounds caused similar high Cu levels in above-ground plant parts (123.2–140.5 mg kg^{-1} d. w.). Although the measured Cu concentration in plant tissues exposed to nano-Cu may not mean a real absorption of Cu. As SEM-EDS analysis has shown, nano-Cu remained on the surface of leaves, notwithstanding the fact that the etching protocol was used to remove the nano-Cu from the outer layer of leaves (Fig. 3C, E). For this reason, the determined metal content in leaves may be overestimated. In a study by Zhao et al. (2017) similar bioaccumulation of $Cu(OH)_2$ was observed on *Zea mays* L. leaves because of significant retention of Cu on the leaf surface. In turn, Cu in barley leaves treated

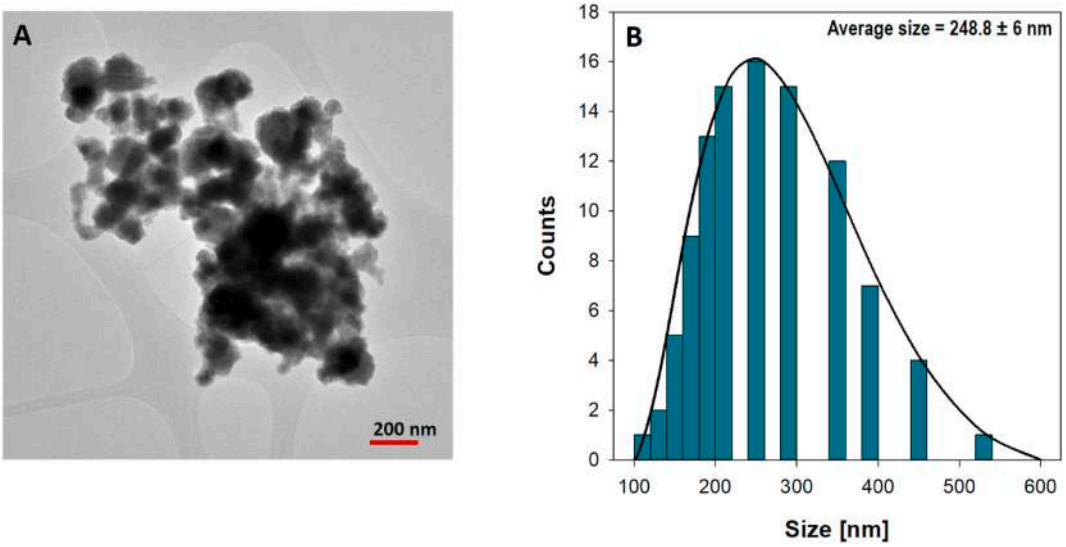

Fig. 2. Nano-Cu characterization in Milli-Q® water with 0.05% (v/v) Tween 20 solution at 100 mg L^{-1}. (A) TEM image of nano-Cu solution; (B) Particle size distribution of nano- Cu aggregates based on DLS technique.

with $CuSO_4$ was almost negligible (Fig. 3D, F), which indicates successful loading of virtually the entire pool of Cu ions cross plant leaves.

Due to the fact that foliar spray may affect the chemistry of leaf surface, FT-IR/ATR analysis of plant samples was performed and the spectra were presented in Fig. 4. The $–CH_3$ and $–CH_2–$ (long-chain aliphatic waxes) and the ester C═O (cutin) have stretching vibrations of much higher intensity for untreated leaf than for other leaf samples (control – redistilled water with surfactant/$CuSO_4$/nano-Cu), suggesting a more hydrophobic surface. This effect on the cuticle components may be the result of degradation of cuticle cells by the surfactant as was observed by Zhang et al. (2020). Subsequently, this cuticle reduction might facilitate the diffusion of ENPs to inner layer of leaves, due to the cuticle being commonly determined as the way of ENPs entry (Du et al., 2015). The analysis of Cu content supported that statement, as Cu accumulation increased after 7 days (Fig. 3B). Moreover, analysis of the spectra shown that the treatment with Cu-compounds (especially $CuSO_4$) provided higher signal intensity of bands of glycosidic C–O–C (1050-1035 cm^{-1}) and δ(OH) at 1261 cm^{-1}, which might indicate the presence of polysaccharides, which are usually located in the inner parts of the cuticle (Heredia-Guerrero et al., 2014). It may suggest an explanation of the burning effect of $CuSO_4$ on leaf surface, which is observed at foliar application.

Cu content in barley roots was unaffected by treatment with both Cu-compounds regardless of the duration of exposure (Table S3). Cu^{2+} has high affinity to be bound with bioligands (A. Blindauer and Schmid, 2010) causing low mobility and translocation in plants (Tan et al., 2018). ENPs might have other capacity of transport, often surface charge- and size-dependent (Avellan et al., 2021). A study by Avellan et al. (2019) revealed that the 10–25% of Au ENPs <50 nm was accumulated in wheat roots after foliar treatment and 2-week exposure. Thus, the lack of translocation of Cu in our study could be also the result of relatively short-term exposure.

3.3. Plant growth under exposure to Cu-compounds

The absence of a Cu source during the growth period before Cu application resulted in the occurrence of the Cu deficiency symptoms such as chlorosis on the top of leaves (Fig. S1) (van Maarschalkerweerd et al., 2013). After 1-day of foliar exposure to both concentrations of nano-Cu and $CuSO_4$, no visible extra symptoms were observed (Fig. S1). However, after 7 days from the application of Cu-compounds, plants exposed to 1000 mg L^{-1} of $CuSO_4$ were characterized with advanced leaf chlorosis, probably due to an excess of Cu in the plants (Martins and Mourato, 2006).

Dry weight (d.w.) of above-ground plants parts was enhanced by both nano-Cu and $CuSO_4$ after 1 and 7-day exposure (Table S4). Regardless of used rates, both Cu compounds increased dry weight of above-ground plant parts by 7–22% compared to untreated plant after 1 day of exposure (Table S4). Whereas, no effect of Cu treatments on dry weights of roots was observed. After 7 days, plants treated with Cu compounds exhibited a positive dose-effect relationship regarding to dry weight of above-ground plant parts, but barley biomass was higher under treatment of $CuSO_4$ (89–115%) than nano-Cu (22.7–85%) compared to control plant. The difference in the d. w. of shoots and leaves measure up to 1.5 to 1.16-fold change in plants exposed to metal salts compared to ENPs. Due to the fact that the plants were grown in Cu-deficiency conditions, the supply of Cu, an essential element, with foliar applied nano-Cu and $CuSO_4$ prompted the biomass growth even in short-term exposure. This relatively quick response of plant mass to Cu application could be also associated with increased nutrient demand occurring during an intense plant growth at the tillering stage (Aspinall, 1961). D. w. of roots was also enhanced in line with increasing ENPs rates (19.5–46.2% compared to control samples), while an opposite tendency was observed for the treatment with $CuSO_4$ (120-82%). The stimulatory effect on plants d. w. by both ENPs and $CuSO_4$ despite the lack of Cu translocation from leaves to roots was previously described by Zhao et al. (2017).

3.4. Biochemical analysis of plant treated with nano-Cu and $CuSO_4$

Chlorophyll *a*, *b* and carotenoid contents were unchanged after 1 day of exposure to nano-Cu and $CuSO_4$, regardless of rates used (Table S5). After 7 days, the nano-Cu at both rates did not induce any significant changes in photosynthetic pigment levels compared to control group. On the contrary, plants treated with $CuSO_4$ at 100 and 1000 mg L^{-1} demonstrated a significant decline in chlorophyll *a* content (14.2% and 24.7%, respectively) compared to untreated plants. This is consistent with the observed chlorosis (Fig. S1), which is probably caused by the loss of chlorophyll due to inhibition of protochlorophyllide reductase, an enzyme involved in the reduction of protochlorophyll to chlorophyll (De Filippins et al., 1981). A study by Kohatsu et al. (2021) reported similar findings on the content of chlorophyll *a* and carotenoids in spinach exposed to 20 ppm of biogenic nano-CuO and their ionic counterparts. This highlights the difference between nanoparticulate and ionic Cu

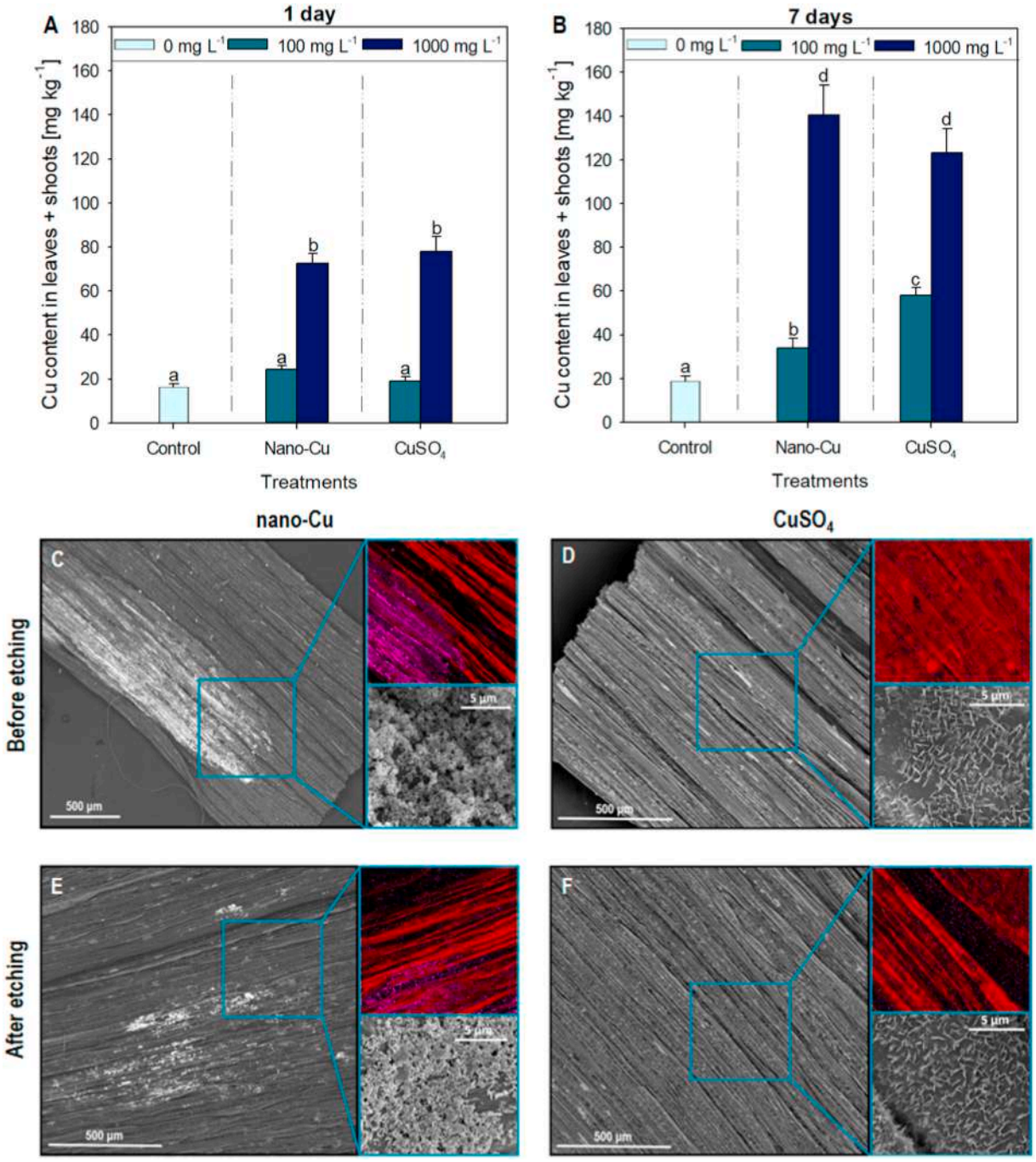

Fig. 3. Analysis of Cu in barley. The total content of Cu (A, B) in aboveground parts of *H. vulgare* (leaves + shoots) exposed to two concentration (100 and 1000 mg L^{-1}) of nano-Cu and $CuSO_4$. Error bars represent standard error (SE, n = 3 tests). Different letters indicate significant differences among the treatments (Tukey's test, $p < 0.05$). Analysis of Cu internalization with the use of SEM-EDS (C, D, E, F) The pictures were taken before (C, D) and after (E, F) etching of *H. vulgare* leaves exposed to nano-Cu and $CuSO_4$ (at 100 mg L^{-1}) to remove adhered Cu nanoparticles. The pink color corresponds with Cu presence. (For interpretation of the references to color in this figure legend, the reader is referred to the Web version of this article).

impact on the photosynthetic pigments in plants, which is indirectly affects the crop yield (Long et al., 2006).

3.5. Oxidative stress and antioxidant response of barley exposed to Cu-compounds

Earlier research demonstrated that both a deficiency (Tewari et al., 2006) and an excess (Kohatsu et al., 2021) of a crucial microelement such like Cu can induce oxidative stress due to imbalance of ROS content. The generation of ROS may trigger plant damage at the molecular level by oxidation of lipids, proteins, pigments, nucleic acid (Lijuan Zhao et al., 2017). The content of MDA, an indicator of lipid peroxidation, was modulated under treatment with Cu compounds, but only at 1000 mg L^{-1} (1-day exposure): nano-Cu declined MDA content by 29%, while $CuSO_4$ caused a 56% increase of MDA amount (Fig. S2). After 7 days, $CuSO_4$ continued increasing MDA content, whereas nano-Cu had no further effect on this parameter. These results suggest that supply of high pool of Cu^{2+} delivered with $CuSO_4$ prompted overproduction of MDA as a result of lipid peroxidation, while nano-Cu caused an attenuation of that process. Previous studies comparing the activity of medium-applied

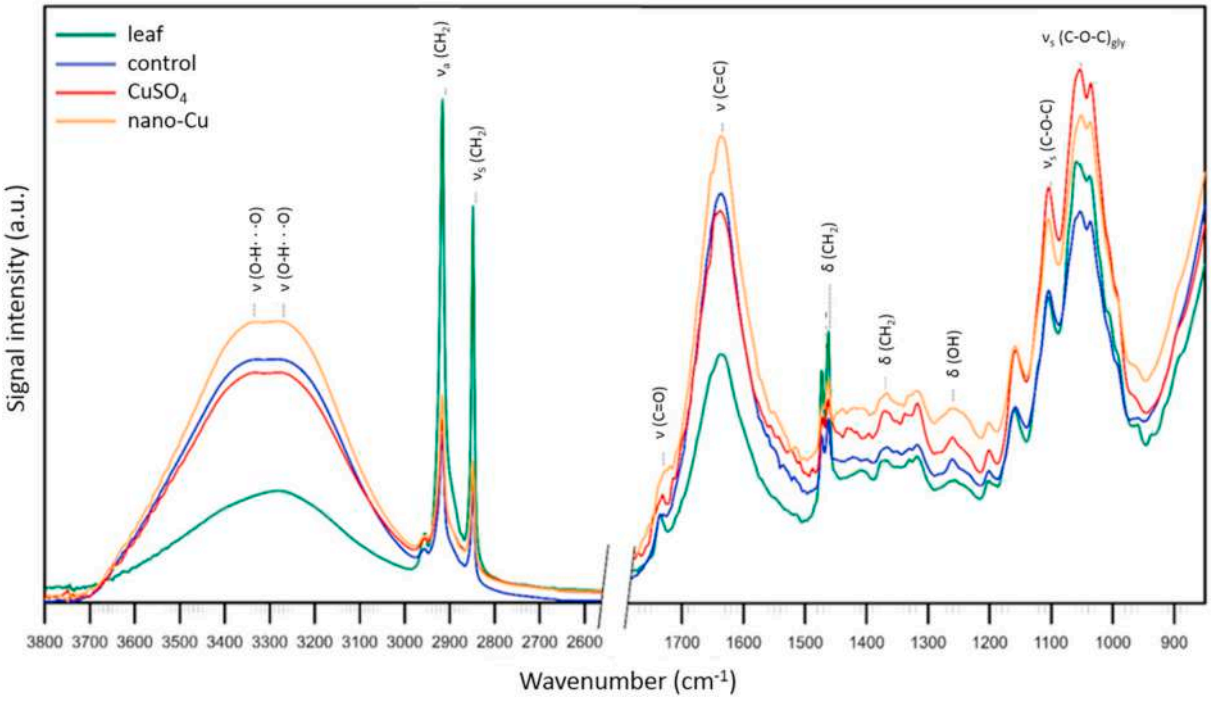

Fig. 4. FT IR/ATR spectra of analyzed samples. H. vulgare leaves was exposed to nano-Cu and $CuSO_4$ (at 100 mg L_{-1}) for 7 days.

nano-Cu and $CuSO_4$ revealed also higher MDA level in wheat under ionic than nanoparticulate Cu (Huang et al., 2022; Zhang et al., 2018).

To combat stress induced by deficient/excessive nutrients, plants activate a defense system consisting of enzymatic and non-enzymatic antioxidants (Fig. 5). The antioxidant capacity measured with ABTS was only increased under $CuSO_4$ at 1000 mg L^{-1} (Fig. S4) by 157.4% compared to untreated plant ($p < 0.05$) in the line with higher MDA content after 1-day of exposure. However, after 7 days ABTS was unchanged under all treatments, even though MDA content was at the highest level under $CuSO_4$. To obtain more in-depth view of antioxidant response of plants on nanoparticulate and ionic Cu-compounds, the activity of enzymes and the content of biomolecules belonging to antioxidant family were further examined.

As presented in Fig. 6, the foliar application of Cu compounds affected only the activity of SOD and GR among the tested enzymes in *H. vulgare* after 1-day of exposure ($p < 0.05$). Our results demonstrated a 1.7-9-fold decrease in SOD activity in plants exposed to nano-Cu and $CuSO_4$ compared to the control (Fig. 6A). SOD is an intracellular metalloenzyme, which is the first line of defense against oxidative stress by catalyzing highly toxic $O_2^{\bullet-}$ to less toxic H_2O_2 and O_2 (Gill and Tuteja, 2010). The decline of SOD activity under Cu treatment might prove the link between enzyme activity modulation and re-establishment of Cu homeostasis (Ravet and Pilon, 2013) as Cu-deprivation can stimulate excessive ROS production (Tewari et al., 2006). On the other hand, previous studies linked the reduction of SOD activity with the occurrence of severe oxidative bursts in the plant cells in response to ENPs-related stress (Rizwan et al., 2017) or with Cu toxicity (Mourato et al., 2009). However, the similar patterns of decreased SOD activity under nano-Cu and $CuSO_4$ may suggest that after 1 day, the other enzymes transforming further reaction products may be induced.

The H_2O_2 generated by SOD can be quenched by CAT, POD and/or the enzymes involved in the ascorbate–glutathione (AsA-GSH) cycle (Fig. 5) (Gill and Tuteja, 2010). Both CAT and POD enzymes convert H_2O_2 into O_2 and H_2O, although on different H_2O_2 detoxification pathways due to localization in different organelles (Gill and Tuteja, 2010). Interestingly, after 1-day exposure CAT (Fig. 6B) and POD

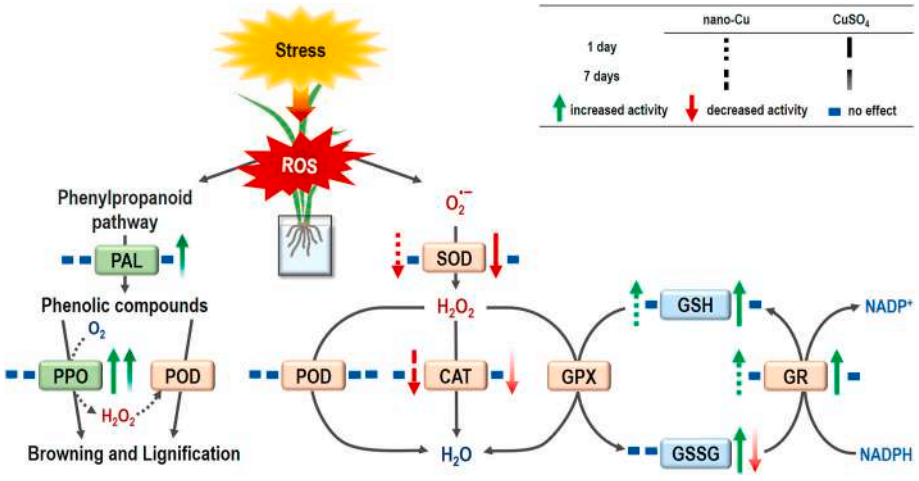

Fig. 5. Activation of enzymatic and nonenzymatic antioxidants in *H. vulgare* to detoxify cellular ROS induced by abiotic stress. ROS, reactive oxygen species; SOD, superoxide dismutase; APX, ascorbate peroxidase; CAT, catalase; GPX, glutathione peroxidase; GR, glutathione reductase; GSH, reduced glutathione; GSSG, oxidized glutathione; H_2O_2, hydrogen peroxide; $O^{2\bullet-}$, superoxide anion; PAL, phenylalanine ammonia-lyase; POD peroxidase; PPO, polyphenol oxidase; $NADP^+$, nicotinamide adenine dinucleotide phosphate; NADPH, reduced form of $NADP^+$.

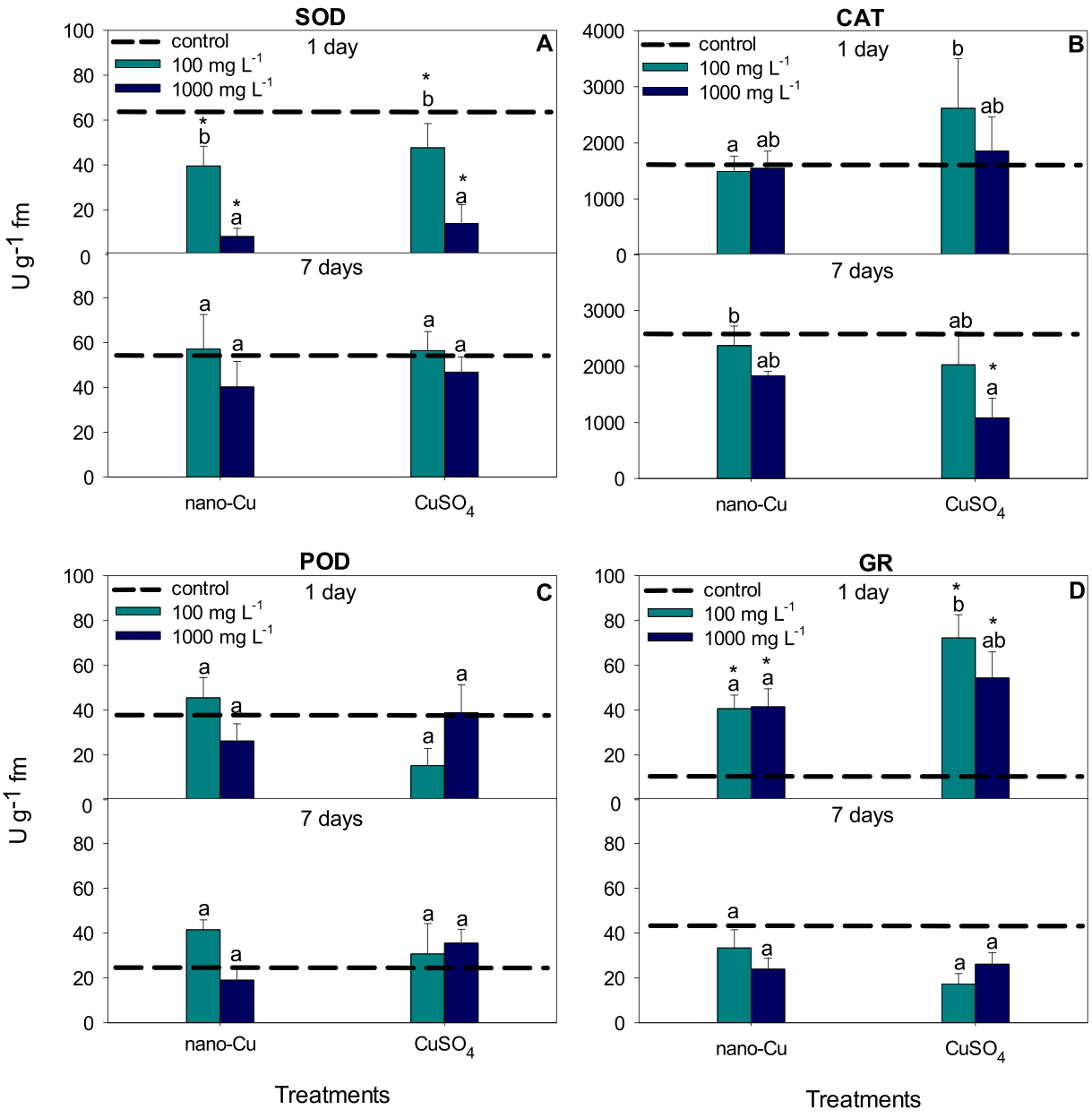

Fig. 6. The activity of SOD (A), CAT (B), POD (C), GR (D) in *H. vulgare* under treatment of nano-Cu and $CuSO_4$ (at 100 and 1000 mg L^{-1}) after 1 and 7 days of exposure. Error bars represent standard error (SE, n = 3 tests). The asterisks indicate significant difference between untreated and treated samples (Tukey's test, $p < 0.05$). Different letters indicate significant differences among the treatments (Tukey's test, $p < 0.05$).

(Fig. 6C) did not present significant differences in activity levels between the treatments and the control plants ($p > 0.05$). No change in CAT and POD activity might stem from the delayed (Martins and Mourato, 2006; Mourato et al., 2009) or species-specific enzymatic response of analyzed plants (Kohatsu et al., 2021; Martins and Mourato, 2006). Moreover, the lack of significant changes in CAT and POD activity might be compensated with the enhancement in GR activity, an enzyme involved in the GSH metabolic pathway (Fig. 5). As presented in Fig. 6D, both Cu compounds were found to strongly boost GR activity after 1 day of exposure. Regardless of the rates used, nano-Cu caused ~3.3-fold rise in GR activity, while the effect of $CuSO_4$ on GR activity was slightly stronger, it was observed that the level of its activity was 4–5.8 higher compared to untreated plant ($p < 0.05$). A high level of GR activity allows to maintain a pool of GSH, which plays a crucial role in the elimination of ROS (Fig. 5), and in the minimization of oxidative stress under the heavy metal stress (Dimkpa et al., 2012; Mostofa et al., 2014; Shaw and Hossain, 2013). This might also stem from higher affinity of AsA-GSH cycle enzymes for H_2O_2 than both CAT and POD (Gill and Tuteja, 2010). Similar results of an initial improvement of GR activity were detected in *O. sativa* under exposure to nano-CuO (1.5 mM) (Shaw and Hossain, 2013), whereas $CuSO_4$ (100 μM) treatment led to a continuous increase of GR activity level by 45–92% (Mostofa et al., 2015). Such an escalation of GR activity was associated with high degree of Cu toxicity and the plant attempt at maintaining cellular redox balance (Mostofa et al., 2015). However, in our study, plants were exposed to relatively low Cu^{2+} released from ENPs compared to $CuSO_4$. Thus, the effect-induced by ENPs may be caused by plant defense response to the combination of alien particles and dissolved Cu^{2+}.

The influence of Cu compounds on foliar GSH pool is presented in Fig. 7. After 1 day of exposure only nano-Cu at 100 mg L^{-1} demonstrated an elevated level of GSH by 102%, compared to the control group ($p < 0.05$) (Fig. 7A). Meanwhile, the GSSG analysis showed an opposite effect: the higher rate of ENPs and both of corresponding metal salt doses have strongly escalated GSSG content (4.5- and 2.8-fold, respectively)

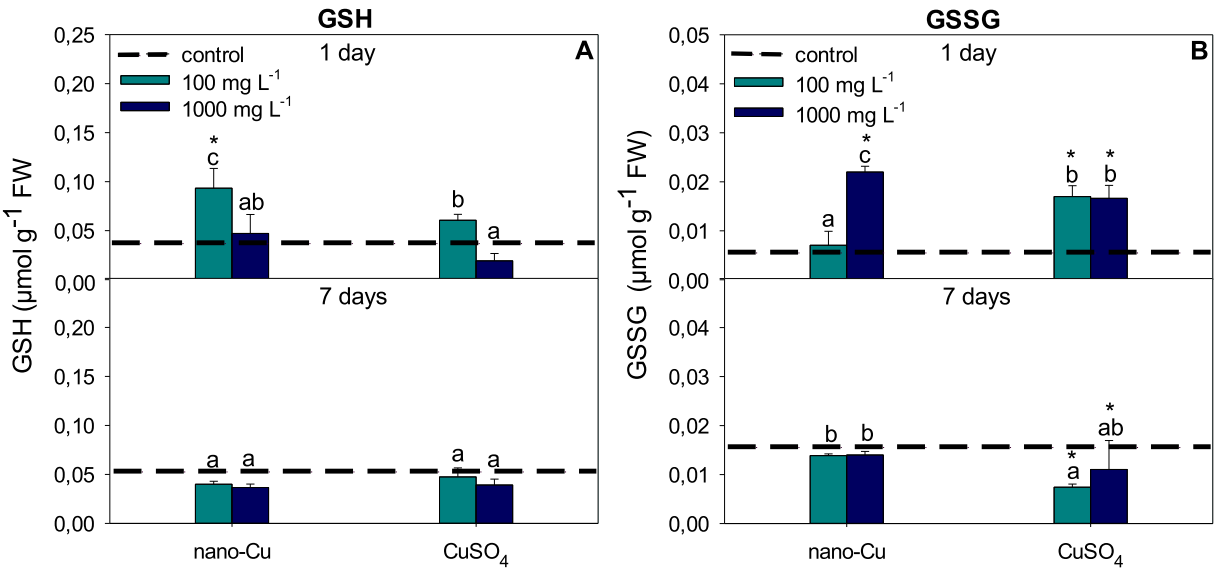

Fig. 7. The effect of nano-Cu and $CuSO_4$ (at 100 and 1000 mg L^{-1}) after 1 and 7 days of exposure on glutathione in both reduced (GSH) (A) and oxidized (GSSG) (B) states in barley leaves. Error bars represent standard error (SE, n = 3 tests). The asterisks indicate significant difference between untreated and treated samples (Tukey's test, $p < 0.05$). Different letters indicate significant differences among the treatments (Tukey's test, $p < 0.05$).

compared to untreated plant ($p < 0.05$) (Fig. 7B). GSH at optimal level is required for appropriate metabolic processes and also plays a crucial role in the non-enzymatic antioxidant defense system, protection of photosynthesis, cell differentiation, death and senescence (Gill and Tuteja, 2010). Moreover, data collected by Cuypers et al. (2000) correlated elevated GSH content with enhanced tolerance of plant toward stress factors. Therefore the rise in GSH content under nano-Cu treatment (100 mg L^{-1}) might have a positive impact on *H. vulgare* growth and yield (Gill and Tuteja, 2010). However, in our study we observed increased biomass under all treatments, and PCA analysis (Fig. 9) and Pearson correlation (Fig. S6) did not show any relation of these endpoints. In conditions of overproduction of ROS, GSH is converted to GSSG, thus the GSH/GSSH ratio is an important marker of cellular redox balance (Cuypers et al., 2000). Therefore, low GSH/GSSH ratio as a result of a growth in GSSG content observed after 1 day in our study could be connected with overproduction of ROS and the high oxidative stress under the higher dose of nano-Cu and both concentrations of corresponding metal salts (Table S6).

None of the tested Cu compounds led to any statistically significant change in PAL activity after 1-day exposure in relation to the control group ($p > 0.05$) (Fig. 8A). As the first committed enzyme in the primary phenolic pathway, PAL activity leads to the biosynthesis of the polyphenol compounds e.g. flavonoids, phenylpropanoids, and lignin (Fig. 5) (Santos-Espinoza et al., 2020). The cited study showed an induction of PAL synthesis by stressors (pathogens, wounding, heavy metals etc.) in response to ROS generation (Santos-Espinoza et al., 2020). As we observed changes in ROS scavenging antioxidant activities in the early period in barley plants in the current study, the lack of PAL response might stem from efficient ROS elimination or delayed enzymatic response (Kováčik and Bačkor, 2007). Moreover, regardless of the doses applied, nano-Cu did not change PPO activity level (Fig. 8B), while both rates of $CuSO_4$ caused ca. 5-fold increase in PPO activity after 1 day of exposure compared to untreated plant ($p < 0.05$). Similarly to PAL, PPO activity can be induced as a plant defense mechanism against abiotic and biotic stressors (Martins and Mourato, 2006). Additionally, PPO is a known Cu-containing enzyme involved in the oxidation of polyphenols into quinones and cell walls lignification (Fig. 5) (Martins and Mourato, 2006). Under Cu-deficiency, PPO activity is strictly

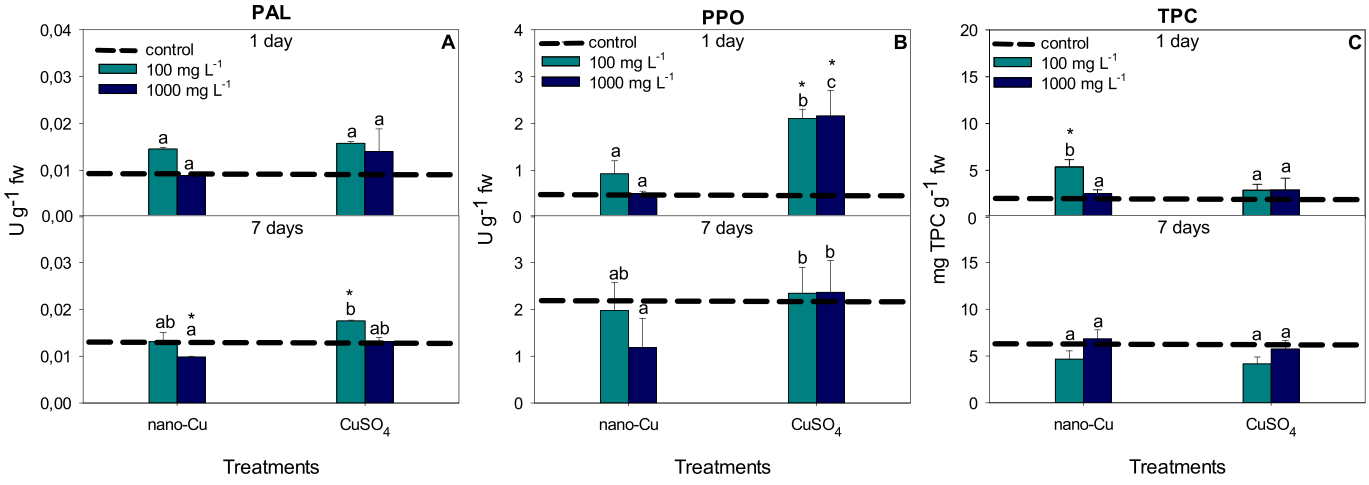

Fig. 8. The changes in activity of PAL (A), PPO (B) and TPC content (C) in *H. vulgare* under treatment of nano-Cu and $CuSO_4$ (at 100 and 1000 mg L_{-1}) after 1 and 7 days of exposure. Error bars represent standard error (SE, n = 3 tests). The asterisks indicate significant difference between untreated and treated samples (Tukey's test, $p < 0.05$). Different letters indicate significant differences among the treatments (Tukey's test, $p < 0.05$).

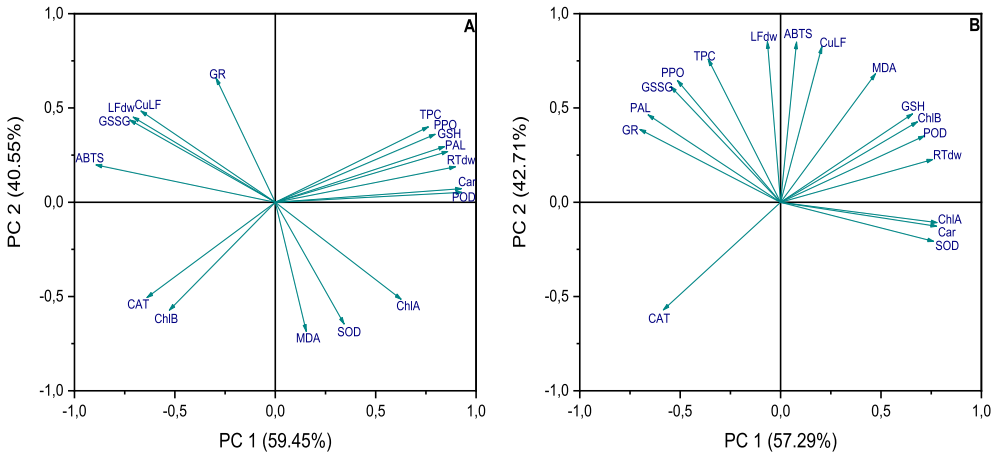

Fig. 9. PCA diagrams of endpoints after treatment of *H. vulgare* with nano-Cu (A) and $CuSO_4$ (B) and 1-day exposure.

restricted as the entire pool of Cu^{2+} present in the plant is redistributed to proteins essential for plant survival, e.g. plastocyanin (Printz et al., 2016). Therefore, significant growth in PPO activity under metal salts treatment most likely resulted from fast release of Cu^{2+} ions and efficient re-supply. Enhanced activity of PPO by ca. 75–90% was also detected after 1 day of exposure to 0.1–0.35 mM $CuSO_4$ in *Lupinus luteus*. Presumably, the lack of impact on PPO activity after nano-Cu application resulted from the low release rate of Cu^{2+} from ENPs (Printz et al., 2016). Surprisingly, TPC was increased by 4.3-fold only under treatment with nano-Cu at 100 mg L^{-1} compared to the control ($p < 0.05$) (Fig. 8C). Phenolic compounds are major secondary metabolites which act as antioxidants and eliminate ROS (Lijuan Zhao et al., 2017). According to Zhao et al. (2017) both 100 and 1000 mg L^{-1} of $Cu(OH)_2$ boost TPC due to Cu-triggered ROS generation. However, since the lower dose of nano-Cu treatment enhanced TPC in plants regardless of the low Cu^{2+} release rate, we suspect that this is impact on *H. vulgare* might be ENPs-dose-specific.

After 7 days, ENPs did not affect the tested enzyme activity in relation to the control sample (Figs. 6–8). As we mentioned earlier, the activity of different components of antioxidant defense system may be delayed under treatment and changed over time. In the case of ENPs, no effect on enzyme activities is in line with unaffected other indicators such as MDA content and ABTS. Previous studies correlated similar results with potential absence of oxidative stress due to restoration of Cu homeostasis (Ravet and Pilon, 2013) without negative effects from ENPs (Kohatsu et al., 2021). Only PAL activity was significantly impacted by nano-Cu treatment after 7 days (decreased by 23.08%), which might be a result of ENPs-specific factor (Rizwan et al., 2017). On the contrary, $CuSO_4$ increased MDA content over time without noticeable changes of tested antioxidants activity. It may suggest a breaking down of defense mechanisms (Martins and Mourato, 2006). Only treatment with $CuSO_4$ at 1000 mg L^{-1} induced a change CAT, the activity of which was unaffected during short-term exposure (Fig. 6B). $CuSO_4$ led to a 60% drop in CAT activity compared to the control. In the literature, a decrease in CAT activity over time is linked with breaking down of defense mechanism in plants due to accumulated H_2O_2 in response to the acute Cu-toxicity (Gill and Tuteja, 2010; Martins and Mourato, 2006). Other endpoints such like chlorosis, decreased biomass and pigment contents as well as high accumulation of Cu in plant tissues may confirm the statement of the failure defense system. Moreover, both rates of $CuSO_4$ also decreased the content of GSSG (Fig. 7B), but the GSH/GSSG ratio was not statistically different than in untreated plant. Previous research showed, that an inability of a plant to efficiently recycle GSSG to GSH correlated with susceptibility to metal-induced oxidative stress (Gill and Tuteja, 2010).

4. Conclusion

This study demonstrated the interactions between nanoparticulate/ionic Cu with plant under conditions regularly used in agronomic practices. Foliar-applied ENPs, especially at 100 mg L^{-1}, revealed promising effect on plant health. Gradually loading of Cu from ENPs triggered an increase of enzyme activity belonging to plant defense system acting as an elicitor. While, $CuSO_4$, which is widely used as fertilizer, induced oxidative stress and leaf surface damage. As the mechanisms behind ENPs-specific responses are not fully understood, further molecular studies on Cu homeostasis in plant under nano-Cu treatment are necessary to ensure long-term safety of potential Cu fertilizer.

Credit author statement

Magdalena Kusiak: Conceptualization, Methology, Investigation, Writing; **Małgorzata Sierocka**: Methology, Investigation; **Michał Świeca**: Methology, Investigation; **Sylwia Pasieczna-Patkowska**: Investigation; **Mohamed Sheteiwy**: Methology, Writing – review & editing. **Izabela Jośko:** Supervision, Conceptualization, Writing – review & editing, Methology, Resources, Funding acquisition.

Declaration of competing interest

The authors declare that they have no known competing financial interests or personal relationships that could have appeared to influence the work reported in this paper.

Data availability

No data was used for the research described in the article.

Acknowledgments

This study was supported by National Science Centre (Poland) in the frame of SONATA project (2017/26/D/NZ9/00067).

Appendix A. Supplementary data

Supplementary data to this article can be found online at https://doi.org/10.1016/j.envpol.2023.121044.

References

Blindauer, C.A., Schmid, R., 2010. Cytosolic metal handling in plants: determinants for zinc specificity in metal transporters and metallothioneins. Metallomics 2, 510–529. https://doi.org/10.1039/C004880A.

Angelé-Martínez, C., Nguyen, K.V.T., Ameer, F.S., Anker, J.N., Brumaghim, J.L., 2017. Reactive oxygen species generation by copper(II) oxide nanoparticles determined by DNA damage assays and EPR spectroscopy. Nanotoxicology 11, 278–288. https://doi.org/10.1080/17435390.2017.1293750.

Aspinall, D., 1961. The control of tillering in the barley plant 1. The pattern of tillering and its relation to nutrient supply. Aust. Jnl. Of Bio. Sci. 14, 493–505. https://doi.org/10.1071/bi9610493.

Assis, J.S., Maldonado, R., Muñoz, T., Escribano, M.I., Merodio, C., 2001. Effect of high carbon dioxide concentration on PAL activity and phenolic contents in ripening cherimoya fruit. Postharvest Biol. Technol. 23, 33–39. https://doi.org/10.1016/S0925-5214(01)00100-4.

Avellan, A., Yun, J., Morais, B.P., Clement, E.T., Rodrigues, S.M., Lowry, G.V., 2021. Critical review: role of inorganic nanoparticle properties on their foliar uptake and *in planta* translocation. Environ. Sci. Technol. 55, 13417–13431. https://doi.org/10.1021/acs.est.1c00178.

Avellan, A., Yun, J., Zhang, Y., Spielman-Sun, E., Unrine, J.M., Thieme, J., Li, J., Lombi, E., Bland, G., Lowry, G.V., 2019. Nanoparticle size and coating chemistry control foliar uptake pathways, translocation, and leaf-to-rhizosphere transport in wheat. ACS Nano 13, 5291–5305. https://doi.org/10.1021/acsnano.8b09781.

Conway, J.R., Adeleye, A.S., Gardea-Torresdey, J., Keller, A.A., 2015. Aggregation, dissolution, and transformation of copper nanoparticles in natural waters. Environ. Sci. Technol. 49, 2749–2756. https://doi.org/10.1021/es504918q.

Cuypers, A., Vangronsveld, J., Clijsters, H., 2000. Biphasic effect of copper on the ascorbate-glutathione pathway in primary leaves of Phaseolus vulgaris seedlings during the early stages of metal assimilation. Physiol. Plantarum 110, 512–517. https://doi.org/10.1111/j.1399-3054.2000.1100413.x.

Dimkpa, C.O., McLean, J.E., Latta, D.E., Manangón, E., Britt, D.W., Johnson, W.P., Boyanov, M.I., Anderson, A.J., 2012. CuO and ZnO nanoparticles: phytotoxicity, metal speciation, and induction of oxidative stress in sand-grown wheat. J. Nanoparticle Res. 14, 1125. https://doi.org/10.1007/s11051-012-1125-9.

Doğaroğlu, Z.G., Köleli, N., 2017. TiO2 and ZnO nanoparticles toxicity in barley (Hordeum vulgare L.). CLEAN – soil. Air, Water 45, 1700096. https://doi.org/10.1002/clen.201700096.

Du, Y., Kopittke, P.M., Noller, B.N., James, S.A., Harris, H.H., Xu, Z.P., Li, P., Mulligan, D. R., Huang, L., 2015. In situ analysis of foliar zinc absorption and short-distance movement in fresh and hydrated leaves of tomato and citrus using synchrotron-based X-ray fluorescence microscopy. Ann. Bot. 115, 41–53. https://doi.org/10.1093/aob/mcu212.

Fageria, N.K., Filho, M.P.B., Moreira, A., Guimarães, C.M., 2009. Foliar fertilization of crop plants. J. Plant Nutr. 32, 1044–1064. https://doi.org/10.1080/01904160902872826.

Galeazzi, M.A.M., Sgarbieri, V.C., Constantinides, S.M., 1981. Isolation, purification and physicochemical characterization of polyphenoloxidases (PPO) from a dwarf variety of banana (musa cavendishii, L). J. Food Sci. 46, 150–155. https://doi.org/10.1111/j.1365-2621.1981.tb14551.x.

Gill, S.S., Tuteja, N., 2010. Reactive oxygen species and antioxidant machinery in abiotic stress tolerance in crop plants. Plant Physiol. Biochem. 48, 909–930. https://doi.org/10.1016/j.plaphy.2010.08.016.

Hasegawa, T., Fujimori, S., Havlík, P., Valin, H., Bodirsky, B.L., Doelman, J.C., Fellmann, T., Kyle, P., Koopman, J.F.L., Lotze-Campen, H., Mason-D'Croz, D., Ochi, Y., Pérez Domínguez, I., Stehfest, E., Sulser, T.B., Tabeau, A., Takahashi, K., Takakura, J., van Meijl, H., van Zeist, W.-J., Wiebe, K., Witzke, P., 2018. Risk of increased food insecurity under stringent global climate change mitigation policy. Nat. Clim. Change 8, 699–703. https://doi.org/10.1038/s41558-018-0230-x.

Heredia-Guerrero, J.A., BenÃtez, J.J., DomÃnguez, E., Bayer, I.S., Cingolani, R., Athanassiou, A., Heredia, A., 2014. Infrared and Raman spectroscopic features of plant cuticles: a review. Front. Plant Sci. 5 https://doi.org/10.3389/fpls.2014.00305.

Hu, P., An, J., Faulkner, M.M., Wu, H., Li, Z., Tian, X., Giraldo, J.P., 2020. Nanoparticle charge and size control foliar delivery efficiency to plant cells and organelles. ACS Nano 14, 7970–7986. https://doi.org/10.1021/acsnano.9b09178.

Huang, G., Zuverza-Mena, N., White, J.C., Hu, H., Xing, B., Dhankher, O.P., 2022. Simultaneous exposure of wheat (Triticum aestivum L.) to CuO and S nanoparticles alleviates toxicity by reducing Cu accumulation and modulating antioxidant response. Sci. Total Environ. 839, 156285 https://doi.org/10.1016/j.scitotenv.2022.156285.

Ippolito, A., El Ghaouth, A., Wilson, C.L., Wisniewski, M., 2000. Control of postharvest decay of apple fruit by Aureobasidium pullulans and induction of defense responses. Postharvest Biol. Technol. 19, 265–272. https://doi.org/10.1016/S0925-5214(00)00104-6.

Iqbal, M.N., Rasheed, R., Ashraf, M.Y., Ashraf, M.A., Hussain, I., 2018. Exogenously applied zinc and copper mitigate salinity effect in maize (Zea mays L.) by improving key physiological and biochemical attributes. Environ. Sci. Pollut. Res. 25, 23883–23896. https://doi.org/10.1007/s11356-018-2383-6.

Jośko, I., Kusiak, M., Oleszczuk, P., Świeca, M., Kończak, M., Sikora, M., 2021. Transcriptional and biochemical response of barley to co-exposure of metal-based nanoparticles. Sci. Total Environ. 782, 146883 https://doi.org/10.1016/j.scitotenv.2021.146883.

Jośko, I., Oleszczuk, P., Skwarek, E., 2017. Toxicity of combined mixtures of nanoparticles to plants. J. Hazard Mater. 331, 200–209. https://doi.org/10.1016/j.jhazmat.2017.02.028.

Kah, M., Navarro, D., Kookana, R.S., Kirby, J.K., Santra, S., Ozcan, A., Kabiri, S., 2019. Impact of (nano)formulations on the distribution and wash-off of copper pesticides and fertilisers applied on citrus leaves. Environ. Chem. 16, 401. https://doi.org/10.1071/EN18279.

Kohatsu, M.Y., Lange, C.N., Pelegrino, M.T., Pieretti, J.C., Tortella, G., Rubilar, O., Batista, B.L., Seabra, A.B., Jesus, T.A. de, 2021. Foliar spraying of biogenic CuO nanoparticles protects the defence system and photosynthetic pigments of lettuce (Lactuca sativa). J. Clean. Prod. 324, 129264 https://doi.org/10.1016/j.jclepro.2021.129264.

Kováčik, J., Bačkor, M., 2007. Phenylalanine ammonia-lyase and phenolic compounds in chamomile tolerance to cadmium and copper excess. Water Air Soil Pollut. 185, 185–193. https://doi.org/10.1007/s11270-007-9441-x.

Kusiak, M., Oleszczuk, P., Jośko, I., 2022. Cross-examination of engineered nanomaterials in crop production: application and related implications. J. Hazard Mater. 424, 127374 https://doi.org/10.1016/j.jhazmat.2021.127374.

Lafmejani, Z.N., Jafari, A.A., Moradi, P., Moghadam, A.L., 2018. Impact of foliar application of copper sulphate and copper nanoparticles on some morpho-physiological traits and essential oil composition of peppermint (*Mentha piperita* L.). Herba Pol. 64, 13–24. https://doi.org/10.2478/hepo-2018-0006.

Lee, W.-M., An, Y.-J., Yoon, H., Kweon, H.-S., 2008. Toxicity and bioavailability of copper nanoparticles to the terrestrial plants mung bean (Phaseolus radiatus) and wheat (Triticum aestivum): plant agar test for water-insoluble nanoparticles. Environ. Toxicol. Chem. 27, 1915–1921.

Long, S.P., Zhu, X.-G., Naidu, S.L., Ort, D.R., 2006. Can improvement in photosynthesis increase crop yields? Plant Cell Environ. 29, 315–330. https://doi.org/10.1111/j.1365-3040.2005.01493.x.

Martins, L.L., Mourato, M.P., 2006. Effect of excess copper on tomato plants: growth parameters, enzyme activities, chlorophyll, and mineral content. J. Plant Nutr. 29, 2179–2198. https://doi.org/10.1080/01904160600972845.

Mosa, K.A., El-Naggar, M., Ramamoorthy, K., Alawadhi, H., Elnaggar, A., Wartanian, S., Ibrahim, E., Hani, H., 2018. Copper nanoparticles induced genotoxicty, oxidative stress, and changes in superoxide dismutase (SOD) gene expression in cucumber (cucumis sativus) plants. Front. Plant Sci. 9 https://doi.org/10.3389/fpls.2018.00872.

Mostofa, M.G., Hossain, M.A., Fujita, M., Tran, L.-S.P., 2015. Physiological and biochemical mechanisms associated with trehalose-induced copper-stress tolerance in rice. Sci. Rep. 5, 11433 https://doi.org/10.1038/srep11433.

Mostofa, M.G., Seraj, Z.I., Fujita, M., 2014. Exogenous sodium nitroprusside and glutathione alleviate copper toxicity by reducing copper uptake and oxidative damage in rice (Oryza sativa L.) seedlings. Protoplasma 251, 1373–1386. https://doi.org/10.1007/s00709-014-0639-7.

Mourato, M.P., Martins, L.L., Campos-Andrada, M.P., 2009. Physiological responses of Lupinus luteus to different copper concentrations. Biologia plant 53, 105–111. https://doi.org/10.1007/s10535-009-0014-2.

Nayek, S., Choudhury, I., Nishika, J.Haque., Roy, S., 2014. Spectrophotometric analysis of chlorophylls and carotenoids from commonly grown fern species by using various extracting solvents. Res. J. Chem. Sci. 4, 2231–2606. https://doi.org/10.1055/s-0033-1340072.

Pagano, L., Servin, A.D., De La Torre-Roche, R., Mukherjee, A., Majumdar, S., Hawthorne, J., Marmiroli, M., Maestri, E., Marra, R.E., Isch, S.M., Dhankher, O.P., White, J.C., Marmiroli, N., 2016. Molecular response of crop plants to engineered nanomaterials. Environ. Sci. Technol. 50, 7198–7207. https://doi.org/10.1021/acs.est.6b01816.

Printz, B., Lutts, S., Hausman, J.-F., Sergeant, K., 2016. Copper trafficking in plants and its implication on cell wall dynamics. Front. Plant Sci. 7 https://doi.org/10.3389/fpls.2016.00601.

Puig, S., Peñarrubia, L., 2009. Placing metal micronutrients in context: transport and distribution in plants. Current Opinion in Plant Biology, Physiology and Metabolism 12, 299–306. https://doi.org/10.1016/j.pbi.2009.04.008.

Rahman, N., Schoenau, J., 2020. Response of wheat, pea, and canola to micronutrient fertilization on five contrasting prairie soils. Sci. Rep. 10, 18818 https://doi.org/10.1038/s41598-020-75911-y.

Ravet, K., Pilon, M., 2013. Copper and iron homeostasis in plants: the challenges of oxidative stress. Antioxidants Redox Signal. 19, 919–932. https://doi.org/10.1089/ars.2012.5084.

Re, R., Pellegrini, N., Proteggente, A., Pannala, A., Yang, M., Rice-Evans, C., 1999. Antioxidant activity applying an improved ABTS radical cation decolorization assay. Free Radic. Biol. Med. 26, 1231–1237. https://doi.org/10.1016/S0891-5849(98)00315-3.

Rizwan, M., Ali, S., Qayyum, M.F., Ok, Y.S., Adrees, M., Ibrahim, M., Zia-ur-Rehman, M., Farid, M., Abbas, F., 2017. Effect of metal and metal oxide nanoparticles on growth and physiology of globally important food crops: a critical review. Journal of Hazardous Materials, SI:Environmental Nanotechnol 322, 2–16. https://doi.org/10.1016/j.jhazmat.2016.05.061.

Santos-Espinoza, A.M., González-Mendoza, D., Ruiz-Valdiviezo, V.M., Luján-Hidalgo, M. C., Jonapa-Hernández, F., Valdez-Salas, B., Gutiérrez-Miceli, F.A., 2020. Changes in the physiological and biochemical state of peanut plants (*Arachis hypogaea* L.) induced by exposure to green metallic nanoparticles. Int. J. Phytoremediation 1–8. https://doi.org/10.1080/15226514.2020.1856037.

Shaw, A.K., Ghosh, S., Kalaji, H.M., Bosa, K., Brestic, M., Zivcak, M., Hossain, Z., 2014. Nano-CuO stress induced modulation of antioxidative defense and photosynthetic performance of Syrian barley (Hordeum vulgare L.). Environ. Exp. Bot. 102, 37–47. https://doi.org/10.1016/j.envexpbot.2014.02.016.

Shaw, A.K., Hossain, Z., 2013. Impact of nano-CuO stress on rice (Oryza sativa L.) seedlings. Chemosphere 93, 906–915. https://doi.org/10.1016/j.chemosphere.2013.05.044.

Sikora, M., Świeca, M., 2018. Effect of ascorbic acid postharvest treatment on enzymatic browning, phenolics and antioxidant capacity of stored mung bean sprouts. Food Chem. 239, 1160–1166. https://doi.org/10.1016/j.foodchem.2017.07.067.

Sikora, M., Złotek, U., Kordowska-Wiater, M., Świeca, M., 2020. Effect of basil leaves and wheat bran water extracts on antioxidant capacity, sensory properties and microbiological quality of shredded iceberg lettuce during storage. Antioxidants 9, E355. https://doi.org/10.3390/antiox9040355.

Singleton, V.L., Orthofer, R., Lamuela-Raventós, R.M., 1999. Analysis of total phenols and other oxidation substrates and antioxidants by means of folin-ciocalteu reagent. In: Methods in Enzymology. Elsevier, pp. 152–178. https://doi.org/10.1016/S0076-6879(99)99017-1.

Tan, W., Gao, Q., Deng, C., Wang, Y., Lee, W.-Y., Hernandez-Viezcas, J.A., Peralta-Videa, J.R., Gardea-Torresdey, J.L., 2018. Foliar exposure of Cu(OH)2 nanopesticide to basil (Ocimum basilicum): variety-dependent copper translocation and biochemical responses. J. Agric. Food Chem. 66, 3358–3366. https://doi.org/10.1021/acs.jafc.8b00339.

Tang, Y., He, R., Zhao, J., Nie, G., Xu, L., Xing, B., 2016. Oxidative stress-induced toxicity of CuO nanoparticles and related toxicogenomic responses in Arabidopsis thaliana. Environ. Pollut. 212, 605–614. https://doi.org/10.1016/j.envpol.2016.03.019.

Tewari, R.K., Kumar, P., Sharma, P.N., 2006. Antioxidant responses to enhanced generation of superoxide anion radical and hydrogen peroxide in the copper-stressed mulberry plants. Planta 223, 1145–1153. https://doi.org/10.1007/s00425-005-0160-5.

van Maarschalkerweerd, M., Bro, R., Egebo, M., Husted, S., 2013. Diagnosing latent copper deficiency in intact barley leaves (Hordeum vulgare, L.) using near infrared spectroscopy. J. Agric. Food Chem. 61, 10901–10910. https://doi.org/10.1021/jf402166g.

Wang, P., Lombi, E., Zhao, F.-J., Kopittke, P.M., 2016. Nanotechnology: a new opportunity in plant sciences. Trends Plant Sci. 21, 699–712. https://doi.org/10.1016/j.tplants.2016.04.005.

Waraich, E.A., Ahmad, R., Ashraf, M., 2011. Role of mineral nutrition in alleviation of drought stress in plants. Aust. J. Crop. Sci. 5, 764–777.

Wazir, S.M., Ghobrial, I., 2017. Copper deficiency, a new triad: anemia, leucopenia, and myeloneuropathy. J. Community Hosp. Intern. Med. Perspect. 7, 265–268. https://doi.org/10.1080/20009666.2017.1351289.

Wessely-Szponder, J., Bełkot, Z., Bobowiec, R., Kosior-Korzecka, U., Wójcik, M., 2015. Transport induced inflammatory responses in horses. Pol. J. Vet. Sci. 18, 407–413. https://doi.org/10.1515/pjvs-2015-0052.

Xiong, T., Dumat, C., Dappe, V., Vezin, H., Schreck, E., Shahid, M., Pierart, A., Sobanska, S., 2017. Copper oxide nanoparticle foliar uptake, phytotoxicity, and consequences for sustainable urban agriculture. Environ. Sci. Technol. 51, 5242–5251. https://doi.org/10.1021/acs.est.6b05546.

Zhang, Y., Yan, J., Avellan, A., Gao, X., Matyjaszewski, K., Tilton, R.D., Lowry, G.V., 2020. Temperature- and pH-responsive star polymers as nanocarriers with potential for in vivo agrochemical delivery. ACS Nano 14, 10954–10965. https://doi.org/10.1021/acsnano.0c03140.

Zhang, Z., Ke, M., Qu, Q., Peijnenburg, W.J.G.M., Lu, T., Zhang, Q., Ye, Y., Xu, P., Du, B., Sun, L., Qian, H., 2018. Impact of copper nanoparticles and ionic copper exposure on wheat (Triticum aestivum L.) root morphology and antioxidant response. Environ. Pollut. 239, 689–697. https://doi.org/10.1016/j.envpol.2018.04.066.

Zhao, L., Hu, Q., Huang, Y., Fulton, A.N., Hannah-Bick, C., Adeleye, A.S., Keller, A.A., 2017. Activation of antioxidant and detoxification gene expression in cucumber plants exposed to a Cu(OH)(2). nanopesticide 4, 1750–1760. https://doi.org/10.1039/c7en00358g.

Zhao, Lijuan, Hu, Q., Huang, Y., Keller, A.A., 2017. Response at genetic, metabolic, and physiological levels of maize (Zea mays) exposed to a Cu(OH)2 nanopesticide. ACS Sustainable Chem. Eng. 5, 8294–8301. https://doi.org/10.1021/acssuschemeng.7b01968.

De Filippins, L. F., Hampp, R., Ziegler, H., 1981. The effects of sublethal concentrations of zinc, cadmium and mercury on *Euglena*. Growth and pigments. Zeitschrift für Pflanzenphysiologie 101, 37-47. doi.org/10.1016/S0044-328X(81)80059-1.

Supplementary material

UNVEILING OF INTERACTIONS BETWEEN FOLIAR-APPLIED CU NANOPARTICLES AND BARLEY SUFFERING FROM CU DEFICIENCY

Magdalena Kusiak[1], Małgorzata Sierocka[2], Michał Świeca[2], Sylwia Pasieczna-Patkowska[3], Mohamed Sheteiwy[4], Izabela Jośko[1]*

[1] Institute of Plant Genetics, Breeding and Biotechnology, Faculty of Agrobioengineering, University of Life Sciences, Lublin, Poland

[2] Department of Biochemistry and Food Chemistry, Faculty of Food Science and Biotechnology, University of Life Sciences, Lublin, Poland

[3] Department of Chemical Technology, Faculty of Chemistry, Maria Curie–Skłodowska University, Lublin, Poland

[4] Department of Agronomy, Faculty of Agriculture, Mansoura University, Mansoura, Egypt

* Correspondence to: Izabela Jośko, Institute of Plant Genetics, Breeding and Biotechnology, Faculty of Agrobioengineering, Univerisity of Life Sciences in Lublin, 20–950 Lublin, 13 Akademicka Street, Poland, tel. +48 81 4456675, fax. +48 81 4456031, e–mail: izabela.josko@up.lublin.pl

Number of pages: 7
Number of tables: 6
Number of figures: 4

METHOLOGY

Plant growth and foliar application conditions of Cu solutions

Tab. S1. The average spray volume deposited on above ground parts of *H. vulgare* plants according to the volume of Cu compounds (100 and 1000 mg L^{1}) applied.

Deposited volume [%]				
Control	Nano-Cu		$CuSO_4$	
	100	1000	100	1000
		1 day		
28.10±4.1	29.53±3.0	31.73±4.9	25.10±3.4	30.83±7.0
		7 days		
32.60±4.2	28.60±4.6	22.83±4.7	27.37±7.5	28.37±4.3

RESULTS

Tab. S2. Concentration of dissolved Cu^{2+} in nano-Cu solutions before and after foliar application.

Treatments of nano-Cu [mg L^{-1}]	Cu^{2+} concentration [mg L^{-1}]	
	Before application	After application
100	0.29 ±0.05	0.21 ± 0.00
1000	0.65 ±0.07	0.56 ± 0.02

Tab. S3. Cu content in roots of *H. vulgare* after foliar application with Cu compounds (100 and 1000 mg L^{1}). Different letters indicate significant differences among the treatments (Tukey's test, $p < 0.05$).

Plant tissue	Cu content [mg kg^{-1} d.w.]				
	Control	Nano-Cu		$CuSO_4$	
		100	1000	100	1000
			1 day		
Roots	1.55±0.12[a]	2.1±0.15[a]	1.01±0.16[a]	2.09±0.23[a]	1.96±0.2[a]
			7 days		
	1.05±0.11[a]	0.98±0.08[a]	1.21± 0.09[a]	0.94±0.07[a]	2.03±0.18[a]

Tab. S4. Impact of nano-Cu and $CuSO_4$ (at 100 and 1000 mg L^{-1}) on protein content and dry weight of roots and above ground parts (shoots and leaves) of *H. vulgare* treated with nano-Cu or $CuSO_4$. Means followed by a different letters indicate significant differences among the treatments (Turkey test $p < 0.05$).

Treatments	Concentration [mg L^{-1}]	Dry weight [mg]	
		Roots	Shoots and leaves
control	-	26.10±1.1[a]	98.72±2.2[a]
nano-Cu	100	28.42±1.3[a]	105.81±1.5[b]
	1000	25.73±1.7 [a]	106.34±3.1[b]
$CuSO_4$	100	29.50±1.3[a]	107.10±1.1[b]
	1000	26.50±1.5[a]	120.61±11.0[c]
control	-	45.21±0.9[a]	102.73±1.4[a]
nano-Cu	100	54.00±1.8[b]	126.09±0.9[b]
	1000	66.10±1.0[c]	190.24±0.8[c]
$CuSO_4$	100	99.50±0.8[e]	192.65±1.5[c]
	1000	81.70±1.6[d]	220.24±1.4[d]

Tab. S5. Impact of different concentrations of nano-Cu and $CuSO_4$ on pigment content of the *H. vulgare* after 1 and 7 days of exposure. Different letters indicate significant differences among the treatments (Tukey's test, $p < 0.05$).

Treatments	Concentration [mg L^{-1}]	Chlorophyll a [ug g^{-1} fw]	Chlorophyll b [ug g^{-1} fw]	Carotenoids [ug g^{-1} fw]
			1 day	
Control	-	14.81±1.33[a]	5.57±0.63[a]	1.67±0.21[a]
nano-Cu	100	13.99±1.96[a]	3.21±4.20[a]	2.26±1.01[a]
	1000	10.88±0.20[a]	4.33±0.15[a]	1.41±0.11[a]
$CuSO_4$	100	11.69±5.45[a]	4.87±2.04[a]	1.17±0.02[a]
	1000	13.74±7.23[a]	5.88±2.88[a]	1.49±0.77[a]
			7 days	
Control	-	13.49±2.85[b]	5.63±0.75[a]	1.63±0.16[a]
nano-Cu	100	14.45±0.37[b]	4.39±0.21[a]	0.94±0.39[a]
	1000	12.32±0.26[b]	5.53±0.02[a]	1.66±0.07[a]
$CuSO_4$	100	11.58±1.51[ab]	3.71±2.09[a]	1.88±1.70[a]
	1000	10.16±5.89[a]	3.64±2.22[a]	1.21±0.23[a]

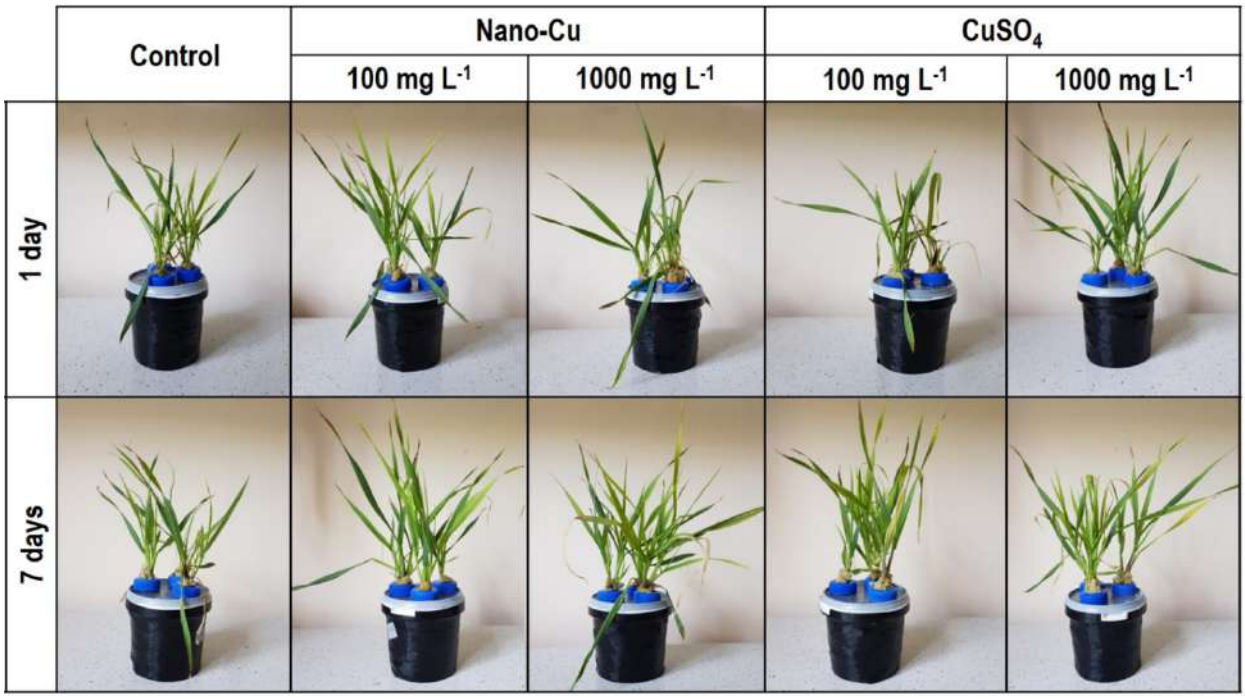

Fig. S1. Photographs of *H. vulgare* taken at 1st and 7th day of exposure to two concentration nano-Cu or $CuSO_4$ at 100 and 1000 mg L^{-1}.

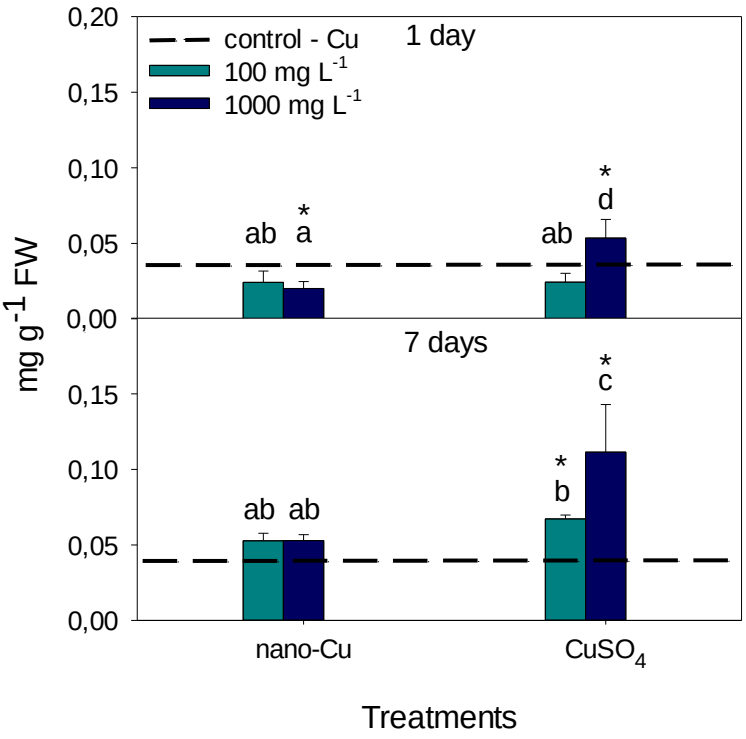

Fig. S2. Malondialdehyde (MDA) content in plants exposed to nano-Cu and $CuSO_4$ at 100 and 1000 mg L^{-1} for 1 and 7 days. Error bars represent standard error (SE, n=3 tests). The asterisks indicate significant difference between untreated and treated samples (Duncan's test, $p < 0.05$). Different letters indicate significant differences among the treatments (Duncan' test, $p < 0.05$).

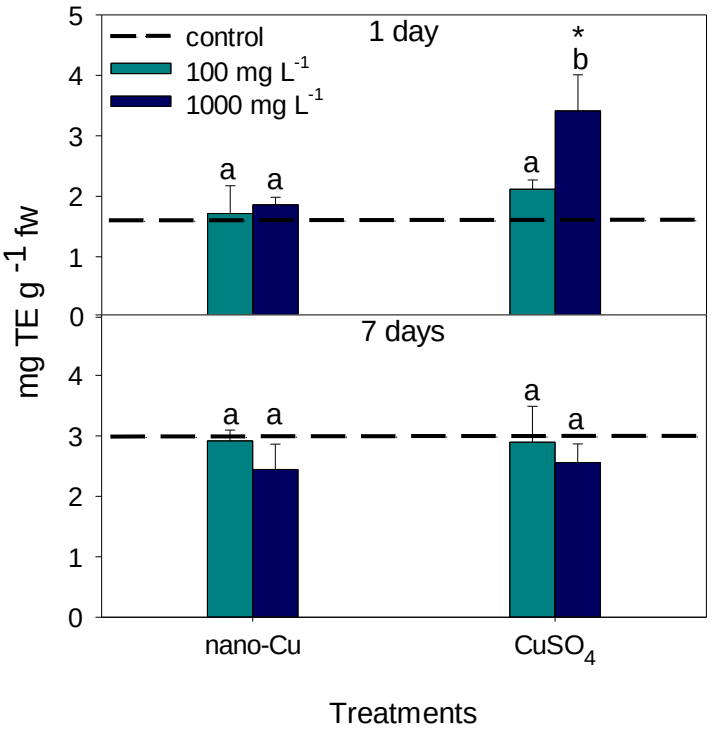

Fig. S3. Radical Scavenging Activity (ABTS) in *H. vulgare* after 1 and 7 days of exposure to nano-Cu and $CuSO_4$ (at 100 and 1000 mg L^{-1}) (Duncan's test, $p < 0.05$). Error bars represent standard error (SE, n=3 tests). The asterisks indicate significant difference between untreated and treated samples (Duncan's test, $p < 0.05$). Different letters indicate significant differences among the treatments (Duncan' test, $p < 0.05$).

Tab S6. Level of total glutathione (C) and the ratio of GSH/GSSH (D) indicate the role of used Cu compounds on the oxidative stress. Error bars represent standard error (SE, n=3 tests).). Different letters indicate significant differences among the treatments (Duncan' test, $p < 0.05$).

	Control	Nano-Cu		$CuSO_4$	
		100	1000	100	1000
			1 day		
GSH/GSSG ratio	7.93 ± 0.9^{c}	14.15 ± 2.9^{d}	1.70 ± 0.6^{a}	1.10 ± 0.3^{a}	3.75 ± 0.8^{b}
			7 days		
	3.08 ± 0.9^{a}	2.88 ± 0.1^{a}	2.62 ± 0.2^{a}	6.35 ± 0.7^{b}	4.95 ± 3.1^{b}

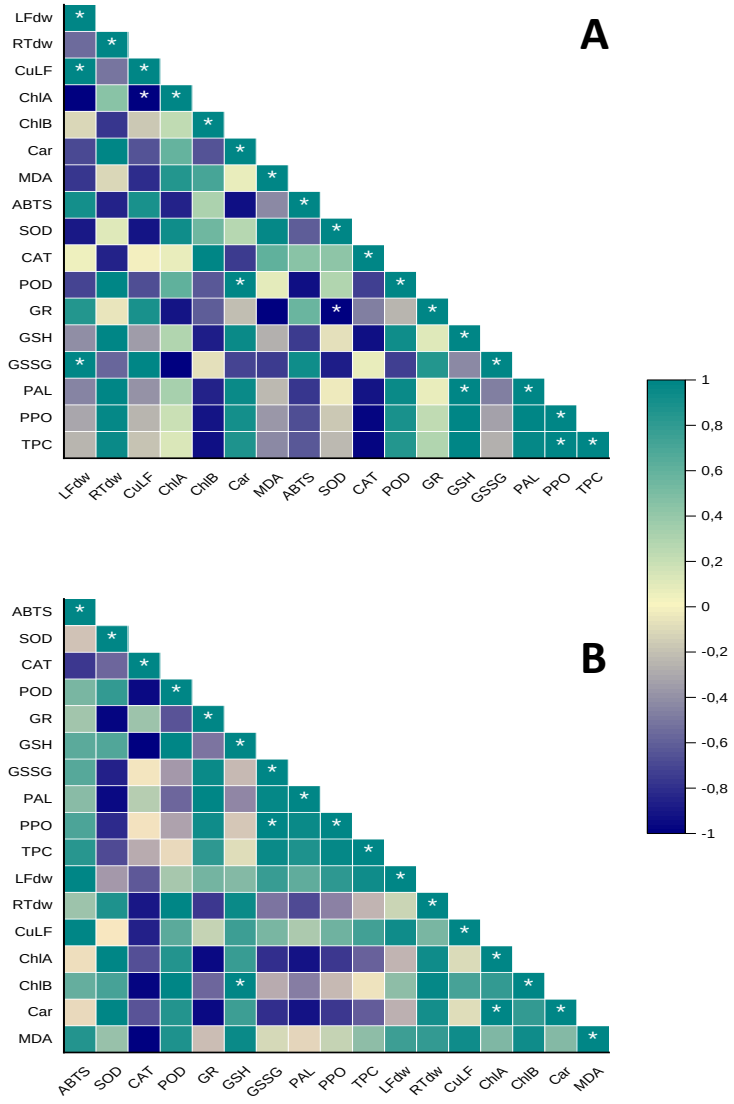

Fig. S4. The correlation plot performed for biochemical parameters of barley leaves exposed to nano-Cu (A) and $CuSO_4$ (B) after 1 day of exposure. The asterisks indicate significant correlation ($p < 0.05$). CuLF – the Cu content in above-ground parts; LFdw – the dry weight of above-ground plant parts; RTdw – the dry weight of roots; ChlA – the content of chlorophyll a; ChlB – the content of chlorophyll b; Car – the content of carotenoids.

Lublin, 30.08.2023

Magdalena Kusiak
Instytut Genetyki, Hodowli i
Biotechnologii Roślin
Uniwersytet Przyrodniczy w Lublinie
Ul. Akademicka 15,
20-950 Lublin
Tel: 508 789 096
magdalena.kusiak@up.lublin.pl

Rada Dyscypliny Rolnictwo i Ogrodnictwo
Uniwersytetu Przyrodniczego
w Lublinie

Oświadczenie o współautorstwie

Oświadczam, że mój udział w pracy "*Unveiling of interactions between foliar-applied Cu nanoparticles and barley suffering from Cu deficiency*" [Environmental Pollution, 2023] wynosi 60%.

Mój wkład polegał na opracowaniu koncepcji badań i metodyki, planowaniu i wykonaniu analiz laboratoryjnych wraz z opracowaniem wyników i ich interpretacją oraz na przygotowaniu manuskryptu i odpowiedzi na recenzje pracy.

Magdalena Kusiak

Podpis

Lublin, 26.06.2023

Dr inż. Małgorzata Sierocka
Katedra Biochemii i Chemii Żywności
Uniwersytet Przyrodniczy w Lublinie
ul. Skromna 8
20-704 Lublin
Tel. 814623328
malgorzata.sierocka@up.lublin.pl

Rada Dyscypliny Rolnictwo i
Ogrodnictwo
Uniwersytetu Przyrodniczego
w Lublinie

Oświadczenie o współautorstwie

Oświadczam, że mój udział w pracy "*Unveiling of interactions between foliar-applied Cu nanoparticles and barley suffering from Cu deficiency*" [Environmental Pollution, 2023] wynosi 5%.

Mój wkład polegał na udziale w opracowaniu metodyki badań oraz na udziale w wykonaniu analiz laboratoryjnych.

Małgorzata Sierocka

Podpis

Lublin, 26.06.2023

Prof. dr hab. Michał Świeca
Katedra Biochemii i Chemii Żywności
Uniwersytet Przyrodniczy w Lublinie
ul. Skromna 8
20-704 Lublin
Tel. 814623327
michal.swieca@up.lublin.pl

Rada Dyscypliny Rolnictwo i Ogrodnictwo
Uniwersytetu Przyrodniczego
w Lublinie

Oświadczenie o współautorstwie

Oświadczam, że mój udział w pracy "*Unveiling of interactions between foliar-applied Cu nanoparticles and barley suffering from Cu deficiency*" [Environmental Pollution, 2023] wynosi 5%.

Mój wkład polegał na udziale w opracowaniu metodyki badań oraz na udziale w wykonaniu analiz laboratoryjnych.

Signed by / Podpisano przez:
Michał Świeca
Uniwersytet Przyrodniczy w Lublinie
Date / Data: 2023-05-30 11:31

.....

Podpis

Lublin, 29.06.2023

Dr hab. Sylwia Pasieczna-Patkowska
Katedra Technologii Chemicznej
Uniwersytet Marii Curie-Skłodowskiej
pl. Marii Curie-Skłodowskiej 3/425
20-031 Lublin
Tel. 81 537 55 72
sylwia.pasieczna-patkowska@mail.umcs.pl

Rada Dyscypliny Rolnictwo i Ogrodnictwo
Uniwersytetu Przyrodniczego
w Lublinie

Oświadczenie o współautorstwie

Oświadczam, że mój udział w pracy "*Unveiling of interactions between foliar-applied Cu nanoparticles and barley suffering from Cu deficiency*" [Environmental Pollution, 2023] wynosi 10%.

Mój wkład polegał na wykonaniu analiz laboratoryjnych.

Sylwia Pasieczna-Patkowska

Podpis

Mansoura, 20.07.2023

Mohamed Sheteiwy Ph.D
Department of Agronomy,
Mansoura University,
60 Elgomhoria Street,
35516 Mansoura, Egyp
salahco_2010@mans.edu.eg

Discipline Council for Agriculture and Horticulture
of University of Life Sciences
in Lublin

Statement of co-authorship

I declare that my contribution to the article "*Unveiling of interactions between foliar-applied Cu nanoparticles and barley suffering from Cu deficiency*" [Environmental Pollution, 2023] is 5%.

My contribution consisted of participation in the writing (review and editing) of the manuscript.

Mohamed Sheteiwy

Signature

Lublin, 03.07.2023

Dr hab. Izabela Jośko, prof. uczelni
Instytut Genetyki, Hodowli
i Biotechnologii Roślin
Uniwersytet Przyrodniczy w Lublinie
Ul. Akademicka 15,
20-950 Lublin
Tel. 814456675
izabela.josko@up.lublin.pl

Rada Dyscypliny Rolnictwo i Ogrodnictwo
Uniwersytetu Przyrodniczego
w Lublinie

Oświadczenie o współautorstwie

Oświadczam, że mój udział w pracy "*Unveiling of interactions between foliar-applied Cu nanoparticles and barley suffering from Cu deficiency*" [Environmental Pollution, 2023] wynosi **15%**.

Mój wkład polegał na kierowaniu projektem naukowym obejmującym badania opisane w tej pracy oraz pozyskaniu funduszy na badania. Ponadto, odpowiadałam za opracowanie koncepcji badań i metodyki oraz za przygotowanie manuskryptu do publikacji i odpowiedzi na otrzymane recenzje pracy.

Izabela Jośko

Podpis

PIII

Kusiak M., Sozoniuk M., Larue C., Grillo R., Kowalczyk K., Oleszczuk P., Jośko I.

Transcriptional response of Cu-deficient barley (*Hordeum vulgare* L.) to foliar-applied nano-Cu: Molecular crosstalk between Cu loading into plants and changes in Cu homeostasis genes

NanoImpact (2023) T. 31 s. 100472,

DOI: 10.1016/j.impact.2023.100472

$IF_{(2023)} = 4.9$

Punkty MEiN = 100

NanoImpact 31 (2023) 100472

Contents lists available at ScienceDirect

NanoImpact

journal homepage: www.elsevier.com/locate/nanoimpact

Transcriptional response of Cu-deficient barley (*Hordeum vulgare* L.) to foliar-applied nano-Cu: Molecular crosstalk between Cu loading into plants and changes in Cu homeostasis genes

Magdalena Kusiak [a], Magdalena Sozoniuk [a], Camille Larue [b], Renato Grillo [c], Krzysztof Kowalczyk [a], Patryk Oleszczuk [d], Izabela Jośko [a,*]

[a] Institute of Plant Genetics, Breeding and Biotechnology, Faculty of Agrobioengineering, University of Life Sciences, Lublin, Poland
[b] Laboratoire Ecologie Fonctionnelle et Environnement, Université de Toulouse, CNRS, Toulouse 31062, France
[c] Department of Physics and Chemistry, School of Engineering, São Paulo State University (UNESP), Ilha Solteira, SP 15385-000, Brazil
[d] Department of Radiochemistry and Environmental Chemistry, Faculty of Chemistry, Maria Curie-Skłodowska University, 20-031 Lublin, Poland

ARTICLE INFO

Editor: Philip Demokritou

Keywords:
Engineered nanoparticles
Gene expression
Metal transporters
Aquaporins
Antioxidants

ABSTRACT

For safe and effective nutrient management, the cutting-edge approaches to plant fertilization are continuously developed. The aim of the study was to analyze the transcriptional response of barley suffering from Cu deficiency to foliar application of nanoparticulate Cu (nano-Cu) and its ionic form ($CuSO_4$) at 100 and 1000 mg L^{-1} for the examination of their supplementing effect. The initial interactions of Cu-compounds with barley leaves were analyzed with spectroscopic (ICP-OES) and microscopic (SEM-EDS) methods. To determine Cu cellular status, the impact of Cu-compounds on the expression of genes involved in regulating Cu homeostasis (*PAA1*, *PAA2*, *RAN1*, *COPT5*), aquaporins (*NIP2.1*, *PIP1.1*, *TIP1.1*, *TIP1.2*) and antioxidant defense response (*SOD Cu—Zn*, *SOD Fe*, *SOD Mn*, *CAT*) after 1 and 7 days of exposure was analyzed. Although Cu accumulation in plant leaves was detected overtime, the Cu content in leaves exposed to nano-Cu for 7 days was 44.5% lower than in $CuSO_4$ at 100 mg L^{-1}. However, nano-Cu aggregates remaining on the leaf surface indicated a potential difference between measured Cu content and the real Cu pool present in the plant. Our study revealed significant changes in the pattern of gene expression overtime depending on Cu-compound type and dose. Despite the initial puzzling patterns of gene expression, after 7 days all Cu transporters showed significant down-regulation under Cu-compounds exposure to prevent Cu excess in plant cells. Conversely, aquaporin gene expression was induced after 7 days, especially by nano-Cu and $CuSO_4$ at 100 mg L^{-1} due to the stimulatory effect of low Cu doses. Our study revealed that the gradual release of Cu ions from nano-Cu at a lower rate provided a milder molecular response than $CuSO_4$. It might indicate that nano-Cu maintained better metal balance in plants than the conventional compounds, thus may be considered as a long-term supplier of Cu.

1. Introduction

Cu is a transition metal and a crucial microelement for plant health and is a cofactor in pivotal metabolic processes such as photosynthesis, mitochondrial respiration, hormone perception, etc. (Shahbaz et al., 2015). Thus, Cu starvation severely affects plants, particularly cereals, manifesting itself in stunted growth, chlorosis, increased susceptibility to diseases, etc. (Rahman and Schoenau, 2020). It is estimated that Cu deficiency occurs in 14% of agricultural soils, mainly in calcareous and organic soils due to the low mobility of Cu at high pH and strong binding of Cu by soil organic matter (Graham, 2008). To alleviate Cu scarcity, Cu fertilization via soil amendment or foliar application is widely used. Due to the low bioavailability of Cu in soil and its mobility in plants, a foliar spray is often appointed for the delivery of Cu to plants. However, the foliar treatment with conventional fertilizing agents such as CuO, $CuSO_4$, and Cu-EDTA is of low efficiency (Deng et al., 2022a). For instance, 50% of the applied nutrients do not reach their target, and high losses of active ingredients cause soil and groundwater pollution (Avellan et al., 2021a). Thus, several strategies are put into improving the effectiveness of agrochemicals, including chemical and

* Corresponding author at: Institute of Plant Genetics, Breeding and Biotechnology, Faculty of Agrobioengineering, Univerisity of Life Sciences in Lublin, 20–950 Lublin, 13 Akademicka Street, Poland.
E-mail address: izabela.josko@up.lublin.pl (I. Jośko).

https://doi.org/10.1016/j.impact.2023.100472
Received 27 February 2023; Received in revised form 15 June 2023; Accepted 27 June 2023
Available online 14 July 2023

biotechnological approaches (Kah et al., 2019b; Kusiak et al., 2022; Wang et al., 2016). Due to the public concern and environmental risk of genetically modified plants (European Commission, 2012), the more intense works focus on the development of the next generation of agrochemicals posing more efficient and sustainable traits (Kusiak et al., 2022). For instance, the implementation of nano-enabled formulations (Fraceto et al., 2016; Guo et al., 2018; Hofmann et al., 2020), or nanocarriers (Bonser et al., 2023a; Xu et al., 2022) including the cutting-edge stimuli-responsive nano-agrochemicals (Bonser et al., 2023a; Xu et al., 2022) are considered. The small size of the engineered nanoparticles (ENPs) can provide unique physico-chemical properties (reactivity, dissolution, aggregation) to the material, and thus increase the efficiency of the product in relation to their bulk counterparts (Tan et al., 2018). ENPs containing microelements such as Cu have a higher dissolution rates than microparticles or bulk materials (Xia et al., 2006). At the same time, the gradual release of Cu ions from ENPs provides a long-term source of microelements in relation to applied metal salts, which are already dissolved upon application (Wang et al., 2016).

To date, numerous studies have demonstrated both positive and negative effects of ENPs on the morphological, physiological, and biochemical traits of plants (Grillo et al., 2021a; Kah et al., 2019a; Kohatsu et al., 2021; Tan et al., 2018). On the other hand, plant responses to ENPs exposure at the molecular level remain relatively unexplored (Jośko et al., 2021a; Landa et al., 2017). Nonetheless, the molecular analysis could provide more in-depth and comprehensive information on plant responses to ENPs treatment (Zhao et al., 2017a). As the impact of nano-Cu on plants is complex, the observed results might be related simultaneously to copper-specific and nanoparticle-specific biological effects (Tan et al., 2018). A study by Valdes et al. (2020a) shown similar upregulating effect of particle size of CuO at 10 mg L^{-1} on *APX* gene expression, and no effect of $CuSO_4$. In turn, the analysis of *Arabidopsis thaliana* L. revealed the similar transcriptional pattern under exposure to nano-Cu and ionic Cu, the different from the activity of bulk CuO (Landa et al., 2017). Moreover, plant species or cultivars determine their response on the ENPs, and their bulk counterparts. For instance, nano-CuO upregulated auxins in grains of both cultivated and weedy rice, while bulk CuO and $CuSO_4$ mostly in cultivated rice (Deng et al., 2022b). Therefore, knowledge regarding the mechanism by which plants modulate the expression of genes involved in Cu translocation to maintain Cu balance can be used as the potential markers of the cellular status of Cu (Landa et al., 2017). Nowadays, much attention is shifting towards investigating changes in the expression of genes and proteins in response to Cu-based ENPs excess (Ren et al., 2022; Roy et al., 2022). However, there are no previous studies assessing the impact of nano-Cu on gene expression in plants grown in Cu deficient conditions. Yet, this might be crucial to determine the optimal dose of nano-fertilizers. Moreover, there is no research on the transcriptional response of plants under the treatment of Cu-based ENPs during the growth stages, when plants demonstrate high sensitivity to Cu starvation (Rahman and Schoenau, 2020). Therefore, we hypothesize that the analysis of transcript levels of genes involved in Cu homeostasis and detoxification in plants grown in Cu deficient conditions might be crucial in the evaluation of nano-Cu safety and efficiency as a fertilizer (del Pozo et al., 2010; Landa et al., 2017).

Due to the importance of Cu in crucial physiological processes and its high reactivity, which can lead to the generation of reactive oxygen species (ROS), all intracellular Cu is precisely controlled (Cota-Ruiz et al., 2020; Wang et al., 2020). Both Cu deprivation and excess induce a cascade of reactions in plants, e.g., the differential expression pattern of gene encoding proteins involved in Cu trafficking and counteracting the stress response (del Pozo et al., 2010; Merakli et al., 2021; Ravet and Pilon, 2013; Wintz et al., 2003). One of the strategies for maintaining Cu homeostasis is the regulation of the expression of genes involved in Cu trafficking via heavy metal transporters (*HMA*) and Cu transporters (*COPT*) in response to changes in the cellular amount of Cu (del Pozo et al., 2010; Printz et al., 2016; Wintz et al., 2003). The *HMA* family includes P-type ATPase: *PAA1* responsible for Cu transport to the stroma and *PAA2* to the lumen of the chloroplast (Blaby-Haas et al., 2014), as well as transporters localized in the endoplasmic reticulum (ER) membrane Responsive-to-Antagonist 1 (*RAN1*), which plays an essential role in Cu delivery and biogenesis of the ethylene receptor 1 (ETR1), crucial for plant growth and development (Binder, 2020). According to del Pozo et al. (2010), *A. thaliana* counteracts Cu excess by down-regulation of *HMA* family genes to hamper absorption of Cu, while Cu starvation increases expression levels of *PAA1*, *PAA2* and *RAN1* genes to induce the uptake and mobilization of Cu (del Pozo et al., 2010). At the same time, there is little to none information regarding changes in Cu transporters gene expression under metal-based ENPs exposure. Moreover, the existing studies were conducted only in Cu excess conditions (Jośko et al., 2021b; Landa et al., 2017; Roy et al., 2022). For an unbiased assessment of ENPs potential as fertilizers, more data on the regulation of Cu transporter genes in plants exposed to Cu-based ENPs under deficient conditions is needed, especially during growth stages with high Cu-demand. On another note, the translocation and accumulation of Cu in various organelles in plants could be controlled via dynamic osmoregulation facilitated by aquaporins (AQs) (Banerjee and Roychoudhury, 2020; Kapilan et al., 2018). The water channels controlled by AQs are involved in bilateral distribution of metal ions into/out of cells (Nodulin 26 like intrinsic proteins, NIPs) (Banerjee and Roychoudhury, 2020; Kapilan et al., 2018) and cellular organelles like chloroplasts (Plasma membrane intrinsic proteins, PIPs) and/or vacuoles (Tonoplast intrinsic proteins, TIPs) (Kholodova et al., 2011; Yue et al., 2017). Recently, some research suggested the involvement of AQs in ENPs translocation in plants (Bárzana et al., 2022; Rico et al., 2011). The existing studies on the expression of *AQs* in response to ENPs are restricted to plant roots exposure to carbon-based ENPs (Khodakovskaya et al., 2012), nano-La_2O_3 (Yue et al., 2017) or nano-Ag (Qian et al., 2013). To the best of our knowledge, the transcriptional response regarding *AQs* in crops under foliar exposure to Cu-based ENPs remains unknown. So far, the majority of studies addressing the changes in gene expression upon ENPs containing Cu are focused on oxidative stress-related genes (Cohu and Pilon, 2007; del Pozo et al., 2010; Roy et al., 2022; Valdes et al., 2020b; Zhao et al., 2017b; Zhao et al., 2017a). Plants counteract the negative effects of both deficiency and excess of Cu through activation of the defense system, including antioxidant enzymes such as superoxide dismutase (SOD) and catalase (CAT) (del Pozo et al., 2010; Zhao et al., 2017b). Thus far, both ionic Cu and Cu-based ENPs have shown the potential to induce defense responses in plants, regardless if applied thru foliar application (Zhao et al., 2017a) or soil irrigation (Jośko et al., 2021a). The study by Zhao et al. (2017a) demonstrated a similar pattern of transcriptomic changes in antioxidant genes of *Cucumis sativus* L. induced by both nano-$Cu(OH)_2$ and $CuSO_4$, which suggests that released Cu^{2+} contributed to the overall effect. Moreover, the modulation of *SOD Cu—Zn* and *SOD Fe* expression patterns has been proven to be a good indicators of plant response to both Cu starvation and Cu excess due to the Fe—Cu crosstalk (Cohu and Pilon, 2007; del Pozo et al., 2010).

To address the aforementioned knowledge gaps, the expression of genes involved in Cu homeostasis and detoxification in barley *Hordeum vulgare* L. treated with nano-Cu or $CuSO_4$ was analyzed. Due to its importance as a food source and ability to adapt to various global climates, *H. vulgare* is considered as the fourth most important cereal in the world (Doğaroğlu and Köleli, 2017). Barley has demonstrated high sensitivity to both Cu deficiency and excess, which results in losses in crop yields (Rahman and Schoenau, 2020). The adverse effects of Cu deficiency are particularly evident during tillering and anthesis stages, leading to a reduction of pollen grains and their lower nutritional values (van Maarschalkerweerd et al., 2013). Although nano-fertilizers demonstrated the potential for effective plant supplementation with microelements than common fertilizers (Wang et al., 2016), little is known regarding their transcriptional response of plants towards nano-Cu supply during periods of increased nutritional demand or severe

deficiency conditions (Deng et al., 2022b; Zhao et al., 2017b). Thus, the overriding objective of this study was to exam the pattern of gene expression of Cu transporters, aquaporins and enzymatic antioxidants under foliar treatment of Cu-compounds to determine actual Cu status in plants, which further may indicate the effectiveness of Cu supplementation. We hypothesize that nano-Cu will be subsequently supplemented plant with Cu compare to dissolved metal salts releasing full/excessive pool of Cu ions.

2. Materials and methods

2.1. Cu compounds and suspensions

Cu nanoparticles (nano-Cu) (purity ≥95.5%) and $CuSO_4$ (purity ≥95.5%) as powders were purchased from Sigma-Aldrich (USA). The preparation and characterization of nano-Cu and $CuSO_4$ solutions for the foliar application have been previously described (Kusiak et al., 2023). In brief, these Cu-solutions were prepared in Milli-Q® water (Ω < 0.05 μS cm^{-3}) containing 0.05% Tween 20 at a total Cu concentration of 100 and 1000 mg L^{-1}. The nano-Cu solutions were sonicated in an ultrasonic bath (25 °C, 250 W, 50 Hz) for 30 min before application.

2.2. Characteristics of nanopowder and nano-Cu suspension

Nano-Cu (a powder) was characterized by the primary particle size of 25 ± 10 nm using a transmission electron microscope (TEM) (JEM–3010 TEM JEOL, Ltd., Japan). The TEM image of nano-Cu was provided in previous work (Kusiak et al., 2023). The surface area of nano-Cu was 8 m^2 g^{-1} as determined by BET analysis. ENPs crystal structure, phase formation and oxidation state were analyzed with powder XRD diffractometer (Empyrean, PANalytical, the Netherlands). The details of XRD analysis were described in our previous article (Jośko et al., 2022). Based on the XRD pattern (Supplementary Materials, Fig. S1), the presence of copper (Cu – 62%) and cuprite (Cu_2O – 38%) was confirmed in nano-Cu powder. The absence of additional peaks attributed to typical possible impurities confirmed the purity of tested nano-powder. The crystallite size of nano-powder was estimated based on the diffraction peak broadening using the Scherrer equation. The average crystallite size of nano-Cu was 32.6 ± 3.7 nm.

The methods used for characteristics of ENPs suspensions (the distribution of aggregate sizes, zeta (ζ) potential and dissolution rate) were described in the Supplementary Materials. The properties of the nano-Cu suspension have been previously described (Kusiak et al., 2023). Briefly, the TEM image and particle size distribution revealed strong aggregation of nano-Cu in stock suspension (Supplementary Materials, Fig. S2). The average particle size of nano-Cu at 100 mg L^{-1} was at the level of 248.8 ± 6 nm, while10 times higher of concentration of ENPs did not allow to measure of the aggregation size. The ζ potential of nano-Cu at 100 and 1000 mg L^{-1} in aqueous solution was −14.6 and − 19.6 mV, respectively. The concentration of Cu^{2+} in 100 and 1000 mg L^{-1} ENPs solutions reached 0.3% (0.3 mg L^{-1}) and 0.065% (0.7 mg L^{-1}) of stock suspensions ready to use (Supplementary Materials, Fig. S3), respectively (Kusiak et al., 2023).

2.3. Plant growth and experimental design

Seeds of *H. vulgare* (cultivar Ella) were soaked for 2 h in Milli-Q® water. The seeds were then surface sterilized with 2% calcium hypochlorite for 15 min and a further 70% ethanol for 1 min. Next, the seeds were rinsed 3 times with Milli-Q® water and germinated in Petri dishes containing filter paper soaked in Milli-Q® water. Prepared Petri dishes were put into a growth chamber at 24 °C in the dark. Further, the 4-day seedlings were transferred into black containers that were filled with Hoagland's solution containing 1.0 mM KNO_3, 1.0 mM $Ca(NO_3)_2$, 0.457 mM $MgSO_4$, 0.1 mM KH_2PO_4, 1.0 μM $MnCl_2$, 3 μM H_3BO_3, 1 μM $(NH_4)_6Mo_7O_{24}$, 1 μM $ZnSO_4$, 0.0672 mM $NaSiO_3$, 60 μM Fe(III)-EDTA buffered with 0.02 MES (4-morpholineethanesulfonic acid, 2-(N-Morpholino) ethanesulfonic acid hydrate)-KOH. Cu was omitted from the nutrient solution to induce Cu deficiency, which usually occurs in the agricultural soil due to the strong immobilization by organic matter or high pH (Graham, 2008). The positive control containing Cu was not used in this experiment due to weak transfer of Cu from the roots to upper parts of plant, not providing an optimal Cu level for plant growth (Graham, 2008). The hydroponic solutions were refreshed every 7 days and continuously aerated. Plants were grown at a relative humidity of 60 ± 10%, a 16 h light/8 h dark cycle at 23 ± 3 °C (day time) and 18 ± 3 °C (night time) and with a light intensity at 450 μmol m^{-2} s^{-1} in a growth chamber (Conviron GEN1000). After 5 weeks of cultivation, when plants reached the advanced tillering stage (BBCH: 23), the foliar treatments with Cu compounds were performed. This time of Cu application is widely practiced under the field conditions, because a tillering stage is an intense growth period characterized by the increased demand for this micronutrient. It should be noted that due to the growth in prolonged adverse conditions (Cu starvation), Cu deficiency symptoms (white tip disease, chlorosis) were apparent on the leaves (Supplementary Materials, Fig. S4). The whole aboveground parts of plant with emerged flag leaf were sprayed with nano-Cu or $CuSO_4$ solutions with 0.05% Tween 20 at concentration of 100 and 1000 mg of Cu L^{-1} using a hand-held diffusive sprayer in three biological replicates. The total volume of solution used for foliar application was 3.3 mL per plant. The Cu-solution at 1000 mg L^{-1} was chosen following the guidelines for agricultural practice (Fageria et al., 2009). The lower concentration of Cu-compounds was selected in a preliminary experiment to assess the fertilizing potential of reduced Cu doses (Kusiak et al., 2023). Milli-Q® water with surfactant was used as a control treatment. To avoid nutrient solution contamination and the entry of solutions into roots, each pot lit was covered with foil. The final volume of solution applied to the plants was assessed by recording the weight of the foil from before and after spraying (Supplementary Materials, Table S1). Approximately 28.5 ± 3.0% of the spray volume was deposited on each plant on average, which demonstrates a comparable, reproducible application process. As we described in the previous work (Kusiak et al., 2023), the leaves sprayed only with the higher rate of $CuSO_4$ (after 7 days) had substantially greater chlorotic changes than control or other treatments (Supplementary Materials, Fig. S4).

2.4. Plant tissues analysis

After 1 and 7 days of exposure, barley plants were harvested and parts of flag leaves (around 500 mg) were immediately ground in liquid nitrogen for RNA isolation. For metal content and microscopic analysis, the flag leaves were Milli-Q® water-rinsed. The analyzes focused on the flag leaves for the following reasons: (i) as the youngest leaves, there are the most sensitive, (ii) to exam a short-term and in situ response, especially since our previous studies indicated the slow translocation of Cu (Jośko et al., 2021b; Kusiak et al., 2023), (iii) to obtain the highest quantify and quality of RNA for the real-time qPCR analysis. The water-rinsed flag leaves were next rinsed with 2.2 M HNO_3 for 30 s and then rinsed 3 times with Milli-Q® water to remove nano-Cu/$CuSO_4$ adhered to the leaf surface. Then leaves samples were air-dried, weighted and stored (in darkness at 20 °C) for Cu spectroscopic and microscopic analysis. The dry weight of flag leaves were provided in Supplementary Material (Supplementary Materials, Table S2). Only nano-Cu at 100 mg L^{-1} after 7 days increased the dry weight by almost 100% compared to control, while other treatments did not affected biomass.

2.4.1. ICP-OES analysis

Dry flag leaves were digested with a mixture of HNO_3:H_2O_2 (4:1) in Teflon vessels in a microwave oven (Milestone, ETHOS EASY, Italy) for 1 h at 200 °C. Cooled samples were filtered (0.45 μm, PTFE), diluted with Milli-Q® –water to 25 mL, and analyzed with ICP–OES (iCAP 7200, Thermo Scientific). All analyses included blanks. Certified material

(tomato leaves, NIST® SRM® 1573a) was used for the quality control of the sample digestion. Recovery of Cu was at the level of 94 ± 2%. Because the etching protocols were not fully effective in removing particles attached to plant leaves, the determined metal content in leaves may be overestimated.

2.4.2. SEM-EDS analysis

Scanning electron microscopy with energy dispersive spectrometry (SEM-EDS) (Quanta™ 3D FEG, FEI with EDAX SDD Apollo detector) was used to detect the occurrence of Cu from nano-Cu suspensions and $CuSO_4$ on flag leaves. The SEM–EDS measurements were made with the high vacuum with accelerating voltage mode. The EDS diagrams present spectra, which show characteristics X-rays of sample atoms induced by electron beam (30 keV). The SEM–EDS maps (with 100-fold magnification) were obtained for a part of leaves after 7 day of exposure.

2.4.3. Total RNA isolation and cDNA synthesis

For gene expression analysis, the total RNA was extracted from *H. vulgare* flag leaves (~50 mg) using the TRIzol™ reagent (Invitrogen, USA) in accordance to the manufacturer's instructions. Isolation of RNA was performed in 3 biological replicates. The RNA was quantified using NanoDrop 2000 spectrophotometer (Thermo Scientific). RNA quality and integrity were confirmed by 2% agarose gel electrophoresis stained with ethidium bromide. RNA was treated with RNase-free DNase I (Thermo Scientific) to remove genomic DNA. The reaction of reverse transcription was performed in 20 μL reactions containing 1 μg RNA with NG dART RT kit (EURx) following the manufacturer's instructions. Obtained cDNA (50 ng μL^{-1}) was used as template in the qPCR analysis.

2.4.4. Real-time qPCR analysis

The transcript levels of genes related to Cu transport in plants (*PAA1*, *PAA2*, *RAN1*, *COPT5*), aquaporins (*NIP2.2*, *PIP1.1*, *TIP1.1*, *TIP1.2*), and antioxidant enzymes (*SOD Cu—Zn*, *SOD Fe*, *SOD Mn*, *CAT*) were determined by the real-time PCR analysis. A total of 7 candidate genes: Actin (*ACT*), ADP-ribosylation factor 1 (*ADP*), Elongation factor 1-alpha (*EF1a*), Alpha-tubulin (*TUBa*), Glyceraldehyde 3-phosphate dehydrogenase (*GAPDH*), Ubiquitin (*UBI*), RNA binding protein (*RNA BP*) were evaluated as potential reference genes in this study using geNorm algorithm (Vandesompele et al., 2002). According to obtained results, *ACT*, *GAPDH* and *ADP* genes were used as internal controls to normalize the data. Gene-specific primers used in the experiment were taken from our previous studies or designed with OligoArchitect™ Online (Sigma-Aldrich) as indicated in Supplementary Materials (Table S3). The full-length cDNA sequences were obtained from the NCBI, The Barley Genome Explorer (BARLEX) and Ensembl Plants databases.

The real-time qPCR reactions were conducted using PowerUp™ SYBR™ Green Master Mix (Applied Biosystems) in accordance to the manufacturer's instructions. The reactions were carried out in a total volume of 20 μL. The real time-qPCR conditions were optimized by adjusting the template cDNA concentration, primer concentration and annealing temperature for each primer pair (Supplementary Materials, Table S4). Real time-PCR was carried out according to the following cycling program: 2 min at 50 °C and 95 °C for 2 min, followed by 40 cycles of: 15 s at 95 °C and 1 min at optimal temperature for each primer pair (Supplementary Materials, Table S4). To verify the specificity of amplification melting curve analysis was performed after each run with continuous data collection from 60 °C to 95 °C (Supplementary Materials, Fig. S5). Reactions were performed in three full biological and three technical replicates along with no template control (NTC). Standard curves were generated from five dilution points and were used to determine the amplification efficiency for each primer pair. All real time-qPCR reactions were performed on the QuantStudio™ 3 Real-Time PCR System (Applied Biosystems™). The results were analyzed using the dedicated relative quantification software module from ThermoFisher Cloud (ThermoFisher Scientific). Relative gene expression was calculated using the $2^{-\Delta\Delta Ct}$ method.

2.5. Statistics

All statistical analyses were performed using Statistica 13.1 software package. The differences between treatments were determined using a one-way and two-way analysis of variance (ANOVA) followed by Tukey's or Dunnett's post hoc test at a significance level of 0.05. Clustering heatmaps were performed with euclidean dissimilarity for distance measure and complete linkage method using Heatmapper (Babicki et al., 2016) to explore the responses of *H. vulgare* to applied Cu compounds. The correlation plot was performed based on Pearson coefficient at significance levels of 0.05, 0.01, 0.001.

3. Results and discussion

3.1. Cu acquisition in flag leaf

After 1 day of exposure (Fig. 1A), no significant differences were found in the concentration of Cu in leaves of *H. vulgare* treated with 100 mg L^{-1} of either nano-Cu or $CuSO_4$ when compared to the control group (52.8 mg kg^{-1} d.w.). Noticeably, leaves exposed to 1000 mg L^{-1} of nano-Cu and metal salt ($CuSO_4$) contained significantly more Cu (101.8 and 150.1 mg kg^{-1} d.w., respectively) than in the control plant ($p < 0.05$). After 7 days (Fig. 1B), the Cu content in leaves treated with both doses of Cu compounds was higher than in the control sample (79.4 mg kg^{-1} d.w.) ($p < 0.05$). While plants exposed to nano-Cu at 100 mg L^{-1} showed the lowest Cu concentration in flag leaf (106.3 mg kg^{-1} d.w.) among all Cu-treated groups, the highest Cu content was observed in plants treated with $CuSO_4$ at 100 mg L^{-1} (191.6 mg kg^{-1} d.w.). On the other hand, at the rate of 1000 mg L^{-1}, no significant difference in Cu content in flag leaves between ENPs and their corresponding salts was noted (135.0–143.1 mg kg^{-1} d.w.). Interestingly, the Cu content in the flag leaf of barley exposed to $CuSO_4$ at 1000 mg L^{-1} did not increase after 7 days compared to 1 day. SEM-EDS analysis (Fig. 2) showed the presence of numerous particulate Cu attached to the leaf surface treated with nano-Cu (100 mg L^{-1}) after 7 days of exposure (Fig. 2B), while definitely lower amount of Cu was detected on the surface leaves of control (Fig. 2A) or $CuSO_4$-applied (Fig. 2C).

3.2. The analysis of genes expression

3.2.1. Metal transporters

The expression pattern of *PAA1*, *PAA2*, *RAN1* and *COPT5* genes in barley plants in response to foliar-applied Cu compounds are demonstrated in Fig. 3. After 1 day of exposure, the transcript level of *PAA1* was ca. 4-fold decreased under 100 mg L^{-1} of nano-Cu, while other treatments did not elicit any significant response compared to untreated plants ($p > 0.05$). Noteworthy, the analysis of *PAA2* gene expression showed the opposite trend: the higher rate of nano-Cu and both doses of $CuSO_4$ caused up-regulation of the gene by 32–47% in relation to control plants ($p < 0.05$). A similar pattern of gene expression was observed for *RAN1* gene (Fig. 3): no effect of nano-Cu at 100 mg L^{-1}, while a higher rate led to a ca. 3.7-fold increase, whereas $CuSO_4$ at 100 and 1000 mg L^{-1} increased *RAN1* expression by ca. 2.7- and 1.6-fold, respectively ($p < 0.05$). On the other hand, our results indicated that compared to control plants, the transcript level of *COPT5* was reduced ca. 2-fold in plants exposed to both ENPs and its corresponding salts, regardless of used rates (Fig. 3).

After 7 days (Fig. 3), the transcript levels of all analyzed genes were down-regulated in response to both doses of nano-Cu and $CuSO_4$ in comparison with untreated plants ($p < 0.05$). The expression of *PAA1* was reduced by both nano-Cu and $CuSO_4$ by 64–85% regardless of used rates compared to the control plants ($p < 0.05$). Meanwhile, the transcript level of *PAA2* dropped under all Cu compounds treatment by ca. 2-fold in relation to the control. Interestingly, nano-Cu at 100 mg L^{-1} led to a 4.6-fold decline in *RAN1* expression, while a higher rate of nano-Cu and both doses of $CuSO_4$ resulted in ca. 90% reduction of gene

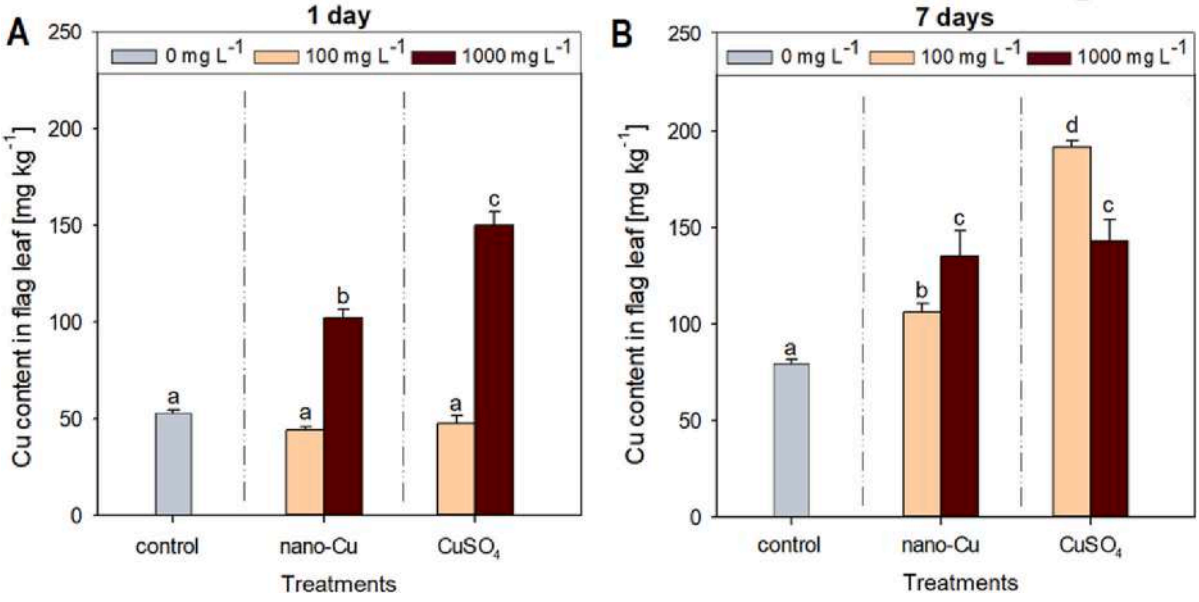

Fig. 1. Analysis of total Cu content in flag leaf of *H. vulgare* exposed to 100 and 1000 mg L^{-1} of nano-Cu and $CuSO_4$ for 1 day (A) and 7 days (B). Error bars represent standard error (SE, $n = 3$ tests). Different letters indicate significant differences among the treatments (Tukey's test, $p < 0.05$).

expression in comparison to the control group (Fig. 3). It is recorded that the transcript level of COPT5 was decreased by ~43% under nano-Cu exposure and ~ 84% by $CuSO_4$ regardless of the used dose (Fig. 3) with respect to untreated plants ($p < 0.05$).

3.2.2. Aquaporins

As presented in Fig. 4, the foliar application of Cu compounds remarkably affected aquaporin gene expression. The transcript level of *NIP2.1* declined after 1-day exposure to both doses of nano-Cu (1.9-fold) and $CuSO_4$ at 100 mg L^{-1} (1.7-fold), whereas no significant changes were observed under 1000 mg L^{-1} $CuSO_4$ treatment (Fig. 4) when compared to control plants ($p < 0.05$). Interestingly, a similar pattern of changes in transcript levels of *PIP1.1* and *TIP1.2* was observed (Fig. 4): only nano-Cu at 100 mg L^{-1} significantly down-regulated genes expression by ca. 2-fold, while remaining treatments did not affect the gene expression ($p > 0.05$). Meanwhile, the lower dose of nano-Cu also caused down-regulation of *TIP1.1* gene by 64%,whereas nano-Cu at 1000 mg L^{-1} and $CuSO_4$ at 100 mg L^{-1} increased *TIP1.1* expression by 78% and 99%, respectively ($p < 0.05$). Surprisingly, no effect was observed in response to $CuSO_4$ at 1000 mg L^{-1} treatment ($p > 0.05$).

After 7 days of exposure (Fig. 4), nano-Cu and $CuSO_4$ at 100 mg L^{-1} resulted in 2 times higher up-regulation of *NIP2.1* (ca. 5.1-fold) than at 1000 mg L^{-1} ($p < 0.05$). Moreover, after 7 days from the application, the transcript levels of both *PIP1.1* and *TIP1.1* (Fig. 4) increased significantly in response to the lower dose of both nano-Cu (by 85% and 73%, respectively) and $CuSO_4$ (by 104% and 49%, respectively) ($p < 0.05$). On the other hand, no significant changes in these gene expression were observed under the treatments with Cu-compounds at 1000 mg L^{-1} (Fig. 4) in relation to control. Interestingly, the expression of *TIP1.2* was higher in barley plants exposed to nano-Cu at 100 mg L^{-1} (5.6-fold) than 1000 mg L^{-1} (3.8-fold), while in plants treated with $CuSO_4$ transcript levels increased in dose-dependent manner (4.7- and 5.7-folds, respectively) (Fig. 4) ($p < 0.05$).

3.2.3. Antioxidants

The influence of nano-Cu and $CuSO_4$ on enzymatic antioxidants in barley leaves is presented in Fig. 5. While both doses of $CuSO_4$ elevated *SOD Cu—Zn* expression after 1 day of treatment almost 4.9- and 3.9-fold compared to the control ($p < 0.05$), nano-Cu induced higher gene expression only at 1000 mg L^{-1} (1.8-fold). Similarly, the lower dose of nano-Cu did not lead to a significant change in *SOD Fe* expression. On the other hand, the transcript level of *SOD Fe* was increased ca. 2-fold under nano-Cu at 1000 mg L^{-1}, while both $CuSO_4$ rates decreased gene expression by ~76% ($p < 0.05$). Interestingly, none of the tested Cu compounds affected the expression of *SOD Mn* after 1-day exposure with respect to the control group ($p > 0.05$). On the contrary, Cu compounds strongly increased *CAT* expression: both doses of nano-Cu caused ca. 1.5-fold rise in *CAT* transcript levels, while both rates of $CuSO_4$ induced stronger up-regulation of *CAT* expression (ca. 4.5-fold) in relation to untreated plants ($p < 0.05$).

Surprisingly, after 7 days of exposure to 100 mg L^{-1} of nano-Cu, the transcript level of *SOD Cu—Zn* declined by 56.3% in reference to the control, while no effect of higher rate was observed ($p > 0.05$) (Fig. 5). Conversely, the increase in *SOD Cu—Zn* expression under 100 and 1000 mg L^{-1} of $CuSO_4$ was dose-dependent (ca. 4- and 13.5-fold, respectively) ($p < 0.05$). Further, *SOD Fe* expression level was decreased by $CuSO_4$ treatment (4- and 12.8-fold), while no significant changes were observed under nano-Cu exposition ($p < 0.05$) (Fig. 5). Even after 7 days, the transcript levels of *SOD Mn* were not influenced by either Cu compound when compared to untreated plants. Noteworthy, after 7 days of all treatments, a down-regulation of *CAT* expression was observed ($p < 0.05$) (Fig. 5). While the lower dose of nano-Cu and both $CuSO_4$ rates caused a ca. 2.6-fold decrease in *CAT* transcript level, 1000 mg L^{-1} of nano-Cu declined the gene expression by 78% comparing to control groups ($p < 0.05$).

4. Discussion

Finding an efficient and suitable way to combat micronutrient deficiency in crops is a long-standing issue which requires an urgent solution for tackling food security (Hasegawa et al., 2018). Here, both nano-Cu and $CuSO_4$ treatments resulted in an dose-dependent increase in Cu content in tissues of *H. vulgare* overtime. However, the Cu loading to plant was higher under exposure to $CuSO_4$ than ENPs in line with studies on other plant species such as *Lactuca sativa* (Kohatsu et al., 2021) and *Cucumis sativus* (Zhao et al., 2017a). One can suppose, that those findings can be explained by the differences in the dissolution kinetics between ENPs and metal salts: while $CuSO_4$ basically provides all of the Cu^{2+} immediately, Cu-based ENPs show the potential to release Cu^{2+} over a prolonged period (Joško et al., 2021b; Landa et al., 2017; Ma

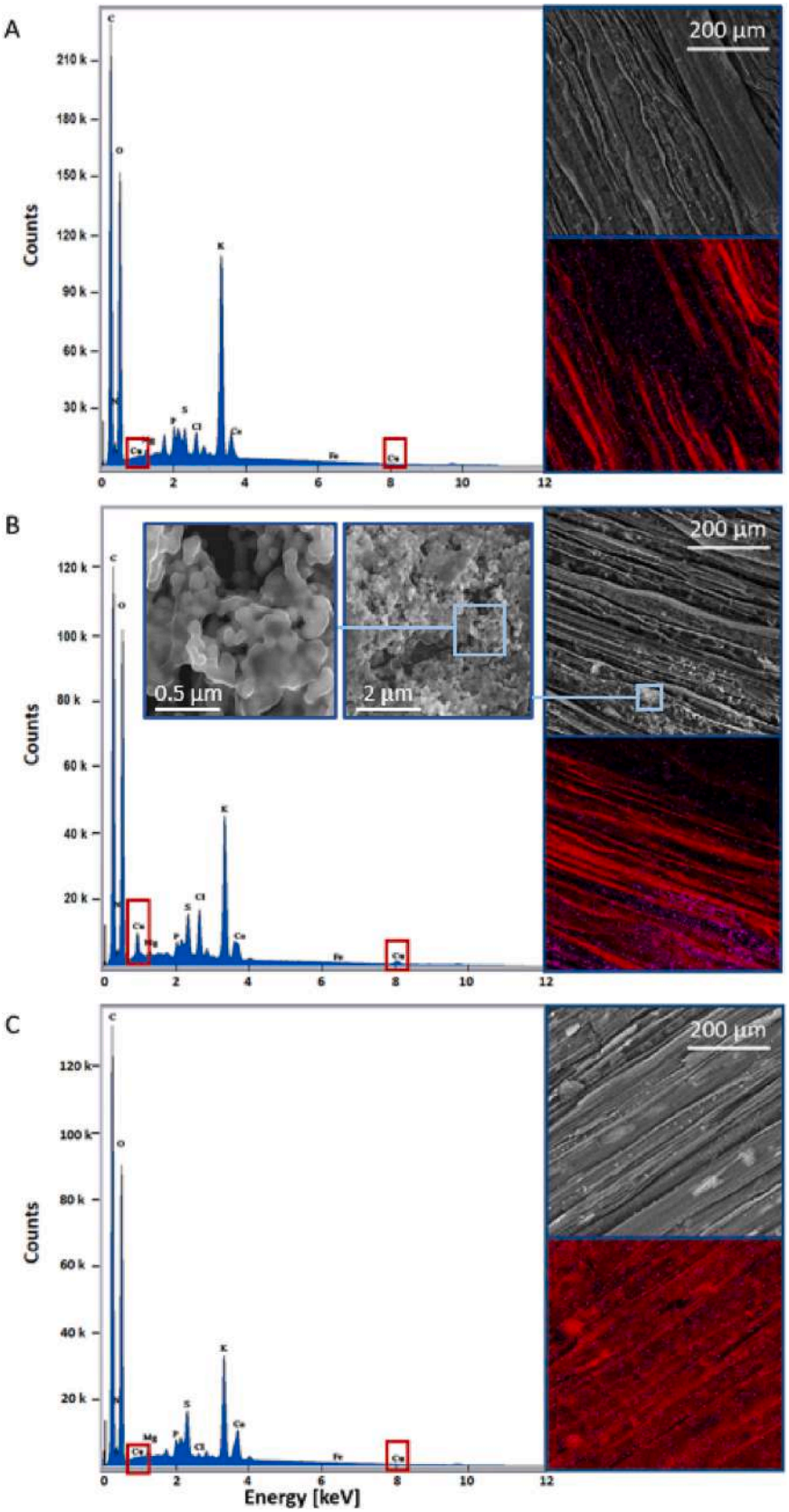

Fig. 2. SEM images with corresponding EDS copper maps of barley leaf surfaces: (A) control, (B) nano-Cu, (C) $CuSO_4$. Plants were treated with Cu compounds at a rate of 100 mg L^{-1} and exposed for 7 days. The pink signals indicate the localization of elemental Cu. The pictures were taken after etching to remove copper particles with 2.2 M HNO_3 for 30s. (For interpretation of the references to colour in this figure legend, the reader is referred to the web version of this article.)

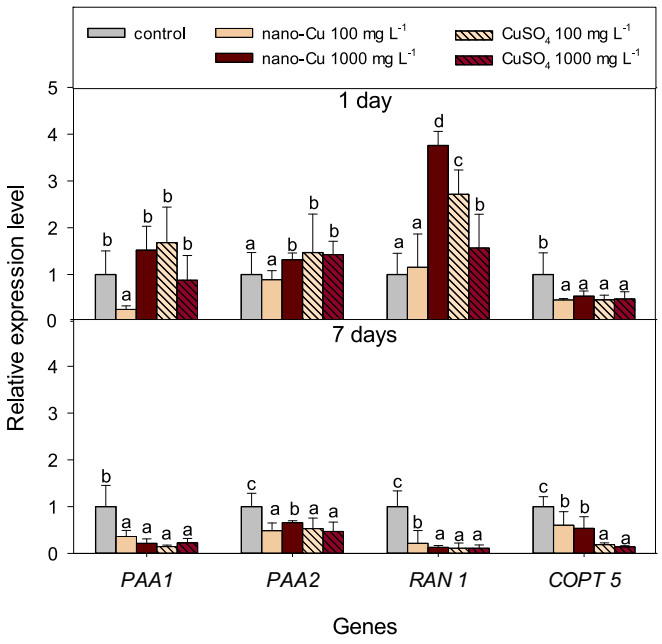

Fig. 3. Relative gene expression of *PAA1*, *PAA2*, *RAN1* and *COPT5* in *H. vulgare* leaves under nano-Cu and $CuSO_4$ (at 100 and 1000 mg L^{-1}) treatment after 1 and 7 days of exposure. Error bars represent standard error (SE, n = 3 tests). Different letters indicate significant differences among the treatments (Tukey's test, $p < 0.05$).

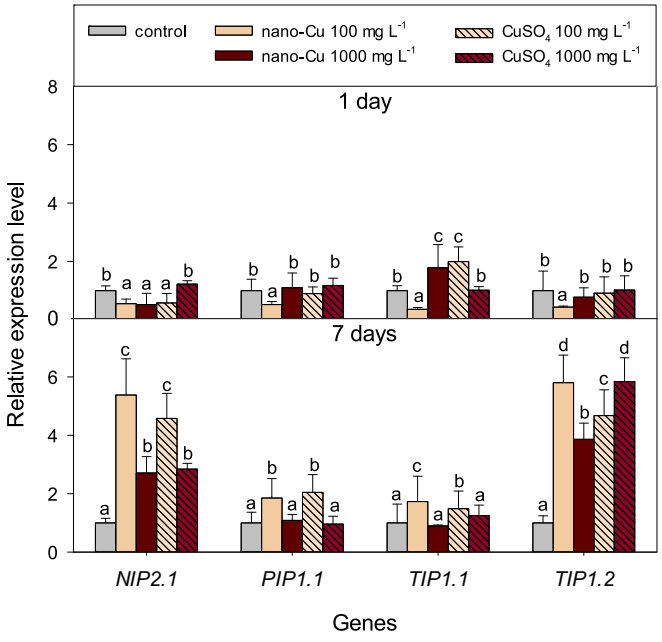

Fig. 4. *AQs* gene expression levels in barley leaves after 1 and 7 days of exposure to ENPs or metal salts (at 100 and 1000 mg L^{-1}). Error bars represent standard error (SE, n = 3 tests). Different letters indicate significant differences among the treatments (Tukey's test, $p < 0.05$).

et al., 2019; Tan et al., 2018; Zhao et al., 2017a). In the dissolution test, the concentration of Cu^{2+} in nano-Cu solution used for foliar application was increased overtime (Fig. S2). However, the question arisen about the dissolution of nano-Cu after their application on plant, that aspect is a methodologically challenging and has not been analyzed so far. However, for example the impact of dew on ENPs dissolution could be a crucial for release of $Cu^{2+}$from attached ENPs to leave surface.

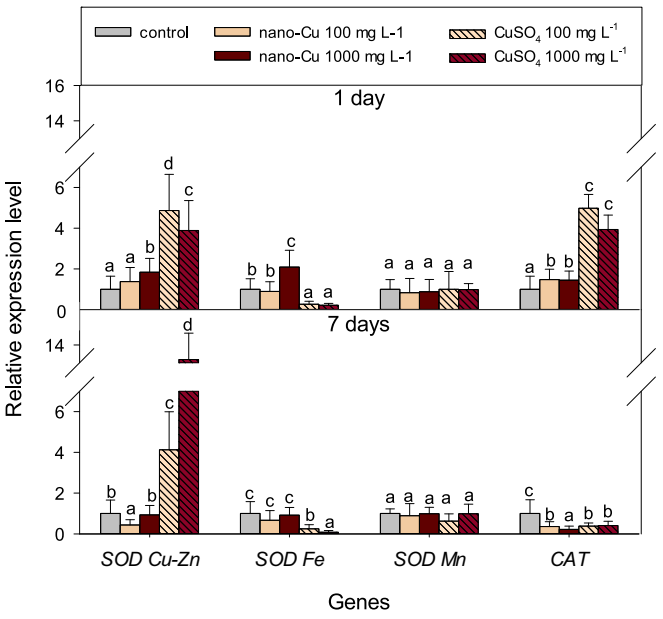

Fig. 5. Relative expression of antioxidant-related genes in response to nano-Cu and $CuSO_4$ (at 100 and 1000 mg L^{-1}) treatment of barley leaves after 1 and 7 days of exposure. Error bars represent standard error (SE, n = 3 tests). Different letters indicate significant differences among the treatments (Tukey's test, $p < 0.05$).

Moreover, the tendency to aggregate on the plant surface (Fig. 2) may constitute a bottleneck for their absorption (Avellan et al., 2021b; Grillo et al., 2021b; Grillo et al., 2021a). Additionally, as it was reported in the literature, the aggregation rate of ENPs correlate with their the concentration, this tendency was also confirmed in our study. Here, it may also contribute to the difference in the Cu level in the flag leaves sprayed with both doses of nano-Cu. Probably the higher weight of aggregates of nano-Cu at 1000 mg L^{-1} may foster their fall from flag leaves, which are usually at vertical position. It should be noted that the used etching protocol for removing adhered ENPs from leaves was not fully sufficient; thus the measured Cu content possibly reflects both surface attached and absorbed Cu. Similarly, the strong retention of negative Cu-based nanoproducts on the leaf surface was confirmed previously in *Zea mays* L. (Zhao et al., 2017a), *Solanum lycopersicum* L. (Ma et al., 2019) and *Myriophyllum spicatum* L. (Roubeau Dumont et al., 2022). The overestimated content of Cu in the flag leaves under nano-Cu treatment obstruct to compare the Cu delivery efficiency with other nanoformulations, including the recently developed "on demand" nanochemicals (Bonser et al., 2023b), even those added to soil (Xu et al., 2022). Surprisingly, after 7 days, the Cu content in the flag leaf of barley plants exposed to both Cu compounds was at a similar level. The explanation of that fact could be (i) the above-mentioned overestimated Cu content under the treatment of nano-Cu, (ii) the dilution of metal concentration by the most increased biomass in case of $CuSO_4$ application, (iii) the leaves treated with $CuSO_4$ at 1000 mg L^{-1} after 7 days were affected by chlorosis, which reduced leaf surface area capable of Cu uptake and translocation. It has to be noted that the translocation from leaves to roots was be excluded, in spite of the fact, that other study reported the transfer of foliar applied Au ENPs from aboveground tissues to the roots. In our experiment the Cu level in roots was unchanged compared to control (Supplementary Materials, Table S5).

As the expression of high-affinity Cu transporters (Fig. 6) depends strictly on the pool of Cu ions present in the plant tissue, the analysis of gene expression might offer valuable information regarding the Cu status at the molecular level (del Pozo et al., 2010; Landa et al., 2017; Wintz et al., 2003). Here, this is particularly justified, because the application of Cu-compounds at 100 mg L^{-1} triggered changes in the

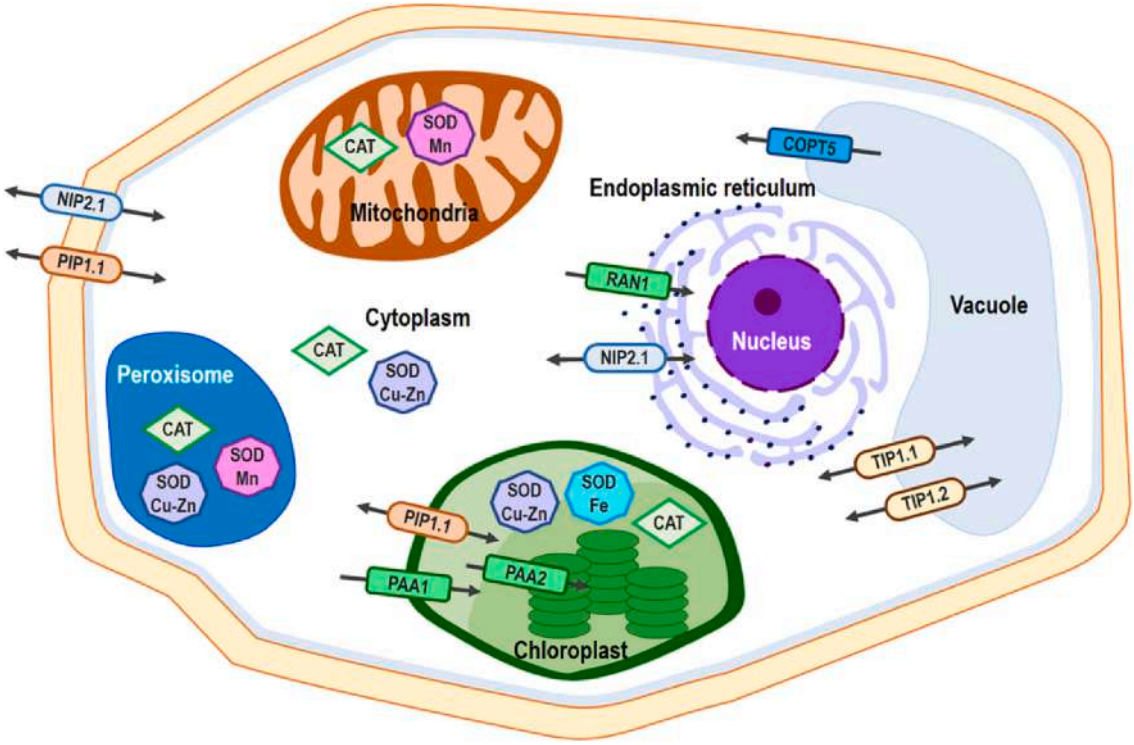

Fig. 6. Schematic diagram of the localization Cu transporters*(*PAA1, PAA2, RAN1, COPT5), aquaporins (NIP2.1, PIP1.1, TIP1.1, TIP1.2) and enzymatic antioxidants (SOD Cu—Zn, SOD Fe, SOD Mn, CAT) in plant cell membrane and organelles.

expression of selected *HMAs* genes, while the Cu content in leaves was unaffected after a short-term exposure. Furthermore, the molecular response was different between the nanoparticulate and ionic form of Cu at a lower rate. Nano-Cu decreased (*PAA1*) or not impacted (*PAA2*, *RAN1*) genes expression while $CuSO_4$ improved both *PAA2* and *RAN1* transcripts, which could be attributed to either higher Cu dosage or a faster dissolution rate ($CuSO_4$). It is worthwhile to note that the transcript levels of high-affinity Cu transporters like *HMAs* were previously shown to significantly decrease soon after Cu treatment and recover overtime (Ma et al., 2021). This could indicate that exposure to nano-Cu at 100 mg L^{-1} led to a delayed plant response due to a slower release of Cu^{2+}. Furthermore, as *PAA1* is responsible for Cu transport to the stroma and *PAA2* to the lumen (Fig. 6), low *PAA1* levels might hinder *PAA2* expression (Wintz et al., 2003). Meanwhile, localized in ER membrane *RAN1* (Fig. 6) is constitutively expressed at comparatively high levels due to its essential role in Cu delivery and biogenesis of the ETR1 (Wintz et al., 2003). Noteworthy, the highest expression of *RAN1* gene was observed after treatment with a higher dose of nano-Cu, which might point out a joint impact of released Cu^{2+} and nanoparticles, although this finding requires further research. Interestingly, after 7 days of exposure, the transcript level of these 3 genes showed a relatively comparable decline among all treatments, despite the extremely different Cu content in tissues. This result could be attributed to the limited Cu translocation to the organelles in plants as a means to prevent or alleviate Cu toxicity in response to Cu excess conditions (del Pozo et al., 2010; Ma et al., 2021; Wintz et al., 2003). Surprisingly, *COPT5* gene remained constantly down-regulated by all treatments at both time-points. As tonoplast-localized *COPT5* plays a crucial role in transporting vacuole-sequestered Cu ions (Fig. 6), the transcript level of *COPT5* gene is known to increase under both Cu deprivation (maintaining Cu content inside the cell) and excess (removing Cu outside the cell) (Garcia-Molina et al., 2011; Klaumann et al., 2011). Interestingly, metal salts in older plants led to a significantly higher decline in *COPT5* expression than nano-Cu, even though Cu content in plant leaves was measured at a similar level. It may suggest that the actual Cu content was higher, upon $CuSO_4$ than nano-Cu resulting in stronger excretion of Cu ions, or the different transcriptional response may stem from the nano-specific impact due to the presence of nanoparticulate and ionic Cu in plants.

Besides high-affinity transporters, AQs are also considered involved in regulating the cellular transport of metal ions and small particles (Kapilan et al., 2018; Wintz et al., 2003). Moreover, as both Cu deficiency and excess impact the osmotic potential, significant changes in *AQs* expression were observed overtime (Kholodova et al., 2011; Merakli et al., 2021; Wintz et al., 2003). It is worth emphasizing that, only nano-Cu at 100 mg L^{-1} led to down-regulation of all tested *AQs* genes under a short-term exposure. Previously, such a drop in *AQs* expression was associated with osmotic adjustments to Cu^{2+} exposure rather than nanoparticles (Landa et al., 2017), however, prolonged Cu deficiency is known to alter plants' responses to stimuli via changes in metabolic processes (Peñarrubia et al., 2015). Moreover, these results may also be related to mechanically-induced stress to sudden ENPs presence as alien solid particles rather than a Cu related response. After 7 days, the up-regulation of all tested *AQs* was noted under almost all treatments. However, that molecular response (*NIP2.1*, *PIP1.1* and *TIP1.*1) was inversely dose-dependent. This is in agreement with previous research, in which low Cu treatment demonstrated a more positive impact on *AQs* expression than high Cu dosage (Landa et al., 2017; Merakli et al., 2021). Noteworthy, *PIP1.1* and *TIP1.1* expressions generally increase in plant tissues during intense growth as a means for effective water and solute circulation (Akdemir, 2021; Banerjee and Roychoudhury, 2020), which demonstrates a positive impact of Cu fertilization with low doses. Surprisingly, no clear pattern of *TIP1.2* stimulation is noticeable. We hypothesize that *TIP1.2* gene expression increased due to its involvement in both Cu remobilization to/out of vacuoles (Banerjee and Roychoudhury, 2020).

Cu homeostasis is regulated not only by the expression of genes involved in Cu transport, but also by the targets for Cu delivery (del Pozo et al., 2010). Generally, plants grown under Cu-deficient conditions down-regulate transcripts of all cuproproteins indirectly involved in

photosynthesis (e.g. *SOD Cu—Zn*), while their expression is improved by Cu-resupply (Cohu and Pilon, 2007; del Pozo et al., 2010; Wintz et al., 2003). This observation was confirmed for $CuSO_4$ treatments, whereas nano-Cu application showed only a slight increase in *SOD Cu—Zn* expression after 1 day of exposure. Similarly to the earlier studies, the inhibition of *SOD Cu—Zn* transcript under Cu-deficiency was counterbalanced by the induction of *SOD Fe* expression, whereas increasing Cu content stimulated the reverse situation (Supplementary Materials, Fig. S6) (Cohu and Pilon, 2007; del Pozo et al., 2010). The increase in *SOD Fe* transcript level under nano-Cu (at 1000 mg L^{-1}) in contrast to the significant drop in the gene expression in barley plants exposed to $CuSO_4$ seems to further prove this assumption. On the other hand, enhanced *SOD Cu—Zn* and *CAT* expression in response to metal salts might signal the overproduction of ROS due to the fast influx of Cu^{2+} (Landa et al., 2017; Zhao et al., 2017a). SOD Cu—Zn and CAT are important components of the enzymatic antioxidant defense system, which convert ROS to less toxic H_2O_2 or neutral O_2 and H_2O, respectively (Ravet and Pilon, 2013). Interestingly, nano-Cu application at low doses did not influence either *SOD Cu—Zn* or *SOD—Fe* transcript levels. It is possible that such low ENPs and/or Cu doses did not activate the antioxidant plant

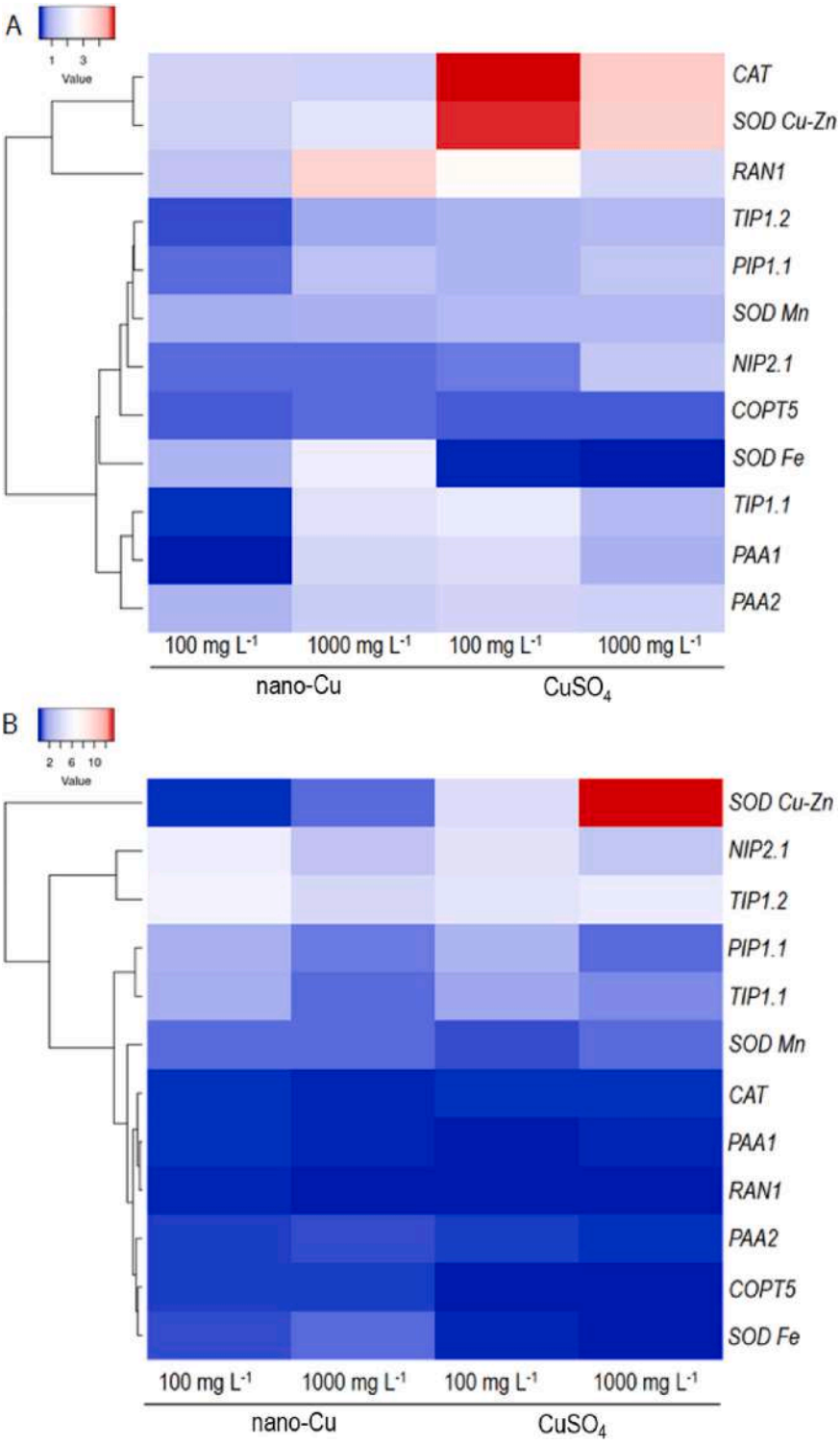

Fig. 7. Heatmaps showing differential gene expression of Cu homeostasis, aquaporins and enzymatic antioxidants genes in *H. vulgare* flag leaves after 1 (A) and 7 days (B) of exposition to Cu-compounds. Each column represents the expression in flag leaves under different Cu treatment (nano-Cu and $CuSO_4$ at 100 and 1000 mg L^{-1}) and each row represents one gene. Scale colour bar in the pictures shows low (blue) to high (red) gene expression. The hierarchical clustering of genes is shown in the dendrograms on the side of the heat map using the complete linkage approach. (For interpretation of the references to colour in this figure legend, the reader is referred to the web version of this article.)

response (Zhao et al., 2017a) or the specific response of different *Cu—Zn SOD* isoenzymes or that other response pathways were induced (Zhao et al., 2017b). Moreover, the observed gene expression pattern may be Cu compound/dose of ENPs (the aggregation rate) specific. Similarly, a study by Cota-Ruiz et al. (2018) revealed the transcriptional defense response in alfalfa was Cu form-dependent. Only nano-$Cu(OH)_2$ induced up-regulation of *SOD Cu—Zn* gene, while Cu sulfate caused the increased in the transcript of *MT* gene related with metallothionines, capable to bind heavy metals, whereas no effect on the selected gene expression was observed for bulk $Cu(OH)_2$. However, considering prolonged Cu deficiency conditions, all released Cu ions from nano-Cu might be efficiently utilized in the process involved in photosynthesis (Cohu and Pilon, 2007), thus avoiding SODs activation. Expression of *SOD Mn* remained unchanged regardless of Cu content in barley leaves or Cu-compound type, which suggests that in barley plants, this SOD isoform is not regulated by Cu status. While similar results were observed in *A. thaliana* (Kliebenstein et al., 1998), *SOD Mn* expression pattern differed significantly depending on Cu exposure in *Solanum nigrum* (Fidalgo et al., 2013), which indicates a species-specific response. SODSSA

To gain further insight into the impact of nanoparticulate and ionic Cu on the 12 analyzed genes, heatmaps were obtained (Fig. 7). According to the received heatmaps, the samples were subdivided into 4 clusters, which corresponded to the Cu-compounds, regardless of the duration of exposure. It is worth noting, that after 1 day of exposure to metal salt, plants showed similar patterns of expression of all genes regardless of the dosage when compared to nano-Cu (Fig. 7A). That modification of gene expression most likely results from the fast dissolution and Cu^{2+} uptake when applied as $CuSO_4$, which directly leads to the quick induction of antioxidant gene expression. However, a clear divide in gene expression patterns is noticeable between lower doses of nano-Cu and the remaining Cu compounds (Fig. 7A). Generally, two clusters of genes with similar expression patterns were recorded: one (upper part) corresponded to up-regulation/ lack of changes to Cu application. The co-expression of *CAT* and *SOD Cu—Zn* under metal salts was most likely a stress response to a sudden influx of Cu^{2+} after a long period of Cu starvation. Meanwhile, another cluster (lower part) included genes, which showed low expression levels, especially in *AQs* and *HMAs* gene expressions under treatment with nano-Cu (100 mg L^{-1}). This consistent pattern of down-regulation most likely results from a combination of low doses and limited dissolution of nano-Cu. Furthermore, after 7 days of exposition, two clusters of similarly expressed genes were achieved (Fig. 7B): interestingly, due to excessively high up-regulation, *SOD Cu—Zn* gene acts as 1 cluster. Meanwhile, all remaining genes were subdivided into another two clusters: highly expressed *AQs* and significantly down-regulated genes, e. g., all high-affinity Cu transporters, as a means to avoid Cu toxicity in plant cells. Moreover, a clear substitution relationship between *SOD Cu—Zn* and *SOD Fe* (for $CuSO_4$ at 1000 mg L^{-1}) depending on the Cu ion pool in plants was observed. In turn, the performed correlation plot of the transcript levels of analyzed genes and the used Cu rate/actual applied Cu amount/Cu content leaves did not show the statistical significant correlation between these endpoints (Supplementary Materials, Fig. S7. A). In case of exposure to ENPs, no relation was also noted for the concentration of Cu^{2+} released from nano-Cu and the transcriptional response (Supplementary Materials, Fig. S7.B). Probably, only actual concentration of cellular Cu/ nano-Cu could be indicate the relationship with the measured transcripts of genes.

5. Conclusion

This study analyzed the impact of foliar applied nano-Cu on *H. vulgare* grown in Cu deficient condition, which could give insight into the further potential use of Cu-based ENPs in plant growth. Prior to this study, the transcriptional mechanisms behind the maintenance of Cu homeostasis in Cu-deficient *H. vulgare* plants exposed to nano-Cu were poorly investigated. Due to the strong retention of nano-Cu on the leaf surface, Cu content measurements were probably overestimated. However, the gene expression analysis involved in the maintenance of Cu homeostasis allowed real-time indication of Cu status in plants. Nano-Cu (1000 mg L^{-1}) and $CuSO_4$ induced fast plant responses at the molecular level as the sudden influx of Cu^{2+} resulted in the induction of oxidative stress. On the other hand, slower dissolution of nano-Cu (100 mg L^{-1}) led to more gradual changes in gene expression, thus limiting the negative impact on the plant at the molecular level, further, this treatment provided the highest biomass among the sprays. The obtained results may be useful for both efficiently optimizing the metal nutrient content in plant and ensuring the long-term safety of nano-enabled products. Moreover, the transcriptional analysis with focus on cellular balance of metals could be valuable marker also for the recent intensively developing a stimuli responsive nano-agrochemicals.

CRediT authorship contribution statement

Magdalena Kusiak: Investigation, Methodology, Visualization, Writing – original draft, Writing – review & editing. **Magdalena Sozoniuk:** Investigation, Methodology, Writing – review & editing. **Camille Larue:** Methodology, Writing – review & editing. **Renato Grillo:** Methodology, Writing – review & editing. **Krzysztof Kowalczyk:** Conceptualization, Writing – review & editing. **Patryk Oleszczuk:** Writing – review & editing. **Izabela Jośko:** Funding acquisition, Investigation, Methodology, Supervision, Writing – review & editing.

Declaration of Competing Interest

The authors declare that they have no known competing financial interests or personal relationships that could have appeared to influence the work reported in this paper.

Data availability

Data will be made available on request.

Acknowledgments

This study was supported by National Science Centre (Poland) in the frame of SONATA project (2017/26/D/NZ9/00067).

Appendix A. Supplementary data

Supplementary data to this article can be found online at https://doi.org/10.1016/j.impact.2023.100472.

References

Akdemir, H., 2021. Evaluation of transcription factor and aquaporin gene expressions in response to Al2O3 and ZnO nanoparticles during barley germination. Plant Physiol. Biochem. 166, 466–476. https://doi.org/10.1016/j.plaphy.2021.06.018.

Avellan, A., Yun, J., Morais, B.P., Clement, E.T., Rodrigues, S.M., Lowry, G.V., 2021a. Critical review: role of inorganic nanoparticle properties on their foliar uptake and *in planta* translocation. Environ. Sci. Technol. 55, 13417–13431. https://doi.org/10.1021/acs.est.1c00178.

Avellan, A., Yun, J., Morais, B.P., Clement, E.T., Rodrigues, S.M., Lowry, G.V., 2021b. Critical review: role of inorganic nanoparticle properties on their foliar uptake and in planta translocation. Environ. Sci. Technol. 55, 13417–13431. https://doi.org/10.1021/acs.est.1c00178.

Babicki, S., Arndt, D., Marcu, A., Liang, Y., Grant, J.R., Maciejewski, A., Wishart, D.S., 2016. Heatmapper: web-enabled heat mapping for all. Nucleic Acids Res. 44, W147–W153. https://doi.org/10.1093/nar/gkw419.

Banerjee, A., Roychoudhury, A., 2020. The role of aquaporins during plant abiotic stress responses, in: plant life under changing environment. Elsevier, pp. 643–661. https://doi.org/10.1016/B978-0-12-818204-8.00028-X.

Bárzana, G., Garcia-Gomez, P., Carvajal, M., 2022. Nanomaterials in plant systems: smart advances related to water uptake and transport involving aquaporins. Plant Nano Biol. 1, 100005 https://doi.org/10.1016/j.plana.2022.100005.

Binder, B.M., 2020. Ethylene signaling in plants. J. Biol. Chem. 295, 7710–7725. https://doi.org/10.1074/jbc.REV120.010854.

Blaby-Haas, C.E., Padilla-Benavides, T., Stübe, R., Argüello, J.M., Merchant, S.S., 2014. Evolution of a plant-specific copper chaperone family for chloroplast copper homeostasis. Proc. Natl. Acad. Sci. U. S. A. 111 https://doi.org/10.1073/pnas.1421545111.

Bonser, C.A.R., Borgatta, J., White, J.C., Astete, C.E., Sabliov, C.M., Davis, J.A., 2023a. Impact of zein and lignin-PLGA biopolymer nanoparticles used as pesticide nanocarriers on soybean growth and yield under field conditions. Agrosystems Geosci & Env 6, e20350. https://doi.org/10.1002/agg2.20350.

Bonser, C.A.R., Borgatta, J., White, J.C., Astete, C.E., Sabliov, C.M., Davis, J.A., 2023b. Impact of zein and lignin-PLGA biopolymer nanoparticles used as pesticide nanocarriers on soybean growth and yield under field conditions. Agrosyst. Geosci. Environ. 6, e20350 https://doi.org/10.1002/agg2.20350.

Cohu, C.M., Pilon, M., 2007. Regulation of superoxide dismutase expression by copper availability. Physiol. Plant. 129, 747–755. https://doi.org/10.1111/j.1399-3054.2007.00879.x.

Cota-Ruiz, K., Hernández-Viezcas, J.A., Varela-Ramírez, A., Valdés, C., Núñez-Gastélum, J.A., Martínez-Martínez, A., Delgado-Rios, M., Peralta-Videa, J.R., Gardea-Torresdey, J.L., 2018. Toxicity of copper hydroxide nanoparticles, bulk copper hydroxide, and ionic copper to alfalfa plants: a spectroscopic and gene expression study. Environ. Pollut. 243, 703–712. https://doi.org/10.1016/j.envpol.2018.09.028.

Cota-Ruiz, K., Ye, Y., Valdes, C., Deng, C., Wang, Y., Hernández-Viezcas, J.A., Duarte-Gardea, M., Gardea-Torresdey, J.L., 2020. Copper nanowires as nanofertilizers for alfalfa plants: understanding nano-bio systems interactions from microbial genomics, plant molecular responses and spectroscopic studies. Sci. Total Environ. 742, 140572 https://doi.org/10.1016/j.scitotenv.2020.140572.

del Pozo, T., Cambiazo, V., González, M., 2010. Gene expression profiling analysis of copper homeostasis in Arabidopsis thaliana. Biochem. Biophys. Res. Commun. 393, 248–252. https://doi.org/10.1016/j.bbrc.2010.01.111.

Deng, C., Wang, Y., Cantu, J.M., Valdes, C., Navarro, G., Cota-Ruiz, K., Hernandez-Viezcas, J.A., Li, C., Elmer, W.H., Dimkpa, C.O., White, J.C., Gardea-Torresdey, J.L., 2022a. Soil and foliar exposure of soybean (Glycine max) to cu: nanoparticle coating-dependent plant responses. NanoImpact 26, 100406. https://doi.org/10.1016/j.impact.2022.100406.

Deng, C., Wang, Y., Navarro, G., Sun, Y., Cota-Ruiz, K., Hernandez-Viezcas, J.A., Niu, G., Li, C., White, J.C., Gardea-Torresdey, J., 2022b. Copper oxide (CuO) nanoparticles affect yield, nutritional quality, and auxin associated gene expression in weedy and cultivated rice (Oryza sativa L.) grains. Sci. Total Environ. 810, 152260 https://doi.org/10.1016/j.scitotenv.2021.152260.

Doğaroğlu, Z.G., Köleli, N., 2017. TiO2 and ZnO nanoparticles toxicity in barley (Hordeum vulgare L.). Clean – Soil, Air Water 45, 1700096. https://doi.org/10.1002/clen.201700096.

European Commission, 2012. A European Strategy for Key Enabling Technologies – A Bridge to Growth and Jobs.

Fageria, N.K., Filho, M.P.B., Moreira, A., Guimarães, C.M., 2009. Foliar fertilization of crop plants. J. Plant Nutr. 32, 1044–1064. https://doi.org/10.1080/01904160902872826.

Fidalgo, F., Azenha, M., Silva, A.F., Sousa, A., Santiago, A., Ferraz, P., Teixeira, J., 2013. Copper-induced stress in Solanum nigrum L. and antioxidant defense system responses. Food Energy Secur 2, 70–80. https://doi.org/10.1002/fes3.20.

Fraceto, L.F., Grillo, R., De Medeiros, G.A., Scognamiglio, V., Rea, G., Bartolucci, C., 2016. Nanotechnology in agriculture: which innovation potential does it have? Front. Environ. Sci. 4 https://doi.org/10.3389/fenvs.2016.00020.

Garcia-Molina, A., Andrés-Colás, N., Perea-García, A., del Valle-Tascón, S., Peñarrubia, L., Puig, S., 2011. The intracellular Arabidopsis COPT5 transport protein is required for photosynthetic electron transport under severe copper deficiency: characterization of the Arabidopsis COPT5 protein. Plant J. 65, 848–860. https://doi.org/10.1111/j.1365-313X.2010.04472.x.

Graham, R.D., 2008. Micronutrient deficiencies in crops and their global significance. In: Alloway, B.J. (Ed.), Micronutrient Deficiencies in Global Crop Production. Springer, Netherlands, Dordrecht, pp. 41–61. https://doi.org/10.1007/978-1-4020-6860-7_2.

Grillo, R., Fraceto, L.F., Amorim, M.J.B., Scott-Fordsmand, J.J., Schoonjans, R., Chaudhry, Q., 2021a. Ecotoxicological and regulatory aspects of environmental sustainability of nanopesticides. J. Hazard. Mater. 404, 124148 https://doi.org/10.1016/j.jhazmat.2020.124148.

Grillo, R., Mattos, B.D., Antunes, D.R., Forini, M.M.L., Monikh, F.A., Rojas, O.J., 2021b. Foliage adhesion and interactions with particulate delivery systems for plant nanobionics and intelligent agriculture. Nano Today 37, 101078. https://doi.org/10.1016/j.nantod.2021.101078.

Guo, H., White, J.C., Wang, Z., Xing, B., 2018. Nano-enabled fertilizers to control the release and use efficiency of nutrients. Curr. Opin. Environ. Sci. Health 6, 77–83. https://doi.org/10.1016/j.coesh.2018.07.009.

Hasegawa, T., Fujimori, S., Havlík, P., Valin, H., Bodirsky, B.L., Doelman, J.C., Fellmann, T., Kyle, P., Koopman, J.F.L., Lotze-Campen, H., Mason-D'Croz, D., Ochi, Y., Pérez Domínguez, I., Stehfest, E., Sulser, T.B., Tabeau, A., Takahashi, K., Takakura, J., van Meijl, H., van Zeist, W.-J., Wiebe, K., Witzke, P., 2018. Risk of increased food insecurity under stringent global climate change mitigation policy. Nat. Clim. Chang. 8, 699–703. https://doi.org/10.1038/s41558-018-0230-x.

Hofmann, T., Lowry, G.V., Ghoshal, S., Tufenkji, N., Brambilla, D., Dutcher, J.R., Gilbertson, L.M., Giraldo, J.P., Kinsella, J.M., Landry, M.P., Lovell, W., Naccache, R., Paret, M., Pedersen, J.A., Unrine, J.M., White, J.C., Wilkinson, K.J., 2020. Technology readiness and overcoming barriers to sustainably implement nanotechnology-enabled plant agriculture. Nat Food 1, 416–425. https://doi.org/10.1038/s43016-020-0110-1.

Jośko, I., Kusiak, M., Oleszczuk, P., Świeca, M., Kończak, M., Sikora, M., 2021a. Transcriptional and biochemical response of barley to co-exposure of metal-based nanoparticles. Sci. Total Environ. 782, 146883 https://doi.org/10.1016/j.scitotenv.2021.146883.

Jośko, I., Kusiak, M., Xing, B., Oleszczuk, P., 2021b. Combined effect of nano-CuO and nano-ZnO in plant-related system: from bioavailability in soil to transcriptional regulation of metal homeostasis in barley. J. Hazard. Mater. 416, 126230 https://doi.org/10.1016/j.jhazmat.2021.126230.

Jośko, I., Krasucka, P., Skwarek, E., Oleszczuk, P., Sheteiwy, M., 2022. The co-occurrence of Zn-and cu-based engineered nanoparticles in soils: the metal extractability vs. toxicity to Folsomia candida. Chemosphere 287, 132252. https://doi.org/10.1016/j.chemosphere.2021.132252.

Kah, M., Navarro, D., Kookana, R.S., Kirby, J.K., Santra, S., Ozcan, A., Kabiri, S., 2019a. Impact of (nano)formulations on the distribution and wash-off of copper pesticides and fertilisers applied on citrus leaves. Environ. Chem. 16, 401. https://doi.org/10.1071/EN18279.

Kah, M., Tufenkji, N., White, J.C., 2019b. Nano-enabled strategies to enhance crop nutrition and protection. Nat. Nanotechnol. 14, 532–540. https://doi.org/10.1038/s41565-019-0439-5.

Kapilan, R., Vaziri, M., Zwiazek, J.J., 2018. Regulation of aquaporins in plants under stress. Biol. Res. 51 https://doi.org/10.1186/s40659-018-0152-0.

Khodakovskaya, M.V., de Silva, K., Biris, A.S., Dervishi, E., Villagarcia, H., 2012. Carbon nanotubes induce growth enhancement of tobacco cells. ACS Nano 6, 2128–2135. https://doi.org/10.1021/nn204643g.

Kholodova, V., Volkov, K., Abdeyeva, A., Kuznetsov, V., 2011. Water status in Mesembryanthemum crystallinum under heavy metal stress. Environ. Exp. Bot. S0098847211000323 https://doi.org/10.1016/j.envexpbot.2011.02.007.

Klaumann, S., Nickolaus, S.D., Fürst, S.H., Starck, S., Schneider, S., Ekkehard Neuhaus, H., Trentmann, O., 2011. The tonoplast copper transporter COPT5 acts as an exporter and is required for interorgan allocation of copper in Arabidopsis thaliana. New Phytol. 192, 393–404. https://doi.org/10.1111/j.1469-8137.2011.03798.x.

Kliebenstein, D.J., Monde, R.-A., Last, R.L., 1998. Superoxide dismutase in Arabidopsis: an eclectic enzyme family with disparate regulation and protein localization. Plant Physiol. 118, 637–650.

Kohatsu, M.Y., Pelegrino, M.T., Monteiro, L.R., Freire, B.M., Pereira, R.M., Fincheira, P., Rubilar, O., Tortella, G., Batista, B.L., de Jesus, T.A., Seabra, A.B., Lange, C.N., 2021. Comparison of foliar spray and soil irrigation of biogenic CuO nanoparticles (NPs) on elemental uptake and accumulation in lettuce. Environ. Sci. Pollut. Res. 28, 16350–16367. https://doi.org/10.1007/s11356-020-12169-x.

Kusiak, M., Oleszczuk, P., Jośko, I., 2022. Cross-examination of engineered nanomaterials in crop production: application and related implications. J. Hazard. Mater. 424, 127374 https://doi.org/10.1016/j.jhazmat.2021.127374.

Kusiak, M., Sierocka, M., Świeca, M., Pasieczna-Patkowska, S., Sheteiwy, M., Jośko, I., 2023. Unveiling of interactions between foliar-applied cu nanoparticles and barley suffering from cu deficiency. Environ. Pollut. 320, 121044 https://doi.org/10.1016/j.envpol.2023.121044.

Landa, P., Dytrych, P., Prerostova, S., Petrova, S., Vankova, R., Vanek, T., 2017. Transcriptomic response of Arabidopsis thaliana exposed to CuO nanoparticles, bulk material, and ionic copper. Environ. Sci. Technol. 51, 10814–10824. https://doi.org/10.1021/acs.est.7b02265.

Ma, C., Borgatta, J., De La Torre-Roche, R., Zuverza-Mena, N., White, J.C., Hamers, R.J., Elmer, W.H., 2019. Time-dependent transcriptional response of tomato (Solanum lycopersicum L.) to cu nanoparticle exposure upon infection with fusarium oxysporum f. sp. lycopersici. ACS Sustain. Chem. Eng. 7, 10064–10074. https://doi.org/10.1021/acssuschemeng.9b01433.

Ma, Y., Wei, N., Wang, Q., Liu, Z., Liu, W., 2021. Genome-wide identification and characterization of the heavy metal ATPase (HMA) gene family in Medicago truncatula under copper stress. Int. J. Biol. Macromol. 193, 893–902. https://doi.org/10.1016/j.ijbiomac.2021.10.197.

Merakli, N., Bulduk, İ., Memon, A., 2021. Cu-induced genes expression in the accumulator plant BRASSICA NIGRA l. Trakya Univ. J. Nat. Sci. https://doi.org/10.23902/trkjnat.978842.

Peñarrubia, L., Romero, P., Carrió-Seguí, A., Andrés-Bordería, A., Moreno, J., Sanz, A., 2015. Temporal aspects of copper homeostasis and its crosstalk with hormones. Front. Plant Sci. 6 https://doi.org/10.3389/fpls.2015.00255.

Printz, B., Lutts, S., Hausman, J.-F., Sergeant, K., 2016. Copper trafficking in plants and its implication on Cell Wall dynamics. Front. Plant Sci. 7 https://doi.org/10.3389/fpls.2016.00601.

Qian, H., Peng, X., Han, X., Ren, J., Sun, L., Fu, Z., 2013. Comparison of the toxicity of silver nanoparticles and silver ions on the growth of terrestrial plant model Arabidopsis thaliana. J. Environ. Sci. 25, 1947–1956. https://doi.org/10.1016/S1001-0742(12)60301-5.

Rahman, N., Schoenau, J., 2020. Response of wheat, pea, and canola to micronutrient fertilization on five contrasting prairie soils. Sci. Rep. 10, 18818. https://doi.org/10.1038/s41598-020-75911-y.

Ravet, K., Pilon, M., 2013. Copper and Iron homeostasis in plants: the challenges of oxidative stress. Antioxid. Redox Signal. 19, 919–932. https://doi.org/10.1089/ars.2012.5084.

Ren, Q.-Q., Huang, Z.-R., Huang, W.-L., Huang, W.-T., Chen, H.-H., Yang, L.-T., Ye, X., Chen, L.-S., 2022. Physiological and molecular adaptations of Citrus grandis roots to long-term copper excess revealed by physiology, metabolome and transcriptome. Environ. Exp. Bot. 203, 105049 https://doi.org/10.1016/j.envexpbot.2022.105049.

Rico, C.M., Majumdar, S., Duarte-Gardea, M., Peralta-Videa, J.R., Gardea-Torresdey, J.L., 2011. Interaction of nanoparticles with edible plants and their possible implications in the food chain. J. Agric. Food Chem. 59, 3485–3498. https://doi.org/10.1021/jf104517j.

Roubeau Dumont, E., Elger, A., Azéma, C., Castillo Michel, H., Surble, S., Larue, C., 2022. Cutting-edge spectroscopy techniques highlight toxicity mechanisms of copper oxide nanoparticles in the aquatic plant Myriophyllum spicatum. Sci. Total Environ. 803, 150001 https://doi.org/10.1016/j.scitotenv.2021.150001.

Roy, D., Adhikari, S., Adhikari, A., Ghosh, S., Azahar, I., Basuli, D., Hossain, Z., 2022. Impact of CuO nanoparticles on maize: comparison with CuO bulk particles with special reference to oxidative stress damages and antioxidant defense status. Chemosphere 287, 131911. https://doi.org/10.1016/j.chemosphere.2021.131911.

Shahbaz, M., Ravet, K., Peers, G., Pilon, M., 2015. Prioritization of copper for the use in photosynthetic electron transport in developing leaves of hybrid poplar. Front. Plant Sci. 6 https://doi.org/10.3389/fpls.2015.00407.

Tan, W., Gao, Q., Deng, C., Wang, Y., Lee, W.-Y., Hernandez-Viezcas, J.A., Peralta-Videa, J.R., Gardea-Torresdey, J.L., 2018. Foliar exposure of cu(OH)2 Nanopesticide to basil (Ocimum basilicum): variety-dependent copper translocation and biochemical responses. J. Agric. Food Chem. 66, 3358–3366. https://doi.org/10.1021/acs.jafc.8b00339.

Valdes, C., Cota-Ruiz, K., Flores, K., Ye, Y., Hernandez-Viezcas, J.A., Gardea-Torresdey, J.L., 2020a. Antioxidant and defense genetic expressions in corn at early-developmental stage are differentially modulated by copper form exposure (nano, bulk, ionic): nutrient and physiological effects. Ecotoxicol. Environ. Saf. 206, 111197 https://doi.org/10.1016/j.ecoenv.2020.111197.

Valdes, C., Cota-Ruiz, K., Flores, K., Ye, Y., Hernandez-Viezcas, J.A., Gardea-Torresdey, J.L., 2020b. Antioxidant and defense genetic expressions in corn at early-developmental stage are differentially modulated by copper form exposure (nano, bulk, ionic): nutrient and physiological effects. Ecotoxicol. Environ. Saf. 206, 111197 https://doi.org/10.1016/j.ecoenv.2020.111197.

van Maarschalkerweerd, M., Bro, R., Egebo, M., Husted, S., 2013. Diagnosing latent copper deficiency in intact barley leaves (Hordeum vulgare, L.) using near infrared spectroscopy. J. Agric. Food Chem. 61, 10901–10910. https://doi.org/10.1021/jf402166g.

Vandesompele, J., De Preter, K., Pattyn, F., Poppe, B., Van Roy, N., De Paepe, A., Speleman, F., 2002. Accurate Normalization of Real-Time Quantitative RT-PCR data by Geometric Averaging of Multiple Internal Control Genes [WWW document]. URL. https://doi.org/10.1186/gb-2002-3-7-research0034 (accessed 8.9.22).

Wang, P., Lombi, E., Zhao, F.-J., Kopittke, P.M., 2016. Nanotechnology: a new opportunity in plant sciences. Trends Plant Sci. 21, 699–712. https://doi.org/10.1016/j.tplants.2016.04.005.

Wang, Y., Deng, C., Cota-Ruiz, K., Peralta-Videa, J.R., Sun, Y., Rawat, S., Tan, W., Reyes, A., Hernandez-Viezcas, J.A., Niu, G., Li, C., Gardea-Torresdey, J.L., 2020. Improvement of nutrient elements and allicin content in green onion (Allium fistulosum) plants exposed to CuO nanoparticles. Sci. Total Environ. 725, 138387 https://doi.org/10.1016/j.scitotenv.2020.138387.

Wintz, H., Fox, T., Wu, Y.-Y., Feng, V., Chen, W., Chang, H.-S., Zhu, T., Vulpe, C., 2003. Expression profiles of Arabidopsis thaliana in mineral deficiencies reveal novel transporters involved in metal homeostasis. J. Biol. Chem. 278, 47644–47653. https://doi.org/10.1074/jbc.M309338200.

Xia, X., Xie, C., Cai, S., Yang, Z., Yang, X., 2006. Corrosion characteristics of copper microparticles and copper nanoparticles in distilled water. Corros. Sci. 48, 3924–3932. https://doi.org/10.1016/j.corsci.2006.04.007.

Xu, T., Wang, Y., Aytac, Z., Zuverza-Mena, N., Zhao, Z., Hu, X., Ng, K.W., White, J.C., Demokritou, P., 2022. Enhancing agrichemical delivery and plant development with biopolymer-based stimuli responsive core–shell nanostructures. ACS Nano 16, 6034–6048. https://doi.org/10.1021/acsnano.1c11490.

Yue, L., Ma, C., Zhan, X., White, J.C., Xing, B., 2017. Molecular mechanisms of maize seedling response to La2O3 NP exposure: water uptake, aquaporin gene expression and signal transduction. Environ. Sci.: Nano 4, 843–855. https://doi.org/10.1039/C6EN00487C.

Zhao, L., Hu, Q., Huang, Y., Fulton, A.N., Hannah-Bick, C., Adeleye, A.S., Keller, A.A., 2017a. Activation of antioxidant and detoxification gene expression in cucumber plants exposed to a Cu(OH)(2). Nanopesticide 4, 1750–1760. https://doi.org/10.1039/c7en00358g.

Zhao, L., Hu, Q., Huang, Y., Keller, A.A., 2017b. Response at genetic, metabolic, and physiological levels of maize (Zea mays) exposed to a cu(OH)2 Nanopesticide. ACS Sustain. Chem. Eng. 5, 8294–8301. https://doi.org/10.1021/acssuschemeng.7b01968.

Supplementary Materials

Transcriptional response of Cu-deficient barley (*Hordeum vulgare* L.) to foliar-applied nano-Cu: Molecular crosstalk between Cu loading into plants and changes in Cu homeostasis genes

Magdalena Kusiak[1], Magdalena Sozoniuk[1], Camille Larue[2], Renato Grillo[3], Krzysztof Kowalczyk[1], Patryk Oleszczuk[4], Izabela Jośko[1]*

[1] Institute of Plant Genetics, Breeding and Biotechnology, Faculty of Agrobioengineering, University of Life Sciences, 20-950 Lublin, Poland.

[2] Laboratoire Ecologie Fonctionnelle et Environnement, Université de Toulouse, CNRS, Toulouse 31062, France.

[3] Department of Physics and Chemistry, School of Engineering, São Paulo State University (UNESP), Ilha Solteira, SP 15385-000, Brazil.

[4] Department of Radiochemistry and Environmental Chemistry, Faculty of Chemistry, Maria Curie-Skłodowska University, 20-031 Lublin, Poland.

* Correspondence to: Izabela Jośko, Institute of Plant Genetics, Breeding and Biotechnology, Faculty of Agrobioengineering, Univerisity of Life Sciences in Lublin, 20–950 Lublin, 13 Akademicka Street, Poland, tel. +48 81 4456675, fax. +48 81 4456031, e–mail: izabela.josko@up.lublin.pl

Number of pages: 13
Number of tables: 5
Number of figures: 7

MATERIALS AND METHODS

Characteristics of nanopowder and nano-Cu suspension

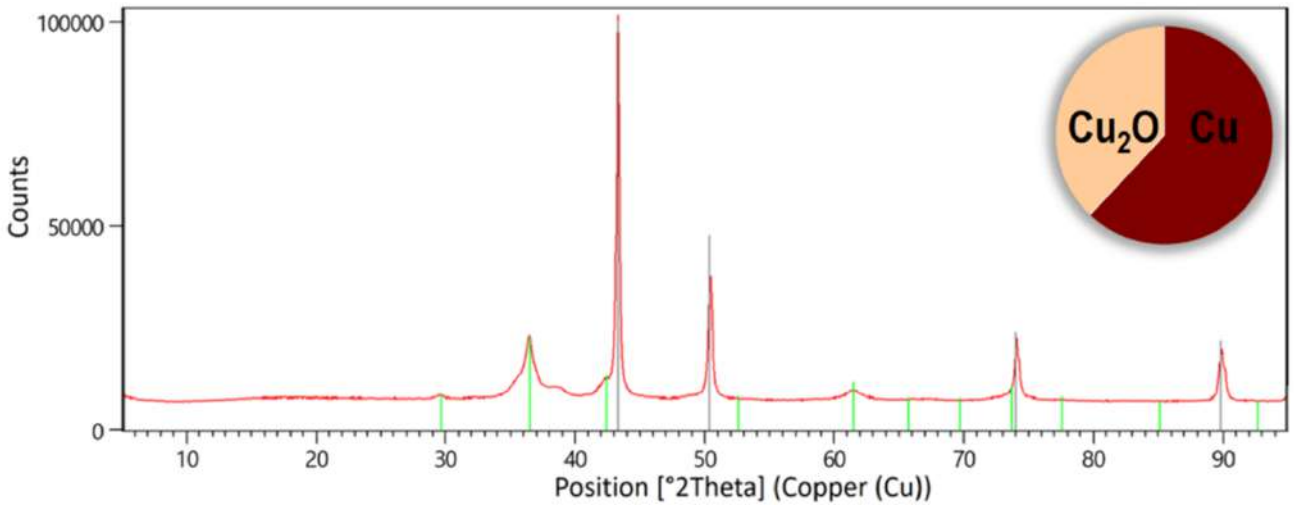

Fig. S1. XRD pattern of nano-Cu.

Dynamic light scattering technique (DLS). The distribution of aggregate sizes and ζ-potential of nano-Cu solution were determined with DLS (Zetasizer 3000, Malven, UK). Moreover, the aggregates of nano-Cu in solution was imaged with TEM (JEM–3010 TEM JEOL, Ltd., Japan) by the application of a drop of solution on the polymeric film.

Dissolution rate. The Cu^{+2} ion fraction was separated from nano-Cu solutions using ultrafiltration with Microsep Advance Centrifugal Devices with Omega Membrane 1K (Pall Corporation). The measurements of the dissolved metal fraction were conducted soon after sonication in an ultrasonic bath (25 ˚C, 250 W, 50 Hz) for 30 min using Inductively Coupled Plasma Optical Emission Spectrometer, ICP-OES (Thermo Fisher Scientific, iCAP 7200, USA). Axial configuration was used for Cu determinations. The spectral line (324.754 nm) was chosen to obtain the highest sensitivity and minimum interference.

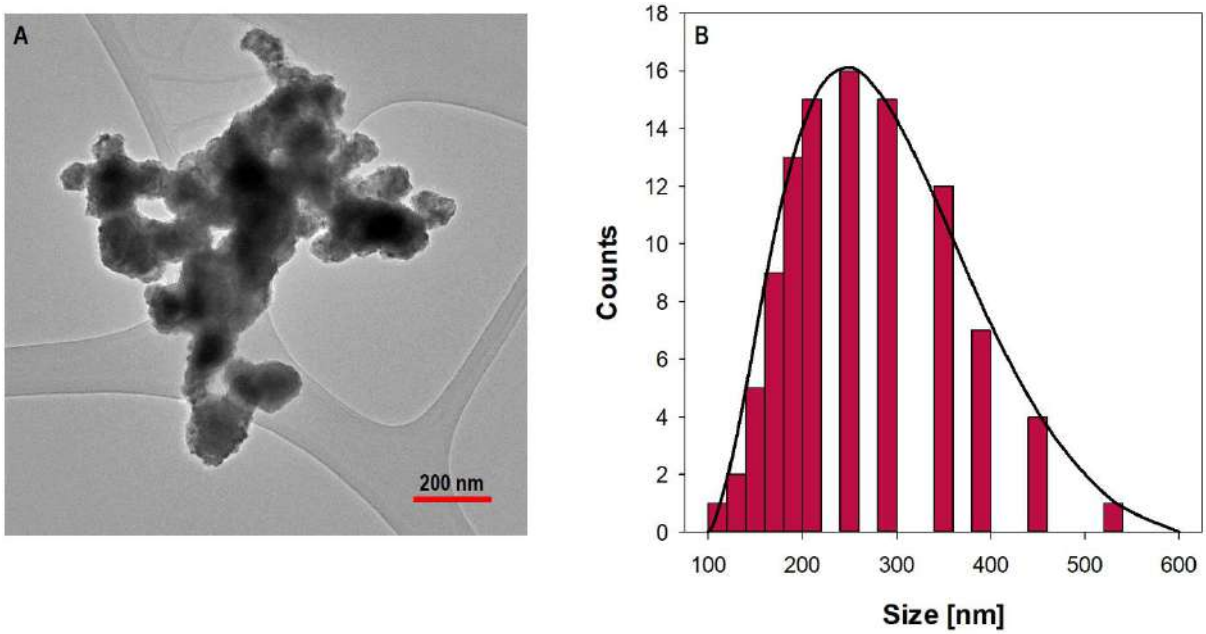

Fig. S2. Characteristics of nano-Cu solution (A) TEM image; (B) particle size distribution.

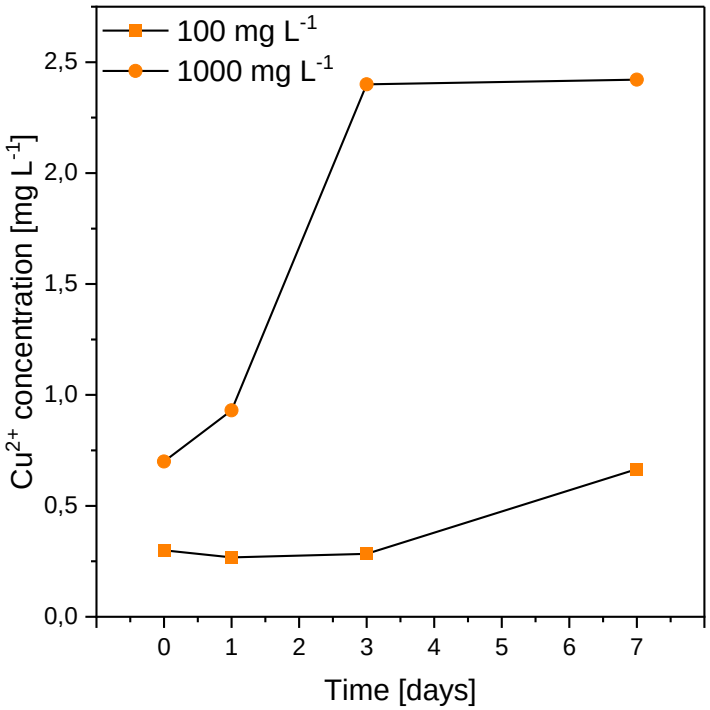

Fig. S3. Concentration of Cu^{2+} released from ENPs in solution used for foliar application.

Tab. S1. The average spray volume deposited on above ground parts of *H. vulgare* plants according to the volume of Cu compounds (100 and 1000 mg L^{1}) applied.

Deposited volume [%]				
Control	Nano-Cu		$CuSO_4$	
	100	1000	100	1000
Plants for 1 day exposure				
28.10±4.1	29.53±3.0	31.73±4.9	25.10±3.4	30.83±7.0
Plants for 7 days exposure				
32.60±4.2	28.60±4.6	22.83±4.7	27.37±7.5	28.37±4.3
Amount of Cu applied on 1 plant [mg]				
Plants for 1 day exposure				
0	0.03	1.05	0.08	1.02
Plants for 7 days exposure				
0	0.09	0.75	0.09	0.94

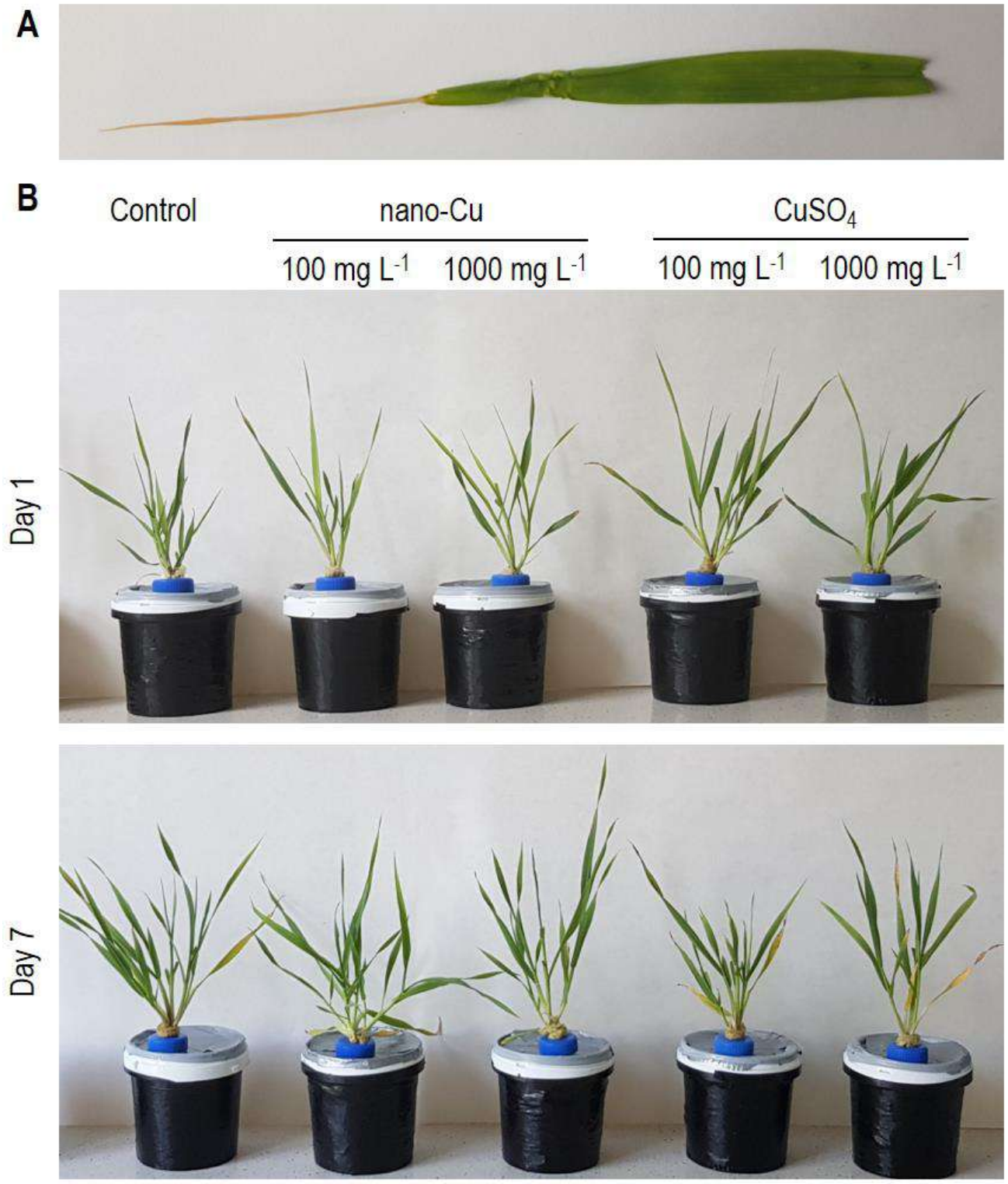

Fig. S4. Images of *H. vulgare* taken at 1 and 7 days after exposure to nano-Cu and $CuSO_4$.

Tab. S2. The dry weight of flag leaves under nano-Cu application. Different letters indicate significant differences among the treatments (Duncan' test, $p < 0.05$).

Exposure time	d.w. [mg kg^{-1}]				
	control	nano-Cu		$CuSO_4$	
		100 mg L^{-1}	1000 mgL^{-1}	100 mg L^{-1}	1000 mgL^{-1}
1 day	15.2±1.2[a]	12.8±1.0[a]	15.7±3.4[a]	16.4±1.5[a]	15.4±0.9[a]
7 days	18.1±1.9[a]	37.5±4.3[b]	23.4±2.9[ab]	20.1±1.9[a]	21.5±2.1[a]

Tab. S3. Sequences of primers used in real-time qPCR

Gene	Primer (5′ → 3′) sequence	NCBI/ Phytozome Acc. number	Reference
ADP	5'-GCGATGAATGCGGCTGAAAT-3' 5'-TCTGAATGTACCAGTGCCGC-3'	AJ508228.2	(Jośko et al.. 2021b)
ACT	5'-AATCCACGAGACGACCTAC-3' 5'-ACCACTGAGCACGATGTT-3'	AY145451.1	(Jośko et al.. 2021b)
GAPDH	5'-GACAGCAGGTCCAGCATCTT-3' 5'-GATCAGGTCGACAACACGGT-3'	X60343.1	This study
COPT5	5'-AAACGAACGTCTGCAATCCC-3' 5'-CCCAAGGTGTGAATGTGTGT-3'	DK830819.1	(Jośko et al.. 2021b)
RAN1	5'-GCATTAGCGACCTCATTAG-3' 5'-GCCTTATCTTGCTCACTAC-3'	HORVU6Hr1G03 1960.1	(Jośko et al.. 2021b)
PAA1	5'-ATGTGCTCTTGGTCTTGCCA-3' 5'-TCCCTCGCTGTGAGAAGCTA-3'	AK355848.1	(Jośko et al.. 2021b)
PAA2	5'-TTCGCCATGACACCATCTCTT-3' 5'-CAGATCATCGGGCCCTGGTC-3'	HORVU0Hr1G00 9080.5	(Jośko et al.. 2021b)
NIP2;1	5'-ATCATCGTCACCTTCAACAT-3' 5'-CTAACCCTGCCAACTCAC-3'	AB540229.1	This study
TIP1;1	5'-TCAGCAGGATCGCCGTGG-3' 5'-GAAGACGAAGATGAGCGTGGAG-3'	AB540221.1	This study
TIP1;2	5'-GTCTGGGAGAACCACTGG-3' 5'-GCCGATGAAGCAGATGTC-3'	AB540226.1	This study
PIP1;1	5'-ATCTACAACAGGGAGCAC-3' 5'-TAGGACTTGGTCTTGAATGG	AB286964.1	This study
SOD Cu-Zn	5'-GGTGACACGACTAATGGAT-3' 5'-TGACGGACTTCATCTTCTG-3'	HORVU7Hr1G06 0130.2	(Jośko et al.. 2021a)
SOD Fe	5'-GTCTCCGAATGCTATCAATC-3' 5'-TTCTCATAATCCAGGTAGTAGG	HORVU7Hr1G00 8390.6	This study
SOD Mn	5'-CTTTGTTGGGAATTGATGTCT-3' 5'-CAGATGTTGGTCAGGTAGT-3'	HORVU2Hr1G11 7740.2	This study
CAT	5'-CACTCAACTACAGGCACAT-3' 5'-ATCATCCAAGAGGCACTTC-3'	HORVU7Hr1G12 1700.1	(Jośko et al.. 2021a)

Tab. S4. Real-time qPCR reaction conditions.

Gene	Temperature [°C]	Primer concentration [nM]	cDNA amount [ng]
ADP	60	300	10
ACT	60	300	10
GAPDH	60	300	10
COPT5	60	300	10
PAA1	60	300	10
PAA2	60	300	10
RAN1	60	300	40
NIP2;1	60	100	10
TIP1;1	62	100	10
TIP1;2	60	300	10
PIP1;1	60	300	10
SOD Cu-Zn	60	300	10
SOD Fe	60	600	10
SOD Mn	60	300	10
CAT	60	300	10

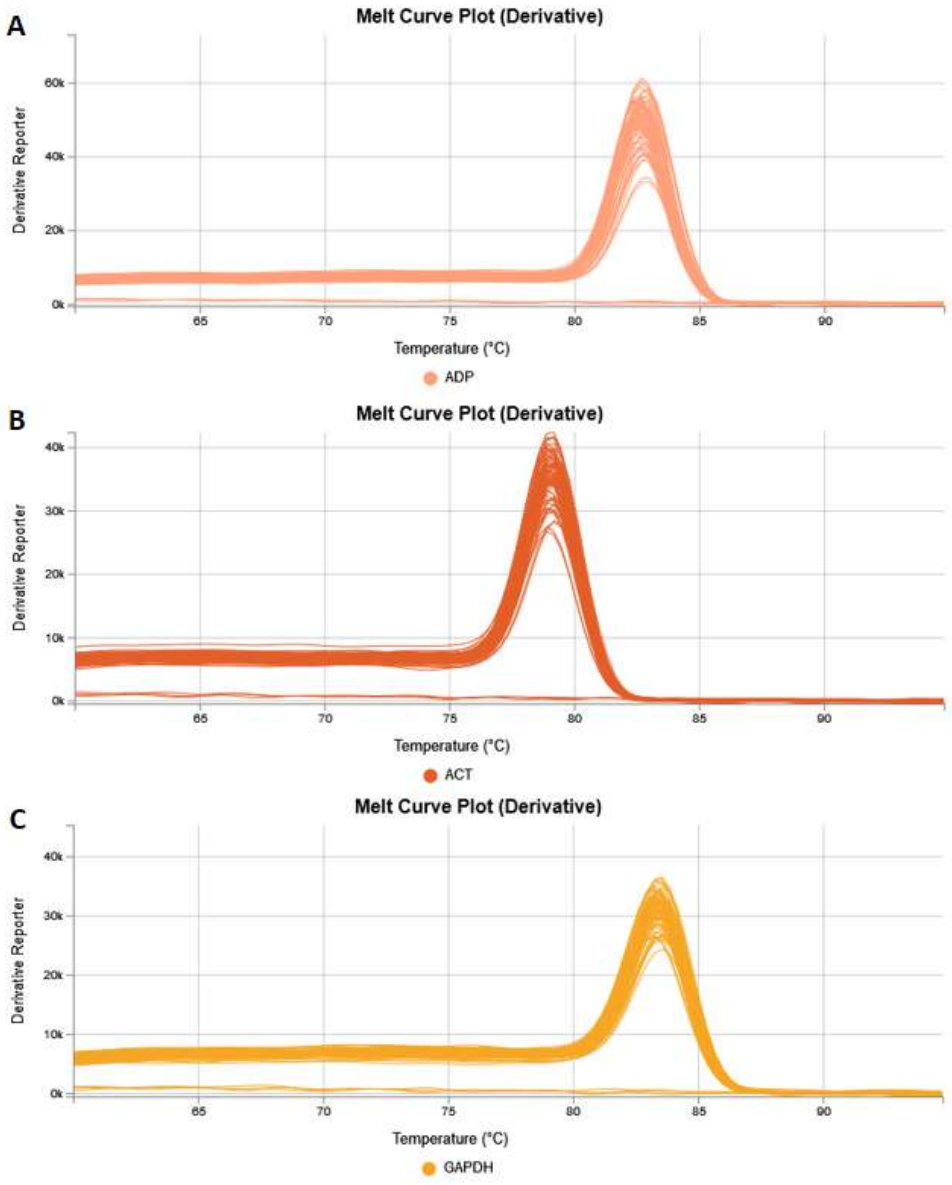
A
Melt Curve Plot (Derivative)
Derivative Reporter
60k
40k
20k
0k
65
70
75
80
85
90
Temperature (°C)
ADP
B
Melt Curve Plot (Derivative)
Derivative Reporter
40k
30k
20k
10k
0k
65
70
75
80
85
90
Temperature (°C)
ACT
C
Melt Curve Plot (Derivative)
Derivative Reporter
40k
30k
20k
10k
0k
65
70
75
80
85
90
Temperature (°C)
GAPDH

D

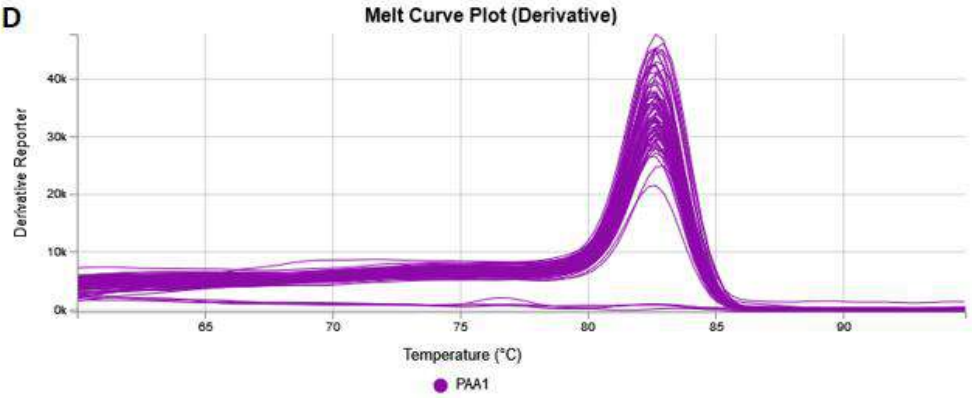
Melt Curve Plot (Derivative)
Derivative Reporter
40k
30k
20k
10k
0k
65
70
75
80
85
90
Temperature (°C)
PAA1

E

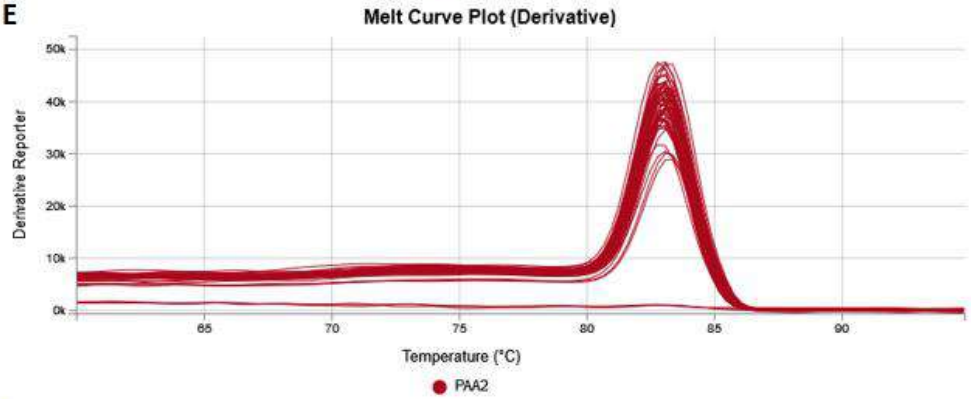
Melt Curve Plot (Derivative)
Derivative Reporter
50k
40k
30k
20k
10k
0k
65
70
75
80
85
90
Temperature (°C)
PAA2

F

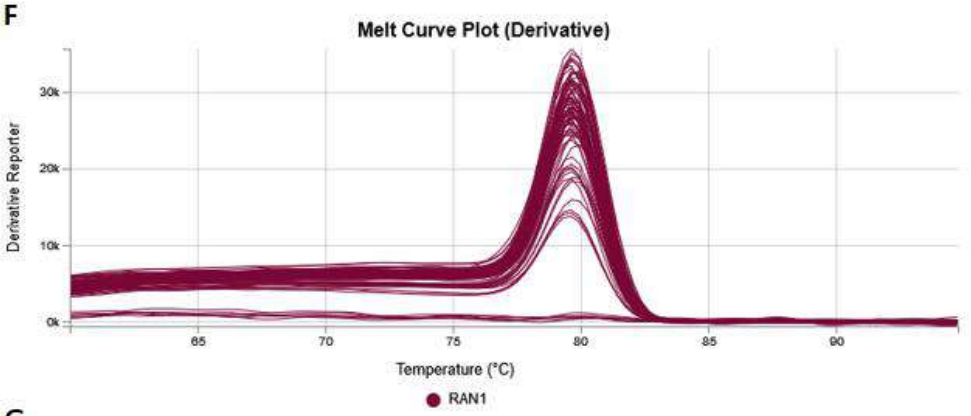
Melt Curve Plot (Derivative)
Derivative Reporter
30k
20k
10k
0k
65
70
75
80
85
90
Temperature (°C)
RAN1

G

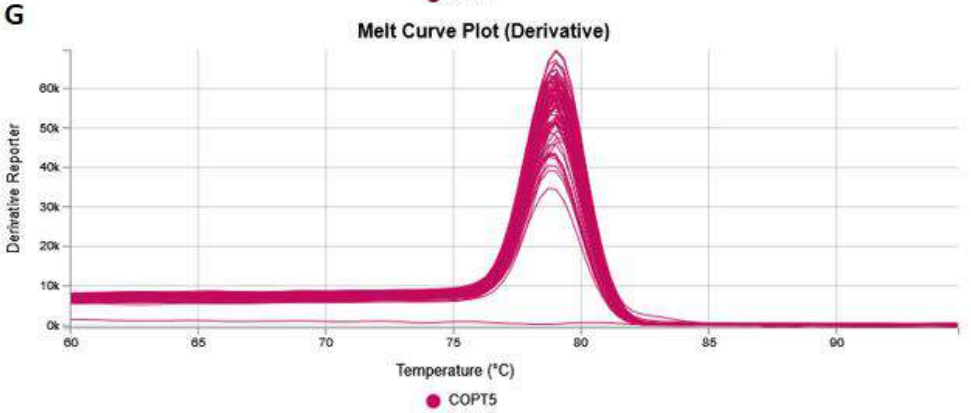
Melt Curve Plot (Derivative)
Derivative Reporter
60k
50k
40k
30k
20k
10k
0k
60
65
70
75
80
85
90
Temperature (°C)
COPT5

H

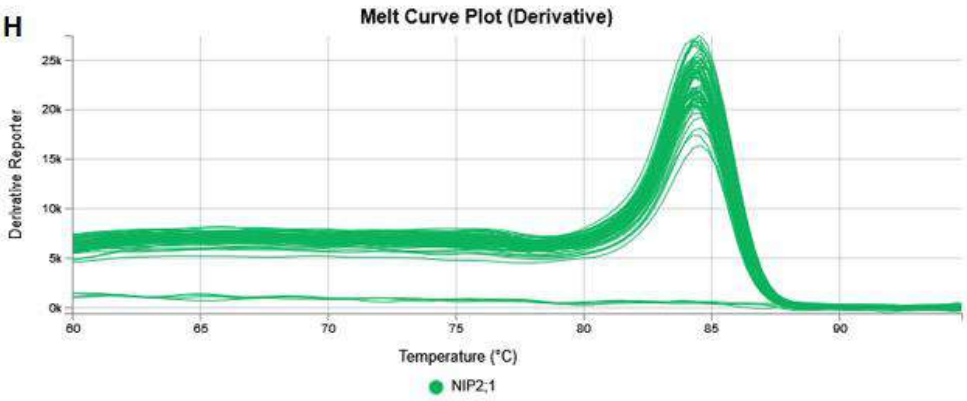
Melt Curve Plot (Derivative)
Derivative Reporter
25k
20k
15k
10k
5k
0k
60
65
70
75
80
85
90
Temperature (°C)
NIP2;1

I

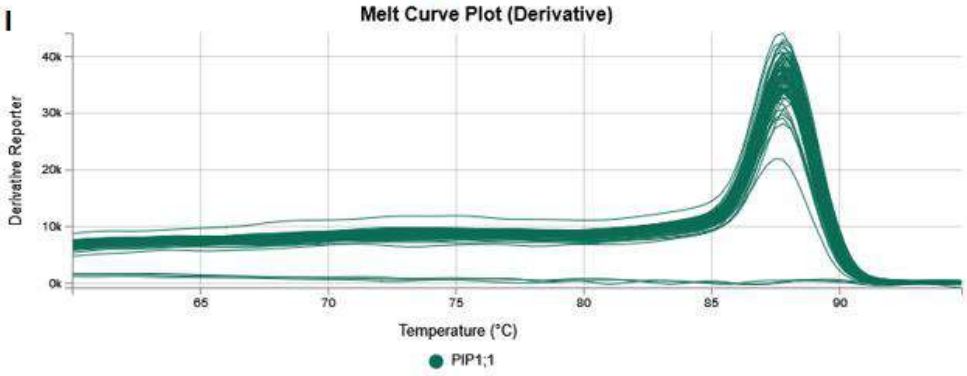
Melt Curve Plot (Derivative)
Derivative Reporter
40k
30k
20k
10k
0k
65
70
75
80
85
90
Temperature (°C)
PIP1;1

J

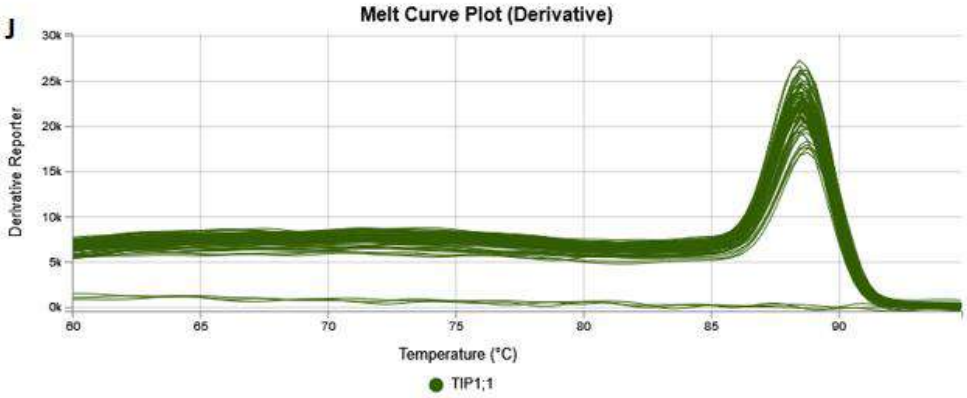
Melt Curve Plot (Derivative)
Derivative Reporter
30k
25k
20k
15k
10k
5k
0k
60
65
70
75
80
85
90
Temperature (°C)
TIP1;1

K

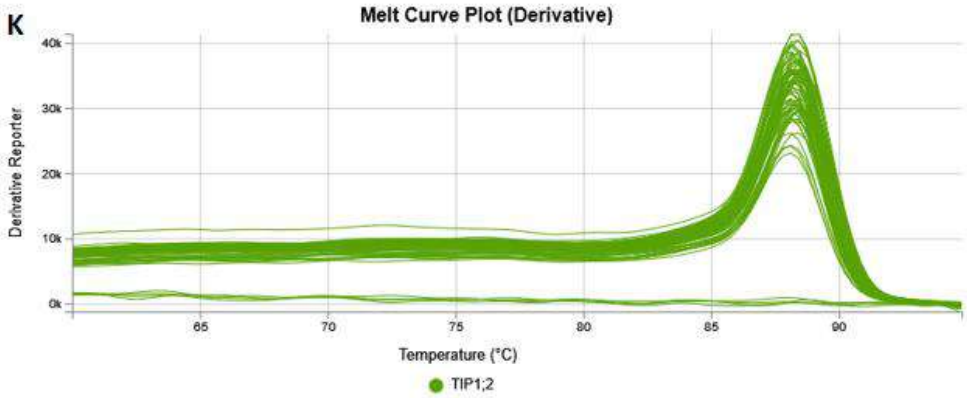
Melt Curve Plot (Derivative)
Derivative Reporter
40k
30k
20k
10k
0k
65
70
75
80
85
90
Temperature (°C)
TIP1;2

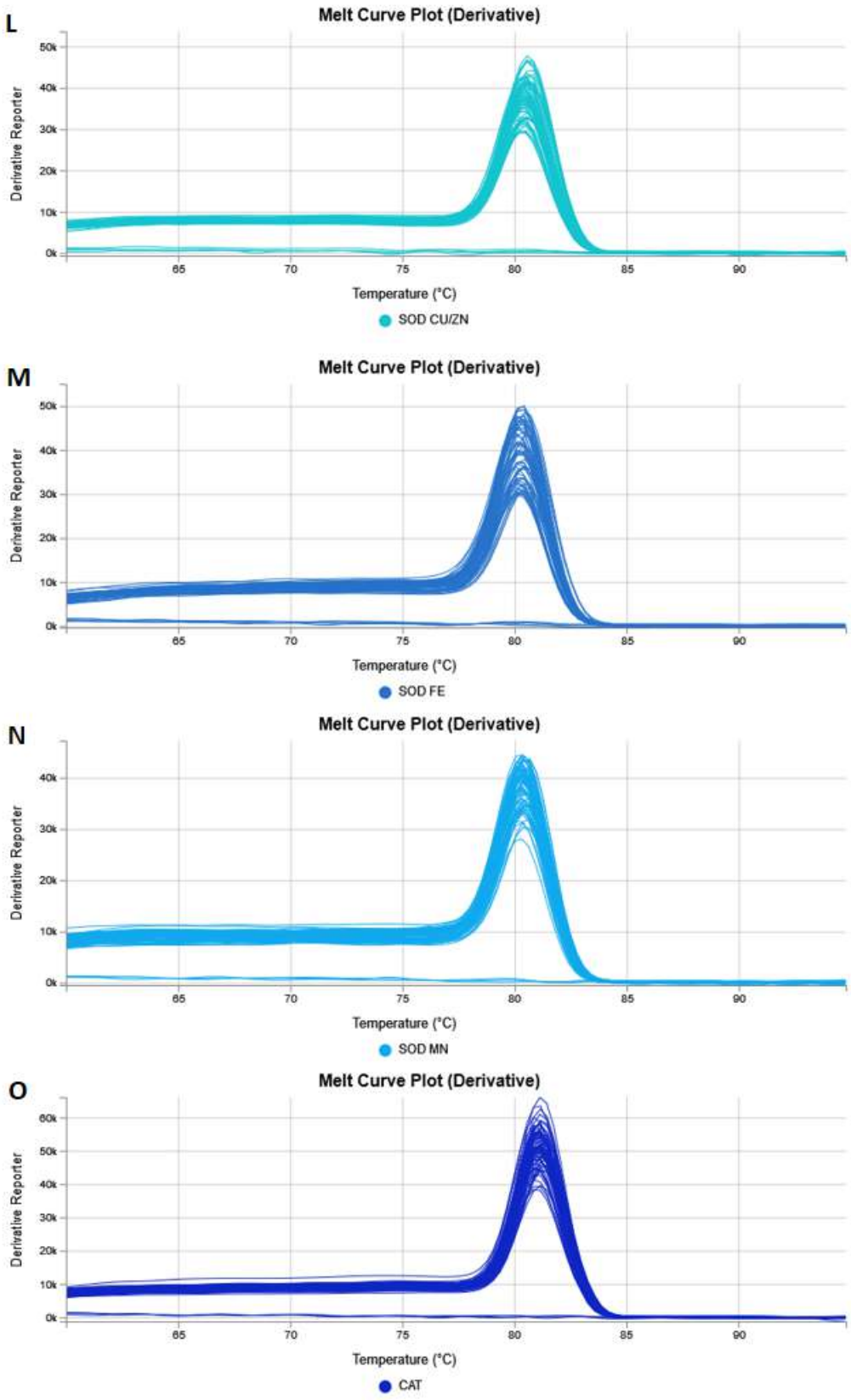

Fig. S5. Melting curve analysis obtained for: (A-C) reference genes (*ACT. ADP. GAPDH*). (D-G) metal transporters (*RAN1. COPT5. PAA1.vPAA2*). (H-K) aquaporins (*NIP2;1. PIP1;1. TIP1;1.TIP1;2*). and (L-O) antioxidant enzymes (*SOD Cu/Zn. SOD Fe. SOD Mn. CAT*) genes. Single peaks indicate specific amplification and lack of primer–dimer artifacts.

Tab. S5. Cu content in the roots and aboveground parts of *H. vulgare* after foliar application with Cu compounds (100 and 1000 mg L^{1}). Different letters indicate significant differences among the treatments (Tukey's test, $p < 0.05$).

Treatments	Concentration [mg L^{-1}]	Dry weight [mg]	
		Roots	Shoots and leaves
control	-	26.10±1.1^{a}	98.72±2.2^{a}
nano-Cu	100	28.42±1.3^{a}	105.81±1.5^{b}
	1000	25.73±1.7^{a}	106.34±3.1^{b}
$CuSO_4$	100	29.50±1.3^{a}	107.10±1.1^{b}
	1000	26.50±1.5^{a}	120.61±11.0^{c}
control	-	45.21±0.9^{a}	102.73±1.4^{a}
nano-Cu	100	54.00±1.8^{b}	126.09±0.9^{b}
	1000	66.10±1.0^{c}	190.24±0.8^{c}
$CuSO_4$	100	99.50±0.8^{e}	192.65±1.5^{c}
	1000	81.70±1.6^{d}	220.24±1.4^{d}

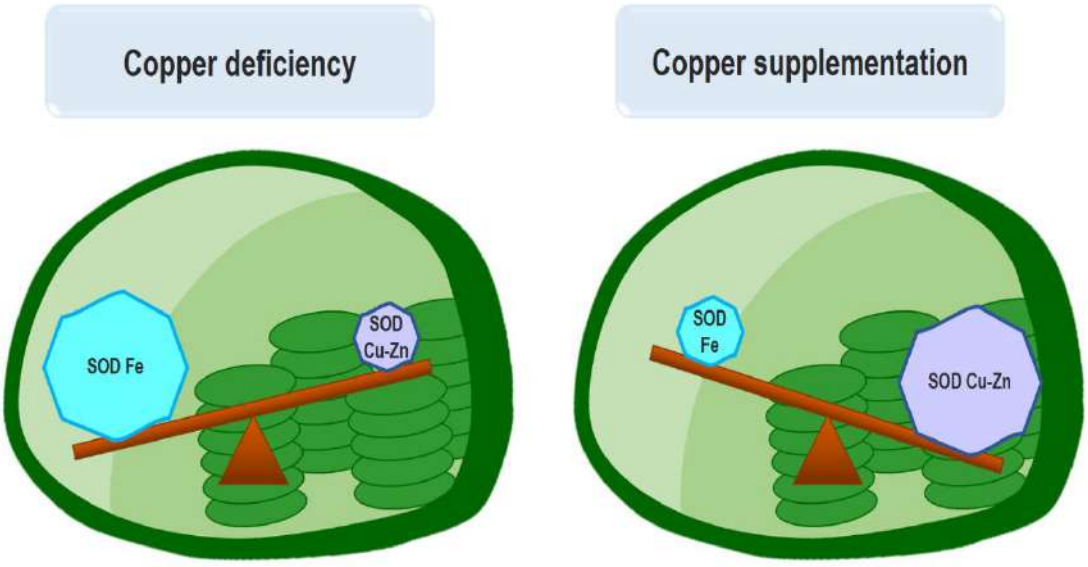

Fig. S6. Schematic representation of substitution relation between *SOD Cu-Zn* and *SOD Fe* depending on Cu status in *H. vulgare* plants.

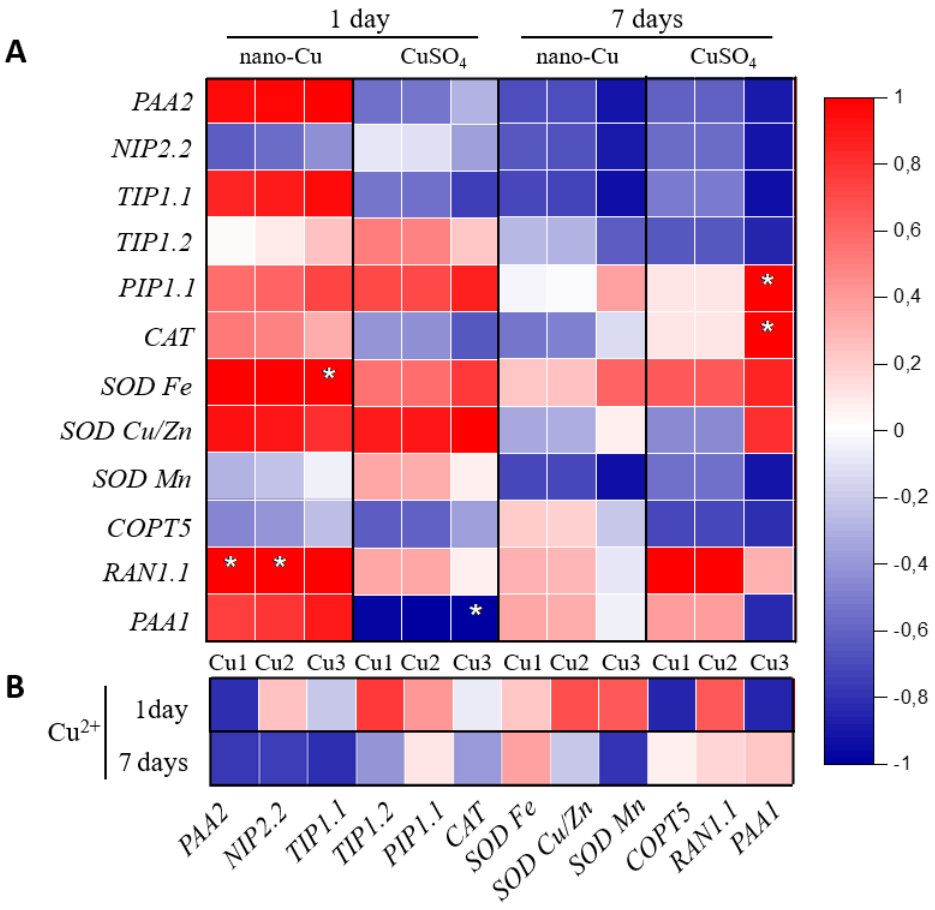

Fig. S7. The correlation plot for the relation between the transcripts of genes and the used rates of Cu compounds (Cu1), the remained Cu amount on plants (Cu2), the Cu content in flag leaves (Cu3) based on Pearson factor (A). The correlation between the selected genes expression and released of Cu ions in nano-Cu solutions used to foliar application. The red and blue colours mean positive and negative correlations, respectively. The asterisks indicate the significant correlation ($p < 0.05$).

References

Jośko. I.. Kusiak. M.. Oleszczuk. P.. Świeca. M.. Kończak. M.. Sikora. M.. 2021a. Transcriptional and biochemical response of barley to co-exposure of metal-based nanoparticles. Science of The Total Environment 782. 146883. https://doi.org/10.1016/j.scitotenv.2021.146883

Jośko. I.. Kusiak. M.. Xing. B.. Oleszczuk. P.. 2021b. Combined effect of nano-CuO and nano-ZnO in plant-related system: From bioavailability in soil to transcriptional regulation of metal homeostasis in barley. Journal of Hazardous Materials 416. 126230. https://doi.org/10.1016/j.jhazmat.2021.126230

Lublin, 29.08.2023

Magdalena Kusiak
Instytut Genetyki, Hodowli i
Biotechnologii Roślin
Uniwersytet Przyrodniczy w Lublinie
Ul. Akademicka 15,
20-950 Lublin
Tel: 508 789 096
magdalena.kusiak@up.lublin.pl

Rada Dyscypliny Rolnictwo i Ogrodnictwo
Uniwersytetu Przyrodniczego
w Lublinie

Oświadczenie o współautorstwie

Oświadczam, że mój udział w pracy "*Transcriptional response of Cu-deficient barley (Hordeum vulgare L.) to foliar-applied nano-Cu: Molecular crosstalk between Cu loading into plants and changes in Cu homeostasis genes*" [NanoImpact, 2023] wynosi 51%.

Mój wkład polegał na opracowaniu koncepcji badań i metodyki, planowaniu i wykonaniu analiz laboratoryjnych wraz z opracowaniem wyników i ich interpretacją oraz na przygotowaniu manuskryptu i odpowiedzi na recenzje pracy.

Magdalena Kusiak

Podpis

Lublin, 04.07.2023

Dr inż. Magdalena Sozoniuk
Instytut Genetyki, Hodowli i
Biotechnologii Roślin
Uniwersytet Przyrodniczy w Lublinie
Ul. Akademicka 15,
20-950 Lublin
Tel. 814456928
magdalena.sozoniuk@up.lublin.pl

Rada Dyscypliny Rolnictwo i Ogrodnictwo
Uniwersytetu Przyrodniczego
w Lublinie

Oświadczenie o współautorstwie

Oświadczam, że mój udział w pracy "*Transcriptional response of Cu-deficient barley (Hordeum vulgare L.) to foliar-applied nano-Cu: Molecular crosstalk between Cu loading into plants and changes in Cu homeostasis genes*" [NanoImpact, 2023] wynosi 14%.

Mój wkład polegał na udziale w opracowaniu metodyki badań, planowaniu i wykonaniu analiz laboratoryjnych wraz z opracowaniem wyników oraz na redagowaniu manuskryptu.

Sozoniuk M.

Podpis

Toulouse, 21.07.2023

Camille Larue Ph.D.
Laboratoire Ecologie Fonctionnelle et Environnement
Université de Toulouse, CNRS
Toulouse 31062, France
camille.larue@ensat.fr

Discipline Council for Agriculture and Horticulture
of University of Life Sciences
in Lublin

Statement of co-authorship

I declare that my contribution to the article *"Transcriptional response of Cu-deficient barley (Hordeum vulgare L.) to foliar-applied nano-Cu: Molecular crosstalk between Cu loading into plants and changes in Cu homeostasis genes"* [NanoImpact, 2023] is 5%.

My contribution consisted of participation in the formulation of investigative methodology and in the writing (review and editing) of the manuscript.

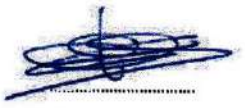

Signature

São Paulo, 21.07.2023

Renato Grillo, Ph.D.
Department of Physics and Chemistry
School of Engineering, São Paulo State University (UNESP)
Ilha Solteira, SP 15385-000, Brazil
renato.grillo@unesp.br

Discipline Council for Agriculture and Horticulture
of University of Life Sciences
in Lublin

Statement of co-authorship

I declare that my contribution to the article *"Transcriptional response of Cu-deficient barley (Hordeum vulgare L.) to foliar-applied nano-Cu: Molecular crosstalk between Cu loading into plants and changes in Cu homeostasis genes"* [NanoImpact, 2023] is 5%.

My contribution consisted of participation in the formulation of investigative methodology and in the writing (review and editing) of the manuscript.

gov.br Documento assinado digitalmente
RENATO GRILLO
Data: 22/07/2023 10:21:10-0300
Verifique em https://validar.iti.gov.br

.....

Signature

Lublin, 05.07.2023r.

Prof. dr hab. Krzysztof Kowalczyk
Instytut Genetyki, Hodowli i
Biotechnologii Roślin
Uniwersytet Przyrodniczy w Lublinie
Ul. Akademicka 15,
20-950 Lublin
Tel. 814456747
krzysztof.kowalczyk@up.lublin.pl

Rada Dyscypliny Rolnictwo i Ogrodnictwo
Uniwersytetu Przyrodniczego
w Lublinie

Oświadczenie o współautorstwie

Oświadczam, że mój udział w pracy "*Transcriptional response of Cu-deficient barley (Hordeum vulgare L.) to foliar-applied nano-Cu: Molecular crosstalk between Cu loading into plants and changes in Cu homeostasis genes*" [NanoImpact, 2023] wynosi 5%.

Mój wkład polegał na udziale w przygotowaniu i redagowaniu manuskryptu.

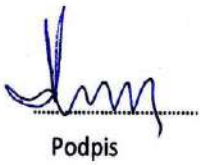

Podpis

Lublin, 28.07.2023

Prof. dr hab. Patryk Oleszczuk
Katedra Radiochemii i
Chemii Środowiskowej
Uniwersytet Marii Curie-Skłodowskiej
pl. Marii Curie-Skłodowskiej 3/425
20-031 Lublin
Tel. 81 537 55 15
patryk.oleszczuk@mail.umcs.pl

Rada Dyscypliny Rolnictwo i Ogrodnictwo
Uniwersytetu Przyrodniczego
w Lublinie

Oświadczenie o współautorstwie

Oświadczam, że mój udział w pracy "*Transcriptional response of Cu-deficient barley (Hordeum vulgare L.) to foliar-applied nano-Cu: Molecular crosstalk between Cu loading into plants and changes in Cu homeostasis genes*" [NanoImpact, 2023] wynosi 5%.

Mój wkład polegał na udziale w przygotowaniu i redagowaniu manuskryptu.

.....
Podpis

Lublin, 03.07.2023

Dr hab. Izabela Jośko, prof. uczelni
Instytut Genetyki, Hodowli
i Biotechnologii Roślin
Uniwersytet Przyrodniczy w Lublinie
Ul. Akademicka 15,
20-950 Lublin
Tel. 814456675
izabela.josko@up.lublin.pl

Rada Dyscypliny Rolnictwo i Ogrodnictwo
Uniwersytetu Przyrodniczego
w Lublinie

Oświadczenie o współautorstwie

Oświadczam, że mój udział w pracy "*Transcriptional response of Cu-deficient barley (Hordeum vulgare L.) to foliar-applied nano-Cu: Molecular crosstalk between Cu loading into plants and changes in Cu homeostasis genes*" [NanoImpact, 2023] wynosi 15%.

Mój wkład polegał na kierowaniu projektem naukowym obejmującym badania opisane w tej pracy oraz pozyskaniu funduszy na badania. Ponadto, odpowiadałam za opracowanie koncepcji badań i metodyki oraz za przygotowanie manuskryptu do publikacji i odpowiedzi na otrzymane recenzje pracy.

Izabela Jośko

Podpis

PIV

Jośko I., **Kusiak M.**, Różyło K., Baranowska-Wójcik E., Sierocka M., Sheteiwy M., Szwajgier D., Świeca M.

The life cycle study revealed distinct impact of foliar-applied nano-Cu on antioxidant traits of barley grain comparing with conventional agents

Food Research International . (2023) T. 164 s. 112303

DOI: 10.1016/j.foodres.2022.112303

$IF_{(2023)} = 8.1$

Punkty MEiN = 140

Food Research International 164 (2023) 112303

Contents lists available at ScienceDirect

Food Research International

journal homepage: www.elsevier.com/locate/foodres

The life cycle study revealed distinct impact of foliar-applied nano-Cu on antioxidant traits of barley grain comparing with conventional agents

Izabela Jośko [a,*], Magdalena Kusiak [a], Krzysztof Różyło [b], Ewa Baranowska-Wójcik [c], Małgorzata Sierocka [d], Mohamed Sheteiwy [e], Dominik Szwajgier [c], Michał Świeca [d]

[a] Institute of Plant Genetics, Breeding and Biotechnology, Faculty of Agrobioengineering, University of Life Sciences, 15 Akademicka Street, 20-950 Lublin, Poland
[b] Department of Agricultural Ecology, Faculty of Agrobioengineering, University of Life Sciences, 13 Akademicka Street, 20-950 Lublin, Poland
[c] Department of Biotechnology, Microbiology and Human Nutrition, Faculty of Food Science and Biotechnology, University of Life Sciences, 8 Skromna Street, 20-704 Lublin, Poland
[d] Department of Biochemistry and Food Chemistry, Faculty of Food Science and Biotechnology, University of Life Sciences, 8 Skromna Street, 20-704 Lublin, Poland
[e] Department of Agronomy, Faculty of Agriculture, Mansoura University, 60 Elgomhoria Street, 35516 Mansoura, Egypt

ARTICLE INFO

Keywords:
Engineered nanoparticles
Biofortification
Microelements
Antioxidants
Hordeum vulgare

ABSTRACT

Despite that the applicability of Cu-based engineered nanoparticles (ENPs) as an antibacterial and antifungal agent for plant protection has been studied widely, little is known about their role in the improvement of crop yield and quality. Here, a full life study was performed to investigate the nutritional quality and bioactivity of barley grains under foliar application of nano-/microparticulate (nano-Cu, nano-CuO, micro-Cu) and ionic Cu compounds ($CuSO_4$, CuEDTA). *Hordeum vulgaris* L. plants were sprayed with Cu compounds at 500 mg/L during the end of tillering and the beginning of heading. Yield, mineral composition, protein and dietary content, antioxidant (phenolic, anthocyanin, flavonoid, tannin, flavanol) content and antioxidant capacity of barley grain were evaluated. Grain yield was unaffected by all treatments. Only nano-Cu and ionic compounds enhanced Cu accumulation in grain: 2-fold increase was observed compared to the control (2.6 μg/kg). Nano-Cu also increased the dietary fiber content by 19.9 %, while no impact of the other treatments was determined. The content of phenolic compounds, the main group of antioxidants, remained unchanged after Cu supply. In general, for all Cu treatment, antiradical and reducing abilities were decreased or were at the similar level in relation to the control. On the other hand, chelating power in grain extracts was 2–4 times higher under nano-Cu/nano-CuO/micro-Cu than in the untreated sample, while the ionic compounds had no impact on the chelating indicator. Our results demonstrated that more favorable effects were triggered by nano-Cu than $CuSO_4$ or CuEDTA on the tested indicators of barley grain, despite that both compounds resulted in similar superior Cu acquisition. It suggests that nano-Cu may be considered as an alternative agent to be used as economic and traditional fertilizers.

1. Introduction

A growing world population, which will be nearly 10 billion by 2050, entails an increase in food demand (FAO, 2018). To meet that need, agricultural production must be increased by 60 % (Alexandratos & Bruinsma, 2012). In the face of shrinkage of arable land, climate change and soil degradation, providing food security is a pressing challenge. Application of conventional fertilizers to meet plant requirements is inefficient (Avellan et al., 2021). As estimated, up to 50 % of applied nutrients do not reach their target (Kah et al., 2019). Consequently, wasted compounds contaminate soil and groundwater causing environmental and public health threats (Avellan et al., 2021). Therefore, new approaches are highly requested to increase yield as well as to improve nutritional quality of strategic crops (biofortification). To address these goals, nano-enabled agrochemicals such as nano-fertilizers have attracted a growing interest in precision agriculture, especially now, that the costs of production of engineered nanoparticles (ENPs) are getting lower (Kah et al., 2019). ENPs, owing to the nano-metric size (1–100 nm) and larger surface area, obtain more efficient physico-chemical properties (e.g. reactivity) than their bulk counterparts (Kusiak et al., 2022). ENPs containing micronutrients belong to promising fertilizing agents due to gradual release of metal ions prolonging

* Corresponding author at: Institute of Plant Genetics, Breeding and Biotechnology, Faculty of Agrobioengineering, Univerisity of Life Sciences, 20-950 Lublin, 13 Akademicka Street, Poland.
E-mail address: izabela.josko@up.lublin.pl (I. Jośko).

https://doi.org/10.1016/j.foodres.2022.112303
Received 11 April 2022; Received in revised form 1 December 2022; Accepted 3 December 2022
Available online 15 December 2022

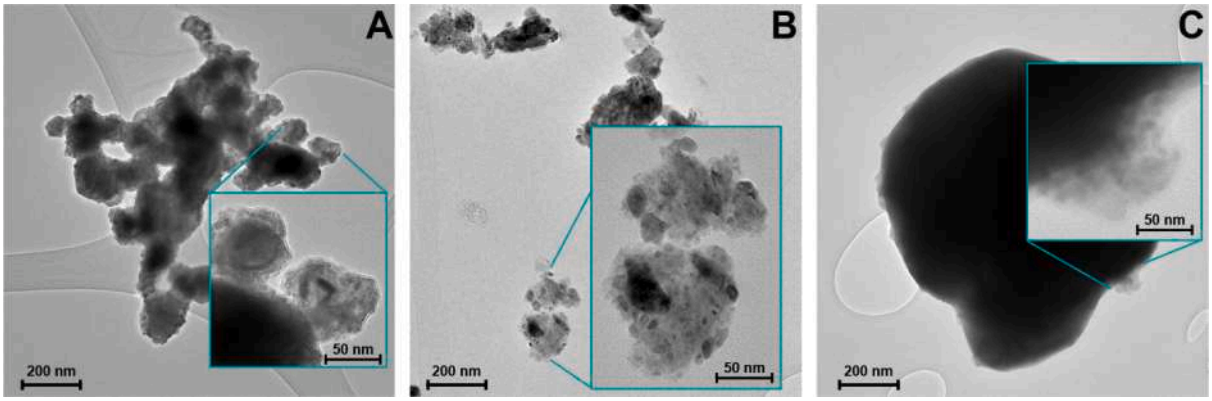

Fig. 1. TEM images of nano-Cu (A), nano-CuO (B), bulk-Cu (C) suspended in Milli-Q® –water.

the access to micronutrients for plants, as opposed to the conventional fertilizers, which are dissolved just after application (Kah et al., 2019). In addition, more effective usage of micronutrients from ENPs than ionic compounds by plants reduces the spread of fertilizer residues and, indirectly, protects environmental resources (Kusiak et al., 2022).

To date, numerous studies have demonstrated beneficial outputs for plant growth and development under treatment of ENPs. However, the majority of these studies included only short-term exposure to ENPs, whereas the full plant life-cycle effect of ENPs containing crucial nutrients (e.g. Zn, Fe, Cu) was scarcely examined in terms of their potential for enhancement of mineral and nutritional quality of crops (Deng et al., 2022; Kadri et al., 2022; Rawat et al., 2018a; Rui et al., 2018; Wang et al., 2019; Zhang et al., 2017). Considering over 2 billion people suffer from micronutrient malnutrition, so-called hidden hunger (Narwal et al., 2020), it is mandatory to assess the efficiency of ENPs for boosting micronutrient accumulation in crops compared with conventional fertilizers. Few studies have compared the mineral composition of crops under ENPs and ionic fertilization (Deng et al., 2022; Rawat et al., 2018a; Zhang et al., 2017), but the advantage of ENPs over metal ions has not been unambiguously confirmed. For instance, a study by Rawat (2018a) did not find significant differences in Cu content in fruits of bell pepper grown in soil treated with nano-CuO, bulk-CuO or $CuCl_2$ at a dose of 125–500 mg/kg. The Cu content of weedy rice grain did not differ between nano-CuO and $CuSO_4$ at 75 and 150 mg/kg, but was higher than under soil amendment with bulk-CuO (Deng et al., 2022). Furthermore, contrary to soil treatment with ENPs, foliar application as widely used technique for delivery of micronutrients has been very rarely examined for plant supplementation with ENPs. It has been reported that foliar-applied nano-ZnO increased Zn content in wheat grain more than $ZnSO_4$ (Zhang et al., 2017). Among ENPs, the potential of Cu-based ENPs for biofortification of crops is far from fully elucidated. One the one hand, Cu is a crucial element for proper plant growth and development (Burkhead et al., 2009) and additionally it has antibacterial and antifungal properties protecting the plant from diseases (Borgatta et al., 2018). On the other hand, however, the phytotoxicity of ENPs containing Cu has been proved towards a wide group of plant species (Burachevskaya et al., 2021; Cota-Ruiz et al., 2018; Jośko et al., 2017; Jośko et al., 2021a; Jośko et al., 2021b; Rawat et al., 2018b). Hence, there is a pressing need to analyse the effect of Cu-based ENPs on the yield and quality of staple crops, such like barley, especially sensitive to Cu deficiency (Narwal et al., 2020).

Barley (*Hordeum vulgare* L.) is an ancient plant belonging to four major agricultural cereal crops (Baik & Ullrich, 2008), which supplies food and feed industries (Mareček et al., 2017). The nutritional value of barley grains was recognized early as they were an essential part of diet of Roman gladiators, so-called "hordearii" (Narwal et al., 2020). Due to a balance of carbohydrates, proteins, vitamins and minerals, barley grains are considered as high energy food (Baik & Ullrich, 2008; Narwal et al., 2020). Moreover, the barley grain is a rich source of phytochemicals and antioxidants playing important role in a prevention of chronic diseases such as cardiovascular disease, cancers, diabetes or Alzheimer's disease (Masisi et al., 2016). Because of the total amount of antioxidant e.g. phenolic compounds and their antioxidant capacity are differentiated by cultivars and growth conditions (Lahouar et al., 2014), it is crucial to include antioxidant properties in evaluation of Cu-based ENPs for plant fertilization. An increase in the content of antioxidants and their antioxidant capacity has already been found in lettuce leaves after foliar spray of biogenic nano-CuO (Kohatsu et al., 2021). However, scarce data exists on the quality of edible parts of plants (e.g. cereal grains) that were not directly exposed to ENPs treatment. Rico et al. (2013) observed a reduction of phenolic content and antiradical abilities in grains of rice grown in soil amended with nano-CeO_2. This finding indicated the potential risk of deterioration of the nutritional value of crops under ENPs exposure. To address the abovementioned gaps, the present study investigated the influence of Cu-based ENPs, their micro counterparts (engineered microparticles, EMPs) and ionic Cu compounds, commonly used as fertilizers on yield quantity and quality of barley. This full life cycle study expands the current knowledge of the role of ENPs in biofortification of crops and food security.

2. Materials and methods

2.1. Cu compounds

Copper and copper oxide ENPs (nano-Cu, nano-CuO) were used for the experiment. For comparison, Cu microparticles (micro-Cu) and two ionic compounds ($CuSO_4$ and ethylenediaminetetra acetic acid copper (II) disodium salt (CuEDTA)) were also included to exam effect of particle size and metal ion activity. All Cu compounds as powders were purchased from Sigma-Aldrich (USA). To determine Cu content in powders, samples were digested with a mixture of HNO_3:H_2O_2 (4:1) in Teflon vessels in a microwave oven (Milestone, ETHOS EASY, Italy) for 1 h at 200 °C. After cooling, the samples were diluted and analyzed using Inductively Coupled Plasma Optical Emission Spectrometer, ICP-OES (Thermo Scientific ICAP7200). Axial view was used for copper determinations. The spectral line 324.754 nm was chosen to obtain the highest sensitivity and minimum interference. Multi-elemental solutions of 1000 mg/L ICP Standard Certipur® (Merck, Germany) containing Cu were used for the calibration. The calibration curves were found to be linear in the range of 0.001 to 1 mg/L for Cu. The quantification limit obtained was 0.001 mg/L for Cu. The quantification limit (LOQ) was calculated as 10 s/m, where s is the standard deviation (n = 10) of the blank and m is the slope of the calibration graph. The precision of the method, expressed as the % relative standard deviation (% RSD) was 8 % for Cu. The primary particle size of ENPs and EMPs determining with a transmission electron microscope (JEM-3010 TEM JEOL, ltd., Japan)

Table 1
Characteristics of ENPs and EMPs solutions.

	Aggregate size [nm]	ζ potential [mV]	Concentration Cu^{2+} [mg/L] before spraying	after spraying
nano-Cu	349.0 ± 5	−14.6 ± 0.4	0.4 ± 0.0	0.4 ± 0.0
nano-CuO	482.0 ± 26	−16.9 ± 1.0	0.5 ± 0.0	0.5 ± 0.0
micro-Cu	5110.0 ± 230	−19.3 ± 0.9	0.1 ± 0.0	0.1 ± 0.0

was 25 ± 10 nm (nano-Cu), 50 ± 10 nm (nano-CuO), 5000 ± 240 nm (micro-Cu). TEM images of ENPs and EMPs were presented in Fig. 1. XRD analysis revealed the crystalline phase of nano-powders. XRD patterns provided in our previous study (Jośko et al., 2022) identified 62 % of copper and 38 % of cuprite (Cu_2O) in nano-Cu powder, while nano-CuO powder characterized by the monoclinic structure tenorite.

2.2. Pot experiment

Plant growth. The sand clay soil collected from Suchodoły, Lubelskie Province, Poland was used as the plant growth matrix. The soil was characterized by a pH of 6.3 and a medium level of available nutrients (P_2O_5 = 124.0 mg/kg, K_2O = 146.0 mg/kg, Mg = 5.8 mg/kg). The background Cu content in the soil was 4.1 mg/kg and the cation-exchangeable concentration of Cu was 0.01 mg/kg. The soil analysis methods were provided in Supporting Material. 50 L pots were filled with fresh soil and dug into the ground. 40 seeds of spring barley *H. vulgare* were sown in each pot. Barley plants were thinned to 20 seedlings per pot at the end of emergence (BBCH 9). The experimental site was surrounded by mesh as a preventive measure against birds, rodents and vermin. The plants were watered with distilled water, and covered during rainfall. The experiment was conducted from 27 March to 27 July in 2020.

Foliar application. Nano-Cu, nano-CuO, micro-Cu, $CuSO_4$, CuEDTA, at concentration of 500 mg Cu/L, were used as treatments in this experiment. The dose of Cu-compounds was calculated to obtain a rate of 2 kg of Cu per ha (Fageria et al., 2009). The powder of Cu compounds was suspended in Milli-Q® water ($\Omega < 0.05$ μS/cm^3) containing 0.1 % of an adjuvant (FASTER, INTERMAG Company, Olkusz, Poland). Anti-foaming adjuvant was used to improve the coverage and maintenance of the Cu solution layer on the plant surface. The Milli-Q® water containing the adjuvant was used as a control treatment. 6 mL of the solutions was sprayed on plants in each pot, corresponding to the commonly used volume of foliar-applied fertilizers (500 L/ha) (Fageria et al., 2009). The foliar application was performed with manual sprayers. Before treatment, the sprayers were calibrated for the same volume and rate application of the solutions. Additionally, the solutions containing nano-Cu, nano-CuO or micro-CuO were sonicated in an ultrasound bath (25 °C, 250 W, 50 Hz) for 30 min immediately prior to application. The solutions were twice applied during plant growth: (i) at the end of tillering (29 BBCH) and (ii) the beginning of heading (51 BBCH) early in the morning. The quality of foliar treatment was controlled by analysis of (i) Cu^{2+} concentrations in solution before and after spraying as well as (ii) Cu content in soil after foliar application. The both analysis of Cu^{2+} in solutions and the total content of Cu in soil was described in detail in the following sections. Due to particulate form, ENPs and EMPs may clog the diffusive element in a sprayer, Cu^{2+} concentration in solutions between and after spraying was analyzed to evaluate if plants were treated with same amount of Cu^{2+}. The Cu^{2+} concentrations in ENPs and EMPs solutions before and after passage through the sprayer were at the same level (Table 1). It indicated the lack of clogging of the sprayer, thus allowing an undisturbed transfer of the solutions to plants. The total Cu content in soil samples after foliar application was provided in Tab. A.1. (Supplementary Material). No difference in Cu content in soil among treated groups confirmed uniform spraying of plants. For foliar application, the pots with plants were placed under a roof to avoid the wind activity and left there until the solutions were dried. Next, the pots were transferred to their previous spot in the ground. Each experimental variant was prepared in three replications.

Sample collection. The barley plants were harvested at the maturity (89 of BBCH) and grains were air-dried to determine grain yield and quality.

2.3. Characteristics of ENPs and EMPs solutions

Solutions of ENPs and EMPs used for foliar spraying were characterized with respect to their zeta potential, the distribution of particle sizes, and Cu^{2+} concentration. These analyses were immediately performed after sonication of solutions in ultrasound bath (30 min, 25 °C, 250 W, 50 Hz). The size of aggregates and zeta potential were measured with the dynamic light scattering technique (Zetasizer 3000, Malvern). In order to determine Cu^{2+} concentration in solutions, the suspensions were centrifuged at 6000 rpm for 60 min in centrifuge tubes (Microsep Advance Centrifugal Devices with Omega Membrane 1 K, Pall Corporation) and acidified with the 65 % nitric acid. Next, Cu was measured with ICP-OES (ICAP 7000, Thermo Scientific, USA).

2.4. The analysis of barley grain

2.4.1. Mineral composition

Air-dried grains were ground and digested with a mixture of HNO_3: H_2O_2 (4:1) in Teflon vessels in a microwave oven (Milestone, ETHOS EASY, Italy) for 1 h at 200 °C. After cooling, the samples were filtered (0.45 μm, PTFE), diluted with Milli-Q® water to 25 mL, and analyzed with ICP-OES (iCAP 7000, Thermo Scientific, USA). All analyses included blanks. Certified material (maize flour, INCT-CF-3, ICHTJ, Poland) was used for the quality control of the sample digestion. The maize flour samples were digested in the same way as the samples of barley samples. The recovery of the selected microelements was in the range of 93.0 – 98.4 % and 87.4 – 95.3 %, respectively.

The assessment of biofortification of crops with microelements needs to be accompanied by food security analysis related to consumption of grain. For the health risk assessment, the daily intake rate (DIR) was calculated following Equation:

$$DIR = [Cu]\ grain \times IR / BW$$

where Cu is the concentration of Cu in grain [mg/kg of dry mass (d.m.)]; IR is the average ingestion rate of barley grain [g of d.m./day/person]. Two values of IR were used: the actual IR by adults in Poland [0.78 g of d.m./day/person] and recommended IR of barley grain by adults [13.3 g of d.m./day/per person] (Gruszecka-Kosowska, 2019); BW is body weight: 60 kg for adults. The DIR values were compared with the tolerable upper intake level (UL), defined as the highest level of daily nutrient intake that is likely to have no risk of adverse health impact for nearly all persons (Trumbo et al., 2001).

2.4.2. Nutritional quality

Protein content and digestibility. For protein extraction, 50 mg of the air-dried wholegrain barley flour was suspended in 600 μL of urea buffer (2 M urea, 10 % glycerol, 65 mM DTT, and 20 mM Tris, pH 8.0) (Hurkman & Tanaka, 2007). The suspension was incubated at room temperature for 1 min, and insoluble material was removed by centrifugation at 16,000 × *g* for 10 min. The protein content was determined according to Bradford (1976) using a calibration curve of albumins, globulins, prolamins, and glutenins as standard protein. *In vitro* protein digestibility was determined by the method of Minekus et al. (2014). Detailed protocol of the wholegrain barley flour digestion was provided in Supplementary Material (Fig. A.1).

The total dietary fiber. The total content of dietary fiber, including soluble and insoluble, was quantified in grain meal according to the AOAC Method 991.43 method using a commercial assay kit (Total

Dietary Fiber Assay Kit, Megazyme International Wicklow, Ireland).

2.4.3. Antioxidants content and antioxidant capacity

Extraction. To determine the content of phenolic compounds and antioxidant properties in grain, the chemical extraction was conducted. Lyophilized samples (100 mg of dry mass) were extracted for 1 h at room temperature in a shaker (300 rpm) in a capped centrifuge tube with 10 mL of different solvents: 50 % methanol, 60 mM HCl in 50 % methanol, and finally with 60 mM HCl in 70 % acetone. The mixture was centrifuged (15 min, 3,000 × *g*, 22 °C) and the supernatants from all steps were combined.

Total phenolic content (TPC). TPC was determined using the modified Folin-Ciocalteu method (Meda et al., 2005). In total, 0.1 mL of the extract, dissolved in DMSO at a concentration of 2 mg/mL, was mixed with 4 mL of distilled water and with 0.5 mL of Folin-Ciocalteu reagent. After 1 min, 2 mL of 20 % sodium carbonate was added and supplemented with distilled water to a total volume of 10 mL. The absorbance was measured at 760 nm after 30 min incubation at dark and at room temperature. A blank sample of water and reagents was used as a reference. TPC was expressed as mg of gallic acid (GAE) equivalent per g of a dry extract (the calibration curve of GAE: $y = 9.8399x + 0.0289$; $R^2 = 0.9993$) in a concentration range of 20 – 80 μg/mL.

Total anthocyanin content (TAC). 250 μL of each extract was mixed with 1.4 mL of 0.4 M acetate buffer (pH 4.5) or HCl/KCl buffer (pH 1.0). Absorbance was measured at 520 nm and 700 nm, while TAC was calculated with a molar extinction coefficient of cyanidin 3-glucoside (Lee et al., 2005).

Total flavonoid content (TFC). 25 μL of each extract was mixed with 350 μL of 80 % (v/v) aqueous EtOH, 12.5 μL of 10 % (v/v) $Al(NO_3)_3$, and 12.5 μL of 1 M aqueous potassium acetate. The sample was left to stand for 40 min at room temperature, after which the absorbance was measured at 415 nm using a microplate reader. The total flavonoid content was calculated using 12 dilutions of quercetin stock solution (250 μg of quercetin dissolved in 250 μL of distilled de-ionized (DDI) water and 250 μL of acetonitrile). TFC was expressed as mg quercetin equivalents per g of dry mass of sample.

Content of condensed tannin (CT). 15 μL of each extract was mixed with 250 μL of 4 % vanillin solution in MeOH and 12.5 μL of HCl (35 – 38 %). The sample was left to stand for 15 min and the absorption was measured at 500 nm against MeOH. A standard curve was prepared using stock (+)-catechin solution (3.45 mg of (+)-catechin dissolved in 2 mL of MeOH) diluted into 15 working solutions as described above (Arancibia-Avila et al., 2011).

Total flavanol content (TFoC). 100 μL was mixed with 0.3 mL of p-dimethylaminocinnamaldehyde (DMACA, 0.1 % in 1 M HCl in MeOH), vortexed, and left to stand for 45 min. Next, the absorbance was read at 640 nm in a microplate reader against a blank without DMACA. The total flavanol content was calculated from 20 dilutions of stock catechin solution (3.3 mg of (+)-catechin dissolved in 1.9 mL of MeOH) mixed with DMACA as described above (Arancibia-Avila et al., 2011).

Antiradical and antioxidant capacity with 2,2- diphenyl-1-picrylhydrazyl radical ($DPPH^{\bullet}$) and 2,2′-azino-bis (3ethylbenzothiazoline-6-sulfonic acid) radical cation ($ABTS^{\bullet+}$). For measurements with $DPPH^{\bullet}$ radical, a slight modification of the method described by Brand-Williams et al. (1995) was used: directly before measurement, the absorbance of DPPH methanol solution was adjusted to 1.5 using methanol (515 nm, 20 °C). A 20 μL volume of the test sample was mixed with 255 μL of methanol and 30 mL of DPPH solution. Absorbance was read at 515 nm after 4 min. The negative blank was composed of 20 μL of DDI water, 255 μL of MeOH, and 30 μL of DPPH solution. The background of the sample was subtracted during the calculations. All samples were run in 8 replicates. The results were expressed in Trolox equivalents (TE), using a calibration curve prepared from 1 L of Trolox solutions (92 – 920 μmol/L). The analysis with $ABTS^{\bullet+}$ radical cation was performed according to the simplified method of Miller et al. (1993) with our own modifications. Prior to the analysis, an aqueous solution of ABTS (15 mmol/L) was stored with potassium persulfate (2.45 mmol/L) for 24 h at room temperature. Directly before measurement, the absorbance of the ABTS solution (734 nm) was adjusted to 1.5 using distilled water (20 °C). The sample (20 μL) was mixed with 180 μL of DDI water and 190 μL of the ABTS solution, and the absorbance was measured after 4 min. The negative blank was composed of 200 μL of DDI water and 185 μL of the ABTS solution. The background of the sample was subtracted during the calculations. All samples were run in 8 replicates. The results were expressed in TE units using a calibration curve prepared with Trolox solutions as described above.

Ferric reducing antioxidant power (FRAP). The sample (20 μL) was mixed with 1.9 mL of FRAP solution, shaken for 30 min at room temperature and the absorbance was read at 593 nm, after shaking for 30 s. The FRAP solution was prepared by mixing 2.5 mL of 5 mM TPTZ solution (prepared in 40 mM HCl solution), 2.5 mL of 5 mM $FeCl_3$ solution, and 25 mL of acetate buffer (0.3 M, pH 3.6) and warming in water bath at 37 °C for 20 min. A blank (reagent) sample was prepared with buffer instead of the sample and the background of the sample was measured (a mixture containing only the studied sample and buffer). A calibration curve was prepared using 510 μg Trolox dissolved in 1 mL of DDI water (stock solution diluted to obtain 20 standard solutions in the range of 25.5 – 510 μg Trolox/mL) (Hanafy et al., 2017).

Cupric reducing antioxidant capacity (CUPRAC). 40 μL of the sample was mixed with 900 μL of ammonium acetate buffer (1 M, pH 7.0), 700 μL of neocuproine (3.75 mM, dissolved in DDI water: ACN 1:1) and 350 μL of 10 mM $CuCl_2$. After 1 h, the absorbance was read at 450 nm against the blank sample (containing 40 μL of the corresponding tested solution mixed with 1950 μL of ammonium acetate buffer). The reagent sample (without the studied samples) was also measured and subtracted from the studied sample. Quercetin was used as antioxidant standard (230 μg of quercetin dissolved in 0.5 mL and 0.5 mL ACN) diluted into 20 standard solutions (17.5 – 350 μmol/L) (40 μL) used as described above (Öztürk et al., 2011).

Hydroxyl radical antioxidant capacity (HORAC). The sample (10 μL) was mixed with 500 μL of DDI and fluorescein solution (200 μL, 60 nM) and incubated at 37 °C for 10 min. Then, 10 μL of 27.5 mM H_2O_2 solution and 10 μL of $CoF_2 \times 4\ H_2O$ solution (230 μM, containing 1 mg of picolinic acid/mL) were added to the solution tested sample. The fluorescence was read (excitation at 485 nm and emission at 520 nm) at start and every 1 min with constant shaking during the whole reaction until stabilization (typically 5 – 10 min). A blank sample containing phosphate buffer instead of the sample was run. Also, the background from the samples was measured (a mixture containing only the studied sample and DDI water). The activity was expressed in GAE equivalents prepared using 15 GAE solutions (equal to 9.6 – 480 μg of GAE/mL) used as described above (Denev et al., 2014).

Chelating power (ChP). ChP was determined using the method developed by Guo et al. (2020). The chelating properties were determined in samples obtained after chemical extraction and expressed as EDTA equivalents in μg of EDTA/g of d.m.

2.5. Data analysis

The data were statistically analyzed using Statistica 13.3 software. The differences between treatments were determined using a one-way analysis of variance (ANOVA) followed by Tukey's post hoc test (parametric analysis) or Kruskal-Wallis test followed by the pairwise multiple comparison of mean ranks (PMCMR) (non-parametric analysis) at a significance level of 0.05. A two-tailed Pearson correlation analysis was performed to test the variables.

3. Results and discussion

3.1. ENPs and EMPs solutions characteristics

Nano-Cu and nano-CuO tended to create aggregates (Table 1), whose

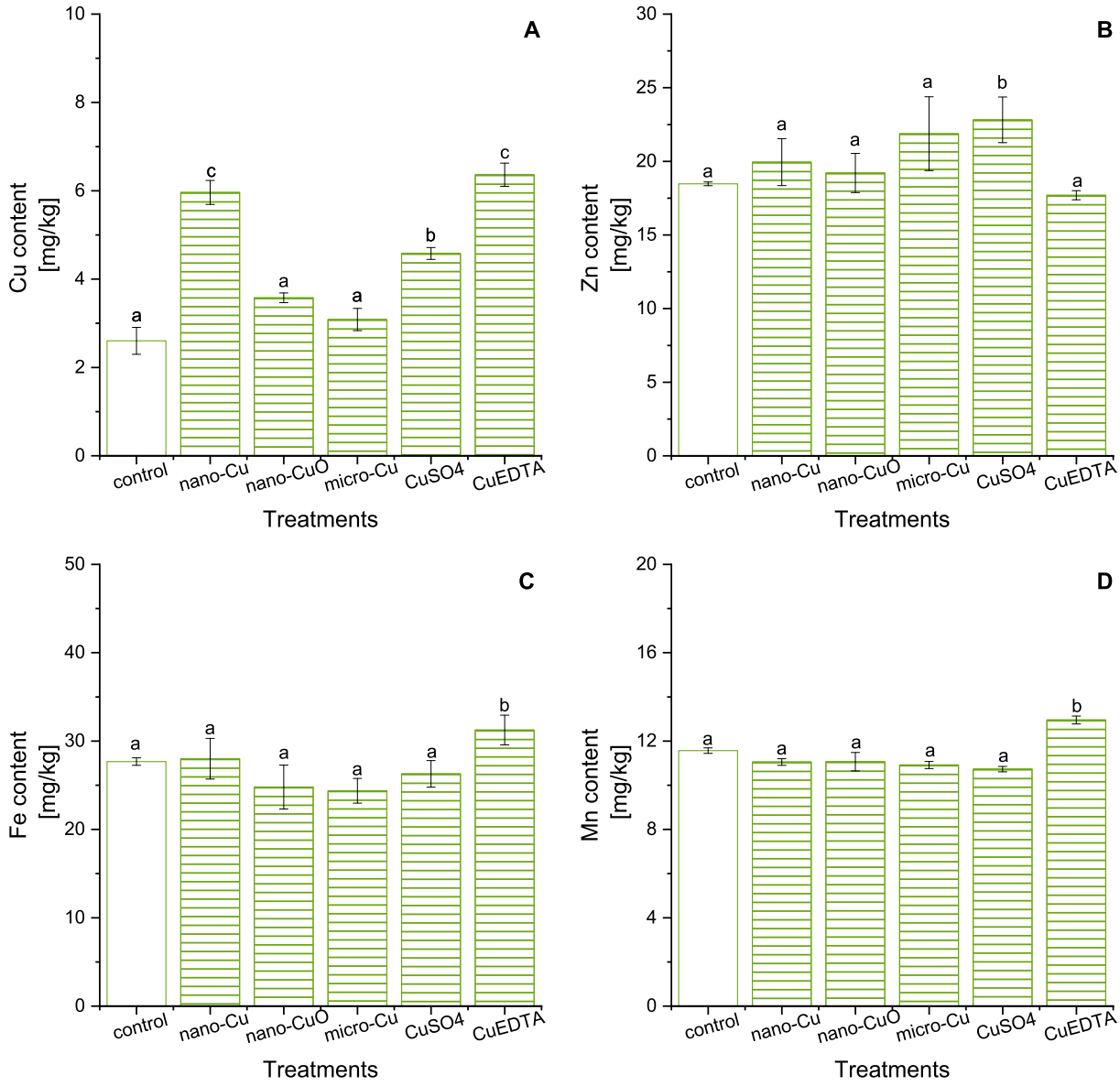

Fig. 2. The content of Cu (A), Zn (B), Fe (C), Mn (D) in grain of barley (dry mass) sprayed with different Cu compounds. Error bars represent standard deviation (SD, n = 3). Different letters indicate significant differences among the treatments ($p < 0.05$).

average sizes (349 – 482 nm) were higher by one order of magnitude than the primary diameter of ENPs determined by TEM (Fig. 1). As was expected, the average size of micro-Cu aggregates was more than 10 times greater than that of ENPs. The values of ζ-potential ranged from −14.6 to −19.3 mV for both ENPs and MNPs (Table 1). The dissolution analysis revealed a low concentration of Cu^{2+} (0.1 – 0.5 mg/L) in the ENPs and EMPs solutions, which was < 1 % of applied Cu. It confirms the low solubility of Cu-based ENPs (Gao et al., 2019). The Cu^{2+} concentration in the micro-Cu solution (0.1 mg/L) was slightly lower in relation to the nano-Cu solutions (0.4 mg/L), which is line with the size effect observed in previous studies (Dai et al., 2018; Kaweeteerawat et al., 2015).

3.2. Effect of Cu treatments on barley grain traits

3.2.1. Agronomic parameters

Overall, foliar application of Cu compounds (ENPs, EMPs, ionic) had no impact on barley grain yield expressed as both grain weight per pot and 1000 grain weight (Tukey test, $p \geq 0.05$) (Tab. A.2). To date, no data on cereal grain yield after foliar application of Cu-based ENPs has been available. As a microelement, Cu could have more significance for quality than quantity of yield. However, studies on vegetables have demonstrated a stimulating effect of Cu-based ENPs (Lasso-Robledo et al., 2022). For example, foliar spraying with nano-CuO at a range of 200 mg/L of cucumber significantly increased fruit fresh weight (Hong et al., 2016), while foliar applied green synthesized nano-CuO at 50 μg/L had a positive effect on lettuce dry weight (Kohatsu et al., 2021). These evidences emphasis the need of optimizing of the application of nano-Cu to deliver essential amount of Cu during the development of barley fruits.

3.2.2. Mineral composition

Copper. The Cu grain content was doubled under nano-Cu and ionic Cu ($CuSO_4$ and CuEDTA) in comparison with control samples (2.6 mg/kg) (Tukey test, $p < 0.05$) (Fig. 2A). Interestingly, for nano-Cu solutions characterized by 1000 lower concentration of Cu^{2+} compared to ionic compounds, the grain Cu content was at a similar level. No difference in grain Cu content between nano-Cu and ionic compounds may suggest that nano-Cu may be up taken and distributed in particulate form. Among the particulate Cu compounds used, nano-Cu featured by the

Table 2
Macroelement content in grain of barley (dry mass) exposed to nano- and micro-particulate and ionic Cu. Different letters indicate significant differences among the treatments ($p < 0.05$).

	Ca [mg/kg]	K [mg/kg]	Mg [mg/kg]
control	304.0 ± 22.5^{b}	5615.7 ± 120.1^{a}	922.3 ± 37.3^{b}
nano-Cu	269.0 ± 36.5^{a}	5991.3 ± 210.2^{b}	913.0 ± 29.8^{b}
nano-CuO	272.6 ± 19.7^{a}	5308.5 ± 320.6^{a}	901.1 ± 21.9^{b}
micro-Cu	269.6 ± 26.0^{a}	5561.4 ± 114.8^{a}	922.9 ± 30.8^{b}
$CuSO_4$	259.2 ± 31.8^{a}	5399.2 ± 213.7^{a}	839.7 ± 37.9^{a}
CuEDTA	298.8 ± 30.2^{b}	5709.0 ± 204.5^{a}	982.3 ± 40.1^{c}

smallest diameter, which might have allowed it to cross through the leaf surface features (stomata, trichomes, cuticule) (Avellan et al., 2021). It should be noted that ENPs were suspended in the solution containing an adjuvant, which may degrade the cuticule, thus paving the way for infiltration of smaller ENPs (Avellan et al., 2019). The fact that no statistically significant effect of nano-CuO (average diameter = 50 nm) and micro-Cu (average diameter = 5 μm) on Cu grain (Fig. 1A) may confirm the size-dependent capacity to take up ENPs by leaves. In previous studies on foliar applied Cu-based ENPs that mostly concerned leafy edible plants (Tan et al., 2018; L. Zhao et al., 2016), an increased Cu content in leaves could have been the sum of uptake of ENPs and adhesion of ENPs to the leaf surface. A study by Laughton et al. (2019) determined a residual amount of Cu on lettuce leaves even after washing lettuce leaves sprayed with Cu-ENPs. Our results shown actual biofortification of grain with Cu, due to the treatments were performed before the grain development. Because of increased Cu grain content, it was necessary to evaluate the possible human intakes and risk assessment. The calculated dietary intake rates of Cu in grain in the control and treated groups based on both the actual and recommended levels of barley grain consumption ranged from 0.03 to 0.08 μg/kg/day and from 0.6 to 3.8 μg/kg/day (Table A.3). Notwithstanding the increased Cu content in barley grain under Cu treatments, the Cu level was definitely below the tolerable upper intake level (40 μg/kg/day) (Xiong et al., 2017), meaning no risk for human health.

Other microelements. The treatment of plants with ENPs and EMPs did not impact the content of other transition metals (Zn, Fe, Mn) (Fig. 2B-D). Ionic Cu compounds had a minor impact on these elements: $CuSO_4$ increased Zn content by 23.5 %, while CuEDTA evoked higher Fe and Mn accumulation in barley grain by 10.1–12.9 % compared to the control (Kruskal-Wallis test, $p < 0.05$). It may indicate the interactions between Cu ions and other transition metals such as competition or substitution (Pilon et al., 2009). As it was mentioned earlier, both nanoparticulate and ionic Cu may be delivered to plants under application nano-Cu, thus it could evoke the different effect on molecular regulation of metal homeostasis (including metal uptake and translocation) compared to Cu ions from dissolved compounds (Jośko et al., 2021b). Existing data on the mineral composition of grain under Cu-based ENPs are limited to soil application ENPs and mainly show a reduction in transition metals in rice grain under both nanoparticulate and ionic Cu (Deng et al., 2022). However, these observations are difficult to refer to our results mostly due to distinct mechanisms of metal uptake *via* roots and foliar routes. No general trend was observed for the grain content of Ca, K and Mg (Table 2) under Cu treatment and their impact was dependent on the type of nutrient and used Cu compounds. The Ca content in grain was 10.3–14.7 % lower under almost all Cu treatment (Kruskal-Wallis test, $p < 0.05$) and only CuEDTA had no impact on the level of this element compared to the control. The accumulation of K in barley grain was only affected after application of nano-Cu resulting in about 7 % increase of that element in relation to the untreated sample. In turn, Mg acquisition was only differentiated by ionic Cu: $CuSO_4$ decreased the Mg content by 9.0 %, while CuEDTA increased the Mg level in grain by 6.5 % compared to the control. No general trends of changes in mineral composition under ENPs exposure were also noted for wheat (Wang et al., 2019) or bell pepper (Rawat et al., 2018a). Further studies including transcriptional analysis of nutrient acquisition in grain at crucial stages of fruit development need to be conducted to more in-depth examination of mineral composition pattern under nano-fertilization (Puig et al., 2007).

Table 3
Nutritional value of air-dried grains of barley after foliar spray with different Cu compounds. Different letters indicate significant differences among the treatments ($p < 0.05$).

	Protein content	Protein digestibility	Dietary fiber		
			Total	Soluble	Insoluble
	[%]	[%]	[%]	[%]	[%]
Control	9.0 ± 1.4^{a}	95.8 ± 1.3^{b}	23.9 ± 1.3^{a}	7.5 ± 0.6^{a}	16.4 ± 0.7^{a}
Nano-Cu	9.5 ± 1.4^{a}	94.1 ± 1.5^{b}	28.7 ± 1.1^{b}	10.8 ± 0.8^{b}	17.9 ± 0.3^{a}
Nano-CuO	8.5 ± 1.6^{a}	93.9 ± 1.8^{b}	23.4 ± 0.6^{a}	6.8 ± 1.3^{a}	16.7 ± 1.9^{a}
Micro-Cu	9.7 ± 1.5^{a}	96.1 ± 1.3^{b}	20.6 ± 0.6^{a}	5.3 ± 0.2^{a}	15.3 ± 0.6^{a}
$CuSO_4$	8.6 ± 2.1^{a}	90.1 ± 2.5^{a}	21.0 ± 3.2^{a}	5.3 ± 1.6^{a}	15.7 ± 1.6^{a}
CuEDTA	10.0 ± 0.7^{a}	95.8 ± 1.2^{b}	22.6 ± 0.3^{a}	7.9 ± 0.4^{a}	14.7 ± 0.7^{a}

Table 4
The content of antioxidant compounds in air-dried grains of barley foliar sprayed with different Cu compounds. Different letters indicate significant differences among the treatments ($p < 0.05$).

	Phenolic [mg GAE/ g]	Anthocyanin [mg cya-3-glu/ g]	Flavonoid [mg quercetin/ g]	Tannin [mg catechin/ g]	Flavanol [mg catechin/ g]
Control	3.0 ± 0.1^{a}	37.1 ± 0.8^{a}	0.2 ± 0.1^{a}	0.4 ± 0.1^{a}	36.0 ± 2.0^{a}
Nano-Cu	3.5 ± 0.6^{a}	33.9 ± 0.1^{a}	0.1 ± 0.0^{a}	0.5 ± 0.1^{a}	43.0 ± 1.0^{b}
Nano-CuO	2.7 ± 0.0^{a}	40.0 ± 0.1^{a}	0.1 ± 0.1^{a}	0.6 ± 0.1^{a}	36.0 ± 2.0^{a}
Micro-Cu	2.7 ± 0.5^{a}	38.7 ± 0.1^{a}	0.1 ± 0.1^{a}	0.7 ± 0.1^{a}	37.0 ± 3.0^{a}
$CuSO_4$	3.0 ± 0.3^{a}	32.6 ± 0.1^{a}	0.1 ± 0.0^{a}	0.3 ± 0.1^{a}	38.0 ± 4.0^{a}
CuEDTA	2.5 ± 04^{a}	44.7 ± 0.1^{b}	0.1 ± 0.0^{a}	0.1 ± 0.1^{b}	34.0 ± 3.0^{a}

3.2.3. Protein and fiber content

Protein content in grain was unchanged under Cu supply (Table 3). Among all treatments, there was also no impact on protein digestibility (Table 3), excluding $CuSO_4$, which slightly reduced it by 6 % (Tukey test, $p < 0.05$). A study by Deng et al. (2022) on nano-CuO dosed to soil did not also showed changes in the protein level of grains of both weedy and cultivated rice. No difference in the total dietary fiber (including soluble and insoluble fiber) content of grain was found between untreated and treated samples (Table 3). The sole exception was nano-Cu, which caused an increased in total dietary fiber and soluble fiber content by 19.9 % and 43.6 %, respectively, compared to the control (Tukey test, $p < 0.05$). These changes are beneficial for the healthy nature of grains because dietary fiber (especially soluble fiber) reduces the concentration of blood cholesterol as well as slows down sugar absorption, thus lowering the risk of prevalence of cardiovascular diseases and diabetes (Narwal et al., 2020).

3.2.4. Antioxidant properties

Whole barley grains as a source of antioxidant phytochemicals help to combat the prevalence of chronic diseases (Madhujith et al., 2006). All treatments did not significantly affect the content of TPC, which are

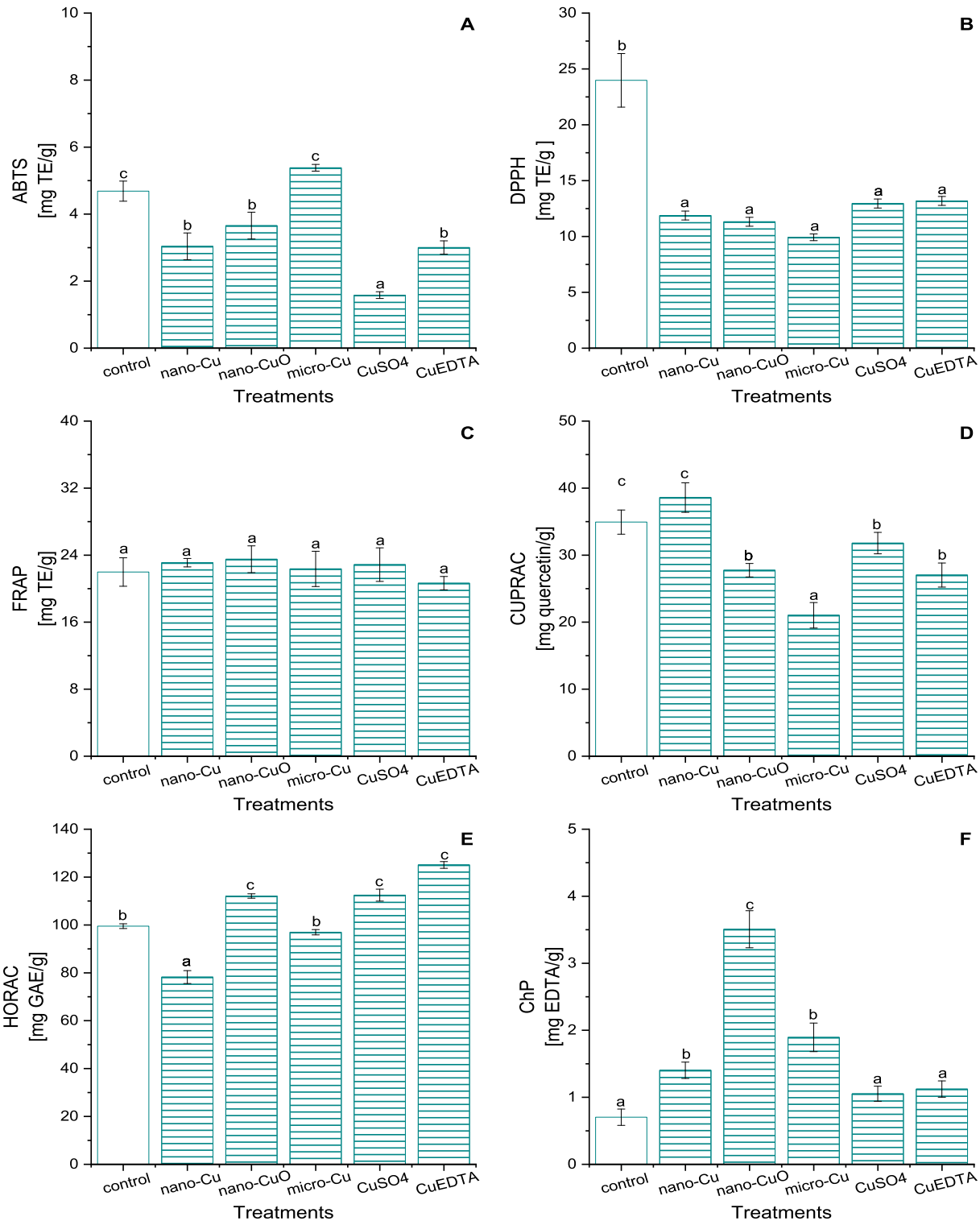

Fig. 3. The antiradical activities against ABTS (A), DPPH radicals (B), FRAP (C), CUPRAC (D), HORAC (E) reducing abilities and chelating power (F) of grain (dry mass). Error bars represent standard deviation (SD, n = 3). Different letters indicate significant differences among the treatments ($p < 0.05$).

considered as main antioxidant compounds (Table 4). Slight changes in individual components of TPC were observed, but only under nano-Cu or CuEDTA. For example, the content of anthocyanin and tannin in grain of plants sprayed with CuEDTA increased by 20 and 140 %, respectively (Kruskal-Wallis test, $p < 0.05$) (Table 4). However, the only effect on the content of flavanol was observed after application of nano-Cu as the accumulation of flavanol increased by 20 % compared to untreated samples (Tukey test, $p < 0.05$) (Table 4). It may indicate a different effect of nanoparticulate and ionic Cu on the accumulation of bioactive compounds, although both compounds provided the same level of Cu content in grain. Despite that both anthocyanin and tannin are characterized by valuable antioxidant capacity, tannins are also considered as a antinutritional factor that reduces the bioavailability of micronutrients, which may reduce the nutritional value of grain (Narwal et al., 2020). To date, scarce and conflicting data on accumulation of antioxidant compounds in crops treated with Cu-based ENPs have

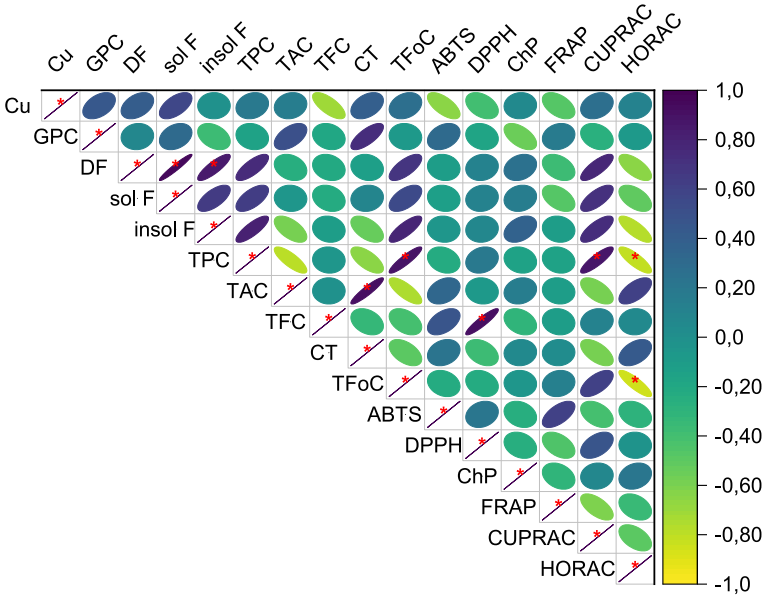

Fig. 4. The correlation plot performed for biochemical parameters of barley grain. Colors indicate Pearson correlation coefficient values ranging from −1 (yellow) to 1 (blue). A narrower ellipse indicates stronger correlation, and a slope of ellipse indicates the direction of the correlation. The asterisks indicate significant correlation ($p < 0.05$). Cu – the Cu content; GPC – the protein content; DF – the dietary fiber content; sol DF – the content of soluble dietary fiber; insol DF – the content of insoluble dietary fiber; TPC – the total phenolic content; TAC – the total anthocyanin content; TFC – the total flavonoid content; CT – the content of condensed tannin; TFoC – the total flavanol content; ABTS – The antioxidant capacity with ABTS; DPPH – The antioxidant capacity with DDPH; ChP – chelating power; FRAP – Ferric reducing antioxidant power; CUPRAC – Cupric reducing antioxidant capacity; HORAC- Hydroxyl radical antioxidant capacity. (For interpretation of the references to colour in this figure legend, the reader is referred to the web version of this article.)

existed. For instance, biogenic nano-Cu applied foliar at (20 mg per plant) significantly increased TPC and flavonoids in lettuce (Kohatsu et al., 2021). In turn, foliar application of $Cu(OH)_2$ nanopesticides at 1050 and 1555 mg/mL evoked a drop in TPC content in lettuce (L. Zhao et al., 2016). Rico et al. (2013) explained a decrease of TPC in grain of rice grown in soil amended with nano-CeO_2 by oxidative stress induced by ENPs. Probably, changes in mineral composition of grains under nano-Cu and ionic Cu found in our study (Fig. 2) may trigger the specific alternation in the antioxidant content.

Besides the total content of antioxidant compounds in grains, an analysis of their bioactivity should be included in evaluation of the effectiveness of Cu supply. Due to antioxidants can be free radical scavengers, a reducing agent and complexing agent of prooxidant (Madhujith et al., 2006), the effect of Cu treatments was determined in the context of antiradical/reducing/chelating activities in grain extracts. The analysis of antiradical activity indicated that Cu treatments decreased the ability of grain extracts to quench both $ABTS^{\bullet+}$ and $DPPH^{\bullet}$ radicals (Fig. 3A, B). Some difference in antioxidant capacity between Cu treatments was observed only in relation to $ABTS^{\bullet+}$ radicals. The lowest antioxidant activity against $ABTS^{\bullet+}$ was noted for $CuSO_4$ treatment (1.6 mg TE/g) since a 66 % decrease was found compared to the control sample (4.5 mg TE/g d.m.) (Tukey test, $p < 0.05$). Antiradical activity of ENPs and CuEDTA, at a similar level of 3.0 – 3.7 mg TE/g, remained higher than for $CuSO_4$ treatments (1.6 mg TE/g), while micro-Cu had no impact on antioxidant capacity. The effect of Cu treatments on reducing power was tested with FRAP and CUPRAC assays. Compounds having reducing power act as electron donors and reduce Fe^{3+} to Fe^{2+} (FRAP assay) or Cu^{2+} to Cu^{+} (CUPRAC assay) (Zengin et al., 2017), which may indicate the potential of grain extracts for reducing intermediates of lipid peroxidation. Regardless of used Cu compounds, FRAP reducing potential remained unchanged (Tukey test, $p \geq 0.05$) (Fig. 3C). The CUPRAC assay indicated that the reducing ability of grain extract decreased by 9.0 – 39.8 % in grain treated with almost all Cu compounds (Tukey test, $p < 0.05$), with the exception of nano-Cu that had no impact on reducing power (Fig. 3D). Whereas nano-Cu lowered HORAC reducing power by 21.4 %, other Cu compounds increased the potential (by 12.7–25.7 %) or did not change it (micro-Cu) (Kruskal-Wallis test, $p \geq 0.05$) (Fig. 3E). The chelating power of grain extracts differed between the particulate and ionic Cu treatment (Fig. 3F). Namely, ENPs and EMPs caused a 2- to 4-fold increase in chelating activity (Tukey test, $p < 0.05$) while both ionic compounds did not impact that parameter. Our results for antiradical properties align with a study by Rico et al. (2013) that revealed reduced radical scavenging in rice grain under nano-CeO_2, which was associated with decreased TPC content, basic antioxidant compounds. As mentioned before, no change in TPC content under Cu treatments was found in our study, but the distinct antioxidant capacity may be related to shifts in the pattern of phenolic compounds. As many biochemical data report, reducing power is correlated with antiradical activity (Lahouar et al., 2014; H. Zhao et al., 2008). Similarly to antiradical response, the CUPRAC reducing power was reduced by Cu treatment, although no correlation was found between these indicators ($p \geq 0.05$) (Fig. 4). However, a significant positive correlation was found between TPC and CUPRAC ($R = 0.86$, $p < 0.05$). As opposed to antiradical and reducing ability, chelating power was increased by ENPs and EMPs. This effect may indicate a distinct effect of particulate and ionic Cu. Chelating activity in grain extracts measured by bounding ferrous ion by chelating agents such as phenolic compounds and phytic acid plays a crucial role in protection against peroxidation of biomolecules (Chandrasekara & Shahidi, 2010). The lack of correlation between antioxidant content/capacity and chelating power (Fig. 4) may suggest that ENPs and EMPs induced shifts in the composition of chelating agents and their ability to complex of Fe ions. Overall, the correlation plot (Fig. 4) did not exhibit a relationship of microelement content and phenolic content with antioxidant properties. Thus, it may be confirmed that Cu treatments affected some of the analyzed indicators by changing the composition of phytochemicals and their bioactivity. However, because of the sum results for all Cu compounds was used to perform the correlation analysis, the antioxidant indicators measured in grain can be related with nanoparticulate or ionic-specific effects.

4. Conclusions

The present study is the first to give insights on the potential role of Cu-based ENPs in enhancement of quality indicators of barely grain including its mineral composition and antioxidant properties, which are crucial for the food industry. Despite that the Cu acquisition of barley grain was similar under foliar treatment of nano-Cu and ionic compounds, the analysis of the content of antioxidants and their activities revealed a distinct impact of these Cu treatments. Some indicators including chelating power and dietary fiber content increased by ENPs render them a promising agent for improvement of grain quality. However, because the antiradical/reducing capacity was mainly decreased by Cu compounds, the nutritive quality of barley grain may be

deteriorated. These findings are valuable to develop a strategy for using ENPs for biofortification of grain crops. Further research needs to be conducted to investigate in more detail changes in the content of phytochemicals and its activities as well as bioaccessibility of Cu to deeply explore the enhancing or inhibiting impact of ENPs on food quality and security.

CRediT authorship contribution statement

Izabela Jośko: Conceptualization, Methodology, Resources, Funding acquisition, Writing - original draft, Writing - review & editing. **Magdalena Kusiak:** Methodology, Investigation. **Krzysztof Różyło:** Investigation. **Ewa Baranowska-Wójcik:** Methodology, Investigation. **Małgorzata Sierocka:** Methodology, Writing – review & editing. **Mohamed Sheteiwy:** . **Dominik Szwajgier:** Methodology, Writing – review & editing. **Michał Świeca:** Methodology.

Declaration of Competing Interest

The authors declare that they have no known competing financial interests or personal relationships that could have appeared to influence the work reported in this paper.

Data availability

Data will be made available on request.

Acknowledgments

This study was supported by the National Science Centre, Poland [2017/26/D/NZ9/00067].

Appendix A. Supplementary data

Supplementary data to this article can be found online at https://doi.org/10.1016/j.foodres.2022.112303.

References

Alexandratos, N., & Bruinsma, J. (2012). *World Agriculture towards 2030/2050: The 2012 revision*. 154.

Arancibia-Avila, P., Toledo, F., Werner, E., Suhaj, M., Leontowicz, H., Leontowicz, M., Martinez-Ayala, A. L., Paśko, P., & Gorinstein, S. (2011). Partial characterization of a new kind of Chilean Murtilla-like berries. *Food Research International, 7*(44), 2054–2062. https://doi.org/10.1016/j.foodres.2011.01.016

Avellan, A., Yun, J., Morais, B. P., Clement, E. T., Rodrigues, S. M., & Lowry, G. V. (2021). Critical review: Role of inorganic nanoparticle properties on their foliar uptake and in planta translocation. *Environmental Science & Technology, 55*(20), 13417–13431. https://doi.org/10.1021/acs.est.1c00178

Avellan, A., Yun, J., Zhang, Y., Spielman-Sun, E., Unrine, J. M., Thieme, J., Li, J., Lombi, E., Bland, G., & Lowry, G. V. (2019). Nanoparticle size and coating chemistry control foliar uptake pathways, translocation, and leaf-to-rhizosphere transport in wheat. *ACS Nano, 13*(5), 5291–5305. https://doi.org/10.1021/acsnano.8b09781

Baik, B.-K., & Ullrich, S. E. (2008). Barley for food: Characteristics, improvement, and renewed interest. *Journal of Cereal Science, 48*(2), 233–242. https://doi.org/10.1016/j.jcs.2008.02.002

Borgatta, J., Ma, C., Hudson-Smith, N., Elmer, W., Plaza Pérez, C. D., De La Torre-Roche, R., Zuverza-Mena, N., Haynes, C. L., White, J. C., & Hamers, R. J. (2018). Copper based nanomaterials suppress root fungal disease in watermelon (Citrullus lanatus): Role of particle morphology, composition and dissolution behavior. *ACS Sustainable Chemistry & Engineering, 6*(11), 14847–14856. https://doi.org/10.1021/acssuschemeng.8b03379

Bradford, M. M. (1976). A rapid and sensitive method for the quantitation of microgram quantities of protein utilizing the principle of protein-dye binding. *Analytical Biochemistry, 72*, 248–254.

Brand-Williams, W., Cuvelier, M. E., & Berset, C. (1995). Use of a free radical method to evaluate antioxidant activity. *LWT - Food Science and Technology, 28*(1), 25–30. https://doi.org/10.1016/S0023-6438(95)80008-5

Burachevskaya, M., Minkina, T., Mandzhieva, S., Bauer, T., Nevidomskaya, D., Shuvaeva, V., Sushkova, S., Kizilkaya, R., Gülser, C., & Rajput, V. (2021). Transformation of copper oxide and copper oxide nanoparticles in the soil and their accumulation by Hordeum sativum. *Environmental Geochemistry and Health, 43*(4), 1655–1672. https://doi.org/10.1007/s10653-021-00857-7

Burkhead, J. L., Reynolds, K. A. G., Abdel-Ghany, S. E., Cohu, C. M., & Pilon, M. (2009). Copper homeostasis. *New Phytologist, 182*(4), 799–816. https://doi.org/10.1111/j.1469-8137.2009.02846.x

Chandrasekara, A., & Shahidi, F. (2010). Content of insoluble bound phenolics in millets and their contribution to antioxidant capacity. *Journal of Agricultural and Food Chemistry, 58*(11), 6706–6714. https://doi.org/10.1021/jf100868b

Cota-Ruiz, K., Hernández-Viezcas, J. A., Varela-Ramírez, A., Valdés, C., Núñez-Gastélum, J. A., Martínez-Martínez, A., Delgado-Rios, M., Peralta-Videa, J. R., & Gardea-Torresdey, J. L. (2018). Toxicity of copper hydroxide nanoparticles, bulk copper hydroxide, and ionic copper to alfalfa plants: A spectroscopic and gene expression study. *Environmental Pollution, 243*, 703–712. https://doi.org/10.1016/j.envpol.2018.09.028

Dai, Y., Wang, Z., Zhao, J., Xu, L., Xu, L., Yu, X., Wei, Y., & Xing, B. (2018). Interaction of CuO nanoparticles with plant cells: Internalization, oxidative stress, electron transport chain disruption, and toxicogenomic responses. *Environmental Science: Nano, 5*(10), 2269–2281. https://doi.org/10.1039/C8EN00222C

Denev, P., Kratchanova, M., Ciz, M., Lojek, A., Vasicek, O., Nedelcheva, P., Blazheva, D., Toshkova, R., Gardeva, E., Yossifova, L., Hyrsl, P., & Vojtek, L. (2014). Biological activities of selected polyphenol-rich fruits related to immunity and gastrointestinal health. *Food Chemistry, 157*, 37–44. https://doi.org/10.1016/j.foodchem.2014.02.022

Deng, C., Wang, Y., Navarro, G., Sun, Y., Cota-Ruiz, K., Hernandez-Viezcas, J. A., Niu, G., Li, C., White, J. C., & Gardea-Torresdey, J. (2022). Copper oxide (CuO) nanoparticles affect yield, nutritional quality, and auxin associated gene expression in weedy and cultivated rice (Oryza sativa L.) grains. *Science of The Total Environment, 810*, Article 152260. https://doi.org/10.1016/j.scitotenv.2021.152260

Fageria, N. K., Filho, M. P. B., Moreira, A., & Guimarães, C. M. (2009). Foliar fertilization of crop plants. *Journal of Plant Nutrition, 32*(6), 1044–1064. https://doi.org/10.1080/01904160902872826

FAO. (2018). *The future of food and agriculture: Alternative pathways to 2050.* Food and Agricultural 8 Organization of the United Nations, Rome.

Gao, X., Rodrigues, S. M., Spielman-Sun, E., Lopes, S., Rodrigues, S., Zhang, Y., Avellan, A., Duarte, R. M. B. O., Duarte, A., Casman, E. A., & Lowry, G. V. (2019). Effect of soil organic matter, soil pH, and moisture content on solubility and dissolution rate of CuO NPs in soil. *Environmental Science & Technology, 53*(9), 4959–4967. https://doi.org/10.1021/acs.est.8b07243

Gruszecka-Kosowska, A. (2019). Human health risk assessment and potentially harmful element contents in the fruits cultivated in the southern Poland. *International Journal of Environmental Research and Public Health, 16*(24), Article 24. https://doi.org/10.3390/ijerph16245096

Guo, J.-T., Lee, H.-L., Chiang, S.-H., Lin, F.-I., & Chang, C.-Y. (2020). Antioxidant properties of the extracts from different parts of broccoli in Taiwan. *Journal of Food and Drug Analysis, 9*(2). https://doi.org/10.38212/2224-6614.2795

Hanafy, D. M., Prenzler, P. D., Burrows, G. E., Ryan, D., Nielsen, S., El Sawi, S. A., El Alfy, T. S., Abdelrahman, E. H., & Obied, H. K. (2017). Biophenols of mints: Antioxidant, acetylcholinesterase, butyrylcholinesterase and histone deacetylase inhibition activities targeting Alzheimer's disease treatment. *Journal of Functional Foods, 33*, 345–362. https://doi.org/10.1016/j.jff.2017.03.027

Hong, J., Wang, L., Sun, Y., Zhao, L., Niu, G., Tan, W., Rico, C. M., Peralta-Videa, J. R., & Gardea-Torresdey, J. L. (2016). Foliar applied nanoscale and microscale CeO2 and CuO alter cucumber (Cucumis sativus) fruit quality. *Science of The Total Environment, 563–564*, 904–911. https://doi.org/10.1016/j.scitotenv.2015.08.029

Hurkman, W. J., & Tanaka, C. K. (2007). Extraction of wheat endosperm proteins for proteome analysis. *Journal of Chromatography. B, Analytical Technologies in the Biomedical and Life Sciences, 849*(1–2), 344–350. https://doi.org/10.1016/j.jchromb.2006.11.047

Jośko, I., Krasucka, P., Skwarek, E., Oleszczuk, P., & Sheteiwy, M. (2022). The co-occurrence of Zn-and Cu-based engineered nanoparticles in soils: The metal extractability vs. toxicity to Folsomia candida. *Chemosphere, 287*, Article 132252. https://doi.org/10.1016/j.chemosphere.2021.132252

Jośko, I., Kusiak, M., Oleszczuk, P., Świeca, M., Kończak, M., & Sikora, M. (2021). Transcriptional and biochemical response of barley to co-exposure of metal-based nanoparticles. *Science of The Total Environment, 782*, Article 146883. https://doi.org/10.1016/j.scitotenv.2021.146883

Jośko, I., Kusiak, M., Xing, B., & Oleszczuk, P. (2021). Combined effect of nano-CuO and nano-ZnO in plant-related system: From bioavailability in soil to transcriptional regulation of metal homeostasis in barley. *Journal of Hazardous Materials, 416*, Article 126230. https://doi.org/10.1016/j.jhazmat.2021.126230

Jośko, I., Oleszczuk, P., & Skwarek, E. (2017). Toxicity of combined mixtures of nanoparticles to plants. *Journal of Hazardous Materials, 331*, 200–209. https://doi.org/10.1016/j.jhazmat.2017.02.028

Kadri, O., Karmous, I., Kharbech, O., Arfaoui, H., & Chaoui, A. (2022). Cu and CuO Nanoparticles Affected the Germination and the Growth of Barley (Hordeum vulgare L.) Seedling. *Bulletin of Environmental Contamination and Toxicology, 108*(3), 585–593. https://doi.org/10.1007/s00128-021-03425-y

Kah, M., Tufenkji, N., & White, J. C. (2019). Nano-enabled strategies to enhance crop nutrition and protection. *Nature Nanotechnology, 14*(6), 532–540. https://doi.org/10.1038/s41565-019-0439-5

Kaweeteerawat, C., Chang, C. H., Roy, K. R., Liu, R., Li, R., Toso, D., Fischer, H., Ivask, A., Ji, Z., Zink, J. I., Zhou, Z. H., Chanfreau, G. F., Telesca, D., Cohen, Y., Holden, P. A., Nel, A. E., & Godwin, H. A. (2015). Cu Nanoparticles Have Different Impacts in Escherichia coli and Lactobacillus brevis than Their Microsized and Ionic Analogues. *ACS Nano, 9*(7), 7215–7225. https://doi.org/10.1021/acsnano.5b02021

Kohatsu, M. Y., Lange, C. N., Pelegrino, M. T., Pieretti, J. C., Tortella, G., Rubilar, O., Batista, B. L., Seabra, A. B., & de Jesus, T. A. (2021). Foliar spraying of biogenic CuO nanoparticles protects the defence system and photosynthetic pigments of lettuce

(Lactuca sativa). *Journal of Cleaner Production, 324*, Article 129264. https://doi.org/10.1016/j.jclepro.2021.129264

Kusiak, M., Oleszczuk, P., & Jośko, I. (2022). Cross-examination of engineered nanomaterials in crop production: Application and related implications. *Journal of Hazardous Materials, 424*, Article 127374. https://doi.org/10.1016/j.jhazmat.2021.127374

Lahouar, L., El Arem, A., Ghrairi, F., Chahdoura, H., Ben Salem, H., El Felah, M., & Achour, L. (2014). Phytochemical content and antioxidant properties of diverse varieties of whole barley (Hordeum vulgare L.) grown in Tunisia. *Food Chemistry, 145*, 578–583. https://doi.org/10.1016/j.foodchem.2013.08.102

Lasso-Robledo, J. L., Torres, B., & Peralta-Videa, J. R. (2022). Do all Cu nanoparticles have similar applications in nano-enabled agriculture? *Plant Nano Biology, 1*, Article 100006. https://doi.org/10.1016/j.plana.2022.100006

Laughton, S., Laycock, A., von der Kammer, F., Hofmann, T., Casman, E. A., Rodrigues, S. M., & Lowry, G. V. (2019). Persistence of copper-based nanoparticle-containing foliar sprays in Lactuca sativa (lettuce) characterized by spICP-MS. *Journal of Nanoparticle Research, 21*(8), 174. https://doi.org/10.1007/s11051-019-4620-4

Lee, J., Durst, R. W., & Wrolstad, R. E. (2005). Determination of total monomeric anthocyanin pigment content of fruit juices, beverages, natural colorants, and wines by the pH differential method: Collaborative study. *Journal of AOAC International, 88*(5), 1269–1278.

Madhujith, T., Izydorczyk, M., & Shahidi, F. (2006). Antioxidant properties of pearled barley fractions. *Journal of Agricultural and Food Chemistry, 54*(9), 3283–3289. https://doi.org/10.1021/jf0527504

Mareček, V., Mikyška, A., Hampel, D., Čejka, P., Neuwirthová, J., Malachová, A., & Cerkal, R. (2017). ABTS and DPPH methods as a tool for studying antioxidant capacity of spring barley and malt. *Journal of Cereal Science, 73*, 40–45. https://doi.org/10.1016/j.jcs.2016.11.004

Masisi, K., Beta, T., & Moghadasian, M. H. (2016). Antioxidant properties of diverse cereal grains: A review on in vitro and in vivo studies. *Food Chemistry, 196*, 90–97. https://doi.org/10.1016/j.foodchem.2015.09.021

Meda, A., Lamien, C. E., Romito, M., Millogo, J., & Nacoulma, O. G. (2005). Determination of the total phenolic, flavonoid and proline contents in Burkina Fasan honey, as well as their radical scavenging activity. *Food Chemistry, 91*(3), 571–577. https://doi.org/10.1016/j.foodchem.2004.10.006

Miller, N. J., Rice-Evans, C., Davies, M. J., Gopinathan, V., & Milner, A. (1993). A novel method for measuring antioxidant capacity and its application to monitoring the antioxidant status in premature neonates. *Clinical Science (London, England: 1979), 84*(4), 407–412. Doi: 10.1042/cs0840407.

Minekus, M., Alminger, M., Alvito, P., Ballance, S., Bohn, T., Bourlieu, C., … Brodkorb, A. (2014). A standardised static in vitro digestion method suitable for food—An international consensus. *Food & Function*. https://doi.org/10.1039/c3fo60702j

Narwal, S., Kumar, D., Kharub, A. S., & Verma, R. P. S. (2020). 11 - Barley biofortification: Present status and future prospects. In O. P. Gupta, V. Pandey, S. Narwal, P. Sharma, S. Ram, & G. P. Singh (Eds.), *Wheat and Barley Grain Biofortification* (pp. 275–294). Woodhead Publishing. https://doi.org/10.1016/B978-0-12-818444-8.00011-0.

Öztürk, M., Duru, M. E., Kivrak, S., Mercan-Doğan, N., Türkoglu, A., & Özler, M. A. (2011). In vitro antioxidant, anticholinesterase and antimicrobial activity studies on three Agaricus species with fatty acid compositions and iron contents: A comparative study on the three most edible mushrooms. *Food and Chemical Toxicology: An International Journal Published for the British Industrial Biological Research Association, 49*(6), 1353–1360. https://doi.org/10.1016/j.fct.2011.03.019

Pilon, M., Cohu, C. M., Ravet, K., Abdel-Ghany, S. E., & Gaymard, F. (2009). Essential transition metal homeostasis in plants. *Current Opinion in Plant Biology, 12*(3), 347–357. https://doi.org/10.1016/j.pbi.2009.04.011

Puig, S., Andrés-Colás, N., García-Molina, A., & Peñarrubia, L. (2007). Copper and iron homeostasis in Arabidopsis: Responses to metal deficiencies, interactions and biotechnological applications. *Plant, Cell & Environment, 30*(3), 271–290. https://doi.org/10.1111/j.1365-3040.2007.01642.x

Rawat, S., R. Pullagurala, V. L., Hernandez-Molina, M., Sun, Y., Niu, G., A. Hernandez-Viezcas, J., R. Peralta-Videa, J., & L. Gardea-Torresdey, J. (2018a). Impacts of copper oxide nanoparticles on bell pepper (Capsicum annum L.) plants: A full life cycle study. *Environmental Science: Nano, 5*(1), 83–95. Doi: 10.1039/C7EN00697G.

Rico, C. M., Hong, J., Morales, M. I., Zhao, L., Barrios, A. C., Zhang, J.-Y., Peralta-Videa, J. R., & Gardea-Torresdey, J. L. (2013). Effect of cerium oxide nanoparticles on rice: A study involving the antioxidant defense system and in vivo fluorescence imaging. *Environmental Science & Technology, 47*(11), 5635–5642. https://doi.org/10.1021/es401032m

Rico, C. M., Morales, M. I., Barrios, A. C., McCreary, R., Hong, J., Lee, W.-Y., Nunez, J., Peralta-Videa, J. R., & Gardea-Torresdey, J. L. (2013). Effect of cerium oxide nanoparticles on the quality of rice (Oryza sativa L.). *Grains. Journal of Agricultural and Food Chemistry, 61*(47), 11278–11285. https://doi.org/10.1021/jf404046v

Rui, M., Ma, C., White, J. C., Hao, Y., Wang, Y., Tang, X., Yang, J., Jiang, F., Ali, A., Rui, Y., Cao, W., Chen, G., & Xing, B. (2018). Metal oxide nanoparticles alter peanut (Arachis hypogaea L.) physiological response and reduce nutritional quality: A life cycle study. *Environmental Science Nano, 5*(9), 2088–2102. https://doi.org/10.1039/C8EN00436F

Tan, W., Gao, Q., Deng, C., Wang, Y., Lee, W.-Y., Hernandez-Viezcas, J. A., Peralta-Videa, J. R., & Gardea-Torresdey, J. L. (2018). Foliar exposure of Cu(OH)2 nanopesticide to basil (Ocimum basilicum): Variety-dependent copper translocation and biochemical responses. *Journal of Agricultural and Food Chemistry, 66*(13), 3358–3366. https://doi.org/10.1021/acs.jafc.8b00339

Trumbo, P., Yates, A. A., Schlicker, S., & Poos, M. (2001). Dietary reference intakes: Vitamin A, vitamin K, arsenic, boron, chromium, copper, iodine, iron, manganese, molybdenum, nickel, silicon, vanadium, and zinc. *Journal of the American Dietetic Association, 101*(3), 294–301. https://doi.org/10.1016/S0002-8223(01)00078-5

Wang, Y., Jiang, F., Ma, C., Rui, Y., Tsang, D. C. W., & Xing, B. (2019). Effect of metal oxide nanoparticles on amino acids in wheat grains (Triticum aestivum) in a life cycle study. *Journal of Environmental Management, 241*, 319–327. https://doi.org/10.1016/j.jenvman.2019.04.041

Xiong, T., Dumat, C., Dappe, V., Vezin, H., Schreck, E., Shahid, M., Pierart, A., & Sobanska, S. (2017). Copper oxide nanoparticle foliar uptake, phytotoxicity, and consequences for sustainable urban agriculture. *Environmental Science & Technology, 51*(9), 5242–5251. https://doi.org/10.1021/acs.est.6b05546

Zengin, G., Nithiyanantham, S., Sarikurkcu, C., Uysal, S., Ceylan, R., Ramya, K. S., Maskovic, P., & Aktumsek, A. (2017). Identification of phenolic profiles, fatty acid compositions, antioxidant activities, and enzyme inhibition effects of seven wheat cultivars grown in Turkey: A phytochemical approach for their nutritional value. *International Journal of Food Properties, 20*(10), 2373–2382. https://doi.org/10.1080/10942912.2016.1238391

Zhang, T., Sun, H., Lv, Z., Cui, L., Mao, H., & Kopittke, P. M. (2017). Using synchrotron-based approaches to examine the foliar application of ZnSO4 and ZnO nanoparticles for field-grown winter wheat. *Journal of Agricultural and Food Chemistry*. https://doi.org/10.1021/acs.jafc.7b04153

Zhao, H., Fan, W., Dong, J., Lu, J., Chen, J., Shan, L., Lin, Y., & Kong, W. (2008). Evaluation of antioxidant activities and total phenolic contents of typical malting barley varieties. *Food Chemistry, 107*(1), 296–304. https://doi.org/10.1016/j.foodchem.2007.08.018

Zhao, L., Huang, Y., Hannah-Bick, C., Fulton, A. N., & Keller, A. A. (2016). Application of metabolomics to assess the impact of Cu(OH)2 nanopesticide on the nutritional value of lettuce (Lactuca sativa): Enhanced Cu intake and reduced antioxidants. *NanoImpact, 3–4*, 58–66. https://doi.org/10.1016/j.impact.2016.08.005

Appendix A. Supplementary material

The life cycle study revealed distinct impact of foliar-applied nano-Cu on antioxidant traits of barley grain comparing with conventional agents

Izabela **Jośko**[a*¥], Magdalena **Kusiak**[a], Krzysztof **Różyło**[b], Ewa **Baranowska-Wójcik**[c], Małgorzata **Sierocka**[d], Mohamed **Sheteiwy**[e], Dominik **Szwajgier**[c], Michał **Świeca**[d]

[a] Institute of Plant Genetics, Breeding and Biotechnology, Faculty of Agrobioengineering, University of Life Sciences, 15 Akademicka Street, 20-950 Lublin, Poland.

[b] Department of Agricultural Ecology, Faculty of Agrobioengineering, University of Life Sciences, 13 Akademicka Street, 20-950 Lublin, Poland.

[c] Department of Biotechnology, Microbiology and Human Nutrition, Faculty of Food Science and Biotechnology, University of Life Sciences, 8 Skromna Street, 20-704 Lublin, Poland.

[d] Department of Biochemistry and Food Chemistry, Faculty of Food Science and Biotechnology, University of Life Sciences, 8 Skromna Street, 20-704 Lublin, Poland.

[e] Department of Agronomy, Faculty of Agriculture, Mansoura University, 60 Elgomhoria Street, 35516 Mansoura, Egypt

[*] Family names are written in bold.

[¥] Correspondence to: Izabela Jośko, Institute of Plant Genetics, Breeding and Biotechnology, Faculty of Agrobioengineering, Univerisity of Life Sciences, 20–950 Lublin, 13 Akademicka Street, Poland, tel. +48 81 4456675, fax. +48 81 4456031, e-mail: izabela.josko@up.lublin.pl

Journal: *Food Research International*

Number of pages: 4

Number of tables: 3

Number of Figures: 1

MATERIALS AND METHODS

Soil characterization

The particle size distribution of the soils was determined with the areometric method. The pH was measured potentiometrically in 1M KCl after 24 h at the liquid/soil ratio of 2.5 (Reeuwijk, 1993). The concentrations of available P_2O_5 and K_2O in soil were determined in 0.1 M $CH_3CH(OH)COONH_4$ in 0.4 M CH_3COOH (in the ratio w:v 1:20) with Egner-Riehm-Domingo method (Salomon et al., 2015). The total content of elements (Mg, Ca, Na, Mn, Fe, Zn, Cu) was measured by ICP-OES (Thermo Scientific iCAP™ 7200 ICP-OES Analyzer). The analysis of cation-exchangeable concentration of Cu was prepared by using batch extraction with $CaCl_2$ (Gao et al., 2018). $CaCl_2$ extraction was performed by mixing 2 g of air-dried soil with 20 mL of 0.01 mol/L $CaCl_2$. The mixtures were shaken at 180 rpm (JW Electronic WL-2000, Poland) for 2 h. After extractions, samples were centrifuged at 4,000 *g* (MPW MED. INSTRUMENTS, MPW-251, Poland) and filtered through a 0.45 μm PTFE filter. Then, the extracts were analyzed using an ICP-OES (Thermo Fisher Scientific, iCAP 7200, USA). For the total content of Cu in soil, dry soil was digested with a mixture of HNO_3:H_2O_2 (4:1) in Teflon vessels in a microwave oven (Milestone, ETHOS EASY, Italy) for 1 h at 200°C. After cooling, the samples were filtered (0.45 μm, PTFE), diluted with Milli-Q® -water to 25 mL, and analyzed with ICP-OES (iCAP 7200).

The analysis of barley grain

Nutritional quality

<u>*Protein digestibility*</u>. For simulated mastication and gastrointestinal digestion, the *in vitro* gastrointestinal model used in the study is presented in Fig. A.1. Water-jacketed glass tanks (250 ml in volume) were used and "digested" samples were continuously purged using sterile CO_2 during the whole "digestion" (analytical grade, Linde Gas Poland, approx. 5 – 8 mL/min, thru syringe PTFE 0.45 μm filter). 200 mg of sample was homogenized in 0.5 mL PBS buffer and 1 mL of simulated salivary fluid [15.1 mmol/L KCl, 3.7 mmol/L KH_2PO_4, 13.6 mmol/L $NaHCO_3$, 0.15 mmol/L $MgCl_2(H_2O)_6$, 0.06 mmol/L $(NH_4)_2CO_3$, 1.5 mmol/L $CaCl_2$, α-amylase (75 U/mL)] and shaken for 10 min at 37°C. Next, the samples were adjusted to pH 3 with 6 mol/L HCl, suspended in 2 mL of simulated gastric fluid [6.9 mmol/L KCl, 0.9 mmol/L KH_2PO_4, 25 mmol/L $NaHCO_3$, 47.2 mmol/L NaCl, 0.1 mmol/L $MgCl_2(H_2O)_6$, 0.5 mol/L $(NH_4)_2CO_3$, 0.15 mmol/L $CaCl_2$, pepsin (2000 U/L) and shaken for 120 min at 37°C. After

simulated gastric digestion, the samples were adjusted to pH 7 with 1 M NaOH and suspended in 4 ml of simulated intestinal fluid [6.8 mmol/L KCl, 0.8 mmol/L KH_2PO_4, 85 mmol/L $NaHCO_3$, 38.4 mmol/L NaCl, 0.33 mmol/L $MgCl_2$ $(H_2O)_6$, 0.15 mmol/L $CaCl_2$, 10 mol/L bile extract, pancreatin (2000 U/mL)]. The prepared samples underwent *in vitro* intestinal digestion for 120 min. For analysis of the potentially bioaccessible fraction of protein, the samples subjected to the gastrointestinal digestion were mixed with an equal volume of methanol to stop the process. A "control" sample containing all components except the studied sample was run simultaneously.

Fig. A.1. *In vitro* gastrointestinal model used in the study.

RESULTS

Tab. A.1. The total content of Cu in soil after foliar treatment. Different letters indicate significant differences among the treatments ($p < 0.05$).

	control	nano-Cu	nano-CuO	micro-Cu	$CuSO_4$	CuEDTA
Cu content [mg/kg]	4.17 ± 0.2^a	4.21 ± 0.3^a	4.47 ± 0.2^a	4.39 ± 0.8^a	4.54 ± 0.1^a	4.60 ± 0.2^a

Tab. A.2. Grain yield of barley treated with different Cu compounds. Different letters indicate significant differences among the treatments ($p < 0.05$).

	control	nano-Cu	nano-CuO	micro-Cu	$CuSO_4$	CuEDTA
Grain weight [g] per pot	41.5 ± 2.5^a	43.6 ± 3.5^a	35.3 ± 4.2^a	43.7 ± 2.0^a	39.6 ± 3.3^a	40.2 ± 3.5^a
1000 grains weight [g]	38.2 ± 1.7^a	$36.0 \pm 2,1^a$	35.6 ± 2.6^a	39.6 ± 2.3^a	36.6 ± 2.6^a	38.7 ± 2.7^a

Tab. A.3. Daily intake rates of Cu calculated based on actual and recommended the average ingestion rate of barley grain (IR) and average body weight (60 kg).

	Daily intake rate [mg/kg/day]					
	control	nano-Cu	nano-CuO	micro-Cu	$CuSO_4$	CuEDTA
Actual IR	0.03	0.08	0.05	0.04	0.06	0.08
Recommended IR	0.06	1.3	0.8	0.7	1.0	1.4

Lublin, 03.07.2023

Dr hab. Izabela Jośko, prof. uczelni
Instytut Genetyki, Hodowli i
Biotechnologii Roślin
Uniwersytet Przyrodniczy w Lublinie
Ul. Akademicka 15,
20-950 Lublin
Tel. 814456675
izabela.josko@up.lublin.pl

Rada Dyscypliny Rolnictwo i Ogrodnictwo
Uniwersytetu Przyrodniczego
w Lublinie

Oświadczenie o współautorstwie

Oświadczam, że mój udział w pracy "*The life cycle study revealed distinct impact of foliar-applied nano-Cu on antioxidant traits of barley grain comparing with conventional agents*" [Food Research International, 2023] wynosi 35%.

Mój wkład polegał na kierowaniu projektem naukowym obejmującym badania opisane w tej pracy oraz pozyskaniu funduszy na badania. Ponadto, odpowiadałam za opracowanie koncepcji badań i metodyki oraz za przygotowanie manuskryptu do publikacji i odpowiedzi na otrzymane recenzje pracy.

Izabela Jośko

Podpis

Lublin, 29.08.2023

Magdalena Kusiak
Instytut Genetyki, Hodowli i
Biotechnologii Roślin
Uniwersytet Przyrodniczy w Lublinie
Ul. Akademicka 15,
20-950 Lublin
Tel: 508 789 096
magdalena.kusiak@up.lublin.pl

Rada Dyscypliny Rolnictwo i Ogrodnictwo
Uniwersytetu Przyrodniczego
w Lublinie

Oświadczenie o współautorstwie

Oświadczam, że mój udział w pracy "*The life cycle study revealed distinct impact of foliar-applied nano-Cu on antioxidant traits of barley grain comparing with conventional agents*" [Food Research International, 2023] wynosi 30%.

Mój wkład polegał na udziale w opracowaniu metodyki badań, planowaniu i wykonaniu analiz laboratoryjnych wraz z opracowaniem wyników i ich interpretacją oraz na redagowaniu manuskryptu.

Magdalena Kusiak

Podpis

Lublin, 28.06.2023

dr hab. Krzysztof Różyło, prof. uczelni
Zakład Ekologii Rolniczej
Uniwersytet Przyrodniczy w Lublinie
ul. Akademicka 13,
20-950 Lublin
Tel. 814456641
krzysztof.rozylo@up.lublin.pl

Rada Dyscypliny Rolnictwo i Ogrodnictwo
Uniwersytetu Przyrodniczego
w Lublinie

Oświadczenie o współautorstwie

Oświadczam, że mój udział w pracy "*The life cycle study revealed distinct impact of foliar-applied nano-Cu on antioxidant traits of barley grain comparing with conventional agents*" [Food Research International, 2023] wynosi 10%.

Mój wkład polegał na wykonaniu badań laboratoryjnych.

Podpis

Lublin, 27.06.2023

dr inż. Ewa Baranowska-Wójcik
Katedra Biotechnologii, Mikrobiologii
i Żywienia Człowieka
Uniwersytet Przyrodniczy w Lublinie
ul. Skromna 8
20-704 Lublin
Tel. 814623394
ewa.baranowska@up.lublin.pl

Rada Dyscypliny Rolnictwo i Ogrodnictwo
Uniwersytetu Przyrodniczego
w Lublinie

Oświadczenie o współautorstwie

Oświadczam, że mój udział w pracy "*The life cycle study revealed distinct impact of foliar-applied nano-Cu on antioxidant traits of barley grain comparing with conventional agents*" [Food Research International, 2023] wynosi 10%.

Mój wkład polegał na wykonaniu badań laboratoryjnych.

Ewa Baranowska-Wójcik

Podpis

Lublin, 26.06.2023

Dr inż. Małgorzata Sierocka
Katedra Biochemii i Chemii Żywności
Uniwersytet Przyrodniczy w Lublinie
ul. Skromna 8
20-704 Lublin
Tel. 814623328
malgorzata.sierocka@up.lublin.pl

Rada Dyscypliny Rolnictwo i Ogrodnictwo
Uniwersytetu Przyrodniczego
w Lublinie

Oświadczenie o współautorstwie

Oświadczam, że mój udział w pracy "*The life cycle study revealed distinct impact of foliar-applied nano-Cu on antioxidant traits of barley grain comparing with conventional agents*" [Food Research International, 2023] wynosi 5%.

Mój wkład polegał na udziale w opracowaniu metodyki badań oraz pisaniu manuskryptu.

Małgorzata Siwecka (z d. Sikora)

Podpis

Mansoura, 20.07.2023

Mohamed Sheteiwy Ph.D
Department of Agronomy
Mansoura University
60 Elgomhoria Street
35516 Mansoura, Egypt
salahco_2010@mans.edu.eg

Discipline Council for Agriculture and Horticulture
of University of Life Sciences
in Lublin

Statement of co-authorship

I declare that my contribution to the article "*The life cycle study revealed distinct impact of foliar-applied nano-Cu on antioxidant traits of barley grain comparing with conventional agents*" [Food Research International, 2023] is 5%.

My contribution consisted of participation in the writing (review and editing) of the manuscript.

Mohamed Sheteiwy

Signature

Lublin, 28.06.2023

Prof. dr hab. Dominik Szwajgier
Katedra Biotechnologii, Mikrobiologii
i Żywienia Człowieka
Uniwersytet Przyrodniczy w Lublinie
ul. Skromna 8
20-704 Lublin
Tel. 81 462 33 74
dominik.szwajgier@up.lublin.pl

Rada Dyscypliny Rolnictwo i Ogrodnictwo
Uniwersytetu Przyrodniczego
w Lublinie

Oświadczenie o współautorstwie

Oświadczam, że mój udział w pracy "*The life cycle study revealed distinct impact of foliar-applied nano-Cu on antioxidant traits of barley grain comparing with conventional agents*" [Food Research International, 2023] wynosi 5%.

Mój wkład polegał na opracowaniu metodyki badań oraz na przygotowaniu manuskryptu.

Dominik Szwajgier

Podpis

Lublin, 26.06.2023

Prof. dr hab. Michał Świeca
Katedra Biochemii i Chemii Żywności
Uniwersytet Przyrodniczy w Lublinie
ul. Skromna 8
20-704 Lublin
Tel. 814623327
michal.swieca@up.lublin.pl

Rada Dyscypliny Rolnictwo i Ogrodnictwo
Uniwersytetu Przyrodniczego
w Lublinie

Oświadczenie o współautorstwie

Oświadczam, że mój udział w pracy "*The life cycle study revealed distinct impact of foliar-applied nano-Cu on antioxidant traits of barley grain comparing with conventional agents*" [Food Research International, 2023] wynosi 5%.

Mój wkład polegał na udziale w opracowaniu metodyki badań.

Signed by / Podpisano przez:
Michał Świeca
Uniwersytet Przyrodniczy w Lublinie
Date / Data:
2023-05-30 11:31

.....

Podpis

Oświadczenie promotora rozprawy doktorskiej

Oświadczam, że niniejsza rozprawa doktorska została przygotowana pod moim kierunkiem i stwierdzam, że spełnia ona warunki do przedstawienia jej w postępowaniu o nadanie stopnia naukowego.

Data ..... Podpis promotora .....

Oświadczenie autora rozprawy doktorskiej

Świadom/a odpowiedzialności prawnej oświadczam, że:

- niniejsza rozprawa doktorska została przygotowana przez mnie samodzielnie pod kierunkiem Promotora/~~Promotorów/Promotora pomocniczego~~* i nie zawiera treści uzyskanych w sposób niezgodny z obowiązującymi przepisami.
- przedstawiona rozprawa doktorska nie była wcześniej przedmiotem procedur związanych z uzyskaniem stopnia naukowego.
- niniejsza wersja rozprawy doktorskiej jest tożsama z załączoną na płycie CD/pendrive wersją elektroniczną.

Data ..... Podpis autora .....

* niepotrzebne skreślić